New York Geological Association
89th Annual Meeting

Field Trip Guidebook

Hosted by
Alfred University
Alfred , New York
October 6-8, 2017

NYSGA
New York State
Geological Association

Alfred University

Edited by
Otto H. Muller

Published by the
New York State Geological Society
www.nysga-online.net

PREFACE AND ACKNOWLEDGEMENTS

The Division of Geology and Environmental Studies, College of Liberal Arts and Sciences at Alfred University is pleased to host the 89th Annual meeting of the New York State Geological Association. Alfred has not hosted an NYSGA meeting since 1957 (it was actually hosted Wellsville, a village nearby), so it was definitely time to bring you all to the Southern Tier of New York state! We hope that you will find this meeting enjoyable and educational and that you will want to return to our beautiful part of the state again.

We wish to express our sincere appreciation to all of the field trip and workshop leaders. We have a wonderful variety of trips thanks to the willingness of the leaders, and we appreciate their hard work and dedication in putting together interesting trips and detailed descriptions/road logs.

We would also like to acknowledge the invaluable assistance of Nicole Munkwitz and Shannon Yocum here at Alfred for their work on organizing the logistics of this conference. Without their help, this conference would not be taking place in Alfred.

Alfred University has a long history of interest in the geology of New York state. One of our first university presidents, Jonathan Allen, and his wife Abigail, were friends of James Hall and avid amateur geologists. The photo on the cover of this guidebook is a building on our campus known as the Steinheim ("rock house"), that President Allen commissioned to be built and was rumored to have a rock from every county in the state on its face (we have proved that rumor to be false, alas, but it is still a fun story and there *is* a nice variety of rock types on the building – we encourage you to go check it out!). The building now houses our Career Development Center, but President Allen lived there during part of his tenure at Alfred.

The Southern Tier also has a long history of oil and gas development with the first commercially successful oil well having been drilled just over the border in Pennsylvania in 1859. Those of you who go on Trip A4 will have the opportunity to learn about the petroleum industry in this part of NYS, visit the Pioneer Oil Museum, a repurposed refinery site and an active lease. No mention of the oil and gas industry in the Southern Tier can be made, however, without acknowledging Arthur Van Tyne, who ran a satellite office of the NYS Geological Survey here on the Alfred University campus for many years, and who contributed enormously to our understanding of the occurrence of fossil fuels in this region.

The bedrock in our region, of course, is comprised of Paleozoic sedimentary rocks, rich in both petroleum and fossils. Professor Daniel Sass, who was a one-man geology department here at Alfred University for many years, studied the Devonian fossil assemblages and introduced hundreds of Alfred geology students to the local geology. But Dan not only taught geology and other liberal arts students – for some time, at least one geology class was also required of ceramic engineering students at Alfred, so countless engineers also benefitted from Dan's enthusiasm and expertise and learned about the raw materials used in their industry.

Atop the Devonian sedimentary strata are glacial deposits, many of which are extracted by local industries. Those of you who choose to go on Trip A6 will visit quarries operated by New Enterprise Stone and Lime Co. and Almond Aggregates, LLC, and we thank those companies for allowing us to visit their operations.

Last, but certainly not least, sincere thanks go to Otto Muller for organizing and editing the guidebook this year. Otto has been laboring all summer getting the guidebook ready. Otto is also our after dinner speaker on Saturday evening. He has been working for several years on the herculean task of putting past NYSGA guidebooks into a searchable digital format and will discuss and demonstrate how you can use his field trip database after the banquet.

We are confident that we have one or more trips to satisfy most geologists' interests at our conference this year. Thank you for coming and we hope you enjoy the weekend.

Michele Hluchy
Conference Organizer

Cover photograph: Benjamin D. Esham / Wikimedia Commons

WEB ACCESS

In order to produce a Guidebook at reasonable expense, it is printed in black and white. Many of the figures and maps, however, are available online at full size and in color. To access them use a URL similar to:

http://www.nysga-online.net/nysga-2017-guidebook-maps-and-images/A5/Fig12

where A5 refers to trip A5 as shown in the Program and Table of Contents, and Fig12 refers to figure 12 in that chapter. Note there are no spaces or underscores in that URL.

The organizers of the 2017 NYSGA conference wish to dedicate this guidebook to the memory of Dr. Bruce Selleck (1949-2017).


Photo by Pam Darwin

The New York State geological community lost an invaluable member in July 2017 when Dr. Bruce Selleck passed away unexpectedly. Bruce spent his entire career studying aspects of New York state geology and contributed to our understanding of the geologic history of the state not only with his own research, but through the hundreds of students he taught in his 43-year career as a professor at Colgate University, many of whom went on to become geologists, environmental scientists, teachers, and other practicing professionals in New York state and elsewhere.

Bruce grew up on a farm in the St. Lawrence lowlands, spent his undergraduate years on the northern edge of the Allegheny plateau at Colgate, went to graduate school in the Genesee Valley, receiving his Ph.D. from the University of Rochester, and then returned to the northern edge of the Allegheny plateau to teach at his alma mater. He initially studied the Paleozoic sedimentary rocks of upstate New York, especially the Potsdam Sandstone and associated formations, but his later research also included work on the tectonic development of the Adirondacks and oil- and gas-bearing strata such as the Marcellus and Utica Shales. Bruce also did research in Alaska and Australia and led student field trips to Wales, Australia, Florida and the southwestern U.S. He published numerous papers in journals such as the *Journal of Sedimentary Research, GSA Bulletin, the American Journal of Science,* and *Geology* by himself, with colleagues, and with his students. Recently, Bruce co-edited a special issue of the *Adirondack Journal of Environmental Science* on the geology and natural environment of the Adirondack region. Bruce also advised dozens and dozens of Colgate undergraduates engaged in research over the years, many of them working on projects in New York state. In his 43 years as part of the Colgate faculty, Bruce was recognized with teaching awards and titled professorships; and he served on several committees and in several administrative positions, including dean of the faculty and provost.


Photo by Ron Parker

Bruce loved being in the field. He was a great friend to the NYSGA, leading or co-leading 12 trips at NYSGA field conferences between 1977 and 2015 and organizing several NYSGA conferences either from Colgate or out of Lake George. In fact, at the time of his passing, Bruce was already planning to help organize a joint NYSGA/NEIGC conference during the fall of 2018. There are others who have also led many NYSGA field trips over the years, for which all of us are grateful, but no one has led trips on such a wide range of topics. Bruce's NYSGA field trips spanned more than a billion years of time, from Mesoproterozoic magmatism of the Adirondacks to surficial geology and soils of Madison county, with many of his trips covering Paleozoic sediments in New York, a subject that was his passion and in which he was a recognized expert. Geographically, these trips covered much of central and northern New York.

Bruce was 67 when he passed away suddenly and unexpectedly and he had no plans to retire or slow down. His love of geology, field work, and teaching was both legendary and contagious. The two organizers of this year's NYSGA conference had the great honor of knowing Bruce as a professor and mentor (Michele) and as a fellow graduate student at the University of Rochester and later colleague at Colgate (Otto) and, while we feel and recognize the great loss to NYS geology, we mostly mourn the loss of a great friend.

Photo by Ron Parker

PROGRAM

Friday (for those from the Buffalo-Fredonia area, especially)

C1 (and B4): Penn Dixie Fossil Park & Nature Reserve -- A Classic and Unique Paleontological and Outdoor Education Center -- Phil Stokes, Holly Schreiber **** Meet at Penn Dixie site, (42.77811, -78.83104) at 10AM ****

Friday Evening Science Center 247, Roon Lecture Hall, 7:00 PM

W1: Workshop: Updates on the glacial, aquifer, and geophysical data in the Genesee Valley, Dansville to Avon, NY -- Richard Young and Lewis Owen; Sam Gowan and John Nadeau; John Williams and William Kappel; Scott Giorgis, Michael Reed, and Eric Horsman

Saturday Morning: Science Center Parking Lot at 8:30 AM unless otherwise noted

A1 (and B1): Depositional Environments Across a Central Trough of the Northern Appalachian Basin, Deep Run Shale Member (Moscow Formation) of the Finger Lakes -- Stephen Mayer, Gordon Baird, Carlton Brett

A2: Upper Devonian Kellwasser extinction events in New York and Pennsylvania: offshore to onshore transect across the Frasnian-Famennian Boundary strata on the eastern margin of the Appalachian Basin **DAY 1**-- Andrew M. Bush, J. Andrew Beard, Gordon Baird, D. Jeffrey Over, Katherine Tuskes, Sarah K. Brisson, Jaleigh Q. Pier **** Meet at Beaver Meadow Creek, Java Village, NY (42.6722, -78.4358) at 10 AM ****

A3 (and B3): Salamanca ("Little Rock City") Conglomerate: Tide-Dominated & Wave-Influenced Deltaic/Coastal Deposits: Upper Devonian (Late Famennian) Cattaraugus Formation -- Jim Craft **** Meet at the DEC sign/State Forest boundary Rock City State Forest – Little Rock City Rd. at the DEC sign - (42.225830, -78.710587) at 10 AM ****

A4: The Bolivar Pioneer Oil Museum, its Environs and the History of Petroleum Production in the Allegany County Region -- Kelly Lounsberry **** Meet at Museum (42.06519, -78.1680) at 9:00 AM ****

A5: Kimberlites in the Cayuga Lake Region of Central New York: The Six Mile Creek, Williams Brook, and Taughannock Creek Dikes -- David Bailey, Marian Lupulescu, Jeffrey R. Chiarenzelli **** Meet at Wegman's Parking Lot, Ithaca, (42.43394, -76.51109) at 9 AM ****

A6: Exploring the Surficial Geology and Hydrology Near Alfred, NY -- David Barclay, Otto Muller, Dick Young

Saturday evening Powell Campus Center Knight Club, 5:30 PM

Banquet

After Banquet Talk: Otto Muller discussing his database of NYSGA field trips from 1956 to 1999, with a demo of how to access all of that info using Excel.

Sunday

B1 (and A1): Depositional Environments Across a Central Trough of the Northern Appalachian Basin, Deep Run Shale Member (Moscow Formation) of the Finger Lakes -- Stephen Mayer, Gordon Baird, Carlton Brett

B2: Upper Devonian Kellwasser extinction events in New York and Pennsylvania: offshore to onshore transect across the Frasnian-Famennian Boundary strata on the eastern margin of the Appalachian Basin **DAY 2**-- Andrew M. Bush, J. Andrew Beard, Gordon Baird, D. Jeffrey Over, Katherine Tuskes, Sarah K. Brisson, Jaleigh Q. Pier ****Meet at Cowanesque Lake Outcrop, Route 49, west of Lawrenceville, PA, (41.9816, - 77.1492) at 10 AM ****

A3 (and B3): Salamanca ("Little Rock City") Conglomerate: Tide-Dominated & Wave-Influenced Deltaic/Coastal Deposits: Upper Devonian (Late Famennian) Cattaraugus Formation -- Jim Craft **** Meet at the DEC sign/State Forest boundary Rock City State Forest – Little Rock City Rd. at the DEC sign - (42.225830, -78.710587) at 10 AM ****

B4 (and C1): Penn Dixie Fossil Park & Nature Reserve - A Classic and Unique Paleontological and Outdoor Education Center -- Phil Stokes, Holly Schreiber **** Meet at Penn Dixie site, (42.77811, -78.83104) at 10 AM****

B5: Glacial Features and the "Great Divide" between Watkins Glen and Ithaca -- Carol Griggs

W2: Key Tools and Strategies for Making and Using Virtual Fieldwork Experiences -- **Don Duggan-Haas and Robert M. Ross**

Table Of Contents

C1 AND B4: THE PENN DIXIE SITE: A CLASSIC AND UNIQUE PALEONTOLOGICAL & OUTDOOR EDUCATION CENTER

PHIL STOKES
Executive Director

HOLLY SCHREIBER
Director of Education

JEROLD C. BASTEDO
Former Executive Director and Author of Guidebook Article

Mailing:
Penn Dixie Fossil Park & Nature Reserve
3556 Lakeshore Rd., Ste. 230, Blasdell, NY 14219
www.penndixie.org

INTRODUCTION

The Hamburg Natural History Society, Inc. (HNHS) is a nonprofit educational corporation that owns and operates Penn Dixie Fossil Park & Nature Reserve in Hamburg, New York (Fig. 1). The HNHS was founded in 1993 to promote the study of the natural sciences, with a particular emphasis on field activities associated with the geological and biological sciences. The HNHS offers a wide variety of hands-on educational programming to students of all ages, both at the Penn Dixie Site and off-site at local schools, libraries, and civic group meetings. Since its inception, the HNHS has expanded its educational curriculum to include public educational programming in astronomy and ornithology to complement its core study in geology and fossil collecting and identification. Unlike conventional museums or research facilities, the Penn Dixie Site is a hands-on outdoor educational facility-one at which visitors of all ages are encouraged to actually collect and keep 380-million-year-old fossils-"*Where Science Comes Alive*".

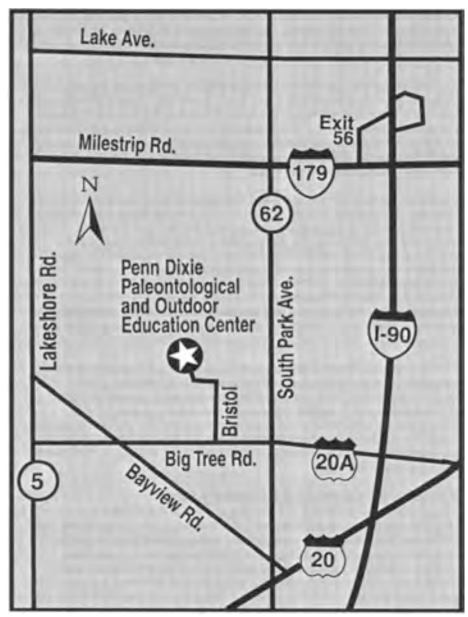

Figure 1. Location of Penn Dixie in Hamburg, New York.

The site of a former quarry operation that was the source of calcareous shale excavated and used for cement aggregate by the Penn Dixie Cement Company. A majority of the 57-acre site was quarried until the late 1960s, during which time 9 to 10 feet of shale was removed from the surface. A gray, somewhat flat "desert-like" or "lunar landscape-appearing" surface now occupies a majority of the site. After quarry operations ceased, weathering forces began to expose 380 million-year-old Devonian fossils preserved within the Windom Shale. This highly fossiliferous unit underlies the entire site and provides an inexhaustible supply of fossils. In addition to the Windom Shale, several limestone units (the Genundewa, North Evans, and Tichenor) outcrop on the surface. The Wanakah Shale is also exposed, underlying the Tichenor Limestone, in a tributary that flows into Rush Creek and in cliffs along Rush Creek on the northern section of the site. All of these units contain a variety of fossils.

Preservation Of Penn Dixie

The HNHS administers and maintains the Penn Dixie, a 32.5-acre former shale quarry that was purchased by the Town of Hamburg in 1995 and deeded to the HNHS in 1996. The HNHS then took immediate steps to clean up the site and establish plans for its transformation into a truly world-class outdoor educational resource center. In 2004, the HNHS purchased 16.75 acres of adjacent land from the Town of Hamburg, increasing the site to 49.25 acres. The HNHS' efforts to preserve the former quarry and its associated wetlands saved one of the richest sites of 380-million-year-old Devonian Era fossils in the eastern United States.

In 1989 and 1990, the site was under the threat of light industrial development, but citizens from the community had other ideas for preserving it for future generations. A group of local residents and geologists collaborated on acquiring and preserving this area for future outdoor educational use. This group worked with members of the Hamburg Town Board to purchase the property. In December 1995 the Town of Hamburg completed the purchase of the property and in January 1996 deeded 32.5 acres to the HNHS.

Fossil collecting and the study of the local geology were the initial intent for the preservation of this former quarry. After acquisition of the property in early 1996, the HNHS reexamined the other resources available for outdoor education programs in the other natural sciences. With over 143 nesting and migratory birds at the site; the deer, turkey, coyote and other animals; the spacious area for viewing the Penn Dixie Skies with telescopes; and the potential for expanding the wetlands, this is a unique location to provide a diversity of programs in the natural sciences. The HNHS also has installed over 2,100 feet of barrier-free paved trails with grants from the East Hill Foundation and the New York State Senate. Eventually, the plan is to install paved and boardwalk trails throughout the entire site. With all these wonderful features and opportunities, the goal continues to be to make Penn Dixie into an outdoor education center and not a museum.

The HNHS hired a full-time Executive Director in 2003 and a full-time educator in September 2004 to manage and develop programs in the natural sciences. As a private non-profit organization, a volunteer board of directors, elected by its membership, governs the HNHS. IINHS staff, volunteer educators and field trip leaders are actively involved in bringing educational programming to the Western New York community.

Geology, Stratigraphy, And Paleontology

Penn Dixie contains an extensive exposure of 380-million-year-old fossiliferous Middle Devonian shales and limestones, serving as an excellent outdoor classroom for introducing students to the local geology and paleontology. The Genudewa Limestone, North Evans Limestone, Windom Shale, Tichenor Limestone, and Wanakah Shale at this site are readily accessible and have the most extensive exposure available for study in Western and central New York. Figure 2 (Brett and Baird, 1982) illustrates the stratigraphic units present at the Penn Dixie Site. Prime exposures of these units are present (except for the West River Shale, which is mostly covered by overburden at the south end of the site). Brett (1974) and Baird and Brett (1982), along with Beuhler and Tesmer (L 963), provide a detailed discussion of the stratigraphy and paleontology of these units. The warm tropical seas that covered this region of Western New York 380 million-years ago, when the region was 20 to 30 degrees south of the equator, provided an environment conducive to a variety of invertebrate and vertebrate animals. The shales and limestones that formed during this time period preserved the remains of the diverse and abundant fauna that occupied these seas. The following brief discussion of the units present on the site begins with the lower Wanakah Shale at the north end through the West River Shale to the south.

Wanakah Shale

The Wanakah Shale is a medium-gray to light-blue gray calcareous shale that weathers to a sticky clay. The Wanakah is exposed in the northeast section of the site in a tributary to Rush Creek and in the high banks on the south side of Rush Creek. The tributary is a popular area for fossil collecting, viewing the large calcareous concretions, and some pyritized burrows, rather than the steeper cliffs along Rush Creek. Brachiopods, bryozoans, trilobites, gastropods, pelecypods, echinoderms, corals, sponges, ostracodes, and some pyritized fossils may be found. Limited area in the tributary does not provide access for large groups.

Tichenor Limestone

The Tichenor Limestone overlies the Wanakah Shale and outcrops at the northern end of the site. Pyrite coating the surface of the Tichenor has weathered, exhibiting a reddish-rusty color that stands out from the surrounding overlying gray Windom Shale. At the northeast section of the site, an unexplained domal feature of the Tichenor, with several feet of relief, is present. This feature is not believed to be a result of the quarrying operation, but possibly from glacial rebound. A large exposure of the eroded limestone surface is adjacent to this feature and extends north to one of the on-site ponds. This area is often referred to as "crinoid heaven" due to the countless number of pelmatozoan columnals that are found lying on the surface. The Tichenor Limestone contains corals, brachiopods, pelecypods, trilobites, bryozoans, and echinoderms, all of which are difficult to remove from the hard limestone. The Tichenor Limestone is approximately 1.5 to 2 feet thick and underlies most of the site, dipping to the south-southwest along with the other units on site.

Windom Shale

The Windom Shale is a medium to dark gray, variably calcareous mudstone with several thin argillaceous limestones, concretionary beds, and pyretic horizons (Beuhler and Tesmer, 1963). In addition, at the southwest portion of the site there is an excellent exposure of phosphate nodules covering the surface. The Windom also weathers to a sticky clay. The Penn Dixie site has the most complete and best exposure of Windom Shale in New York State, approximately 42 feet thick. Brett and Baird (1982) described 14 subdivisions within the Windom that could be recognized at this location (Fig. 2). Fossil assemblage zones were described in Brett (1974) and Brett and Baird (1982). A disconformable basal contact with the Tichenor Limestone is exposed in the domal outcrop in the northeast section of the site. The upper Windom beds have been scoured, and shale clasts can be observed in the overlying North Evans Limestone. The Windom contains a variety of corals, brachiopods, pelmatozoan columnals, bryozoans, trilobites, gastropods, pelecypods, cephalopods, and more rarely fish remains, plant material, and blastoid and crinoid calices. The upper Windom has a variety of pyritized fossils, burrows, and most likely fecal remains weathering out on the surface. Some of the pyritized fossils include brachiopods, pelecypods, cephalopods, trilobites, and blastoids (Fig. 3). The weathering shale exposes thousands of specimens lying on the surface, waiting to be found after 380 million years.

Enrolled trilobites can be commonly found washed out of the shale after a good rainstorm, along with horn corals, brachiopods, and pelmatozoan columnals. Multiple complete trilobites on a slab have been collected from the Lower Windom and complete specimens of *Phacops rana*, like the specimen in Figure 4, keep collectors returning for their perfect specimen. Sections of the Windom are not as fossiliferous as others (Figure 5), but careful study of the stratigraphic subdivisions identified by Brett and Baird (1982) will yield some interesting discoveries. In addition, Penn Dixie staff and volunteer guides will direct visitors to the better collecting areas on the site.

North Evans Limestone

The North Evans Limestone is a buff-colored, weathered dark-gray crinoidal limestone that is 1.5 to 4 inches thick and contains angular clasts derived form the underlying Windom Shale. Erosional lag concentrations of hiatus concretions, pelmatozoan fragments, conodonts, fish plates, teeth, and mandibles, along with some brachiopod valves, are present (Brett and Baird, 1982). Carbonized plant remains are also found in this unit. Although a variety of fish remains have been found at the Penn Dixie Site (Fig. 4), they are difficult to find even with the good exposure of North Evans present. The buff-colored weathered surface of the North Evans and bone material make this unit easily recognizable.

Genundewa Limestone

The Genundewa Limestone is a nodular, medium dark-gray, poorly bedded limestone that weathers to a light gray, which has been referred to as the "Styliolina Limestone" directly overlying the North Evans Limestone (Buehler and Tesmer, 1963). Carbonized wood can be frequently found, but other examples of the fauna are more difficult to obtain.

West River Shale

The West River Shale is dark gray to black in color and overlies the Genundewa Limestone. Most of this unit is covered by overburden at Penn Dixie and Eighteen Mile Creek provides a better opportunity to view this unit. Conodonts, cephalopods, pelecypods, and fish remains have been reported from the West River Shale at other localities in Western New York (Buehler and Tesmer, 1963).

The preservation, diversity, abundance of fossils, and the extensive bedrock exposures at the Penn Dixie Site makes this an excellent outdoor classroom for students as well as amateur and professional paleontologists to be introduced to Western New York geology and paleontology. In addition, students and possible future scientists from pre-school through college are being introduced to the rich geologic history of Western New York by the thousands each year. Plates 1 through 4 illustrate some of the more common fossils that can be found at the Penn Dixie Site. Weathering of the Windom Shale results in many corals, brachiopods, pelmatozoan columnals, and trilobites being continually exposed on the surface. Those who extend the effort to dig into shale are rewarded with an extensive introduction to the variety of fossils preserved within the Windom. The northern section of the site provides an excellent outdoor classroom for students and visitors to be introduced to fossils and the local geology. Many specimens found at Penn Dixie can be viewed on the web site at www.penndixie.org.

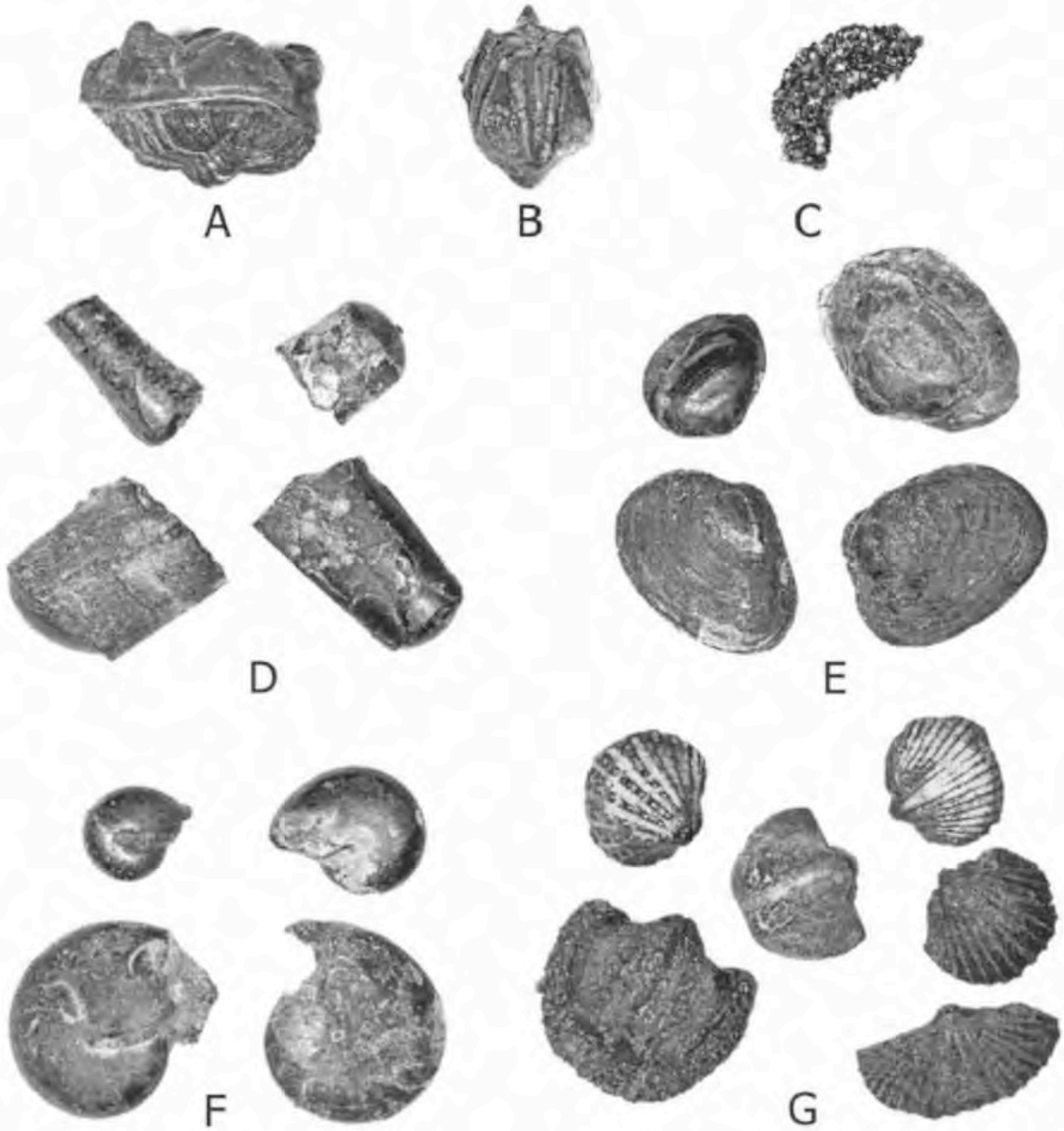

Figure 3. Pyritized fossils that weathered out of the Penn Dixie pyrite beds at the southern end of the site from the Upper Windom Shale. A-*Greenops* sp., enrolled, 0.7 cm wide; B- Blastoid calyx, 0.5 cm wide; C-pyrite, 1 cm long – burrows, nodules, or other shapes may weather out; D-Cephalopods, *Michlinoceras* sp. , largest 1 cm across; E-Pelecypods, largest 1 cm; F-Cephalopods, *Tornoceras* sp. , smallest is 0.4 cm across; G-Brachiopods, largest is 1 cm across; Blastoid was collected by Amanda Czechowski, pyrite specimens collected by Richard Spencer, and all other specimens collected by the author.

Plate 1
Fossils of the Penn Dixie Site

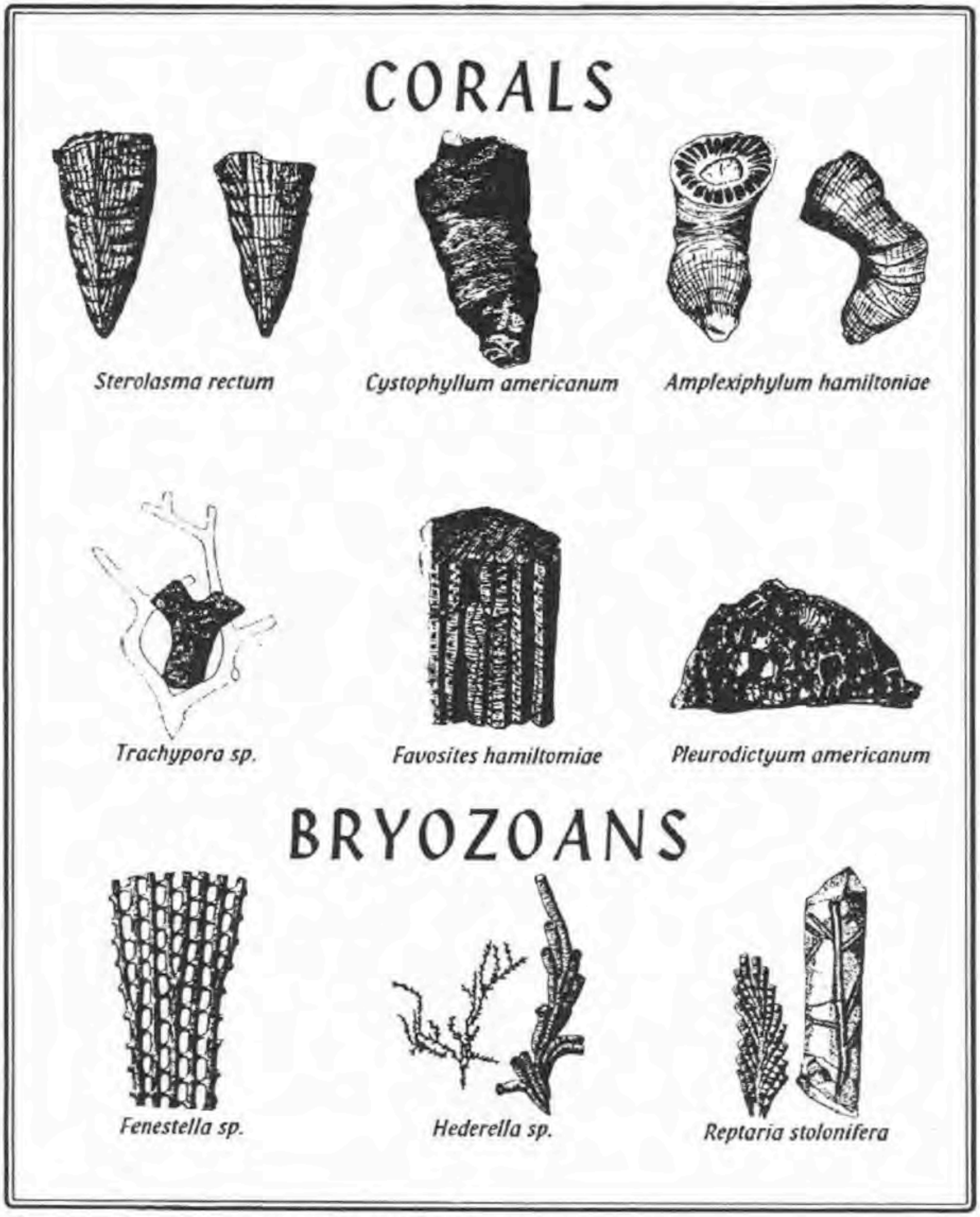

Drawings from "Geology and Palaeontology of Eighteen Mile Creek" by Amadeus Grabau
Plates compiled by Scott Clark

Plate 2
Fossils of the Penn Dixie Site

BRACHIOPODS

Orbiculiodea sp.

Rhipidomella sp.

Stropheodonta demissa

Mucrospirifer mucronatus

Spinocyrtia granulosa

Mediospirider auduculus

Athyris spiriferoides

Spinatrypa spinosa

Pseudoatrypa devonica

Drawings from "Geology and Palaeontology of Eighteen Mile Creek" by Amadeus Grabau
Plates compiled by Scott Clark

Plate 3
Fossils of the Penn Dixie Site

TRILOBITES

Greenops boothi

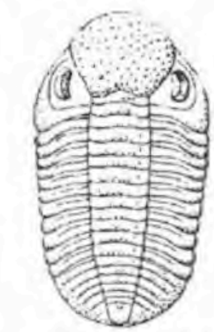

Phacops rana

CRINOIDS

Ancyrocrinus bulbosus

Various Crinoid segments

Drawings from "Geology and Palaeontology of Eighteen Mile Creek" by Amadeus Grabau
Plates compiled by Scott Clark

Plate 4
Fossils of the Penn Dixie Site

CEPHALOPODS

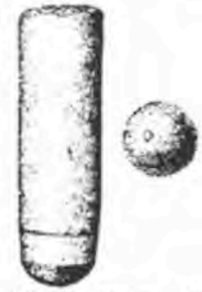

Michlenoceras sp.

Tornoceras uniangulare

Spyroceras sp.

GASTROPODS

Naticonema lineata

PELECYPODS

Pterinopecten sp.

Palaeoneilo sp.

Plethomytilus sp.

Drawings from "Geology and Palaeontology of Eighteen Mile Creek" by Amadeus Grabau
Plates compiled by Scott Clark

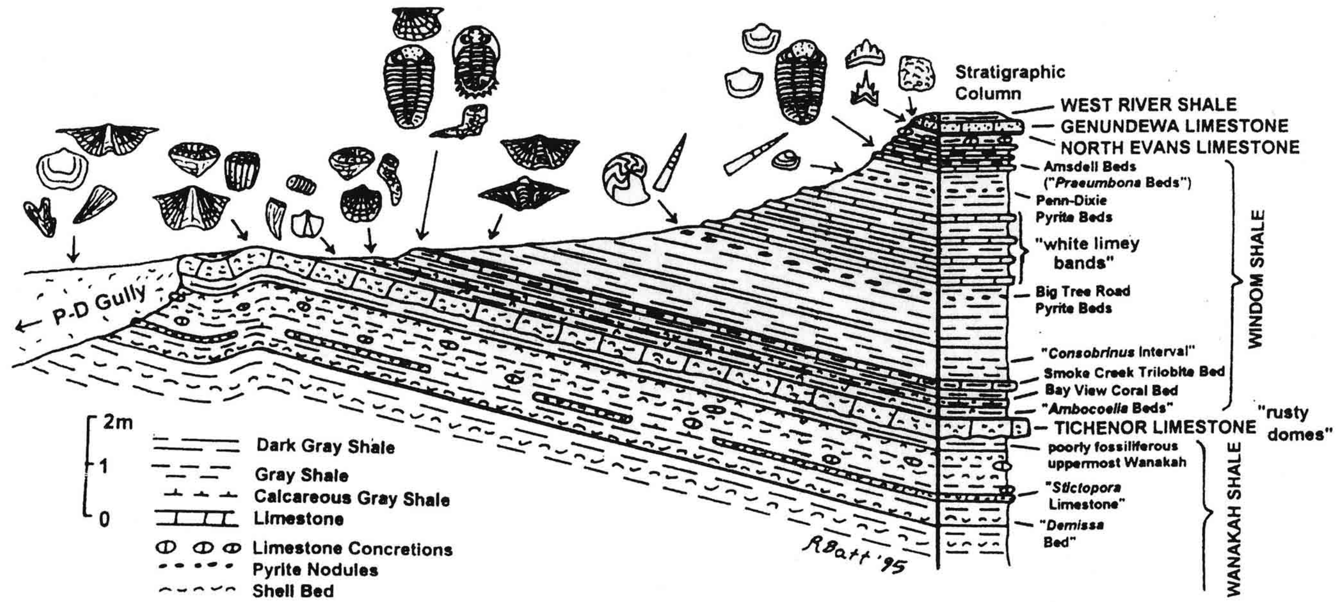

Cross section of Penn Dixie geology by Rick Batt. Regional dip is two degrees south (to the right).

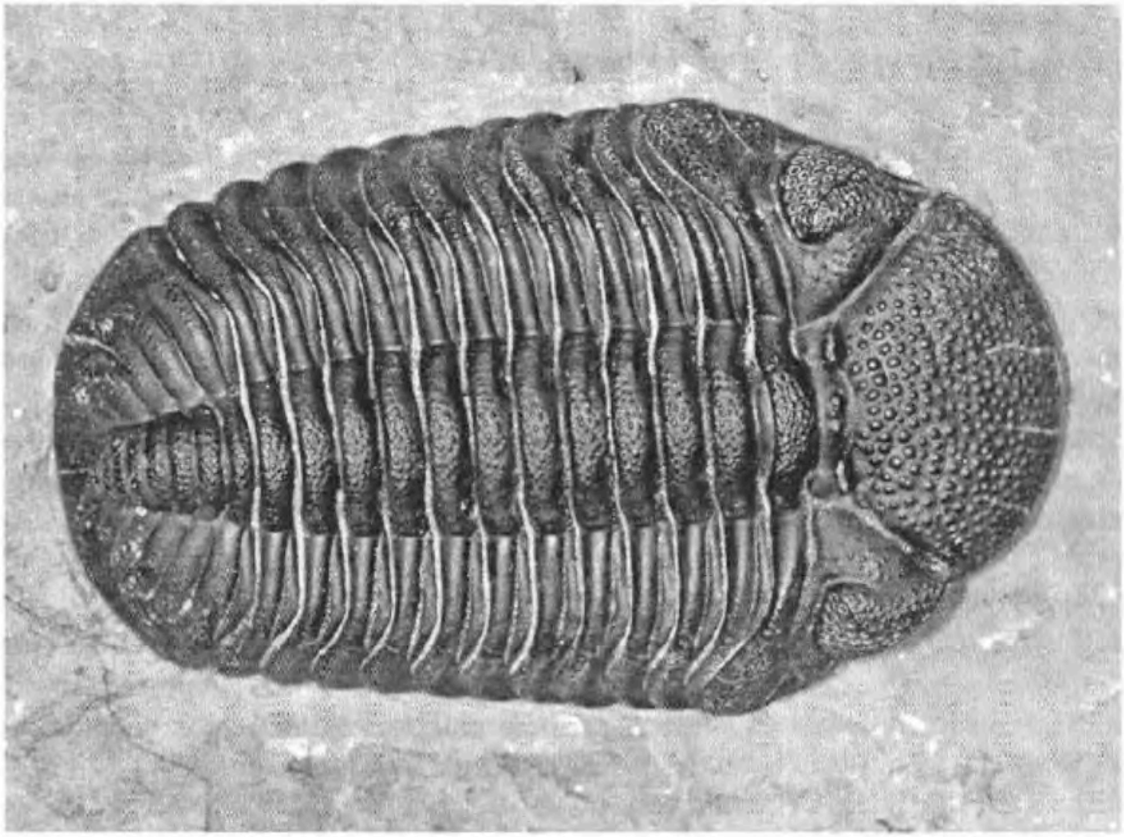

Figure 4. ***Phacops rana*** **collected by Jon Luellen and prepared by Gerry Kloc. Collected during the Dig with the Experts in May 2005 from the Lower Windom Shale at Penn Dixie. Trilobite is 2 inches long.**

W1A: UPDATING THE LATE WISCONSIN GEOLOGY OF THE GENESEE VALLEY, DANSVILLE TO AVON, NY: VALLEY HEADS MORAINE (HEINRICH EVENT H1?) TO FOWLERVILLE MORAINE COMPLEX (YOUNGER DRYAS, HEINRICH EVENT H0?)

(A brief summary to accompany an illustrated oral workshop presentation)

RICHARD A. YOUNG
Department of Geological Sciences (Emeritus), SUNY at Geneseo, Geneseo, NY 14454

LEWIS A. OWEN
Department of Geology, University of Cincinnati, Cincinnati, OH, 45221

INTRODUCTION

Geological Setting and Previous Investigations

Reevaluation of radiocarbon dates in light of the extended and revised calendar-year chronology for the last 50,000 years has provided important revisions to the Late and Middle Wisconsin glacial stratigraphy of the middle Genesee Valley in west-central New York. The previously unrecognized Middle Wisconsin ice advance at ca. 39,000 calendar years BP (Heinrich Event H4) has been described in detail, based on a sequence of 68 AMS ages by Young and Burr (2006), for exposures at the adjacent Elam and Dewitt sand and gravel excavations along the west bank of the Genesee River 4.5 miles north of Avon, NY (opposite the confluence with Honeoye Creek). The borrow pit exposures are largely overgrown at present, but the stratigraphy is extensively documented with 14 years of photography taken during nearly continuous excavations (Young, 1990 to 2004). Another nearby location with wood of Middle Wisconsin age is located 11 miles southwest of the Elam-DeWitt locality. Well preserved wood was encountered at a depth of 85 feet during water-well drilling by B. Moravic, Inc. on a moraine segment near the Late Wisconsin peccary site described below (see Fowlerville moraine). The age of the well preserved wood from that well is 43,300±1800 ^{14}C years BP or a corrected calendar age of 46,667 YBP (Young and Burr, 2004). This suggests that the Middle Wisconsin advance reached at least as far south as the younger Fowlerville moraine described below. Given the nature of the local buried valley topography, it is likely that a finger of ice (narrow lobe) extended southward from the main ice mass along the buried bedrock valley, a feature that approaches the larger Finger Lake bedrock troughs in scale [See also Karig and Miller (2013) for similar chronology of events in Cayuga Lake trough].

Mike Wilson (1981) completed 1:24,000-scale glacial mapping of portions of the area under the direction of Dr. Ernest Muller in the mid-1970s, before extensive excavations of clay to construct the Monroe County Mill Seat (Riga) landfill at the Elam-DeWitt site exposed the deeper Middle Wisconsin sequence. The basic geology of the Genesee Valley as updated during that general era is described in the Friends of the Pleistocene 51st Annual Meeting guidebook for 1988 (Brennan, 1988), as well as in the contemporaneous article by Muller et al. (1988). The present workshop presentation focuses on the revision of the timing for the Late Wisconsin history from the formation of the Valley Heads moraine (Fig. 1) to a previously undated ice advance corresponding to the time of the Younger Dryas cold interval (ca. 13,000 to 12,000 calendar years BP). All radiocarbon ages mentioned subsequently in this brief summary are calendar corrected ages (1Σ mean; labeled YBP) as determined using the Calib 7.1 program (http://calib.org/calib/) of Stuiver et al., unless otherwise labeled as ^{14}C years BP. Ages done after 1990 are ^{14}C AMS by the Univ. of Arizona lab (AA), by Beta Analytic (#), or Lawrence Livermore Lab (CAMS).

REVISION OF GLACIAL CHRONOLOGY

Calendar Year Corrections of ^{14}C Ages

Much of the revision of the Genesee Valley history is based on the fact that ages in the ca. ^{14}C 11,000 ± years BP range (uncorrected) are now known to be approximately 2000 years older in actual calendar years. During the 1970s and 1980s the ^{14}C calendar correction programs were in their infancy, were usually calculated by the relevant laboratory prior to the advent of the Internet, and generally did not include calendar corrections for results much beyond ca. 6000 ^{14}C years. From the late 1960s through the early 1980s R.A. Young and students at SUNY Geneseo obtained several ^{14}C ages from miscellaneous wood samples that were in the ca. 11,000 ^{14}C BP range. These were generally obtained from samples at the glacial-postglacial transition horizon, mostly from subsurface borings for highways, bridges, or from USGS studies during those decades (see Table 8 in Mansue et al., 1991, p. II-30 to II-31). At that time, the age of glacial Lake Iroquois was generally believed to be in the 11,500 to 12,600 ^{14}C years BP range (Calkin, 1970), and most of the uncorrected published ^{14}C ages for that lake were greater than 12,000 ^{14}C. Accordingly, this implied that the conventional (pre-AMS) ca. 11,000 ^{14}C year BP ages obtained by R.A. Young were too recent to represent true late "glacial" events and were simply recording random postglacial events associated with a variable and unknown time lag following the last ice recession in the Genesee Valley until organic growth accumulated in various depositional environments (such as bogs, or the base of the Genesee River floodplain sediments). Ages younger than the inferred, but uncorrected, ^{14}C age of the Lake Iroquois shoreline were assumed to be unrealistic as true measurements documenting previously unrecognized late glacial advances south of Lake Ontario. However, the majority of those ages in the ca. 11,000 ^{14}C year BP range are now known to be closer to 13,000 "calendar corrected" years old, and correspond approximately to the Younger Dryas cold episode as determined from GISP2 ice core studies and numerous other dated localities throughout the northern hemisphere (Carlson, 2013). [See end note on laboratory dates following references list.]

Valley Heads Moraine: An advance coincident(?) with Heinrich Event H1

The morphology of the Valley Heads moraine varies considerably across its southern Finger Lakes extent (illustrated by additional images in the accompanying oral workshop). Near Dansville, the moraine is very lobate (Fig. 2) and contains large masses of reworked, deformed lacustrine varves that attest to the readvancing ice reincorporating older proglacial sediments following a recession of unknown magnitude. The headwaters of Canaseraga Creek exhibit an interesting stream capture of the originally south-flowing drainage that has resulted from headward erosion through the moraine at Poag's Hole (Fig. 2).

The age of the glacial readvance to the position of the Valley Heads moraine from the literature is estimated to be approximately 16,600 YBP (Ellis et al., 2004), but we are unaware of any absolute age that is based directly on wood or organics located within the moraine itself. A new limiting age for the moraine that is consistent with that estimated age has been obtained from an apparent buried kettle pond near Geneseo (19 miles north of Dansville) that was subsequently covered by a migrating sand dune (Figs. 3,4). A pre-dune AMS age of 16,545 YBP was obtained from organic debris at the dune-pond sediment contact near a depth of 5 feet (Fig. 3). This age, if accurate, implies that the dune sand may have formed as a result of strong katabatic winds off a nearby ice sheet (a second ^{14}C age on wood as well as an optically stimulated luminescence (OSL) age on the dunes by Lewis Owen are in progress). There was no evidence observed during a large excavation into the dune (Fig. 4) that it had advanced across a surface where small trees or tundra vegetation had become well established. This further supports the suggestion that the dune records unimpeded aeolian deposition immediately following ice recession, across a relatively open landscape close to the ice front. The current age at the Geneseo site strengthens the evidence that the glacial readvance to the Valley Heads position coincides with Heinrich Event H1 in the Atlantic Ocean deep sea sediment records. Heinrich Event H1 is estimated to have occurred at 16,800 YBP (Bond and Loti, 1995).

Fowlerville Moraine Complex: An advance corresponding(?) with the Younger Dryas (YD) cold episode and Heinrich Event H0

Site 1

The broad Fowlerville moraine complex (Figs. 1,5) consists of a series of subparallel till ridges (gray lines, Fig. 5) spread over a north-south distance stretching approximately 4 miles south of Fowlerville, NY. The Genesee River has a notably narrow channel and lacks a wide floodplain where it has eroded through this broad moraine. One of the three small moraine crests on the west side of the valley near Linwood, NY, was the site of the excavation of a complete peccary skeleton (Figs.1,5) on the Lawrence Hill property in 1978 (borrow excavation, east side of Federal Road, 2000 feet south of junction with Fowlerville Rd.; lat. 44.8879, long. 77.9200). The glacial stratigraphy exposed at the peccary excavation demonstrated that the immature animal foundered in quicksand (south-dipping, stratified and ripple laminated outwash sand) at the margin of an active ice sheet, then was buried under a thin till sheet by the continued advance of the nearby ice (Young et al., 1978). Figures 6 through 10 provide some of the evidence explained in more detail in the accompanying workshop presentation. Two dates on the peccary (bone and collagen extract) are 13,002 YBP and 13,045 YBP.

Site 2

During a Genesee River study, funded by the US Army Corps of Engineers (Young, 2003), several partial logs and associated organic debris were uncovered in a thin till sandwiched between two sets of glacial varves on the east bank of the Genesee River near Avon, NY (Figs. 1,5,11,12). The thirteen ^{14}C ages obtained from this section are shown on the accompanying diagram (Fig. 11). Despite the well exposed “apparent” glacial stratigraphy, the site was tentatively and hesitantly described by Young (2012) as representing logs buried by a local landslide in order to account for the relatively young age and diamict-like texture. A large landslide did occur in 1972 on the same side of the river 2 miles further south at Oxbow Lane (See photo, Young and Rhodes, 1973, p. E-5). Young’s (2012) tentative landslide interpretation was based exclusively on the relatively young ^{14}C ages, as related to the purported older age of the glacial Lake Iroquois shoreline. However, the wood-bearing diamict is in normal conformable contact with the varved lacustrine sediments above and below the till, a relationship not indicative of a heterogeneous, gravity-driven deposit (Figs. 11-14). As a result of subsequent reviews and calendar corrections of the accumulating radiocarbon chronology for glacial events ca. 13,000 YBP, as well as unpublished data from other sites in western NY, the landslide assumption has been abandoned in favor of the obvious glacial nature of the preserved stratigraphic section, in addition to the orderly and thousand-year-long chronologic span of ^{14}C ages (Fig. 11). In support of the glacial transport interpretation, the logs buried in the till have no attached branches, are stripped entirely of bark, and are aligned in parallel, north-south orientations

(Fig. 13). Had this been a landslide along the Genesee River, any such catastrophically buried trees would have preserved evidence of branches and bark from a rapid, gravity-related burial, whereas subglacial transport of small trees would likely trim both bark and branches from the trunks. The slight age reversals in units 2 and 3 (Fig. 11) indicate scouring by advancing ice from progressively deeper organic horizons of older (re-incorporated) bog deposits.

Additional glacial recession dates

There are additional Younger-Dryas-linked ^{14}C ages from two drill hole samples shown on Figure 1 and located: 1) Below the Canaseraga Creek floodplain 6.5 miles south of Geneseo (Keshequa Ck at railroad; Interstate I-390 test boring), and 2) Five miles northwest of Avon (Dugan Creek channel, Muller et al., 1988). The Keshequa Creek sample was a 1-inch diameter piece of wood (with branch stubs) from a depth of approximately 32 feet at the contact of Keshequa Creek (Genesee Valley) sediments with the underlying glaciolacustrine sediments of the youngest recessional proglacial lake in the valley.

The Dugan Creek channel sample is from woody debris at the basal peat-till contact (depth 8.8 ft) that was hand cored by R. A. Young and students near Baker (old RR stop at Lacy Rd.) in the late Wisconsin outwash channel that discharged southwestward into the Genesee Valley (Young, in Muller et al, 1988, p. 63; Young, 1988). The wood age of the basal floodplain sample recovered at Keshequa Creek has a calendar corrected age of 13,012 ± 160 YBP. The Dugan Creek sample is slightly younger with an age of 12,917 ± 160 YBP, consistent with its more northerly location.

Both of these samples appear to record the rapid or contemporaneous revegetation of the valley following recession of the most recent (Younger Dryas) glacial event. The conclusion that revegetation occurred essentially coincident with the brief ice advance and withdrawal is based on observations of modern glaciers, plus the fact that the *juvenile** peccary's burial by quicksand on the crest of the moraine implies that the animals were living and breeding close to the active ice front, which implies an adequate source of appropriate vegetation. **Peccary's molars and tusks were still erupting (Fig. 8).*

In addition to the corrected calendar ages of these numerous Genesee Valley deposits, with ages largely in the 12,900 to 13,500 YBP range, the Greenland ice core project (GISP2) and other detailed studies have now provided a detailed and well dated climatic history back through this critical interval of unusual climatic diversity (Anderson, 2006; Brauer et al., 2014; Lemieux-Dudon, B. et al., 2010; Svensson et al., 2008). The approximate ages of the key events are on Figure 15. Based on this chronology, the two sites on and near the Fowlerville moraine, as well as the glacial-postglacial contact samples, appear to coincide closely with the timing of the Younger Dryas cold interval, which is also recorded in the oceanic sediments as Heinrich layer H0. Dates on wood in glacial till naturally must be older than the associated glacial advance, thus accounting for dates that slightly overlap the ca. 14,000+ YBP range.

CONCLUSIONS

There is now ample evidence of a late glacial advance along the Genesee Valley to a position approximately 3.5 miles north of Geneseo, NY, culminating in a ca. 13,000 YBP moraine. Additional sites with similar wood-in-till ages are the subject of ongoing field studies for which the supporting data cannot be released at the present time, pending approval and release of a final report. The close correspondence of the Genesee Valley ages reported here with the well documented age of the Younger Dryas cold interval (approximate 1000-year length) seems to establish that this northern hemisphere event was accompanied by a late glacial advance well south of the modern Lake Ontario shoreline at a time that coincides closely with the proposed age for the initiation of glacial Lake Iroquois in the Ontario basin (Anderson and Lewis, 2012). This implies that either the proposed age of Lake Iroquois is slightly too old, and/or that the recession of the ice front from the Genesee Valley was a very rapid event. Mickelson et al. (2007) describe significant new evidence of new sites with similar Younger Dryas-age, post Two Creeks, chronology in Wisconsin. These upper Midwest localities are described as documenting rapid ice advances involving proposed wet-bed conditions, a scenario that may fit the Genesee Valley history.

The Pinnacle Hills kame moraine, located along the southern edge of Rochester, NY, was capped by a till sheet that postdated the stratified kame deposits below in many places. The photographs taken by Fairchild (1923, 1928) of the numerous exposures in working sand and gravel pits indicate that the till was at least 20 feet thick in places (estimated from wagons and human figures included in the photographs). It is possible that the Pinnacle Hills moraine was overridden by the Younger Dryas ice advance without destroying the basic relief and morphology of the kame moraine. Such ice readvances over preexisting morainal topography without destroying the older morphology have been reported elsewhere in PA and OH (Fleeger, 2005; Thomas et al., 1987). If such were the case for the Pinnacle Hills moraine it would be compatible with a rapid withdrawal of the ice from Fowlerville to the Ontario basin. This would avoid the necessity for having the retreating glacier stall near Rochester, build the impressive Pinnacle Hills kame moraine, and then readvance some distance over the kame moraine sediments, before rapidly retreating again in time to allow glacial Lake Iroquois to form within the narrow time frame. Alternatively, the estimated age of glacial Lake Iroquois may need to be reconsidered.

Overall there is increasing evidence that some North Atlantic Heinrich glacial surges (Hemming, 2004) are approximately contemporaneous or nearly synchronous with glacial advances that are represented by prominent terrestrial moraines (Moores and Lehr, 1997). This is especially true for the Middle to Late Wisconsin glacial history of the Genesee Valley. Additional information on the general revision of the Late Wisconsin time-stratigraphic classification scheme are reviewed in Karrow et al., (2000).

FIGURES

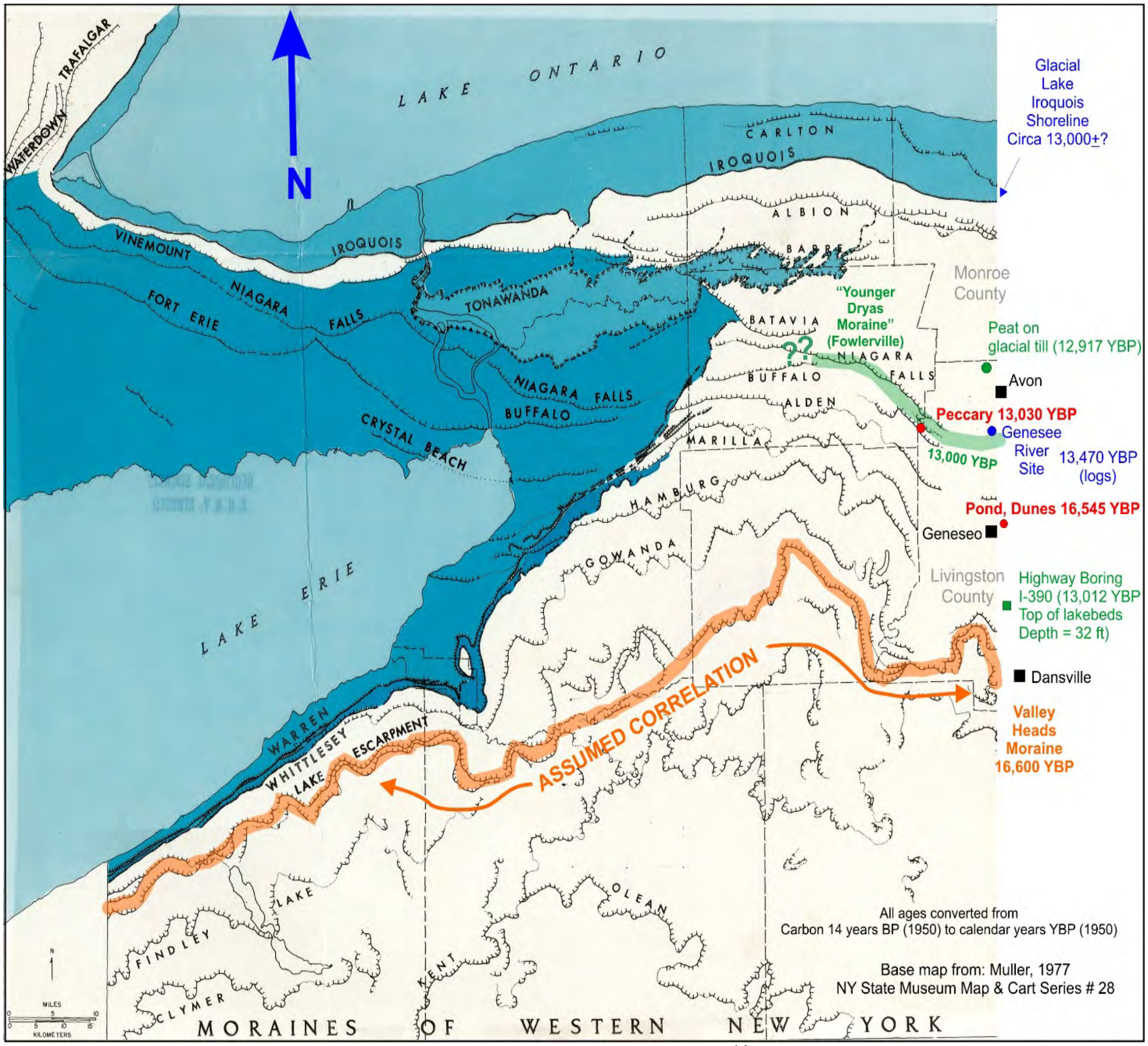

Figure 1. Generalized diagram of major moraines and some of the ^{14}C ages discussed in this presentation. The assumed correlation of the Valley Heads moraine with the Lake Escarpment moraine is from literature sources, such as Calkin (1970) and Muller and Calkin (1993). The age and westward correlation of the ca. 13,000 YBP Fowlerville moraine containing the complete buried peccary skeleton is uncertain, because the original Muller Niagara sheet map did not appear to recognize the Fowlerville moraine complex, presumably due to its broad and subdued topography (compare with Figure 5). Note: Moraine base map with color additions by authors is taken from descriptive legend portion of the original edition of the Niagara sheet of the Quaternary Geology of New York (Muller, 1977), which was subsequently revised to conform to USGS standards for colors and descriptive sedimentary unit labels. Squares are towns, circles are ^{14}C sample sites.

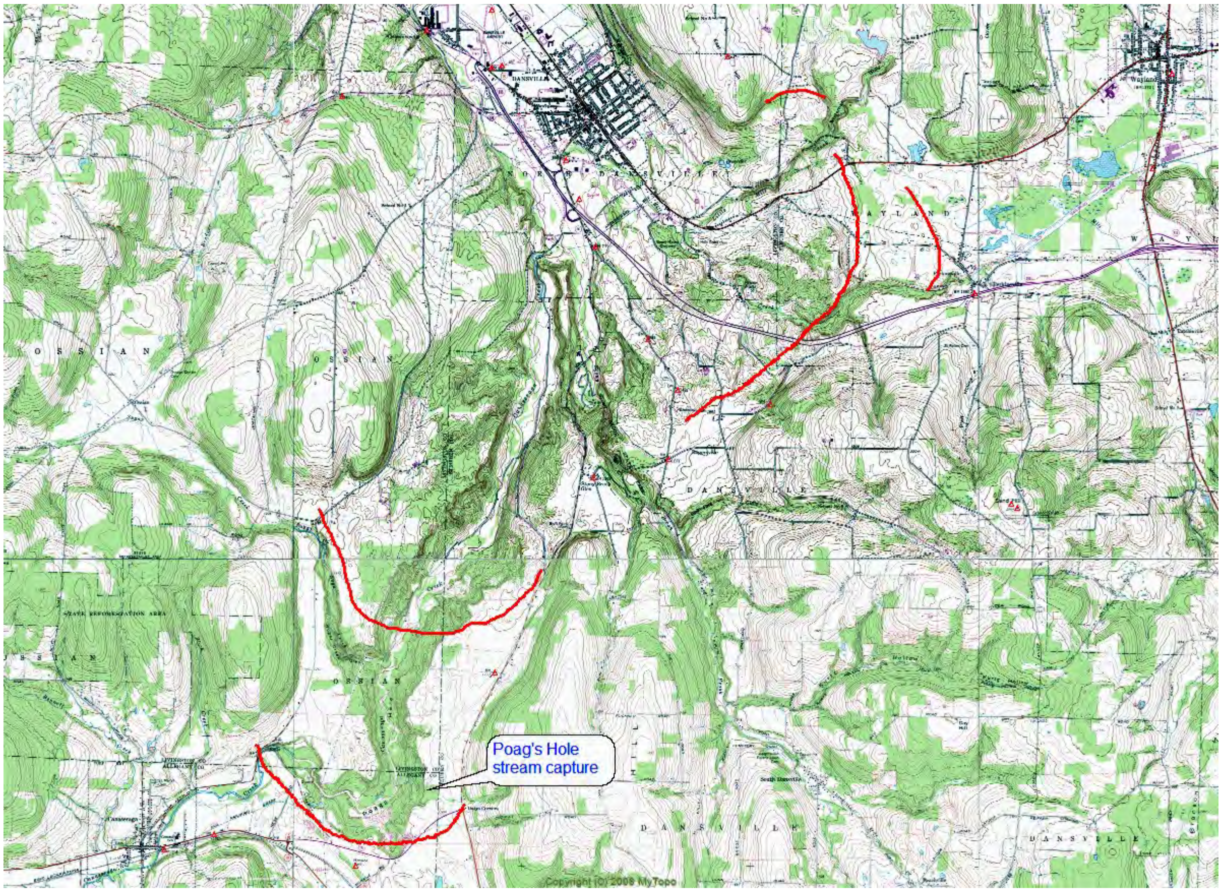

Figure 2. Numerous morainal crests (red curves) near Dansville-Wayland section of Valley Heads moraine. Dansville, NY 1:24,000 scale (7.5 minute) topographic map.

Figure 3. Left is Geneseo dune/pond contact; right is debris in dark organic layers (1 mm grid).

Figure 4. Five foot deep trench exposing dune covering Geneseo kettle pond site.

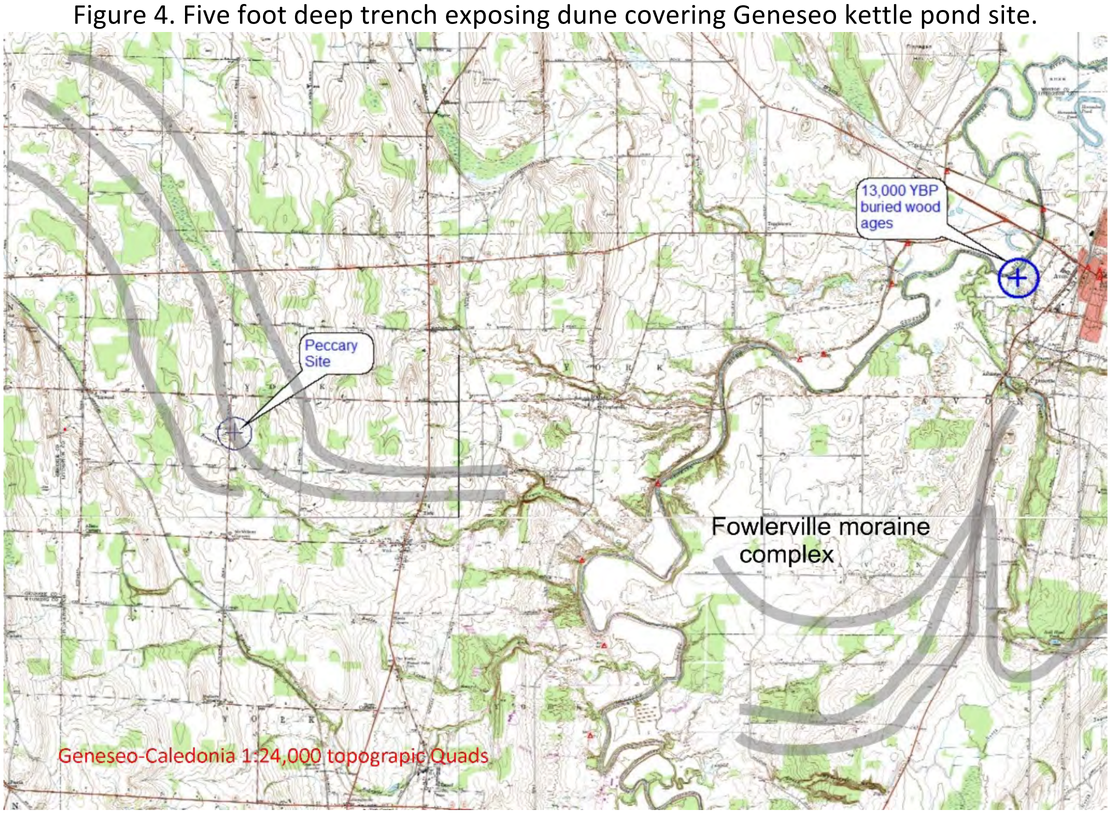

Figure 5. Fowlerville moraine complex with two dated sites; Avon at upper right edge.

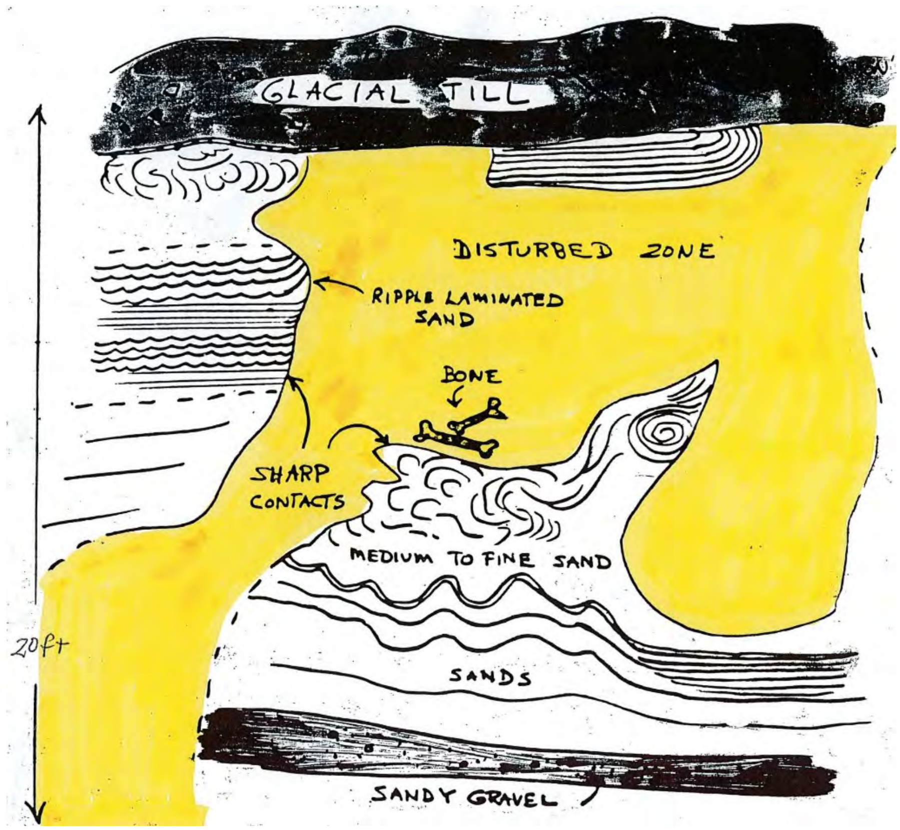

Figure 6. Original field sketch of peccary skeleton quicksand burial site near Linwood, NY.

Figure 7. Contact between completely liquefied sand above (at trowel) and less fluidized but disrupted sand layers at base of peccary burial (bones), as sketched near center of Figure 6.

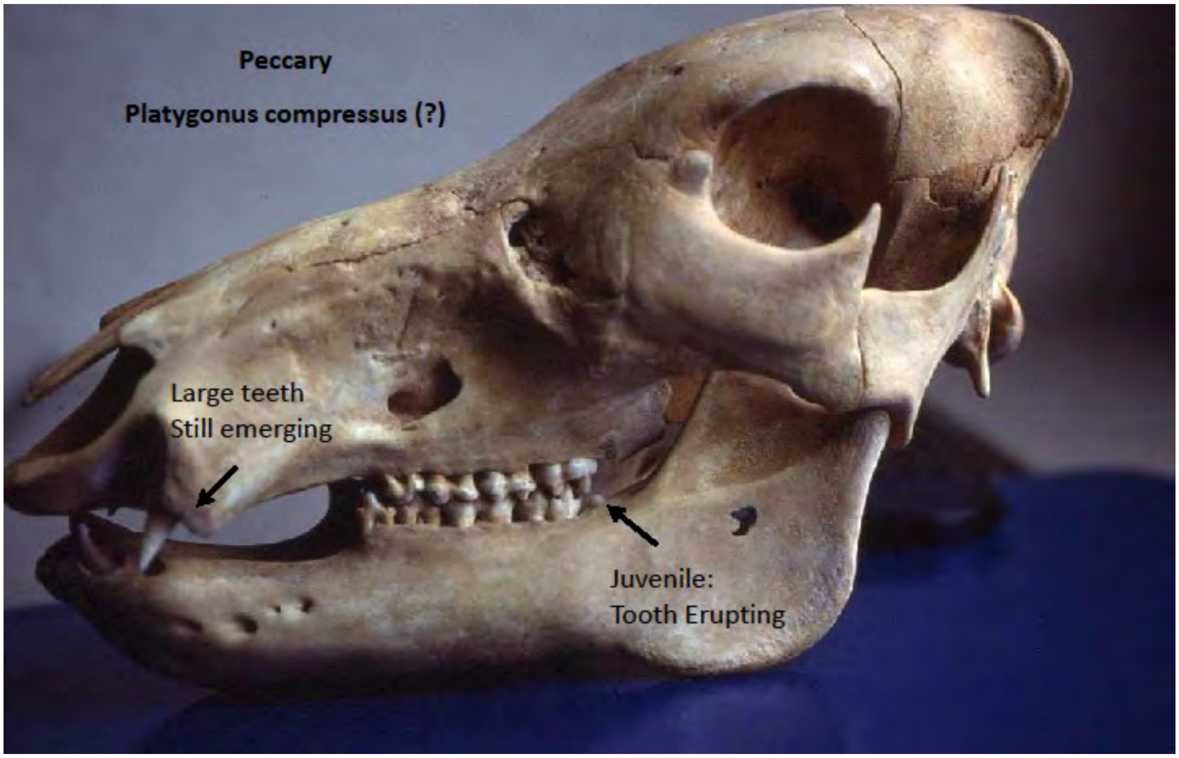

Figure 8. Juvenile peccary skull showing excellent preservation and tooth-tusk eruption stages.

Figure 9. Upwelling of glacial meltwater at glacier margin, illustrative of potential quicksand mechanism. Photo by Gordon King, Lost Coast, Alaska.

Figure 10. Similar quicksand structures at ice marginal outwash site 5 miles SW of Albion, NY.

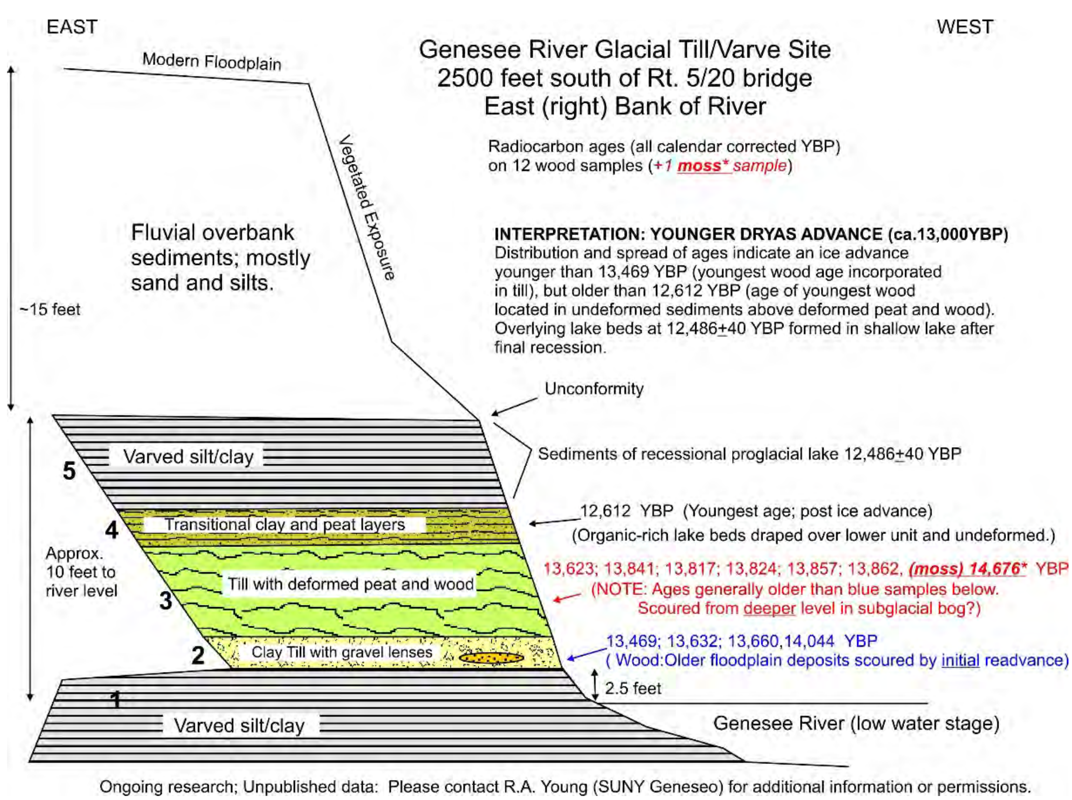

Figure 11. Radiocarbon age profile for stratigraphic section at Genesee River site near Avon, NY.

Figure 12. Unexcavated glacial till and varve site of Fig. 11, east bank, Genesee River, Avon, NY.

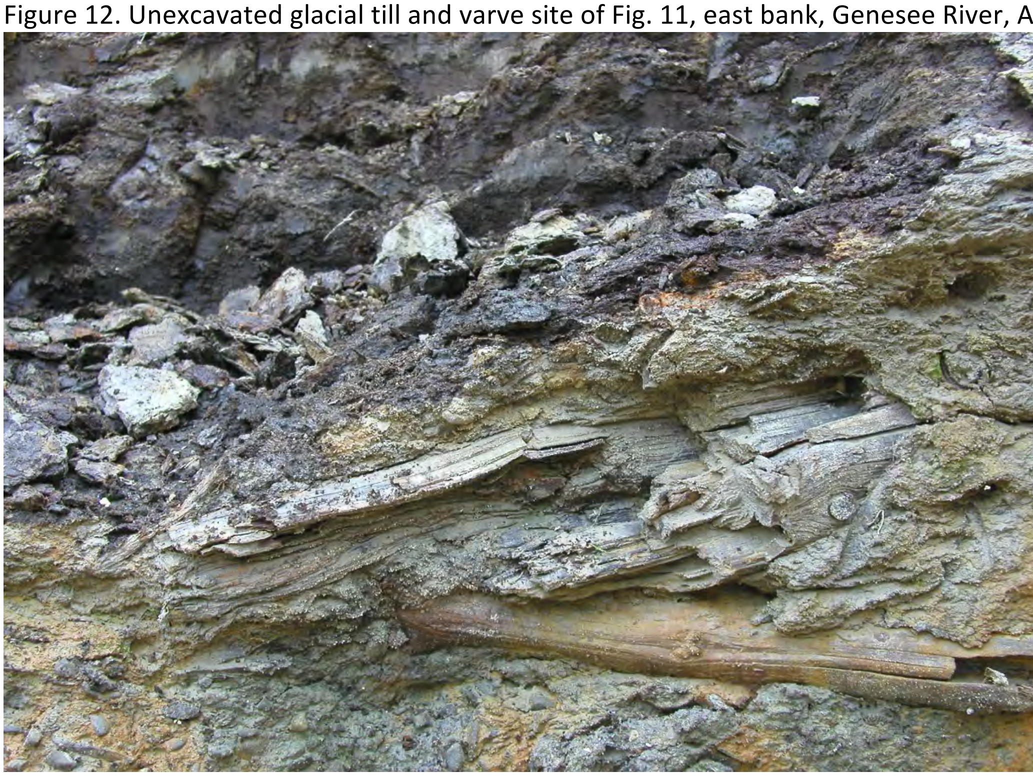

Figure 13. Logs (6” dia.) stripped of bark and limbs in glacial till, Genesee River bank, Avon, NY.

Figure 14. Close-up of unit 3 (gray till) and 4 (clay & peat) as on Figure 11 (Scale under #7 is 2").

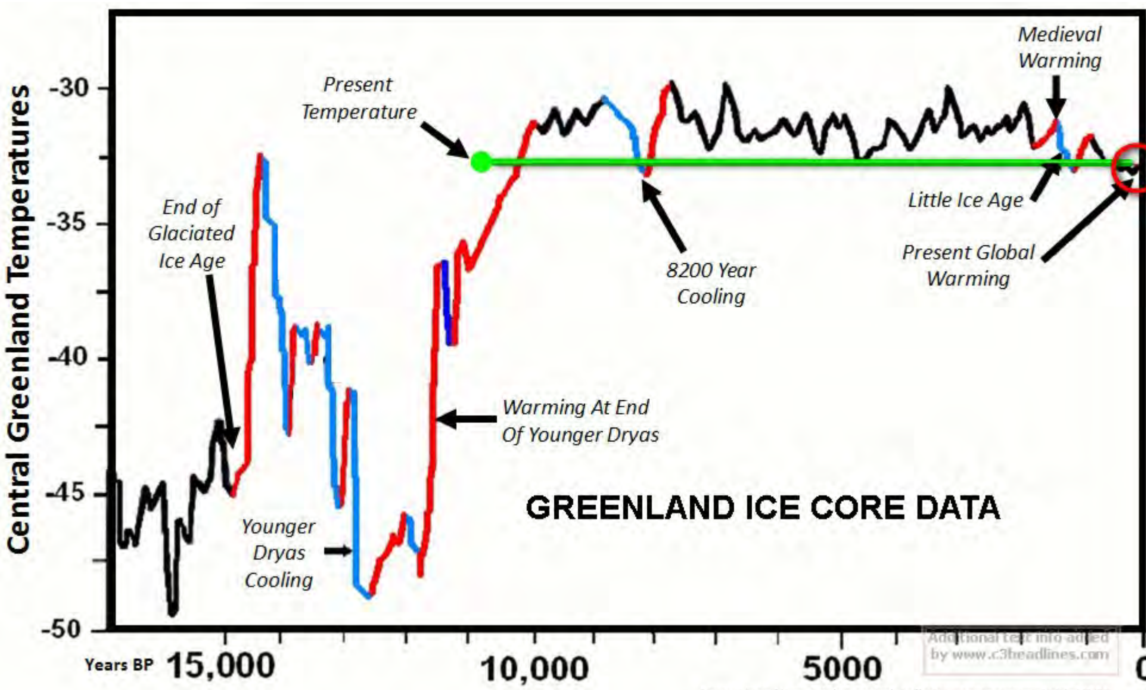

Figure 15. Diagram from Esterbrook (online posting), showing the major temperature oscillations during the past 15,000 years (YBP) as determined from the GISP2 and other studies. Source: https://wattsupwiththat.com/2012/06/19/the-intriguing-problem-of-the-younger-dryas.

REFERENCES CITED

Andersen, K.K., 2006, The Greenland Ice Core Chronology 2005, 15-42 ka. Part I: Constructing the time scale: Quaternary Science Reviews, v. 25, p. 3246-3257.

Anderson, T.W. and Lewis, C.F.M., 2012, A new water-level history for Lake Ontario basin: Evidence for a climate-driven early Holocene lowstand: Journal of Paleolimnology, v. 47, no. 3, p. 513-530.

Bond, G. and Loti, R., 1995, Iceberg discharges into the North Atlantic on millennial time scales during the last glaciation: Science, v. 267, p. 1005-1010.

Brauer, A., et al., 2014, The importance of independent chronology in integrating records of past climatic change of the 60-8 ka INTIMATE time interval: Quaternary Science Reviews, v. 106, p. 47-66.

Brennan, W.J. (Ed.), 1988, Late Wisconsin Deglaciation of the Genesee Valley: in Guidebook for the 51st Annual Meeting of the Friends of the Pleistocene, SUNY Geneseo, p. 1-87.

Calkin, P.E., 1970, Strand lines and chronology of the glacial Great Lakes in northwestern New York: Ohio Journal of Science, v. 70(2), p.78-96.

Carlson, A.E. 2013, The Younger Dryas Climate Event: Encyclopedia of Quaternary Science, v. 3, pp.126-134, Elsevier, Amsterdam.

Ellis, K. G., H. T. Mullins, and W. P. Patterson, 2004, Deglacial to middle Holocene (16,600 to 6000 calendar years BP) climate change in the northeastern United States inferred from multi-proxy stable isotope data, Seneca Lake, New York: Journal of Paleolimnology, v. 31, p. 343–361.

Fairchild, H.L., 1923, The Pinnacle Hills or The Rochester Kame Moraine: Proc. of the Rochester Academy of Science, v. 6, p. 141-194, Plates 24-77.

Fairchild, H.L, 1928, Geologic story of the Genesee Valley and western NY: pp. 1-215, published by the author, distributed by Scrantom's Inc.

Fleeger, G. M., 2005, Summary of the Glacial Geology of Northwestern Pennsylvania, in: Type Sections and Stereotype Sections in Beaver, Lawrence, Mercer, and Crawford Counties: Glacial and Bedrock Geology: 70th Field Conference of Pennsylvania Geologists (Host: Pennsylvania Geological Survey), Sharon, PA, p. 1-11.

GISP2, Greenland Ice Sheet Project, The Greenland Ice Sheet Project (GISP) was a decade-long project to drill ice cores in Greenland that involved scientists and funding agencies from Denmark, Switzerland and the United States. Besides the U.S. National Science Foundation (NSF), funding was provided by the Swiss National Science Foundation and the Danish Commission for Scientific Research in Greenland. The ice cores provide a proxy archive of temperature and atmospheric constituents that help to understand past climate variations. Website, http://www.gisp2.sr.unh.edu/

Hemming, Sidney R.,2004, Heinrich events: Massive late Pleistocene detritus layers of the North Atlantic and their global climate imprint: Reviews of Geophysics, v. 42 (1).

Karig, D.E. and Miller, G.M., 2013, Middle Wisconsin glacial advance into the Appalachian Plateau, Sixmile Creek, Tompkins Co., NY: Quaternary Research, v. 80, p. 522-533.

Karrow, P.F., Dreimanis, A., and Barnett, P.J., 2000, A proposed diachronic revision of Late Quaternary time-stratigraphic classification in the eastern and northern Great Lakes area: Quaternary Research, v. 54, p.1-12.

Lemieux-Dudon, B., et al., 2010, Consistent dating for Antarctic and Greenland ice cores: Quaternary Science Reviews, v. 29, p. 8-20.

Mansue, L. J, Young, R.A., and Soren, J., 1991, Hydrologic influences on sediment-transport patterns in the Genesee River Basin, NY: In: Genesee River Watershed Study, Volume IV, Special Studies, U.S. Geological Survey, U.S. Environmental Protection Agency Publication EPA-905/9-91-005D, GL-07D-91, v. IV, p. II-1 to II-33.

Mickelson, D.M., Hooyer, T.S., Socha, B.J., and Winguth, Cornelia, 2007, Late-glacial ice advances and vegetation changes in east-central Wisconsin: In Hooyer, T.S. (Ed.), Late-glacial history of east-central Wisconsin: Guide book for the 53rd Midwest Friends of the Pleistocene Field Conference, May 18-20, 2007, Oshkosh, Wisconsin. 2007-01 Open-file report, p 73-87.

Mooers, H.D., and Lehr, J.D., 1997, Terrestrial record of Laurentide Ice Sheet reorganization during Heinrich events: Geology, v. 25(11), p.987-990.

Muller, E. H., and P. E. Calkin, 1993, Timing of Pleistocene glacial events in New York State: Canadian Journal of Earth Sciences, v. 30, p. 1829–1845.

Muller, E., Braun, D., Young, R.A., and Wilson, M., 1988, Morphogenesis of the Genesee Valley: Northeastern Geology, v. 10(2), p.112-133.

Svensson, A., Andersen, K.K., Bigler, M., Clausen, H.B., Dahl-Jensen, D., Davies, S.M., Johnsen, S.J., Muscheler, R., Parrenin, F., Rasmussen, S.O., Rothlisberger, R., Seierstad, I., Steffensen, J.P., and Vinther, B.M., 2008, A 60,000 year Greenland stratigraphic ice core chronology: Climate of the Past, v. 4, p.47-57.

Thomas, D.J., Delano, H.L., Buyce, M.R., and Carter, C.H., 1987, Pleistocene and Holocene geology on a dynamic coast, Glacial Geology of Northwestern Pennsylvania: In: 52nd Annual Field Conference of Pennsylvania Geologists, Pennsylvania Geological Survey, Department of Environmental Resources, Bureau of Topographic and Geologic Survey, Harrisburg, PA, p. 1-39.

Wilson, M.P., 1981, Catastrophic Discharge of Glacial Lake Warren in the Batavia - Genesee Region. PhD Dissertation, Syracuse University.

Young, R.A., 1988, Late Wisconsin Deglaciation of the Genesee Valley: Guidebook for 51st Annual meeting of the Friends of the Pleistocene, May 27-29, p. 63, Figs. 3 and 4.

___________, 2003, Recent and long-term sedimentation and erosion along the Genesee River floodplain in Livingston and Monroe Counties, NY: U.S. Army Corps of Engineers, U.S. Army Engineering District, Buffalo (Final report for SUNY Research Foundation Award No. 25106), Buffalo, NY, 140 pages, CD Rom images.

___________, 2012, Genesee Valley Glacial and Postglacial Geology from 50,000 Years Ago to the Present: A Selective Annotated Review: Rochester Academy of Science (online at http://www.rasny.org/), p. 1-24 (*Note: landslide section to be revised*).

Young, R.A. and Burr, G.S., 2006, Middle Wisconsin glaciations in the Genesee Valley, NY: A stratigraphic record contemporaneous with Heinrich Event, H4: Geomorphology, v. 75, p. 226- 247.

Young, R.A. and Rhodes, W.D., 1973, late glacial and postglacial geology of the Genesee Valley in Livingston Co., NY, A preliminary report: in NY State Geological Association 45th Annual Meeting Field Trip Guidebook, New York State Geological Association, SUNY Brockport, p. E-1 to E-21

Young, R.A., Scatterday, J.W., and Hill, L. 1978, Significance of the remains of a Pleistocene Peccary (Platygonus compressus Le Conte) beneath glacial till in Livingston County, NY. Rochester Academy

of Science, Pre-Meeting Abstracts, Fifth Annual Sessions for Scientific Papers, SUNY, Geneseo, NY, p. 46.

NOTE: Previously unpublished ^{14}C lab results are the subject of a longer article in preparation for a peer-reviewed journal, so only calendar corrected ages are presented for unpublished ages in this brief workshop summary.

Preliminary results for two OSL samples from the dunes in Figure 4 are included in Table 1. These two ages overlap in the 14.2 to 13.4 ka range using their respective "average and standard" errors, or from 13.1 to 12.9 ka using their "weighted average" errors. These results suggest that the dunes were formed by possible katabatic wind activity associated with the Younger Dryas event, thus accounting for the underlying organics to have accumulated in the interval following withdrawal of the ice from the Valley Heads position.

Table 1: Summary of OSL dating results from extracted from sediment, sample locations, radioisotope concentrations, moisture contents, total dose-rates, D_E estimates and optical ages.

Sample number	Location (°N/°W)	Altitude (m asl)	Depth (cm)	U[a] (ppm)	Th[a] (ppm)	K[a] (%)	Rb[a] (ppm)	Cosmic[b, c] (Gy/ka)	Dose-rate[b, d] (Gy/ka)	n[e]	Weighed mean equivalent dose[f] (Gy)	Average equivalent dose[g] (Gy)	OSL Age[f,h] (ka)	OSL Age[g,h] (ka)
A- DUNE	42.8080/ 77.7513	308	152	1.1	3.5	1.3	37	0.19± 0.02	1.80±0.12	29	24.95± 0.32	26.67± 1.88	13.8±0.9	14.8±1.4
B- DUNE	42.8080/ 77.7513	308	152	1.4	4.2	1.4	42	0.19± 0.03	2.03±0.13	26	25.01± 0.35	26.76± 1.17	12.3±0.8	13.2±1.0

[a] Elemental concentrations from NAA of whole sediment measured at Activation Laboratories Limited Ancaster, Ontario Canada. Uncertainty taken as ±10%.

[b] Estimated fractional day water content for whole sediment is taken as 10% and with an uncertainty of ± 5%.

[c] Estimated contribution to dose-rate from cosmic rays calculated according to Prescott and Hutton (1994). Uncertainty taken as ±10%.

[d] Total dose-rate from beta, gamma and cosmic components. Beta attenuation factors for U, Th and K compositions incorporating grain size factors from Mejdahl (1979). Beta attenuation factor for Rb is taken as 0.75 (cf. Adamiec and Aitken, 1998). Factors utilized to convert elemental concentrations to beta and gamma dose-rates from Adamiec and Aitken (1998) and beta and gamma components attenuated for moisture content.

[e] Number of replicated equivalent dose (D_E) successfully measured determined from replicated single-aliquot regenerative-dose method (SAR; Murray and Wintle, 2000). These are based on recuperation error of < 10%.

[f] Weighted average for equivalent doses (D_E) of all aliquots. The uncertainty includes an uncertainty from beta source estimated of ±5%.

[g] Average and standard error for equivalent doses (D_E) of all aliquots. The uncertainty includes an uncertainty from beta source estimated of ±5%.

[h] Uncertainty incorporate all random and systematic errors, including dose rates errors and uncertainty for the D_E.

W1B: GEOLOGY, HYDROGEOLOGY, AND REMEDIATION OF THE ENVIRONMENTAL IMPACTS ASSOCIATED WITH THE RETSOF MINE COLLAPSE, CUYLERVILLE, NEW YORK

SAMUEL W. GOWAN AND JOHN M. NADEAU
Alpha Geological Services, Inc.

ABSTRACT

The Retsof Mine in Livingston County, New York had completely filled with saturated brine by 1996 following a collapse on March 12, 1994 and subsequent flooding with ground water. Monitoring revealed salinity was increasing in the fractured rock above the mine in the collapse area, and it was connected to the upward rise of brine from the mine. A remedial plan was developed in 2003 to prevent the saline water and brine from entering the overlying aquifer system at the base of the glacial valley. The remedial plan consisted of pumping brine from the fractured bedrock in the collapse zone at a rate equal to the calculated brine squeeze rate from mine closure. The remedial plan was designed based on data collected from well drilling, geophysical logging, ground water sampling and analysis, geochemical modeling, and subsidence monitoring. Caliper and gamma-ray geophysical logging were employed to confirm the location of significant stratigraphic contacts, to refine the monitoring program. Caliper and acoustic televiewer logging were used to locate and evaluate the extent of fracture zones in the bedrock to determine the optimal placement of the pumps in the brine remediation wells. The remedial pumping program was initiated in May of 2006, after a period of pre-pumping monitoring, and was continued until December of 2013. Monitoring continued after cessation of pumping until November of 2014. The monitoring shows that the pumping program was successful in controlling the brine migration. The subsidence and geochemical modeling results show that no differential subsidence was induced by pumping induced dissolution of anhydrate and halite. The subsidence data also show that the brine squeeze rate is approximately 15.7 gpm, which is much lower than initially projected and that it would take 2,240 years for full mine closure at this rate. Approximately 47 percent of the mine area is at a closure rate of zero; consequently, it is likely that the overall mine closure rate will approach zero in the distant future.

Figure 1. Site Location Map

INTRODUCTION

The Retsof Mine in Livingston County, New York (Figure 1) collapsed on March 12, 1994 and began to flood with ground water. The mine was completely filled with saturated brine by 1996. The collapse occurred when the roof fell within two panels of small yield pillars located near the southern, downdip extremity of the mine (panels 2YS and 11YW) (Gowan et al, 1999; Gowan and Trader, 2000). Sinkholes formed at the land surface after the support for the underlying bedrock and glacial sediments was eroded by the influx of fresh water into the mine (Gowan and Trader, 2003). Brine began rising through rubblized zones in the bedrock above the collapse panels as the mine began gradually closing under the weight of the overlying rock and glacial deposits

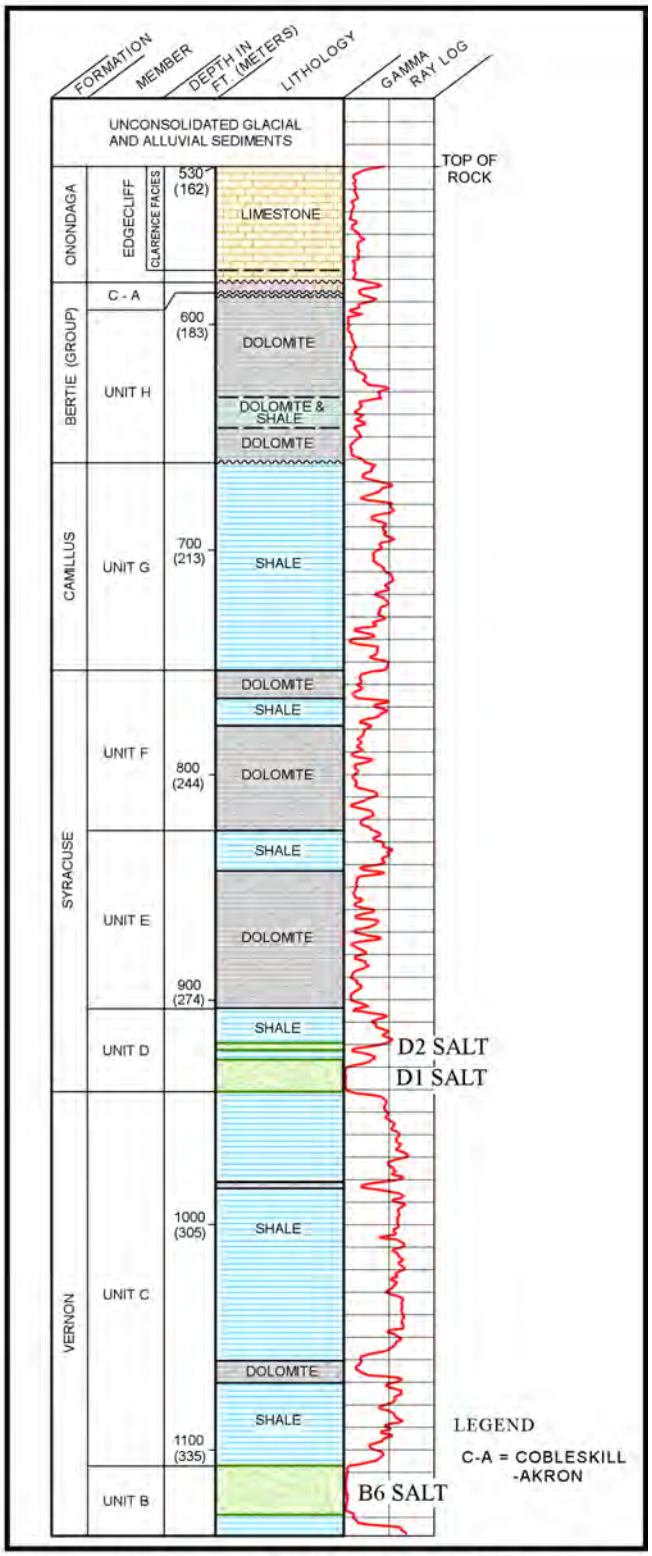

Figure 2. Detailed stratigraphic section for the Retsof Mine area with approximate formation depths for the collapse area.

A ground water monitoring program was initiated in 1996 to monitor the rising brine. This monitoring program revealed that elevated concentrations of brine were approaching the top of rock and entering the unconsolidated glacial aquifer system by 2003. These elevated concentrations triggered a legal agreement between New York State and the mine owner to protect the natural resources contained within the aquifer system from brine contamination. A remedial plan was designed to remove brine from the collapse zone by pumping from deep bedrock wells at a rate equivalent to the mine closure rate. It was anticipated that this balanced removal rate would simultaneously stop the brine from rising while preventing less saline water from being drawn into the salt horizons where further salt dissolution could occur and result in associated surface subsidence.

The remedial plan was an integrated system of subsurface monitoring, brine pumping, and brine disposal by on-site desalination. The development of these elements of the plan required the application of various subsurface investigation and data analysis techniques that included: geophysical logging of monitoring well and pumping well boreholes, ground water sampling and analysis, geochemical modeling, and subsidence monitoring. The objective of this paper is to describe the application and findings from the various sampling and analysis approaches, describe the remedial system, and summarize the results of the monitoring and remediation project.

Hydrogeologic Setting

The 11.2 square-mile Retsof Mine lies within the 20 feet (ft) thick B6 salt bed of Unit B of the Vernon Formation. The mine within the area of the collapse is approximately 1,100 ft beneath the surface and is overlain by 600 ft of

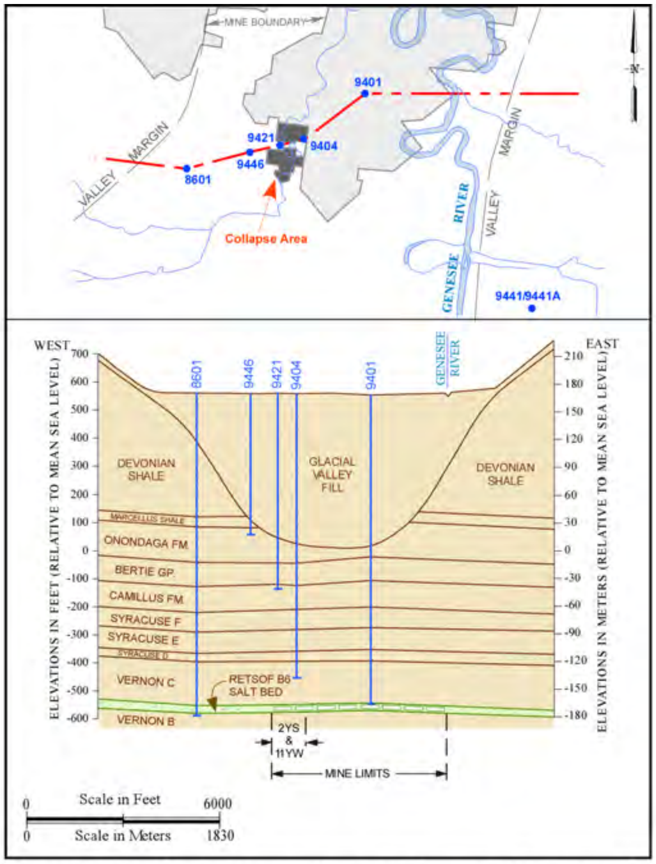

Figure 3. Geologic Cross Section Through Collapse Area Under Panel 2YS and 11YW.

dolostone, limestone and shale (Figure 2) and approximately 500 ft of glacial and alluvial deposits (Figure 3). The dolostone and shale layers of Unit C of the Vernon Formation and Unit D of the Syracuse Formation occupy the 190 ft of strata immediately above mine level and contain lenses and beds of salt and anhydrite (Gowan et al, 2006).

The B-6 salt bed dips southward at an angle of 0.65°. The updip extent of the mined section of the B-6 is at an approximate elevation of -273 ft below mean sea level (bmsl), and the bed at the collapse area is at an approximate elevation of -555 ft bmsl (Figure 4). Mining was progressing southward when the collapse occurred near the downdip limit of the mine (Figure 3).

Mining was conducted using a room and pillar method that extracted approximately 12 ft of the 20-ft bed and left between 35 to 40 percent of the salt as pillars. Ground water from overlying aquifers entered the mine through the collapse zone (Figure 5), dissolved salt, and filled the mine by 1996 with approximately 18 billion gallons of 100 percent saturated brine. The overlying aquifers that contributed to the mine inflow included the pre-existing brine pool in Unit D of the Syracuse Formation (Gowan et al, 1999; Gowan and Trader, 2000), the regional fracture zone at the Onondaga/Bertie contact (Bertie aquifer), the fractured zone at the top of the Onondaga Formation, and the glacial aquifer system at the base of the valley fill. The fracture zone at the top of rock combined with the glacial aquifer at the base of the valley fill is the Lower Confined Aquifer as identified by Yager et al (2001, 2009, and 2012).

The fractured top of rock (Onondaga Formation), in conjunction with the overlying basal glacial aquifer, form the most critical aquifer zone because of the high transmissivity, the extent of the aquifer across the valley, and the relative freshness of the water at some locations (Dunn Geoscience, 1992; Haley and Aldrich of New York, 1988; Yager et al., 2001, 2009, and 2012; Alpha Geoscience, 2003). The basal glacial Limestone aquifer consists of a mixture of sand, gravel and boulders and contains variable quantities of silt and clay and the basal glacial aquifer together provided most of the water that entered the mine, and as the result of being either a glacial till or glacial outwash deposit. The combined fractured Onondaga

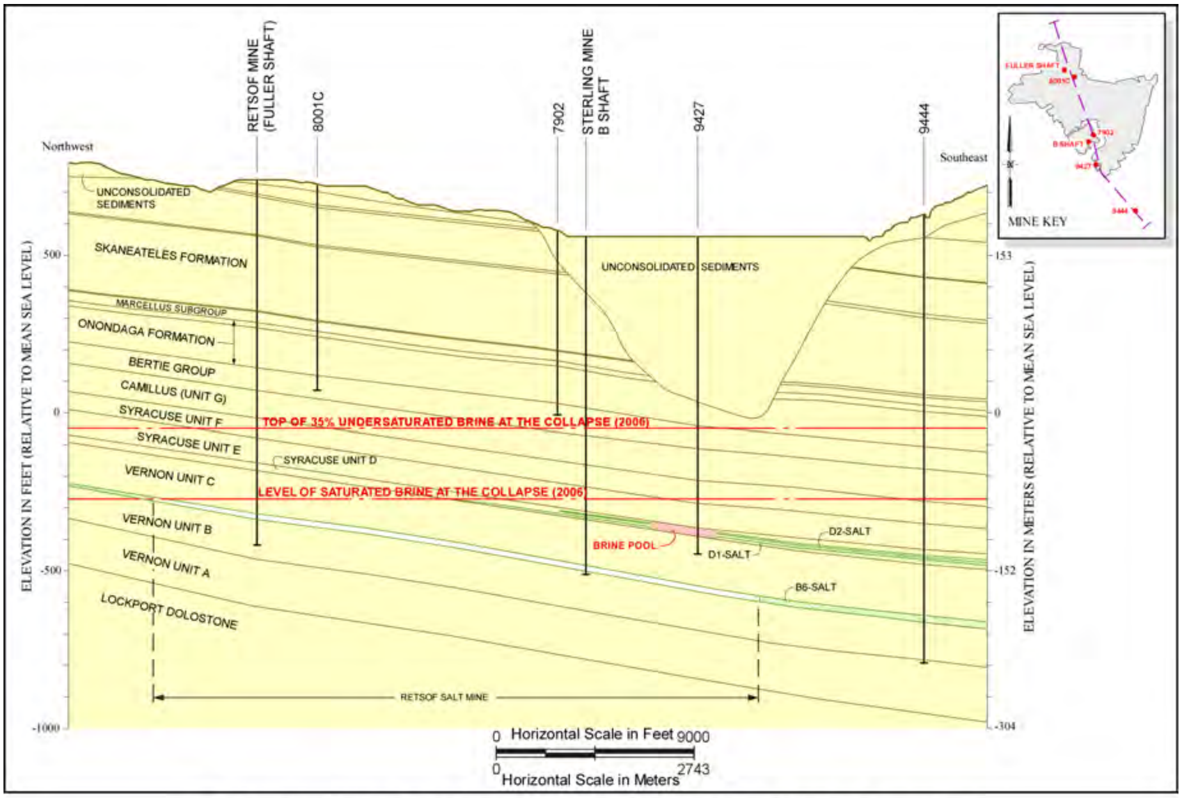

Figure 4. Geologic Cross Section Across the Retsof Mine Area

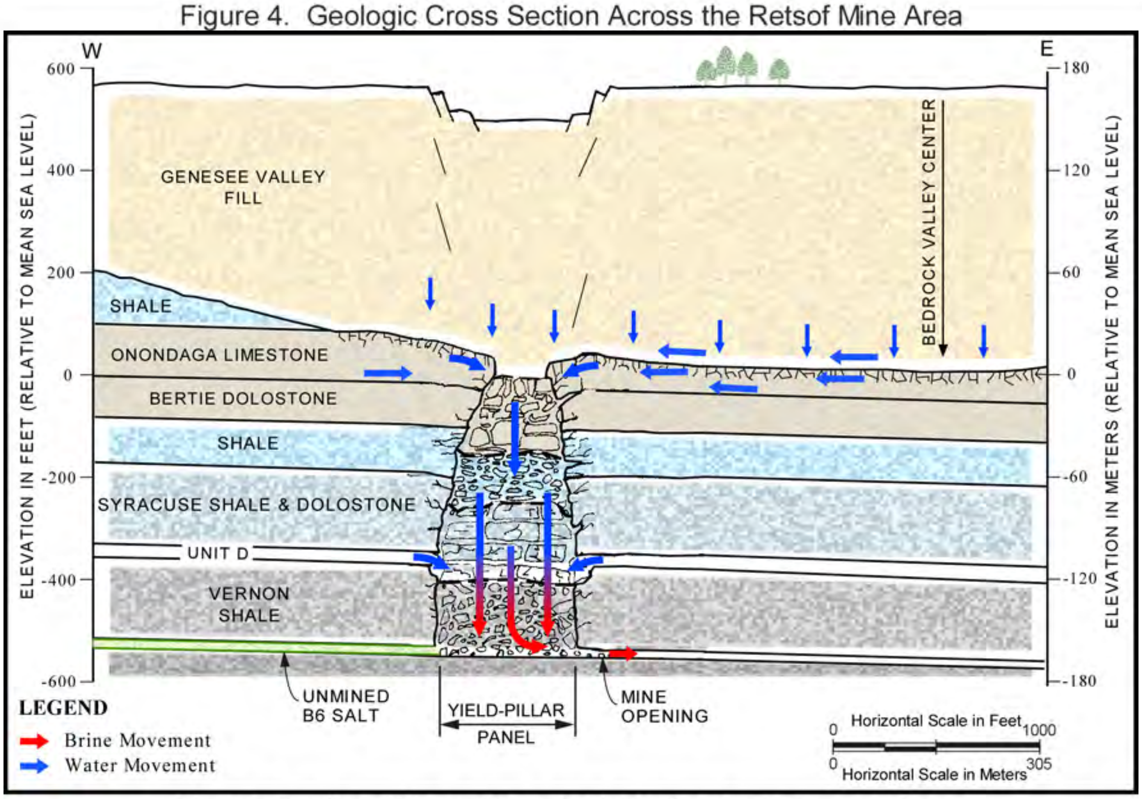

Figure 5. Condition after sinkhole formation at surface.

Limestone and the basal glacial aquifer together provided most of the water that entered the mine, and this aquifer system was considered by the State of New York to have a high potential for future use as a potable water supply.

The Bertie aquifer has limited importance due to poor water quality and limited yield. The Bertie may be connected to the top of rock aquifer through vertical fracturing throughout the valley system. The Unit D brine pool within the Syracuse Formation was of little importance as a source of inflow to the mine due to its limited extent. The Bertie aquifer and the Unit D brine pool are not considered potential water resources for future use.

Rising Brine in the Collapse Zone

It was understood that the gradual compression of the mine was squeezing saturated brine out of the mine, back through the collapse zone and into the overlying aquifers (Figure 6); however, it was not known whether the brine would remain within the deeper, saline bedrock aquifer zones or be pushed up into the basal aquifer system. A monitoring well system was installed in 1996 to track the movement of brine out of the mine and to observe whether the brine would remain in the deeper saline aquifer or be pushed up into the more significant top of bedrock/basal glacial aquifer system. This monitoring well network was initially limited to two basal glacial aquifer wells (9422 and 9568) and two of the top of rock wells (9446 and 9409), which are shown of Figure 7. Salinity, which was monitored in these wells regularly from 1996 through November of 2014, indicated that it had begun to increase in the ground water at the top of rock and in the basal glacial aquifer zone by 2003 as the result of brine rising up through the collapse zone from the mine. Data from the monitoring of zones near the top of the rock at monitoring wells 9409 and 9422 illustrate this steady increase in salinity until a remedial pumping system was started in May 2006 (Figure 8).

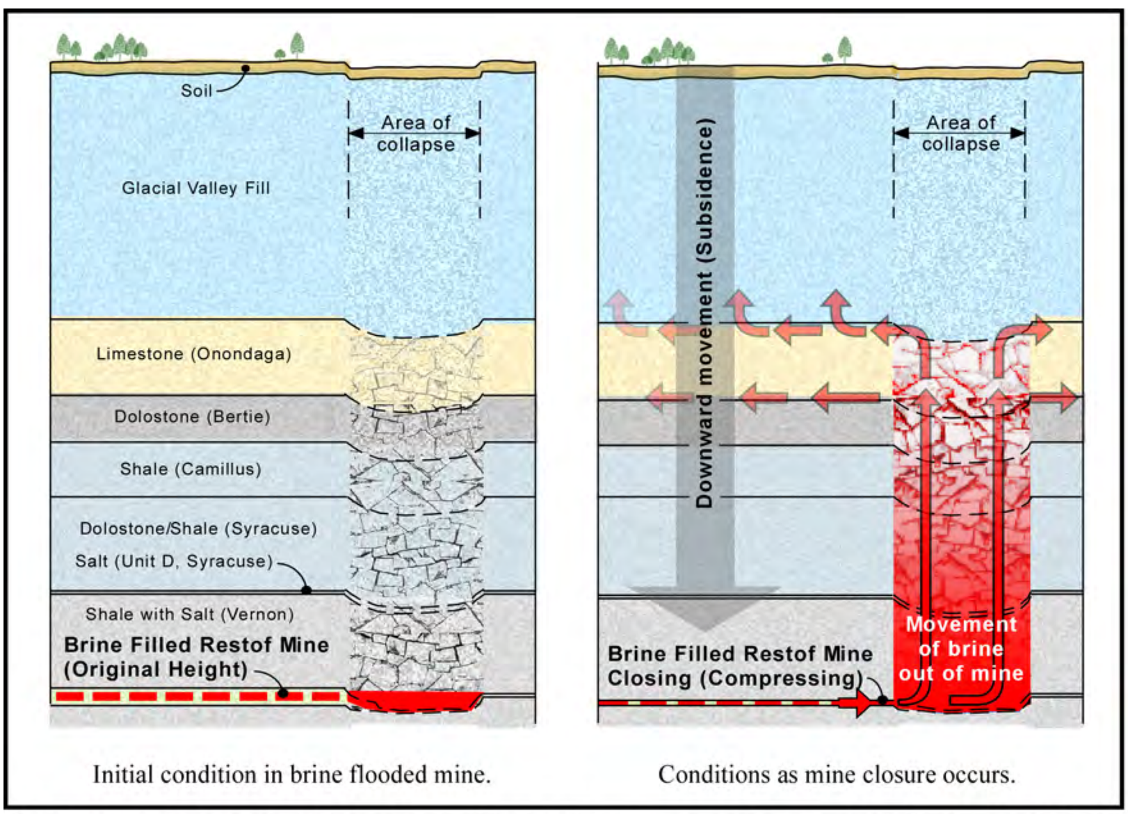

Figure 6. Schematic illustration of brine being squeezed out of the Retsof Mine.

BRINE REMEDIATION PROGRAM

The appearance of mine-impacted saline water at the top of rock triggered a State requirement that the mine owner (Akzo Nobel Salt Incorporated (ANSI)) protect the basal fresh water aquifer system. A brine remedial plan was developed and implemented on behalf of ANSI, in 2004, by: upgrading the monitoring well network around the collapse, increasing the frequency of water level and water quality monitoring, installing and pumping from six (ultimately five) pumping wells, increasing the number of subsidence monuments and constructing and operating a desalinization plant to treat the pumped brine. The program also included geophysical logging of all wells, geochemical modeling, interpretation of the data and reporting of the data and interpretations to the State of New York and other stakeholders.

Monitoring Wells

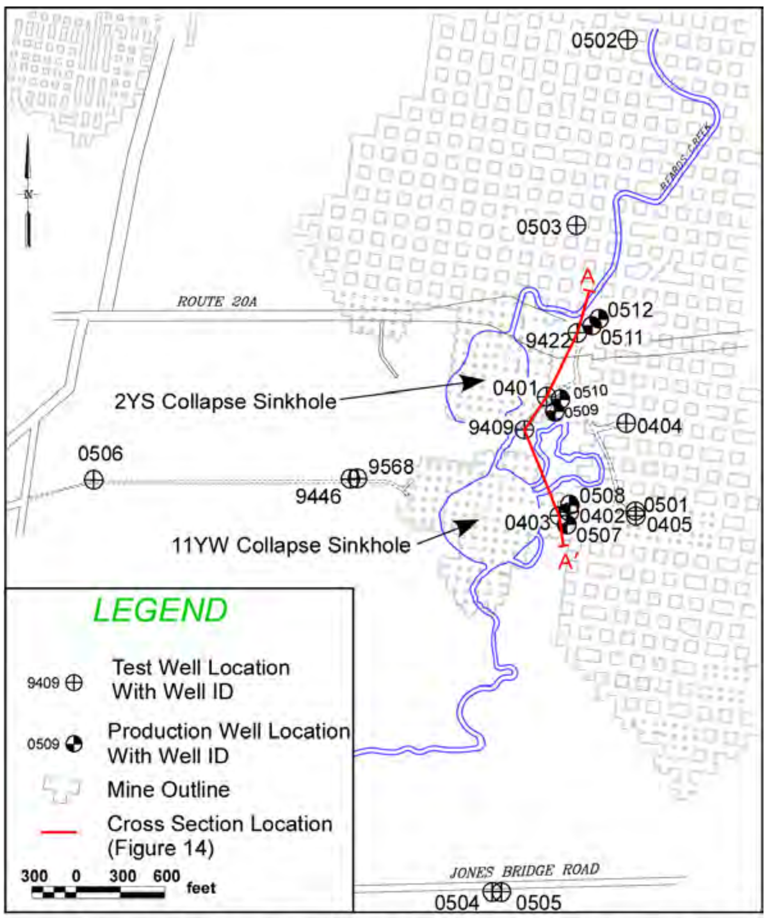

Figure 7. Location Map of Brine Monitoring and Remediation Wells

Eleven new monitoring wells were added to the existing network of four wells in the vicinity of the collapse. This brought the total in the immediate area to 15 wells (Figure 7). A water level and quality monitoring program from the monitoring well network was designed and implemented to maintain real-time knowledge of the vertical and lateral distribution of the brine profile so that pumping-induced changes to that profile were known as close to real time as possible. Detailed knowledge of the vertical and lateral extent of the profile and changes to that profile while pumping also were used to assess the efficacy of pumping and to make adjustments in the pump placements and pumping rates. The effects of remedial pumping were also monitored to prevent dissolution of the salt at mine level or of gypsum and anhydrite minerals in the dolostone and shale layers of Units C and D above mine level (Figures 2 and 4). It was desirable to prevent dissolution of these zones to prevent further catastrophic collapses and sinkhole formation.

Brine Pumping Wells

A total of six wells were installed for pumping on the east side of the collapse area (Figure 7) to provide maximum lateral coverage on the down slope (bedrock valley) side of the collapse. The wells were positioned at these locations to avoid the rock instability within the collapsing chimney while taking advantage of enhanced fracture permeability that was anticipated to occur above the panel entries where inflow-induced dissolution would have been focused. Four of the pumping wells (0507, 0508, 0509, and 0510) were located above the entryways to the collapsed mine panels, and wells 0511 and 0512 were located on the north side of 2YS to provide coverage in accessible areas where more extensive fracturing was also predicted to have occurred as the water was flowing out to the north during the mine flooding phase. The location and spacing of the wells was chosen to allow for an even drawdown of the brine level across the collapse region.

The six wells were grouped into three sets of well pairs. The well pairs were each designed with a shallow and deep well (Figure 9) to cover the 200-ft zone from the middle of the Bertie Group down to

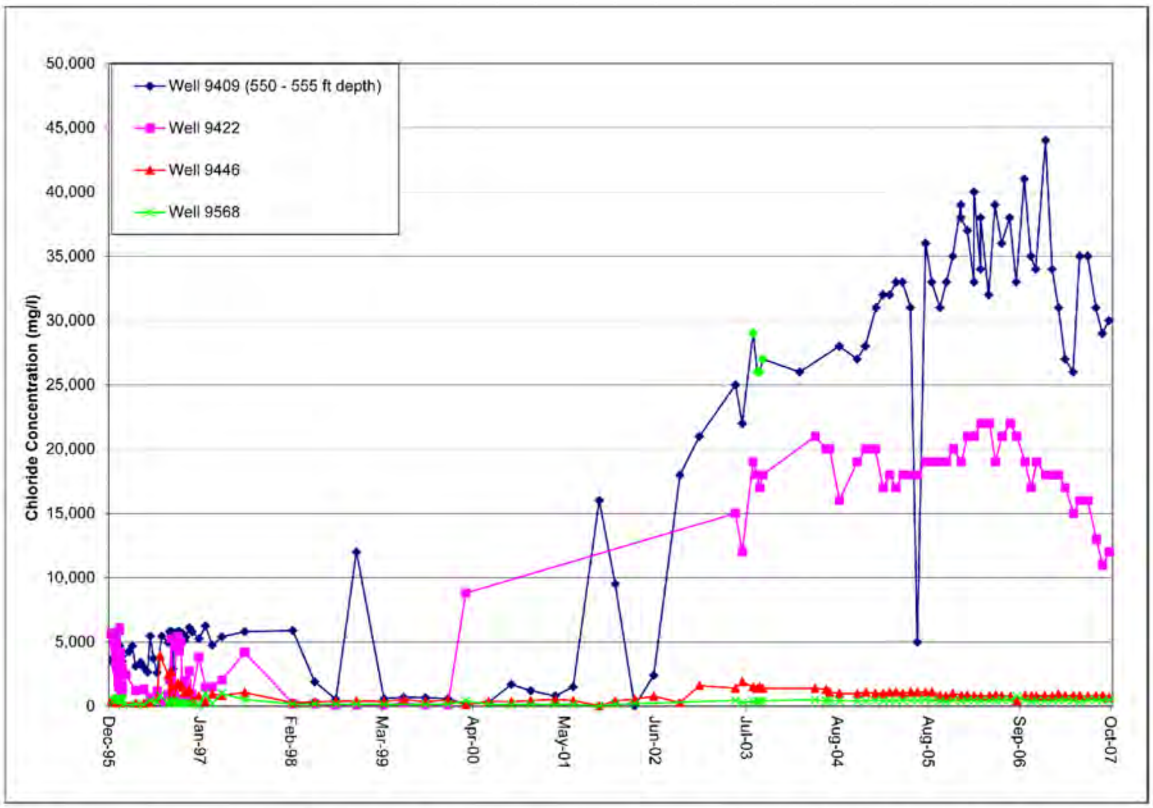

Figure 8. Historical Chloride Concentrations in Wells 9409, 9422, 9446, and 9568 from January 1996 through October 2007

the top of the 100% saturated brine. This interval covers the brine saturation range of approximately 50 to 100 percent. The wells were each designed with a screen length of 100-ft for a total screened interval of 200 ft at each well pair location. This combined interval covered the elevation range from approximately -75 ft bmsl to -275 ft bmsl. The lowest elevation in the deep wells corresponded with the elevation of the mine at its upgradient limit, which is illustrated on Figure 4. This well depth limit was established to avoid drawing the top of the 100 percent saturation line below the elevation of the updip (northern) limit of the mine. This depth limit prevented the potential for further mine-level salt dissolution.

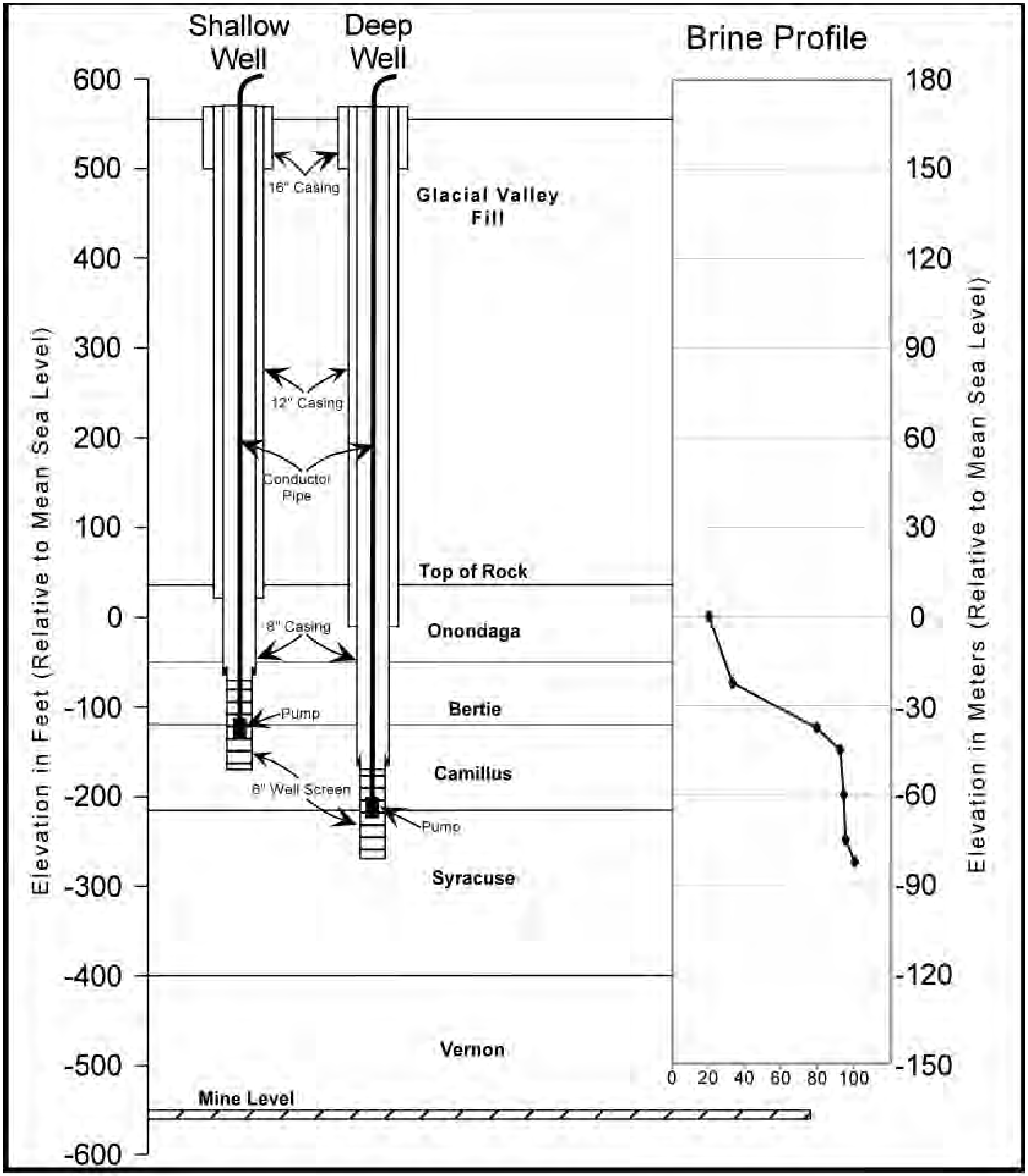

Figure 9. Brine Suppression Well Pairs

The initial pump settings in each respective well were established within the unsaturated portion of the brine profile based on the water quality monitoring and fracture zones identified during drilling and subsequent geophysical logging; however, there was a need for flexibility to respond to actual conditions encountered during pumping. Flexibility was accommodated by designing pump systems that could be adjusted readily to various depths within the 100 ft screen interval in each well. This was accomplished by attaching the pumps to as much as 730 ft of flexible Angus Wellmaster 200 hose (Kidde, 2006) to allow for rapid removal of the pump from the well and to avoid corrosion of steel pipe in contact with the brine. Small sections of stainless steel are used at the top of the assembly to allow for relative easy and quick adjustments to pump intake depths.

The desalination plant had an estimated maximum feed rate from the pumping of 100 gpm. The rate was estimated based on the previously calculated maximum brine squeeze rate of 106 gpm (RE/SPEC, 2003).

The pumping rates of the individual wells ranged from 10 gpm to 25 gpm with a combined rate of 100 gpm. The overall objective was to pump at low enough rates to result in a brine skimming effect to minimize the potential for upwelling of saturated brine by pressure drawdown or the drawdown of fresh water into the profile. The rates in the individual wells were adjusted periodically based on water quality results from each pumping well and the monitoring wells.

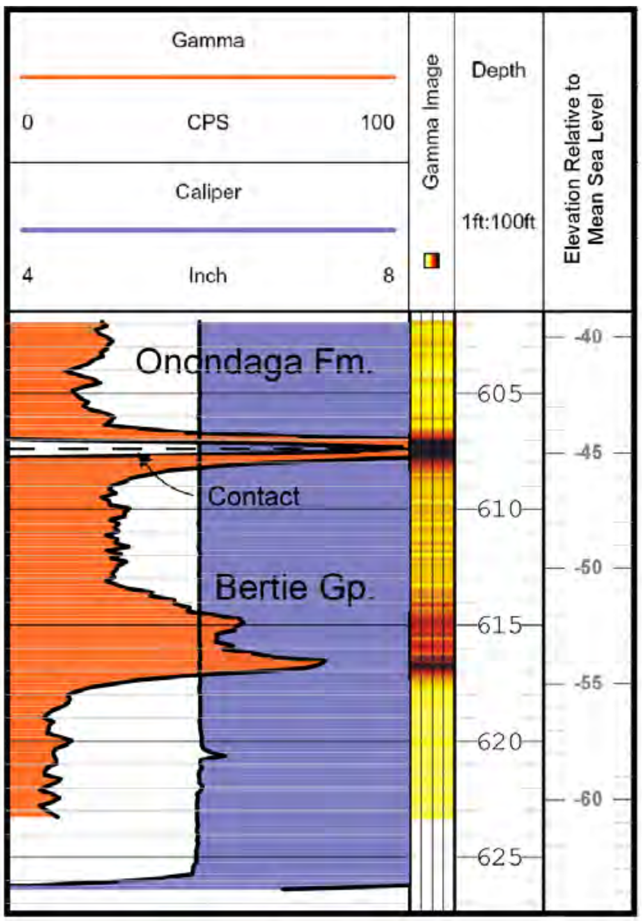

Figure 10. Gamma and Caliper Log of the Onondaga-Bertie Contact.

Geophysical Logging

Geophysical logging has been conducted in fifteen of the monitoring and pumping wells across the site. Gamma-ray and caliper logging tools were applied to confirm the location of significant stratigraphic contacts that were estimated initially from observations during drilling. Figure 10 is an example of the confirmation of the distinctive Onondaga-Bertie contact, which is a significant regional stratigraphic marker and one of the more important water-bearing fracture zones in the Genesee Valley. The location of this and other formation contacts, such as the basal aquifer at the interface between the fractured top of rock and overlying glacial valley fill sediments, were important for the refinement of the ground water monitoring program, the physical visualization of the brine rise, and the development of the geochemical model.

Heat pulse flow logging was conducted in four monitoring wells to detect vertical fluid movement within the wells. The intent of this logging was to measure fluid movement in order to quantify hydraulic flow potentials between fracture sets in the bedrock; however, the initial results showed no measurable flow. Apparently, the vertical flow was below the detection limit of the equipment despite the fact that water level monitoring indicated vertical pressure gradients between fracture sets within each hole.

Caliper and acoustic televiewer logging were used to locate specific fractures and correlate fracture sets between wells. Optical televiewer logging was attempted in the wells but was unsuccessful due to discoloration caused by hydrogen sulfide. The acoustic televiewer logs in Figures 11, 12 and 13 graphically represent an example of a fracture set that is correlatable throughout the collapse area. The televiewer log of well 0510 displays an extensive fracture set from a depth of 664 ft below grade (bg) to 674 ft bg (Figure 11). The log from well 0508 (Figure 12), which was located approximately 700 ft down dip from well 0510, displays a similar fracture set from 672 ft bg to 677 ft bg. The third shallow pumping well 0512 (Figure 13), which was located approximately 600 ft updip of 0510, displays fractures within the 670 ft bg to 680 ft bg depth range that are less numerous and not as well developed as those noted in wells 0508 and 0510. These results suggest the presence of a fracture zone that could be laterally extensive and transmissive in the rock interval above the collapse entries but diminishes further away from the collapse area (Figure 14).

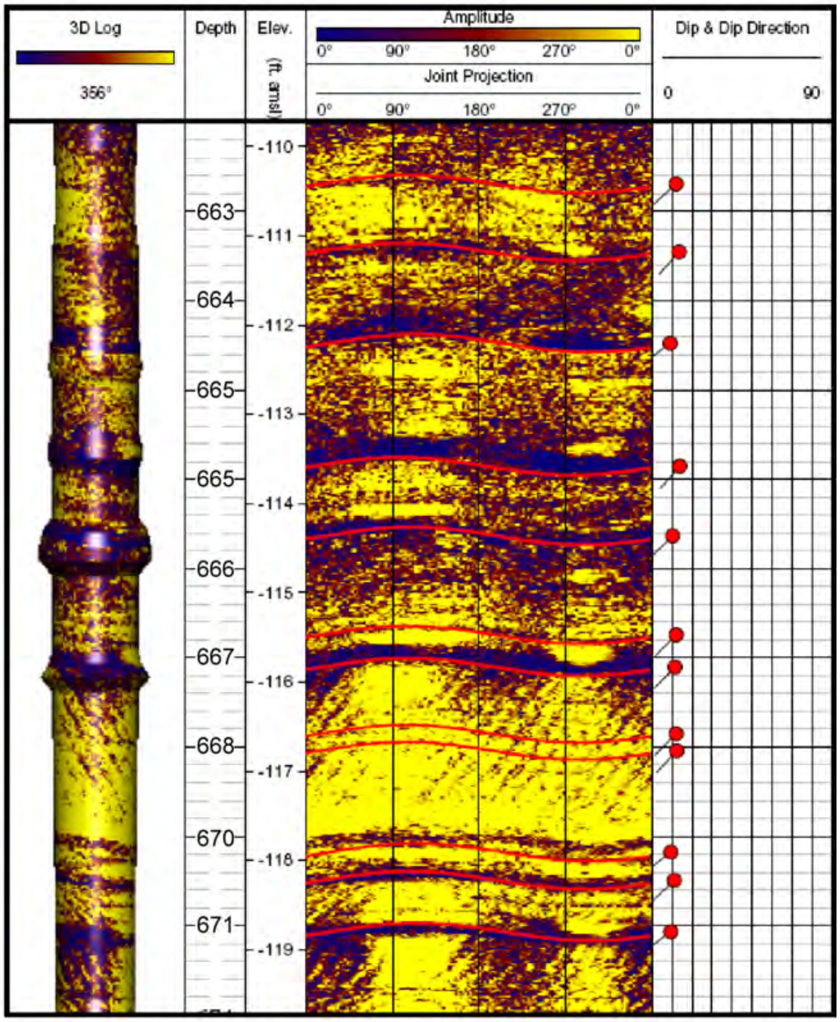

Figure 11. Acoustic Televiewer Log of Production Well 0510.

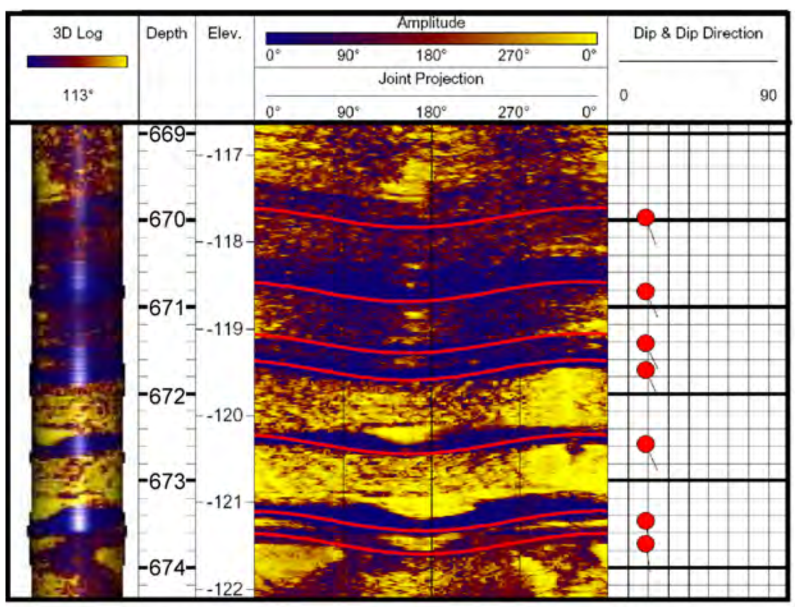

Figure 12. Acoustic Televiewer Log of Production Well 0508.

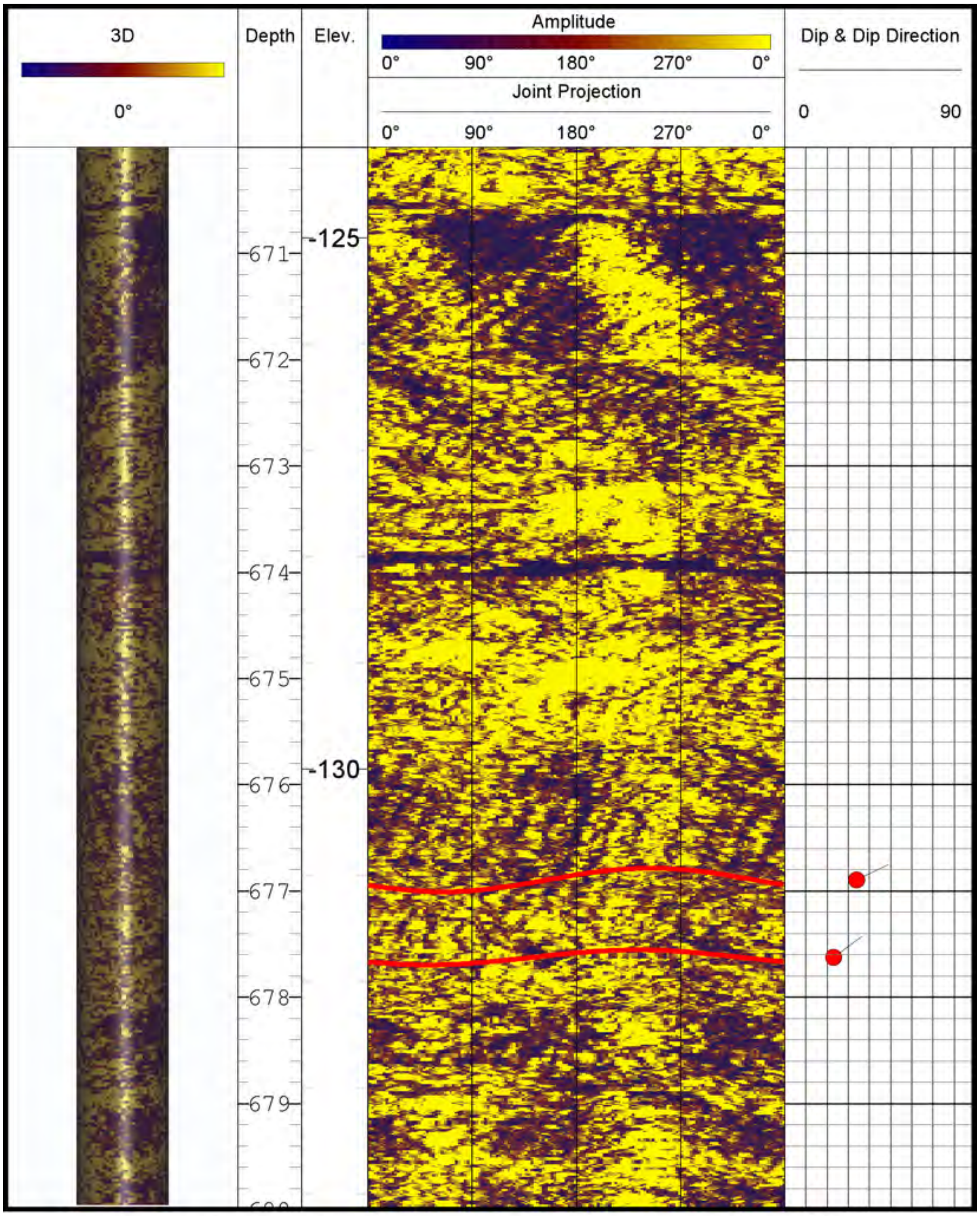

Figure 13. Acoustic Televiewer Log of Production Well 0512.

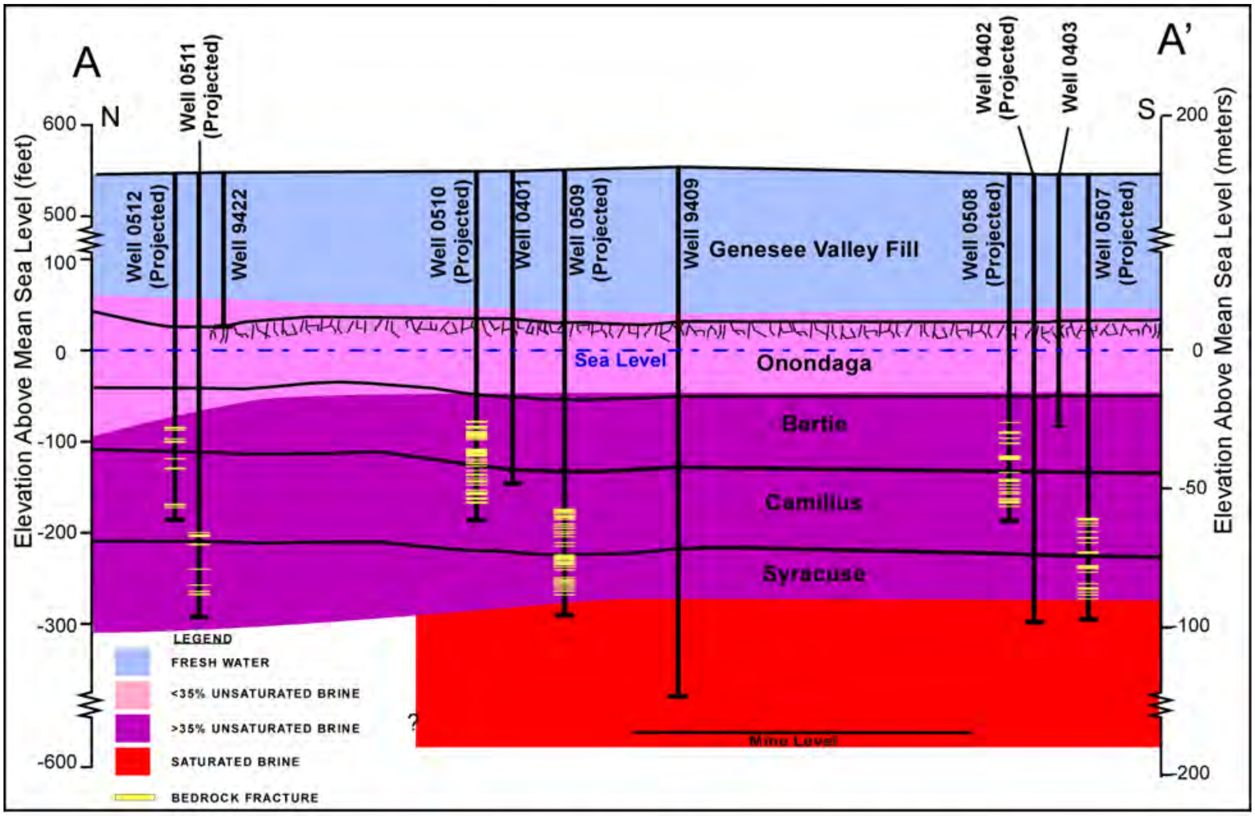

Figure 14. North-South directed cross section through monitoring and remediation wells showing the location of significant fracture sets.

Laterally extensive and potentially transmissive fracture sets were found elsewhere within the 200 ft interval intersected by each well pair. The shallow wells, (0508, 0510, and 0512) display an extensive fracture set between 635 ft bg and 655 ft bg. Two of the deeper wells (0507 and 0509) were found to have extensive fracturing across the entire 100 ft zone. Well 0511 displayed less extensive fracturing and fewer sets than the other deeper wells, likely because there was less dissolution and subsidence in this area than originally predicted. The placement of the pumps in each well was based upon the potential transmissivity of the fracture sets and the concept of lowering the brine concentration via the skimming effect. The existence of multiple fracture sets that are laterally extensive allowed for the installation of the pumps at varying depths/elevations across the region.

Water Quality and Hydraulic Flow Monitoring

Field salinity was tested at specific horizons throughout the collapse area to chronicle the rate and nature of changes in the brine profile. This testing was the primary focus of the water quality monitoring program. The particular horizons of interest included the top of bedrock, the 35% saturated brine level, and the top of the 100% saturated brine level.

Hydraulic flow monitoring within the collapse vicinity was conducted to quantify brine and saline water movement. The monitoring consisted of collecting hydraulic head (water level) measurements associated with the Onondaga-Bertie contact and mean sea level elevation across the region. The water level data collected from the wells had to be adjusted to equivalent pressure head of fresh water by multiplying the column height above the measuring points by the density of the fluid.

Geochemical Modeling

Geochemical modeling was utilized to simulate the dissolution and precipitation of minerals as the salinity. This is being accomplished by using PHREEQC (Parkhurst and Appelo, 1999) to calculate saturation indices that would result when subsurface layers containing anhydrite and gypsum are exposed to water with a range of chemical characteristics. Saturation indices represent the potential for minerals to dissolve or precipitate in a solution (Freeze and Cherry, 1979). Saturation indices of halite and anhydrite were calculated for the historical data set and trends were established for the pre-pumping environment. These indices were monitored during the pumping of brine to watch for sudden or drastic changes from the baseline trends in order to determine if dissolution was occurring at specific zones.

Subsidence Monitoring

Monitoring of the pre-existing surface subsidence monument network in the collapse region was used to detect short-term increases in subsidence related to pumping activities and to track the overall subsidence rate above the mine. This monitoring was conducted during the design and construction of brine mitigation plan to provide pre-pumping background information. Each set of data was evaluated to detect localized changes in elevation during pumping that could have been indicative of collapse related to pumping-induced dissolution. The subsidence data was also used as a proxy for mine closure which is directly related to the brine squeeze rate. This squeeze rate was coupled with the water quality monitoring to assess the percentage of pumped brine that was coming from the mine and the amount that may have been pre-existing in the saline aquifers below the top of the rock.

RESULTS OF THE BRINE REMEDIATION PROGRAM

The installation of additional monitoring wells was completed in 2005. Some of these wells were completed with multi-level tubing for monitoring various depths within the brine profile. A few of the wells were also completed with multi-level packers, but those proved to be ineffective due to vertical fracture connection around the packers, and the packers proved to be unnecessary due to high transmissivities in the wells and the density stratification in the brine profile.

The pumping wells were completed in 2006, and pumps were installed in five of these wells. No pump was installed in Well 0512 due to low yield as the result of limited fractures. Pumping was initiated in late May 2006 after a desalinization plant was constructed at the site. The wells were pumped intermittently until February of 2007 due to the need to modify the plant to accommodate the challenges of processing a multi-chloride brine that contained Mg/Ca/NaCl and several other constituents such as sulfate. The system was operated successfully with relatively continuous pumping from February 2007 through mid-December 2013 when the State of New York allowed ANSI to shut down the remediation system during negotiations to determine the future of the remedial program. The brine profile monitoring continued through November 2014 when it was determined that no further remediation was required.

Pre-Pumping Brine Profile and Hydraulic Pressures

The brine profile through the collapse zone, as it appeared in November 2005 (six months prior to initial pumping), is illustrated on a west-east cross section through the collapse chimney (Figure 15). It was apparent to Alpha Geoscience (2003) and The U.S. Geological Survey (Yager et al, 2009) that a significant percentage of the saline water (bedrock zone with less than 35% saturation) was a brine that pre-dates the collapse. This pre-existing brine was being displaced and partially mixed with the upwelling, mine-derived brine. The domed surface of the more saturated, upwelling brine illustrated by Figure 15 is based on a percent salinity map (Figure 16) that represents conditions at the regionally extensive aquifer at the Bertie/Onondaga contact as it existed in November of 2005. The highest concentration is

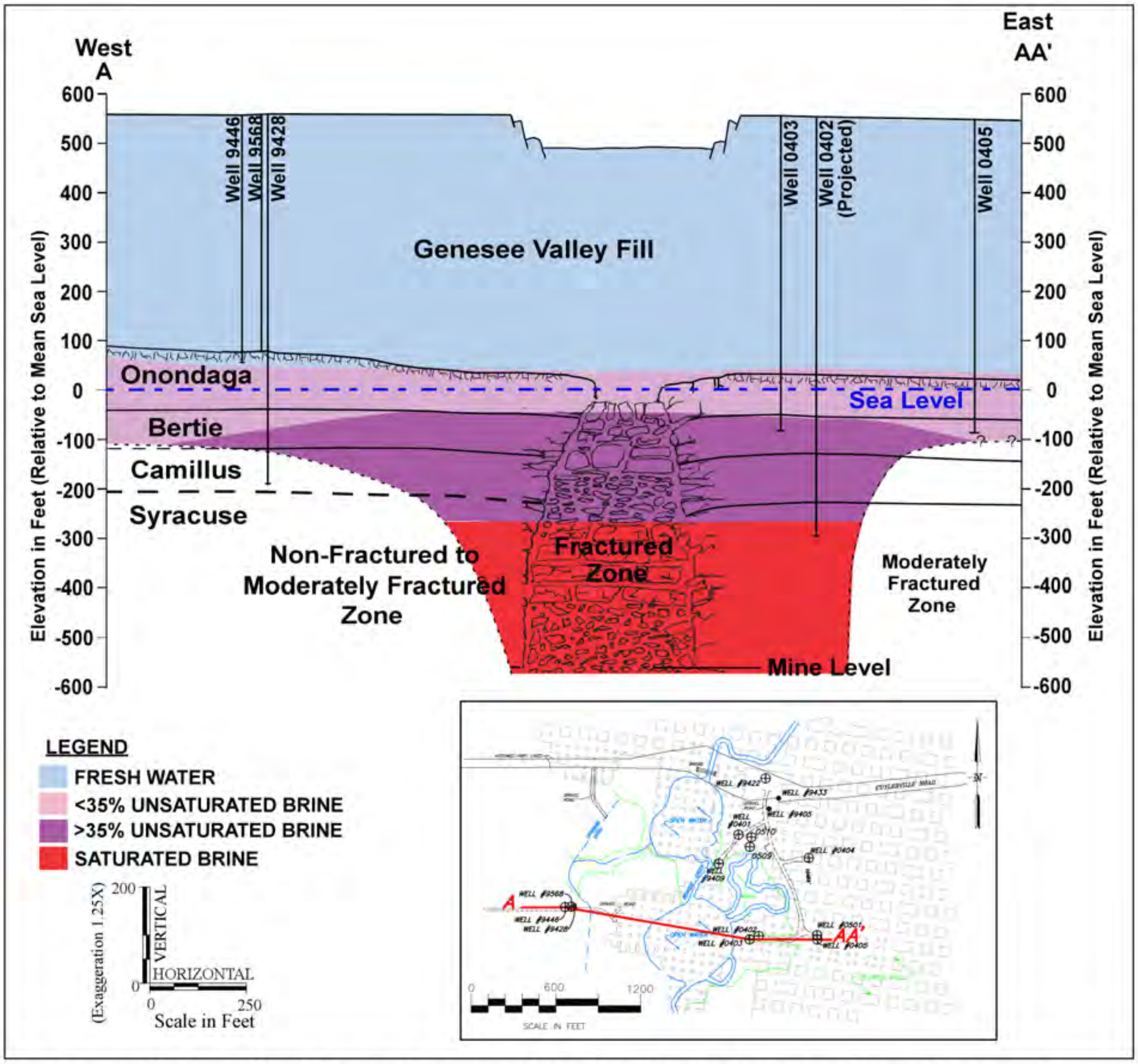

Figure 15. East-West directed cross section through monitoring and remediation wells showing upwelling brine

centered at the two adjacent collapse chimneys represented by the open water of the surface sinkholes.

The brine upwelling indicated by the saturation map is consistent with the distribution of pressures at the Onondaga/Bertie contact (Figure 17). This map shows a distinctive pattern of pressure mounding and outward radial flow centered on the collapse chimneys.

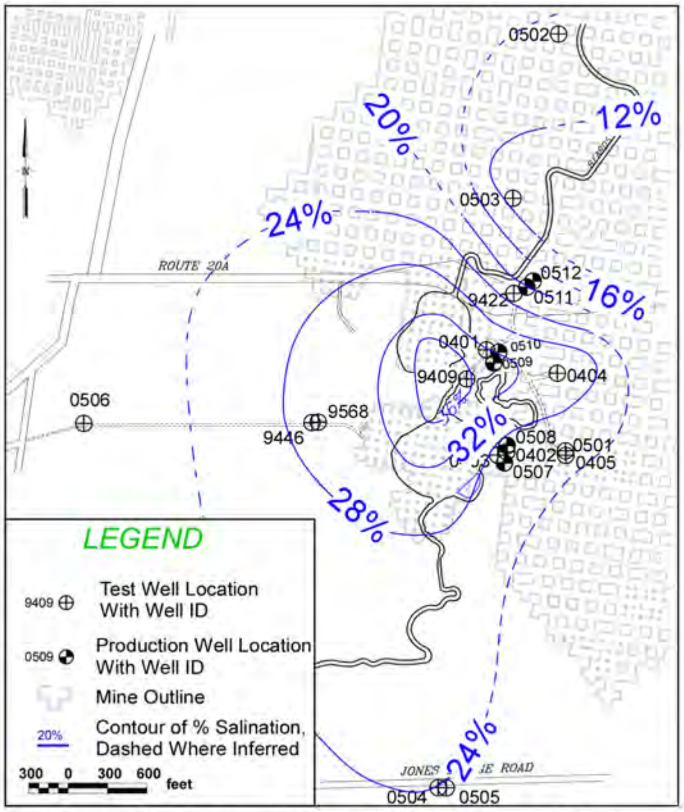

Figure 16. Percent Salinity Contour Map at Mean Sea Level, November 2005

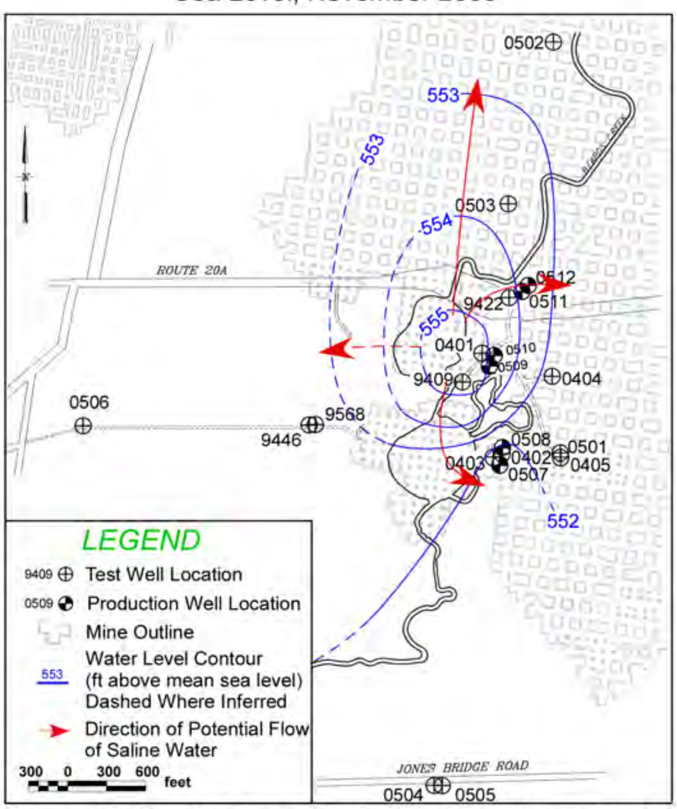

Figure 17. Contour map of water level elevations at the Mean Sea Level, November 2005

Brine Profiles and Hydraulic Pressures during Brine Pumping

The brine saturations at the top of rock essentially stopped increasing at the start of intermittent pumping in May of 2006 and were clearly decreasing after more continuous pumping began in February of 2007 (Figure 8). Pumping-induced drawdown effects at the Bertie/Onondaga contact are evident on the hydraulic head pressure contours for July 2013 (Figure 18). A contour map for chloride concentration at mean sea level in July 2013 shows the reduction in salinity in the collapse zone (Figure 19).

The pumping was spread out over the east side of the collapse zone with the intent of not creating significant drawdown or upwelling effects. This was achieved and allowed the maintenance of stable pressures through an increase in water levels as the denser brine was replaced by less saline water. This is illustrated by the increase in measured fluid level at the Onondaga/Bertie contact that was correlated with a decrease in salinity (field measured density) as the pumped brine was replaced by less saline fluid (Figure 20). This increase in water levels related to a decrease in salinity (density) required an adjustment (normalization) of all field measured salinity (density) to a fresh water equivalent hydraulic head for piezometric mapping purposes.

Post-Pumping Conditions

Pumping was discontinued in December of 2013, and there was a more immediate response exhibited by an increase in salinity and a corresponding decline in directly measured fluid levels in response to the increase in fluid density (Figure 21). For example, the saturation at the Onondaga-Bertie Contact increased by approximately 10%, and the directly measured fluid level declined by approximately 10 feet in Well 0403.

All monitoring was discontinued after November 2014. The wells were plugged and abandoned in 2015 and 2016, and the brine treatment plant was dismantled in 2015. This closure activity was conducted through a settlement agreement between ANSI and the stakeholders.

Summary of Geochemical Modeling and Subsidence Monitoring

The geochemical modeling was focused towards the pumping effects on dissolution in the anhydrite-bearing formations below the Onondaga-Bertie Contact. The ideal condition was to have a saturation index close to zero. The data input into the PHREEQC model resulted in a high potential for anhydrite dissolution above the anhydrite-bearing Camillus Shale, as illustrated in Well 9409 (Figure 22), but little or no apparent potential at the more critical anhydrite-bearing zones below that level. No dissolution conditions occurred during the pumping test for either the anhydrite or the more soluble halite intervals. These results are consistent with the subsidence data, which did not show any evidence of differential (sinkhole-type) settlement occurring throughout the area.

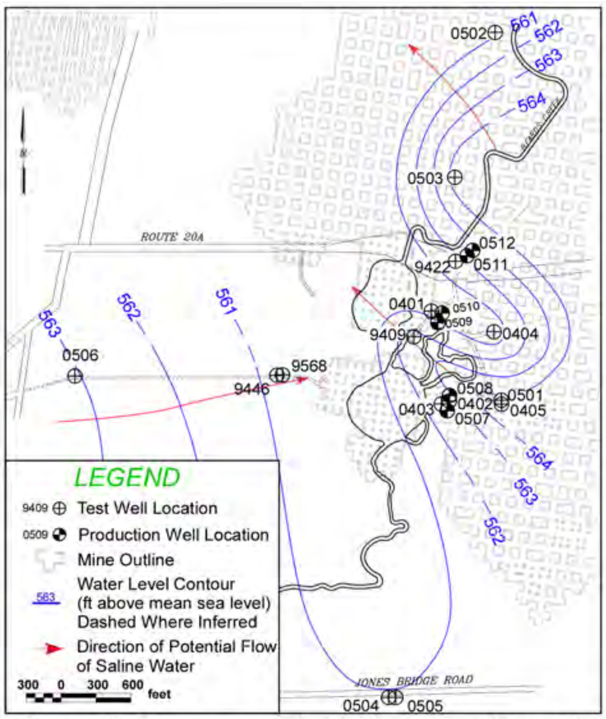

Figure 18. Contour map of water level elevations at the Onondaga-Bertie Contact, July 2013

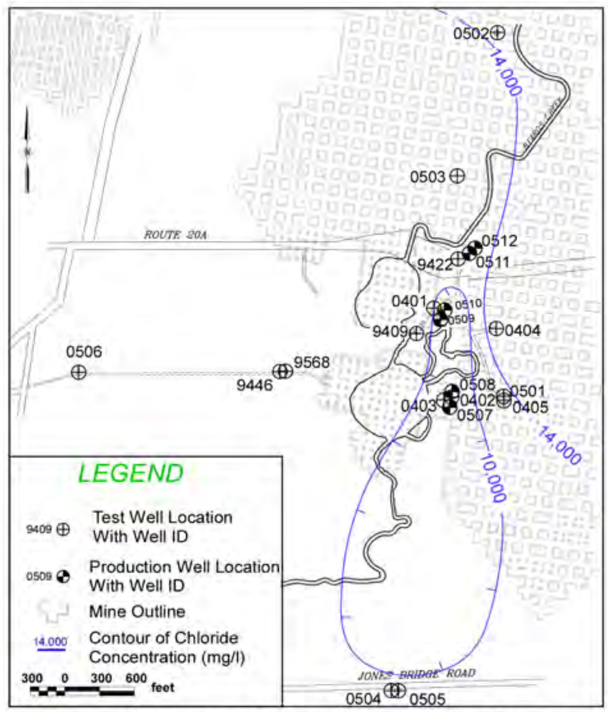

Figure 19. Chloride Concentration Contour Map at Mean Sea Level, July 2013

The subsidence monitoring data showed that subsidence above approximately 47 percent of the mine was effectively zero. The remaining 53 percent of the footprint had a subsidence rate that was equivalent to a brine squeeze rate of 15.7 gallons per minute (gpm) with a range of +/- 4 gpm. This rate was well below the maximum estimated squeeze rate of 106 gpm and had apparently declined significantly due to the buoyancy effects of hydrostatic pressure. It is estimated that it would take approximately 2,240 years for the 11.2-square mile mine to push out all of the brine at the current closure rate; however, the non-measurable rate of subsidence over approximately half of the mine footprint suggests that further declines in the closure rate will occur, and ultimately, the mine closure will approach zero.

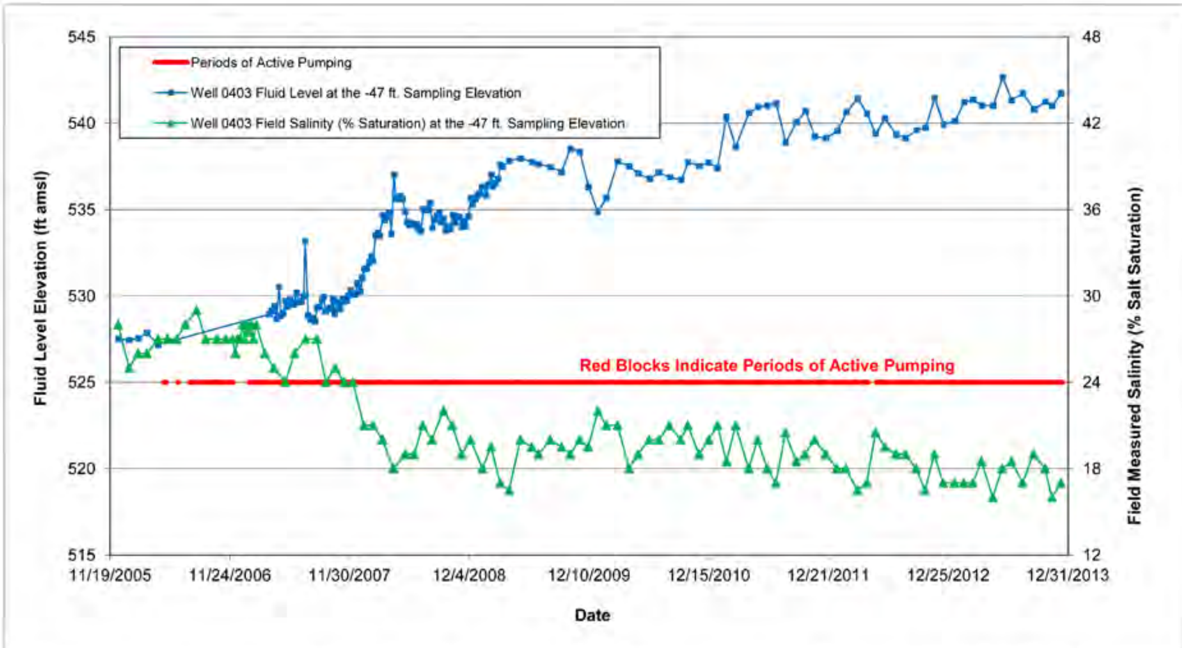

Figure 20. Unadjusted Fluid Level Elevation vs. Field Measured Salinity, Well 0403 at the Onondaga - Bertie Contact (-47 ft. Sampling) Elevation

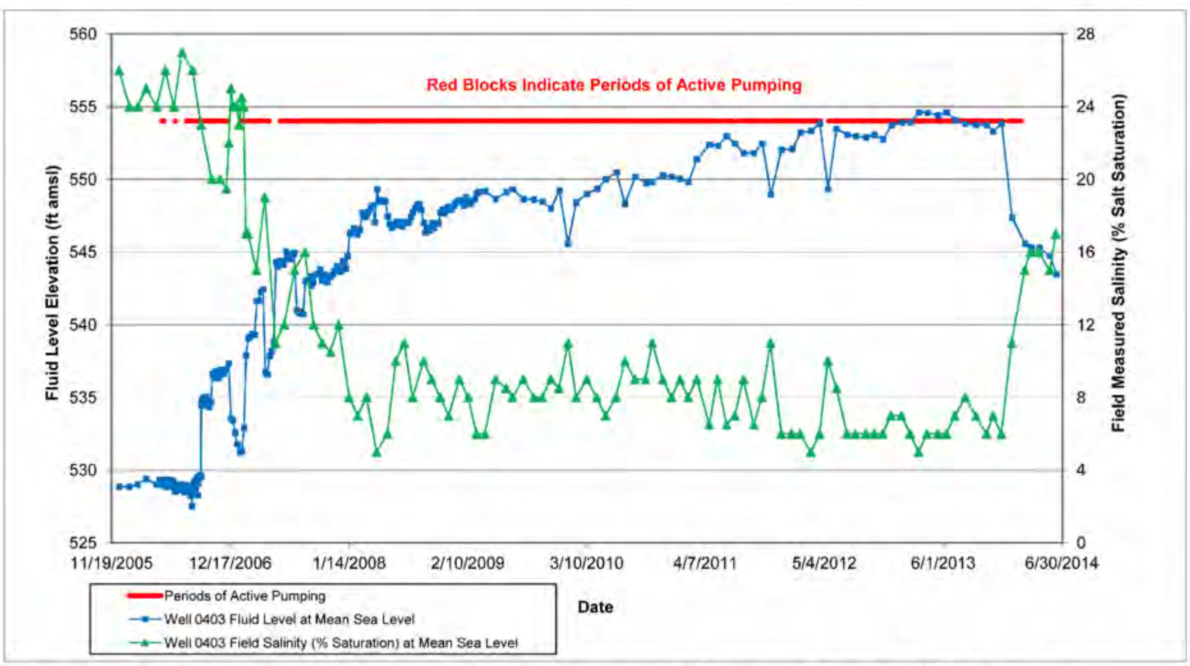

Figure 21. Unadjusted Fluid Level Elevation vs. Field Measured Salinity, Well 0403 at Mean Sea Level Elevation

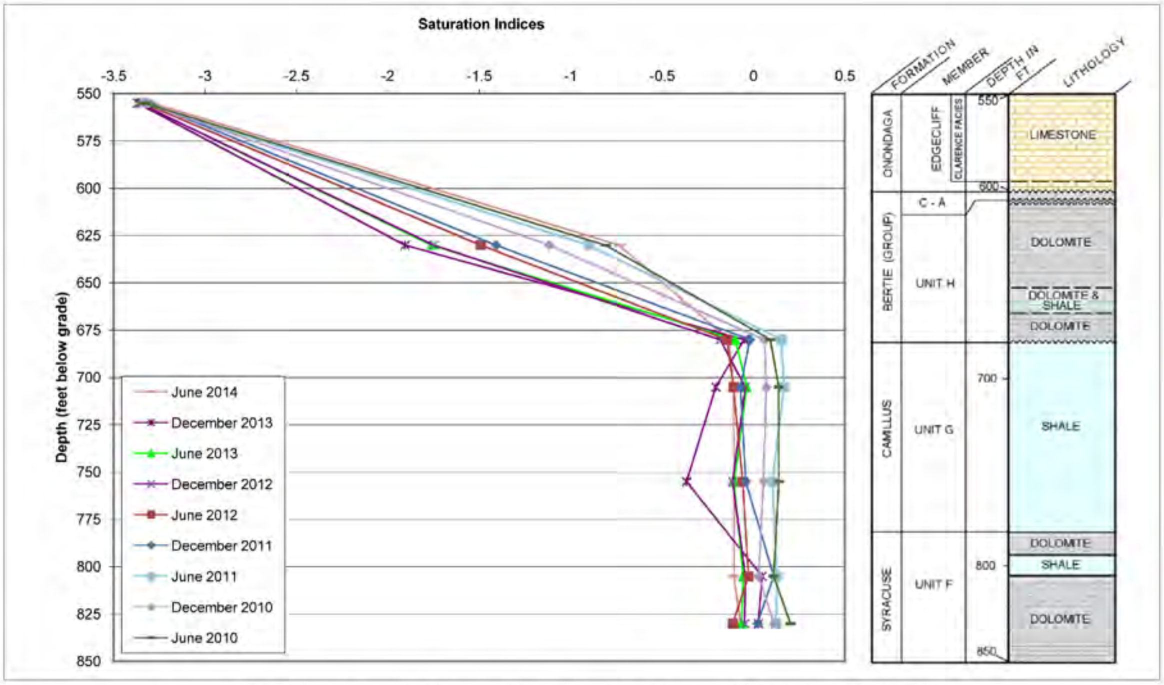

Figure 22. Anhydrite Saturation Index Versus Depth at Well 9409

CONCLUSION

The ANSI brine remediation project at the collapsed Retsof Salt Mine yielded detailed data about the stratigraphy and hydrogeology of the bedrock and glacial deposits in the mine collapse area. This detailed data, which included vertical water quality profiles throughout the collapse area, showed that the brine was being squeezed out of the Retsof Mine and up through the collapse zone chimneys toward a fresh water aquifer at the top of the rock and base of the overlying glacial sediments. The data provided the basis for developing a brine remediation system consisting of pumping from the unsaturated zones of the bedrock adjacent to the collapse chimneys. The objective of the remedial pumping was to prevent the brine from entering the fresh water aquifer at the top of the rock. The results demonstrated that this remedial objective was achieved while pumping. The results also demonstrated that pumping was occurring at a higher rate than the rate that the brine was being expelled from the mine and that some of the brine being extracted by pumping was pre-existing saline water that was located within the fractured bedrock aquifer system and locally within the glacial aquifer base above the mine.

REFERENCES CITED

Alpha Geoscience, 2003, Discussion of Hydrogeologic Conditions in the Genesee River Valley and Assessment of Remedial Options to Address the Rise of Brine into the Valley and the Retsof Salt Mine Collapse," unpublished consulting report by Alpha Geoscience, Clifton Park, NY, for Zurich America Insurance Group, Troy, Michigan, 17 p.

Dunn Geoscience Corporation, 1992, Hydrogeologic Report for the Akzo ash processing plant, unpublished consulting report by Dunn Geoscience, Albany, NY, for Akzo Nobel Salt Inc., Clarks Summitt, PA, 44 p.

Freeze, R.A., and Cherry, J.A., 1979, Groundwater: Englewood Cliffs, N.J., Prentice-Hall, 604 p.

Gowan, S. W.; Van Sambeek, L.L.; and Trader, S.M., 1999, "The Discovery of an Apparent Brine Pool Associated with Anomalous Closure Patterns and the Eventual Failure of the Retsof Salt Mine," Proceedings, October 1999 Meeting of the Solution Mining Research Institute, Washington, D.C., USA, pp 242-272.

Gowan, S. W.; and Trader, S.M., 2000, "Mine Failure Associated with a Pressurized Brine Horizon: Retsof Salt Mine", Western New York, Environmental and Engineering Geoscience, Vol. VI, No.1, pp 57-70.

Gowan, S. W.; and Trader, S.M., 2003, "The Mechanism of Sinkhole Formation in Glacial Sediments above the Retsof Salt Mine, Western New York", in Johnson, K. S.; and Neal, J. T. (eds.); Evaporite Karst and Engineering/Environmental Problems in the United States:@ Oklahoma Geological Survey Circular 109, p. 321-336.

Gowan, S. W.; Trader, S. M.; Piel, M. E.; Milliken, L D.; 2006, Stratigraphy of the Devonian and Upper Silurian in the Vicinity of the Retsof, Sterling and Hampton Corners Mines in Livingston County, New York", New York State Museum Map and Chart Series No. 45, 72 p.

Haley and Aldrich of New York, 1988, Report of Geologic and Hydrogeologic Conditions Adjacent to the Retsof Salt Mine, prepared by H&A of New York, Rochester, NY, for Geostock US, Inc., 28 p.

Kidde, 2006, Wellmaster - The flexible drop pipe system, Retrieved August 31, 2006, from http://www.kidde-fire.com/utcfs/ws-465/Assets/wellmasterbrochure.pdf.

Langevin, C.D., Shoemaker, W.B., and Guo, Weixing, 2003, MODFLOW-2000, the U.S. Geological Survey Modular Ground-Water Model-Documentation of the SEAWAT-2000 Version with the Variable-Density Flow Process (VDF) and the Integrated MT3DMS Transport Process (IMT): U.S. Geological Survey Open-File Report 03-426, 43 p.

Parkhurst, D.L. and Appelo, C.A.J., 1999, User's guide to PHREEQC (version 2)—A computer program for speciation, batch-reaction, one-dimensional transport, and inverse geochemical calculations: U.S. Geological Survey Water-Resources Investigations Report 99-4259, 312 p.

RE/SPEC, 2003, Draft calculation of brine squeeze rate from the Retsof (NY) Mine, Prepared by RE/SPEC Inc., Rapid City, SD, for Alpha Geoscience, 9 p.

Yager, R.M.; Miller, T.S.; Kappel, W.M., 2001, Simulated effects of salt-mine collapse on ground water flow and land subsidence in a glacial aquifer system, Livingston County, New York: U.S. Geological Survey Professional Paper 1611, 85 p.

Yager, R.M.; Misut, P.E., Langevin, C.D., Parkhurst, D.L., 2009, Brine Migration from a Flooded Salt Mine in the Genesee Valley, Livingston County, New York: Geochemical Modeling and Simulation of Variable Density Flow: U.S. Geological Survey Professional Paper 1767, 51 p.

Yager, R.M.; Miller, T.S.; Kappel, W.M., Misut, P.E., Langevin, C.D., Parkhurst, D.L., deVries, M.P., 2012, Simulated Flow of Groundwater and Brine from a Flooded Salt Mine in Livingston County, New York, and The Effects of Remedial Pumping on an Overlying Aquifer: U.S. Geological Survey Open-File Report 2011-1286, 15 p

W1C: TIME-DOMAIN ELECTROMAGNETIC SOUNDINGS FOR THE DELINEATION OF SALINE GROUNDWATER IN THE GENESEE RIVER VALLEY, WESTERN NEW YORK

JOHN H. WILLIAMS[1], WILLIAM M. KAPPEL[2], CAROLE D. JOHNSON[3],
ERIC A. WHITE[3], AND PAUL M. HEISIG[1]
USGS New York Water Science Center, [1]Troy, NY; [2]Ithaca, NY; [3]USGS Branch of Geophysics, Storrs, CT

INTRODUCTION

The U.S. Geological Survey, in cooperation with the New York State Department of Environmental Conservation, is investigating the distribution of saline groundwater in the Genesee River Valley near the former Retsof salt mine (fig. 1). As part of this study, paired time-domain electromagnetic (TEM) soundings and horizontal-to-vertical spectral ratio (HVSR) seismic soundings were made at 39 locations during the fall of 2016 to determine the presence of saline groundwater and depth to the bedrock surface, respectively. All measurement sites were west of Geneseo, New York, on the Genesee River valley floor north and south of the sinkhole area that developed as a result of the roof collapse and flooding of the Retsof mine in 1994 (fig. 1). An integrated analysis of the TEM and HVSR soundings with borehole logs, coupled with groundwater-sample data from previous investigations, allowed the delineation of zones of high electrical conductivity associated with saline water in the lower part of the valley fill and underlying bedrock to depths greater than 1,000 feet (ft). This article describes the TEM sounding method and its application in the ongoing investigation, presents results of the TEM analysis at two of the sounding sites, and identifies proposed sites for additional TEM/HVSR sounding data collection during the fall of 2017. Supporting data for this study are available in a separate data release (Johnson and others, 2017).

TIME-DOMAIN ELECTROMAGNETIC METHOD (TEM)

The TEM sounding system used in this study consisted of a wire transmitter loop deployed in a square configuration on the ground, small receiver coils placed in the center of the square loop, a control unit, and a power source (fig. 2). An electric current generated by a battery was pulsed through the transmitter wire, and the resulting electromagnetic field and its decay was measured at the receiver, and the decay data was recorded as a function of time with the control unit. Inversion of the TEM data produced a layered geo-electric model of the subsurface electrical conductivity beneath the sounding site. (See also ‘Basic Principles of TEM’, at the end of the article).

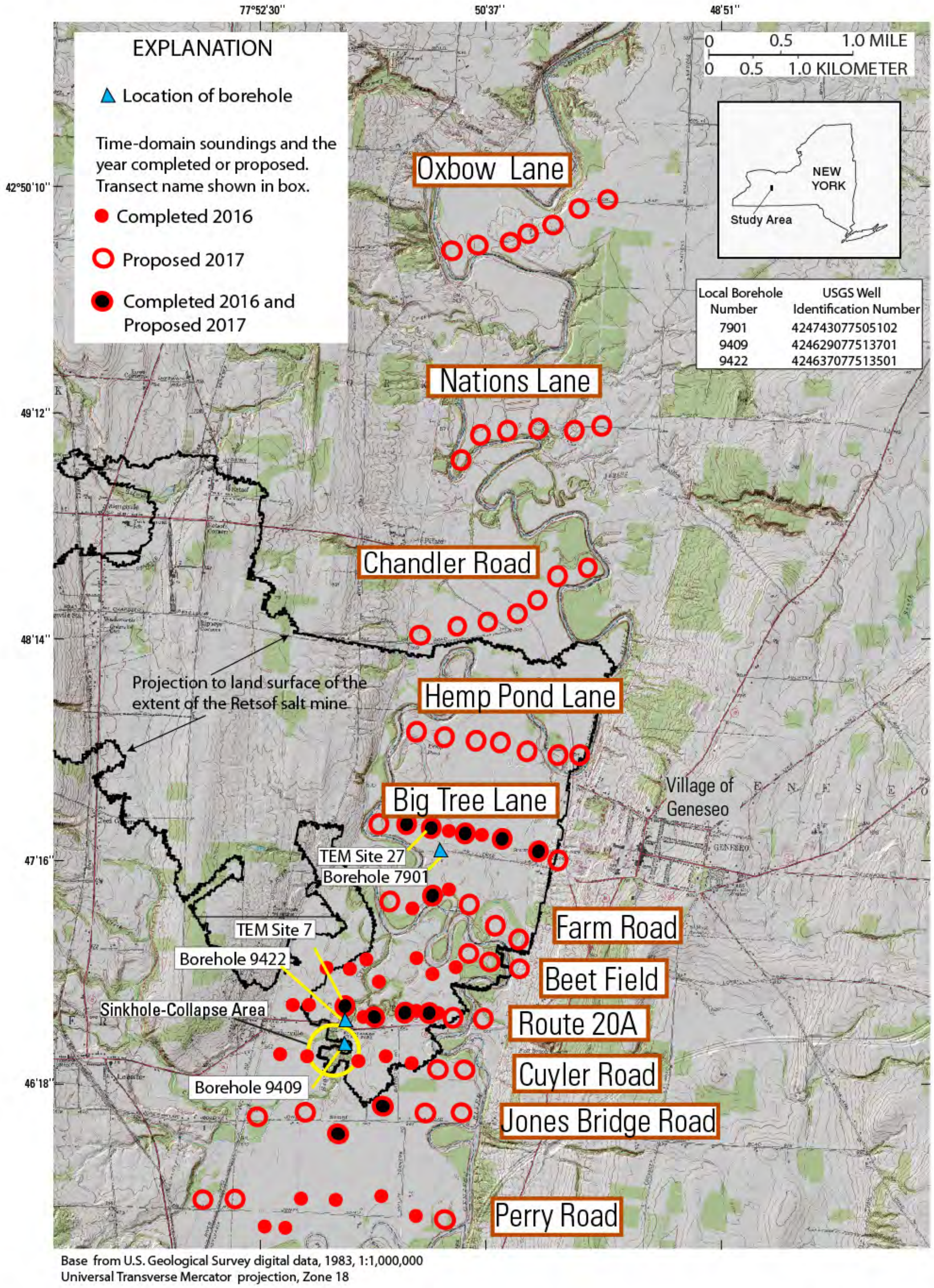

Figure 1 - Location of study area west of Geneseo, New York, sinkhole-collapse area, time-domain electormagnetic (TEM) and horizontal-to-vertical seismic resonance (HVSR) soundings and transects, and selected boreholes.

TIME-DOMAIN ELECTROMAGNETIC SOUNDING RESULTS

The results of the TEM soundings for site 7 of the Route 20A transect and for site 27 of the Big Tree Lane transect (fig. 1) are presented below. Although no borehole logs or groundwater-quality sample data were collected near these sites or any of the other sounding sites as part of the present study, information from previous investigations related to mine development and operation, sinkhole (chimney) collapse, and brine migration and mitigation were used to evaluate the results of the TEM and HVSR methods. These data include the Empire State Organized Geologic Information System (https://esogis.nysm.nysed.gov/) and reports by Yager and others (2001, 2009, and 2012), Gowan and others (2005), and Gowan (2013).

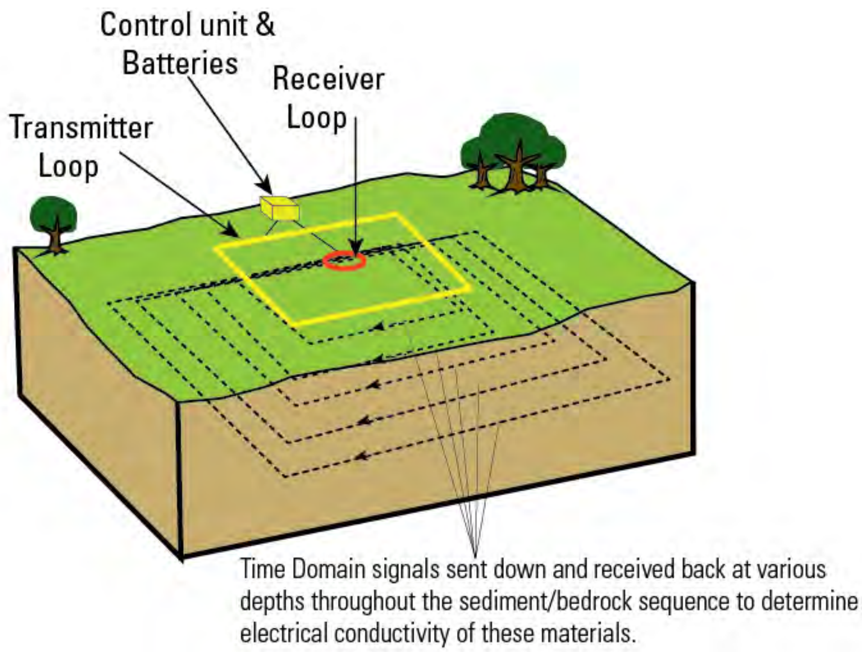

Figure 2. Time-domain electromagnetic equipment and signal propogation schematic.

TEM Sounding Site 7

TEM sounding site 7 and borehole sites 9409 and 9422 are at the edge of the sinkhole-collapse area just north and south of New York State Route 20A (fig. 1). Borehole 9409 was originally installed in 1994 with 527 ft of casing through the valley-fill deposits and 311 ft of open hole in bedrock, but was later deepened to about 900 ft. Geophysical logs were collected from the borehole in 1994 and in 2004 (fig. 3). Borehole 9422 was installed in 1994 with a 10-ft well screen in the basal valley-fill deposits that extended slightly into the top of bedrock. Both boreholes were periodically sampled for chlorides from 2004 to 2014, prior to and following pumping at the sinkhole-collapse area to mitigate the migration of brine. Analysis of the geophysical logs and borehole-sample results indicated that the chloride concentration of groundwater from the basal valley-fill deposits and the fractured bedrock surface in 2004 was about 23,000 mg/L, a more than 40-fold increase from that estimated for this interval in 1994. Analysis of the geophysical logs and borehole-sample results indicated that chloride levels in groundwater from the Onondaga Limestone interval in 2004 were about 35,000 mg/L, and that from the lower Syracuse Formation (saline) interval were about 185,000 mg/L. This latter chloride concentration was representative of the saturated brine moving upward from the flooded mine through the sinkhole-collapse chimney.

The geo-electric model developed for TEM sounding site 7 (right side column of fig. 3) displays an increase in electromagnetic conductivity that is consistent with the distribution of salinity indicated by the geophysical logs and chloride concentrations in groundwater sampled from boreholes 9409 and 9422 in 2004. Below the top of bedrock at 515 ft below land surface (bls), the geo-electric model displays increasing conductivity with depth that reflects the upward movement of brine from the collapsed mine roof at 1,100 ft bls and upward flow of saline water from the Onondaga Limestone-Bertie Formation contact at 600 ft bls through the fractured and solutioned bedrock in and near the collapse area. Above the top of bedrock, the model displays high conductivity in the lower part of valley-fill deposits with the highest conductivity zone within the glaciofluvial deposits between 400 to 480 ft bls.

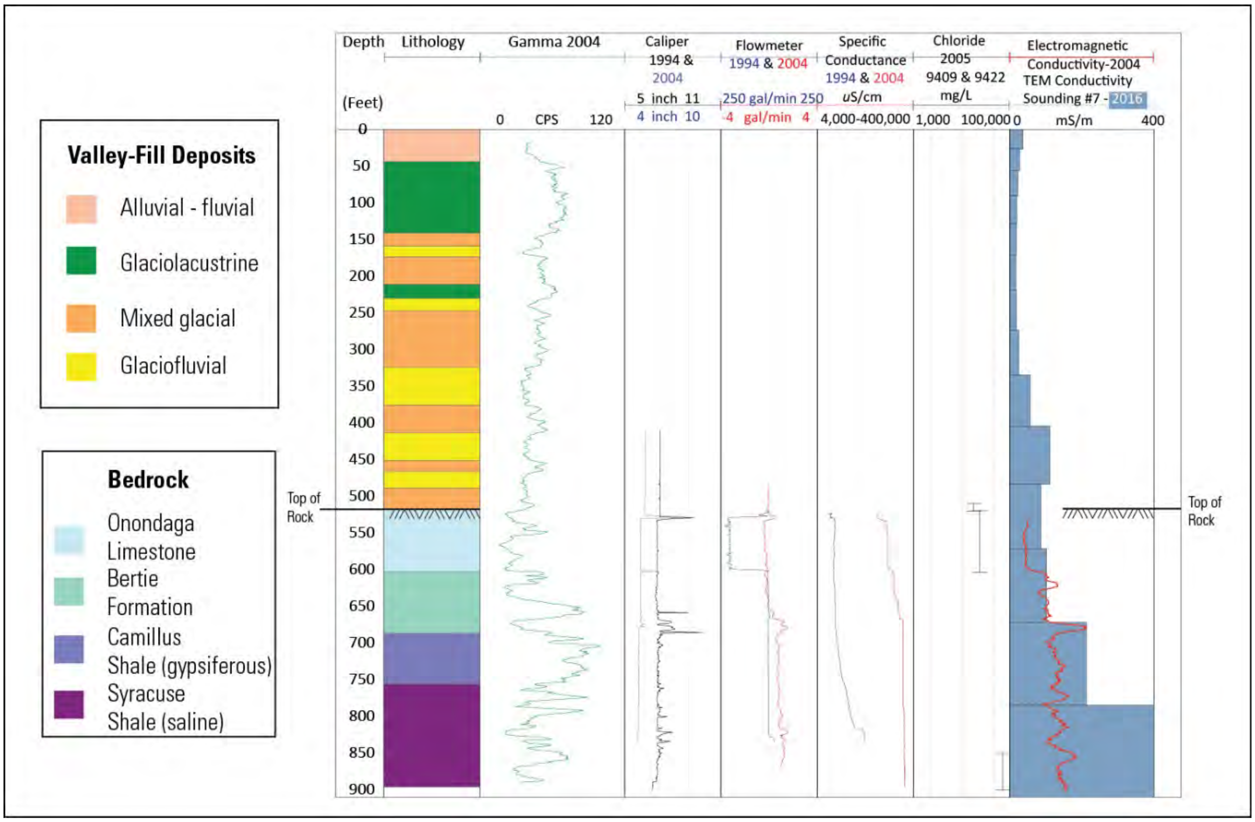

Figure 3 - Lithostratigraphic and geophysical logs collected from borehole 9409 in 1994 and 2004, chloride concentrations in groundwater samples from boreholes 9409 and 9422, and the geo-electric model developed for the TEM sounding site 7. [CPS - counts per second; gal/min-gallons per minute; uS/cm-microsiemens per centimeter; mg/L-milligrams per liter; mS/m millisiemens per meter.]

TEM Sounding Site 27

TEM sounding site 27 and borehole site 7901 are near the western end of Big Tree Lane (fig. 1). Borehole 7901 was drilled in 1979 to provide access for power to the mine, close to where active mining was occurring at the time. Analysis of a focused guard conductivity log collected in the mudded hole prior to the installation of casing to the bottom of the Onondaga Limestone indicated that saline water was present in the basal glaciofluvial deposits and fractured top of bedrock at 470 to 495 ft bls and freshwater was present in glaciofluvial deposits at 415 to 440 and at 230 to 275 ft bls (fig. 4). In 1995, the bottom of borehole 7901 was plugged and grouted up to near the top of bedrock, and the casing was perforated from 400 to 455 ft bls. During 1995, the chloride concentration in groundwater sampled from this retrofitted borehole was about 13,700 mg/L.

The geo-electric model developed for TEM sounding site 27 (the far right column of fig. 4) displays 1) an elevated-conductivity distribution consistent with the distribution of salinity in the lower part of the valley-fill deposits and fractured top of bedrock indicated by the focused guard conductivity log from borehole 7901 in 1979, and 2) the subsequent increase in conductivity in the basal glacial deposits as indicated by the chloride concentration of about 13,700 mg/L in groundwater sampled from 400 to 455 ft bls in the retrofitted borehole in 1995. The geo-electric model displays the highest electrical conductivity between 415 and 495 ft bls. The lowest electrical conductivity in the model is associated with the freshwater-bearing glaciofluvial deposits at 230 to 275 ft bls.

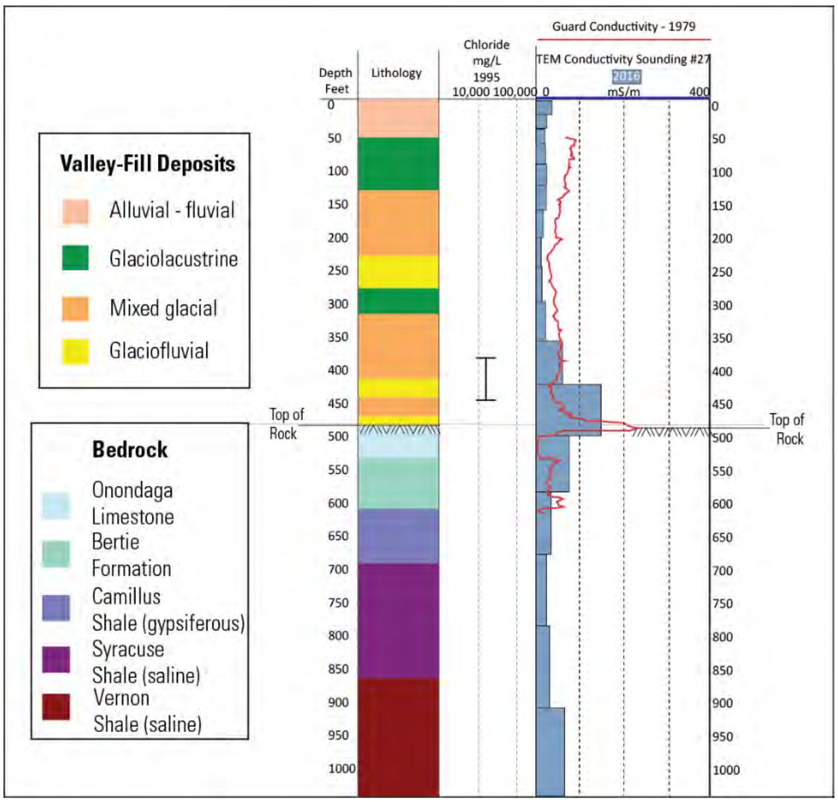

Figure 4 - Lithostratigraphic log from borehole 7901, chloride concentration in a groundwater sample from retrofitted borehole 7901 in 2005, and conductivity log from 1979 with the geo-electric model developed for the TEM sounding site 27. [mg/L - milligrams per liter; mS/m - millisiemens per meter.]

PROPOSED FALL-2017 GEOPHYSICAL SURVEY

The results from the fall 2016 geophysical survey indicated that TEM is an effective and efficient method for the delineation of saline groundwater in the Genesee River Valley and further application of this non-invasive technique is warranted. The following geophysical survey program is proposed for late October-early November 2017 (fig.1):

1) Collect paired TEM and HVSR soundings at 23 new sites west and east of the existing Perry Road, Jones Bridge Road, Cuyler Road, Route 20A, Beet Field, Farm Road, and Big Tree Lane transects to provide more complete coverage across the valley floor;

2) Collect TEM soundings at 12 previously established sites along the existing Jones Bridge, Route 20A, Farm Road, and Big Tree Lane transects to evaluate if the subsurface conductivity at any of those sites has changed between the fall of 2016 and the fall of 2017; and

3) Collect paired TEM and HVSR soundings at 28 new sites along the Hemp Pond Lane, Chandler Road, Nations Lane, and Oxbow Lane transects to track the northward extent of the high-conductivity zone delineated in the lower part of the valley-fill deposits found along the Big Tree Lane transect.

BASIC PRINCIPLES OF THE TIME-DOMAIN ELECTROMAGNETIC METHOD (TEM)

The time-domain electromagnetic method uses a transmitter that drives an electrical current through a square loop of insulated cable laid on the ground. The current consists of equal periods of time-on and time-off, with base frequencies that generally range from 30 to 300 Hertz (Hz), producing an electromagnetic field. Termination of the current flow is not instantaneous, but occurs over a very brief period of time (a few microseconds) known as the ramp time, during which the magnetic field is time-variant. The time-variant nature of the primary electromagnetic field creates a secondary electromagnetic field in the ground beneath the loop, in accordance with Faraday's Law, that generally mirrors the transmitter loop (Halliday and Resnick, 1974). This secondary field immediately begins to decay, in the process generating additional eddy currents that propagate downward and outward into the subsurface like a series of smoke rings. Measurements of the secondary currents are made only during the time-off period by a receiver located in the center of the transmitter loop. The signal strength of the decaying currents at specific times and depths is controlled by the bulk conductivity of subsurface rock units and their contained fluids (Stewart and Gay, 1986; Mills and others, 1988; Goldman and others, 1999; McNeill, 1994). The voltage decay curve collected at the receiver is related to the subsurface conductivity (geo-electrical model) by a process of inversion (for example HydroGeophysics Group, http://hgg.au.dk/software/spia). The depth of investigation (DOI) depends on the time interval after shutoff of the current and the signal strength of the late-time signal, since at later times the receiver is sensing eddy currents at progressively greater depths. The DOI was determined for this investigation using methods described by Christiansen and Auken (2012).

BASIC PRINCIPLES OF HORIZONTAL-TO-VERTICAL SEISMIC RESONANCE SOUNDINGS (HVSR)

The HVSR ambient-noise seismic method, sometimes referred to as "passive seismic" is used to estimate unconsolidated sediment thickness and map the bedrock surface. The HVSR method uses a single, broad-band three-component (two horizontal and one vertical) seismometer to record ambient seismic noise. In areas that have a strong acoustic contrast between the bedrock and overlying sediments, the seismic noise induces resonance at frequencies that range from about 0.1 to 64 Hz. The ratio of the average horizontal- to- vertical spectrums produces a spectral-ratio curve with peaks at fundamental and higher-order resonance frequencies. The spectral ratio curve (the ratio of the averaged horizontal-to-vertical component spectrums) is used to determine the fundamental resonance frequency, which can be interpreted using either an average shear-wave velocity or a regression equation to estimate sediment thickness and depth to bedrock (Lane and others, 2008) and Johnson and Lane, 2016.

ACKNOWLEDGEMENTS

We thank the farmers and land owners of the Genesee River Valley for graciously granting access to the geophysical sounding sites. Without their cooperation, these soundings would not have been possible. We thank Mr. Robert Stryker of the Livingston County Soil and Water Conservation District who helped coordinate land access with the farming community. Alton Anderson, Mike Izdebski, and Adam Baldwin of the USGS are acknowledged for their able support during field data collection.

REFERENCES CITED

Christiansen, A. V. and Auken, E., 2012 , A global measure for depth of investigation, Geophysics, v 77, no. 4, p. WB171-WB177 7 p. doi: 10.1190/geo2011-0393.1.

Goldman, M., Ezersky, M., Hurwitz, S., and Gvirtzman, H., 1999, Geophysical (time domain electromagnetic model) delineation of a shallow brine beneath a freshwater lake, the Sea of Galilee, Israel: Water Resources Research, v. 35, no. 12 pp. 3631-3638.

Gowan, S.W., Nadeau, J. M., and Smith, J. N., 2005, Movement and control of brine rising from the Retsof salt mine eleven years after the collapse: Solution Mining Research Institute, Spring 2005 Meeting, Syracuse, New York, 17 p.

Gowan, S. W., 2013, Report of the results of the Akzo brine pumping test and recommendations for the future: Alpha Geoscience, Clifton Park, New York, 73 p., 16 appendices, 5 plates.

Halliday, D., and Resnick R., 1974, Fundamentals of physics: New York, John Wiley and Sons, Inc., 655p.

HydroGeophysics Group – Department of Geoscience, SPIA-Processing and inversion of ground based TEM data. Accessed June, 2017, at http://hgg.au.dk/software/spia/.

Johnson, C.D., White, E.A., Williams, J.H., and Kappel, W.M., 2017, Transient electromagnetic surveys collected for delineation of saline groundwater in the Genesee Valley, New York, October-November 2016: U.S. Geological Survey data release https://doi.org/10.5066/F79C6VXX.

Johnson, C.D. and Lane, J.W., Jr., 2016, Statistical comparison of methods for estimating sediment thickness from horizontal-to-vertical spectral ratio (HVSR) seismic methods: An example from Tylerville, Connecticut, USA *in* Symposium on the Application of Geophysics to Engineering and Environmental Problems, March 20-24, 2016, Denver, Colorado, Proceedings: Denver, Colorado, Environmental and Engineering Geophysical Society, 7 p.

Lane, J.W., Jr., White, E.A., Steele, G.V., and Cannia, J.C., 2008, Estimation of bedrock depth using the horizontal-to-vertical (H/V) ambient-noise seismic method, in Symposium on the Application of Geophysics to Engineering and Environmental Problems, April 6–10, 2008, Philadelphia, Pennsylvania, Proceedings: Denver, Colo., Environmental and Engineering Geophysical Society, 13 p.

McNeill, J.D., 1994, Principles and application of time domain electromagnetic techniques for resistivity sounding: Geonics Limited, Mississauga, Ontario Canada, 16 p.

Mills, T., Hoekstra, P., Blohm, M., and Evans, L. 1988, The Use of Time Domain Electromagnetic Soundings for Mapping Sea Water Intrusion in Monterey County, CA: A Case History: Ground Water, v. 26, No. 6, Nov.-Dec., pp. 771-782.

Stewart, M. and Gay, M. C. (1986), Evaluation of transient electromagnetic soundings for deep detection of conductive fluids, Ground Water, 24, p. 351–356.

Yager, R.M., Miller, T.S., and Kappel, W.M., 2001, Simulated effects of 1994 salt-mine collapse on groundwater flow and land subsidence in a glacial aquifer system, Livingston County, New York: U.S. Geological Survey Professional Paper 1611, 85 p., at http://pubs.usgs.gov/pp/pp1611/.

Yager, R.M., Misut, P.E., Langevin, C.D., and Parkhurst, D.L., 2009, Brine migration from a flooded salt mine in the Genesee Valley, Livingston County, New York: Geochemical modeling and simulation of variable-density flow: U.S. Geological Survey Professional Paper 1767, 59 p., at http://pubs.usgs.gov/pp/pp1767/.

Yager, R.M., Miller, T.S., Kappel, W.M., Misut, P.E., Langevin, C.D., Parkhurst, D.L., and deVries, M.P., 2012, Simulated Flow of Groundwater and Brine from a Flooded Salt Mine in Livingston County, New York, and Effects of Remedial Pumping on an Overlying Aquifer: U.S. Geological Survey Open-File Report 2011–1286, 16 p., at http://pubs.usgs.gov/of/2011/1286.

W1D: 3D GRAVITY SURVEY OF GLACIAL LAKE GENESEO, LIVINGSTON CO, NY

SCOTT GIORGIS, MICHAEL REED
Department of Geological Sciences, SUNY Geneseo, Geneseo, NY 14414

ERIC HORSMAN
Department of Geological Sciences, East Carolina University, Greenville, NC 27858

ABSTRACT

Much of western New York's landscape has been shaped by the Pleistocene glacial advance and retreat of the Laurentide Ice Sheet, which carved the Finger Lakes within the region. The Middle and Late Wisconsin glaciations from ~35,000-12,000 years ago have since filled in some of these lakes, including Glacial Lake Geneseo (previously the region's westernmost Finger Lake), with glacial till and sediment fill from the Genesee River. Glacial Lake Geneseo was a proglacial lake dammed by the Fowlerville Moraine to the north in Avon and bounded by bedrock valley walls in Dansville to the south. The lake spanned 35 km in length, with a total area of 135 km2 at its 189 meter highstand. The less consolidated glacial till and fluvial sediment filling this paleo-valley has a lower density than the surrounding shale and limestone. This density contrast creates a local gravitational anomaly, which was measured using a Lacoste and Romberg gravimeter. After removal of a strong regional gradient, the buried paleo-valley is clearly visible in the Bouguer anomaly and has a range up to 15 mGals. As expected, relative highs occur along the west and east valley walls, and the lows characterizing the center of the valley. The shape of the Bouguer anomaly interpolation suggest a more complex valley geometry than previously proposed models using sparse well log data. A valid structure contour map of depth to bedrock can be drawn using these data and will be useful for hydrologic processes in the largely agricultural community, as well as assistance in the planning of local mining efforts.

A1 AND B1: DEPOSITIONAL ENVIRONMENTS ACROSS A CENTRAL TROUGH OF THE NORTHERN APPALACHIAN BASIN, DEEP RUN SHALE MEMBER (MOSCOW FORMATION) OF THE FINGER LAKES

STEPHEN M. MAYER
5475 East Lake Rd. Romulus, NY 14541

GORDON C. BAIRD
Dept. of Geosciences, SUNY at Fredonia, Fredonia, NY 14063

CARLTON E. BRETT
Dept. of Geology, University of Cincinnati, Cincinnati, OH, 45221

INTRODUCTION

The Middle Devonian Givetian Hamilton Group is well known for its thick sequence of variably fossiliferous siliciclastics. Many naturalists and scientists including James Hall (1843), Amadeus Grabau (1899), and J.M. Clarke (1903) studied the fossil faunas preserved in these shales and limestones. Other early workers including Cooper (1930), attempted to correlate the distinct lithologic units within western and central New York. During the last 20-30 years detailed microstratigraphic and paleontological studies (Brett and Baird, 1985, 1994, Mayer, 1994, Mayer et al, 1994, Miller, 1991 and numerous others) have resulted in high resolution correlations and improved the general understanding of the dynamics of the Hamilton Group. The extensive stratigraphic field analysis by Baird (1979) firmly established the sedimentary relationships between the lithologic units at the boundary between the Ludlowville and Moscow Formations.

The purpose of the present study was to identify and correlate isochronous horizons and beds within the Deep Run Shale Member of the lower Moscow Formation across the Finger Lakes Region of New York State. Moreover, biofacies gradients were surveyed from west to east, facilitating interpretation of depositional history and environments. The study also examined the nature and character of this unit and its westward erosional truncation beneath the Menteth Limestone. Lastly, previously undescribed Ludlowville - Moscow sections were investigated along the west shore of Seneca Lake.

PALEOGEOGRAPHY

During Middle Devonian Givetian time (~ 380-385 Ma), the regional geology of eastern North America was influenced by the breakup of Gondwana and the amalgamation of terranes and intense mountain building (Benton, 2004}. The convergence and collision of crustal fragments comprising the Avalon terrane (Blakey, 2008) resulted in the accretion of Avalonia to Laurentia. This orogenic event and associated deformation gave rise to the Acadian Mountains and concurrent loading was predominantly responsible for subsidence of the Appalachian Foreland Basin (Van der Voo, 1983, 1988, Ettensohn, 1985). Sediments eroding from these mountains were shed westward into the foreland basin. Hamilton Group mudstones and carbonates accumulated as a clastic wedge within the prograding Catskill Delta Complex in the northern arm of the Appalachian Basin.

Over 15 meters (50 feet) of sediments of the Deep Run Shale Member were deposited in a central subsiding trough located in the present day Canandaigua Lake Valley. This central depocenter was migrating westward due to structural flexure of the basinal crust through time. Successively higher units of the Ludlowville-Moscow Formations are observed to obtain their greatest thickness from east to west across New York (Brett et al, 2013). Furthermore, sections of the Deep Run Member thin to less than 5 meters (15 feet) toward the Seneca –Cayuga Valleys across an east-southeast trending shelf where the facies become equivalent to the Portland Point Limestone Member (Baird, 1979). Similarly, on the opposite, western side of the trough, Deep Run sediments dramatically thin to less than 2.5 meters (8 feet) in the present day Genesee Valley. The sediments, in turn, are completely removed by erosional truncation prior to the deposition of the Menteth Limestone across a west-northwest trending sediment starved carbonate shelf. Key Ludlowville-Moscow outcrops studied in western and central Finger Lakes of New York are shown in Figure 1.

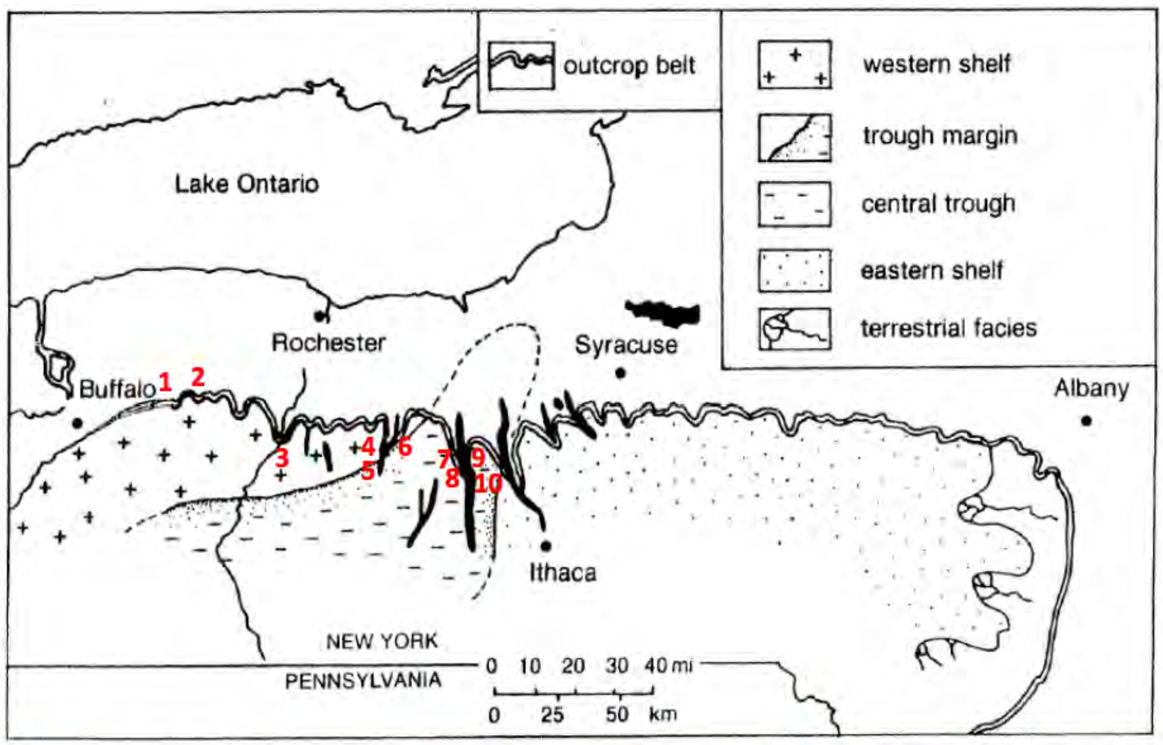

1. **Eleven-Mile Creek**
2. **Murder Creek**
3. **Jaycox Creek**
4. **Tichenor Gully**
5. **Menteth Gully**
6. **Deep Run Gully**
7. **Kashong Creek**
8. **Houston Rd. Gully**
9. **Shale banks along Seneca Lake**
10. **Indian Creek**

Figure 1. Ludlowville – Moscow outcrop belt in New York. Numbered locations correspond to studied sections. (Modified from Brett and Baird, 1986).

PRINCIPLES AND METHODOLOGY

The regional stratigraphy and paleoecology of the Deep Run Shale Member was determined by precise measurement of the individual beds contained within the sequence. A common steel tape and an eye level were used to determine the exact thickness of each bed, centimeter by centimeter. Furthermore, the biofacies of each bed was determined by the careful attention to the smallest of details and collecting and recording all fossils found.

Initially, a general and broad spectrum of fossils was observed from each bed at all localities. However, to better understand and enhance paleoenvironmental interpretations, a detailed sampling of the fossils present or absent in key layers was conducted in three regions which included from west to east: Jaycox Creek (Genesee Valley), Deep Run Gully (Canandaigua Valley), and Kashong Glen (Seneca Valley). Whenever it was difficult to positively identify the fossil at the outcrop, field samples were brought back to the laboratory for further analysis. Species abundance is an estimate due to the shelly debris in these beds is commonly disarticulated and not in-situ. It is to this extent that the correlation of the beds and the interpretation of the paleoecological environments across the basin can be deduced for the Deep Run Shale Member.

STRATIGRAPHY OF THE DEEP RUN SHALE MEMBER CANANDAIGUA LAKE VALLEY –SENECA LAKE VALLEY

On the east side of Canandaigua Lake, about 5.6 km (3 ½ miles) south of Routes 5 & 20 and the city of Canandaigua, a small creek named Deep Run Gully cuts downward into the bedrock exposing the complete type section of the Deep Run Shale Member. This unit is 15.95 meters (52.3 ft) thick and is overlain by the Menteth Member and underlain by the Tichenor Limestone and Jaycox Shale Members. Moreover, the upper strata of the Wanakah Member are also exposed at the base of the Deep Run Gully section. Cooper (1930) first designated the shale between the Menteth and Tichenor as the Deep Run Shale Member, which Baird (1979) supported. However up until now, the detailed microstratigraphy and paleontology of the Deep Run Shale Member has remained largely unstudied.

The Deep Run Shale Member conformably overlies the Tichenor, which typically exhibits a hummocky top surface (Fig. 2). The strata directly above the Tichenor, were interpreted by Brett and Baird (1986) to be part of a transitional phase of the Tichenor into the Deep Run Shale Member. This transitional phase of interbedded fossiliferous calcareous siltstone and calcareous shale was understood to merge downward both westward and eastward into condensed Tichenor deposits. At Deep Run, this unit is 1 meter (37 inches) thick and forms erosionally resistant ledges. This unit is hereby designated the Kipp Road Bed of the Deep Run Shale Member for strata at Deep Run Gully along Kipp Rd. The Kipp Rd Bed is regionally widespread and traceable in outcrop across the western Finger Lakes region of New York and is noticeably different from the Tichenor. The unit ranges regionally from a bluish-gray calcareous mudstone in the Genesee Valley to a medium-gray moderately calcareous siltstone in the Canandaigua Valley to a dark- gray blocky siltstone in the central Finger Lakes region (see also Baird et al 1988,1991 – thermal color effects).

The Kipp Road Bed contains a distinct and diverse well-preserved assemblage of fossils. Particularly noteworthy are very large *Eldredgeops rana* trilobites which are commonly articulated and up to 8 cm in length and 4.5 cm in width. *Greenops boothi*, typically represented only by a pygidium, and rare *Monodechenella macrocephala* trilobites can be found in this bed. Moreover, the trilobite *Bellacartwrightia whiteleyi* has been found in the Kipp Road Bed at Jaycox Creek in the Genesee Valley.

Additionally, large camerate crinoids including *Megistocrinus, Dolatocrinus* and *Gennaeocrinus* species, as well as associated holdfasts systems or “runners “are conspicuously abundant throughout the region. These “runners” commonly are about 1.25 cm in diameter and up to 30 cm long and can be found throughout the Kipp Road Bed regionally making them an exceptionally useful marker. Additionally, rare *Placoblastus* blastoids are even found in conjunction with the other pelmatozoans.

Both tabulate and rugose corals are observed in the Kipp Road Bed but species type changes laterally from west to east across the Finger Lakes region. Whereas the corals *Favosites hamiltonaie* and *Heliophyllum halli* dominate in the Genesee Valley, large aggregations of *Cystiphyllum conifollis* as well as the colonial coral *Eridophyllum subcaespitosum* are abundant throughout the Canandaigua Valley. Eastward the Eridophyllum corals replace the Cystiphyllum corals in the Seneca Lake Valley.

Furthermore, various brachiopods including *Mucrospirifer mucronatus, Mediospirifer audaculous, Meristella, Nucleospira*, and chonetids as well as bivalves and fenestrate and fistuliporoid bryozoans are observed in the Kipp Road Bed.

Stratigraphically above the Kipp Road Bed up to the Menteth Limestone Member, in both the Canandaigua Lake Valley and Seneca Lake Valley, the Deep Run Shale Member is predominately a thick depocenter wedge of silty mudstone to siltstone. This interval is hereby designated the Willard siltstone interval for the excellent exposure of beds on the east shore of Seneca Lake immediately north of the town of Willard, New York. Although this medium-gray siltstone interval obtains its maximum thickness around Deep Run Gully, 15 meters (49.25 ft), it is easily recognized in eastern sections. On the west side of Seneca Lake at Kashong Creek, the interval thins to 12 meters (39.4 ft) and on the east shore of the lake, at Willard it further thins to 4 meters (13.1 ft). Similarly this interval thins dramatically west of the Canandaigua Valley.

At the top of the Kipp Road Bed to basal Willard transition there is an important interval of similar fossils at several localities. Articulated crinoid crowns of *Taxocrinus* commonly occur associated with the gastropod *Naticonema lineata.* On the east side of Canandaigua Lake, at the Deep Run type section, a major assemblage of these fossils is developed in the creek floor downstream from the Deep Run high falls. Similarly, on the west side of the lake, at both Tichenor Point and Menteth Gully are localized abundances of *Naticonema* and *Taxocrinus* columnals in this interval.

The Willard siltstone interval is conspicuously barren to poorly fossiliferous. Evidence of pervasive bioturbation exists from the numerous *Zoophycos* spreiten and pyritized marginal tubes throughout the interval. However, when macrofossils are found in the interval, they appear to be concentrated into shell-rich horizons or localized lenses or aggregations. Fossils are moderately abundant in these shelly horizons but of low diversity, and dominated by either a few in-situ brachiopods and/or bivalves. Brachiopods include *Mucrospirifer mucronatus, Mediospirifer audaculus, Tropidoleptus carinatus, and Devonochonetes coronatus* at Deep Run Gully. Likewise, bivalves include *Paleoneilo*, *Plethomytilus*, *Orthonata*, *Modiomorpha*, *Cypricardella*, and *Goniophora* at Kashong Glen as well as at the lake shore near Willard. Other typical fossils include scattered trilobites and crinoid debris.

A horizon in the middle of the Willard siltstone interval of harder siltstone appears to be spatially correlative between the Canandaigua Valley and the Seneca Valley, although the bed may be manifested slightly differently between outcrops. At Deep Run Gully and Kashong Glen, the bed is in the same stratigraphic position forming an erosionally resistant ledge in the face of the waterfalls of those creeks. In Deep Run Gully, the bed is 7.5-10 cm (3-4 inches) thick and is a prominent layer whereas at Kashong Glen it is only 2.5-5 cm (1-2 inches) thick cryptic layer. This isochronous horizon does not contain fossils and may have been deposited as a single large tempestite event.

The uppermost subunit of the Willard siltstone interval is characterized by coarse-grained, very wavy and undulating or irregular and jagged surfaces suggestive of increased silt content and is disconformably overlain by the Menteth Limestone Member. This erosional surface can be traced both east and west of the Canandaigua Lake Valley truncating the Deep Run Shale Member.

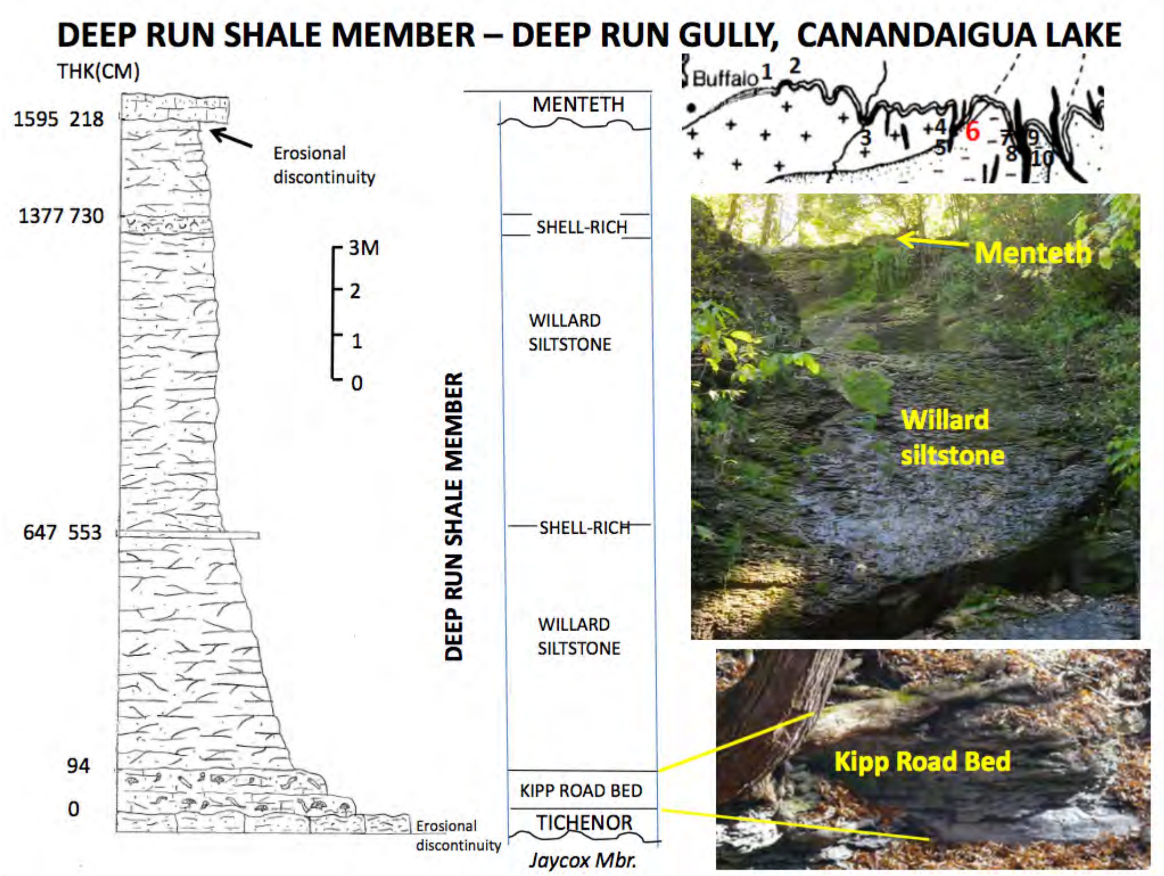

Figure 2. Generalized stratigraphic column of the Deep Run Shale Member type section at Deep Run Gully, Canandaigua Lake Valley.

STRATIGRAPHY OF THE DEEP RUN SHALE MEMBER
CANANDAIGUA LAKE VALLEY – ERIE COUNTY

The Deep Run Shale Member thins dramatically west of Canandaigua Lake. At Jaycox Creek in the Genesee River Valley, the Kipp Road Bed and the Willard siltstone interval, are still observed but notably thinner (Fig. 3). The complete section comprising the Deep Run interval is only 2.4 meters (8 ft) thick in which the Kipp Road Bed is 29 cm (11.4 inches) thick and the Willard siltstone interval is 2.1 meters (7 ft) thick.

DEEP RUN SHALE MEMBER – JAYCOX CREEK, GENESEE RIVER VALLEY

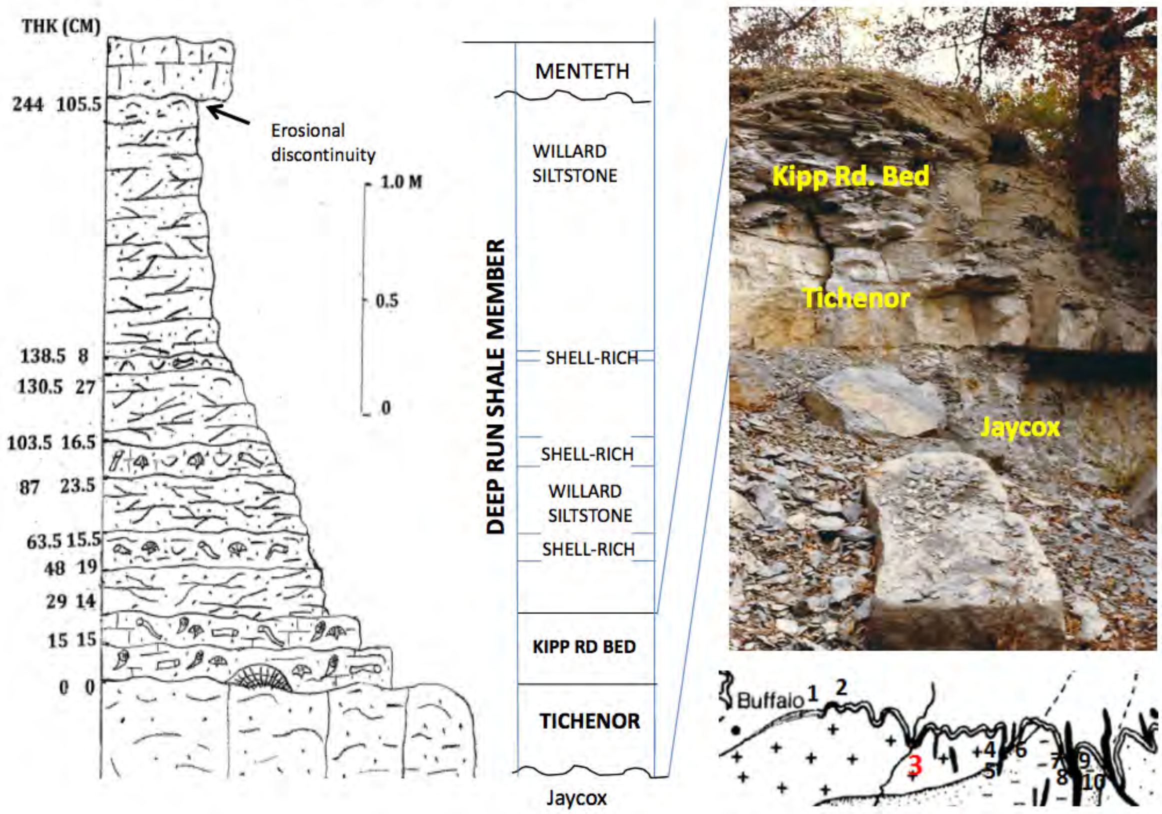

Figure 3. Generalized stratigraphic column of the Deep Run Shale Member at Jaycox Creek, Genesee River Valley.

The Kipp Road Bed is a bluish-gray calcareous mudstone in the Genesee Valley rich in fossils including large rugose and tabulate corals, large phacopid trilobites, crinoids and blastoids, brachiopods and bivalves as well as fenestrate and fistuliporoid bryozoans. The Willard siltstone interval contains three distinct shelly horizons separated by barren to poorly fossiliferous, *Zoophycos* churned mudrock.

The Deep Run Shale Member continues to thin westward across Genesee County to 28-30 cm (less than 1 foot) thick at Murder Creek. The Kipp Road Bed is a gray, very calcareous, blocky mudstone about 13-15 cm (5-5.9 inches) thick and contains conspicuous crinoid "runners" and corals. Moreover, the Willard siltstone interval is also about 15 cm (5.9 inches) thick and contains a sparse fauna predominately of the brachiopod *Mucrospirifer mucronatus* and a few bivalves. In turn, the Menteth Limestone sharply overlies this unit. The upper contact of the Deep Run Shale Member with the Menteth is highly irregular and has been erosionally overstepped by the Menteth.

Still further west, the unit if at all present is only a few centimeters thick at Elevenmile Creek. Here in places the Menteth Limestone directly overlies the Tichenor Limestone with only a vestige of the Deep Run Shale Member remaining sometimes between those units. In Erie County, west of Buffalo Creek and Cazenovia Creek, the condensed sequence comprising both the Menteth Limestone and Deep Run Shale Members are completely missing due to erosional overstep by the Windom Shale Member (Baird, 1979).

ANALYSIS OF UPPER LUDLOWVILLE-LOWER MOSCOW STRATIGRAPHY, SENECA LAKE VALLEY - A REINTERPRETATION OF BASIN AXIS DEPOSITION

Previous research by Baird (1979), Brett and Baird (1986), and Mayer (1994) examined in detail the Ludlowville – Moscow stratigraphy on the western side of Seneca Lake particularly at Kashong Glen (Fig. 4). However, investigation of these rock layers as the units intersect and dip beneath the shoreline of the lake, only 7.4 km (4.6 miles) south of Kashong Glen, has been hindered due to their inaccessibility from summer homes along the lake. By initially exploring the shoreline with a small boat, direct access was gained at the most pertinent points which provided important information about the geology of these previously undescribed sections. Additionally, a very small, unnamed stream gully emptying into the lake in this area and adjacent to Houston Road down cut into the rocks exposing the Jaycox through Menteth strata (Fig. 5).

Moreover, these sections have revealed additional beds, which may have been deposited only in the central trough of the Appalachian Basin prior to Deep Run time. At Houston Road Gully, the Jaycox Shale Member is overlain unconformably by the Tichenor which is 71 cm (28 inches) thick of interbedded crinoid-rich shale and recrystalline limestone. These layers grade upward into the Kipp Road Bed, which is 10 cm (3.9 inches) thick and exhibits the typical trilobite, crinoid "runner", brachiopod fauna. The Willard siltstone interval consists primarily of 14.53 m (47.67 ft) thick of barren to poorly fossiliferous calcareous siltstone intermixed with three very thin shell-rich horizons. The uppermost strata is 32 cm (12.6 inches) thick of wavy, coarse-grained siltstone which resemble "stacked" ripple marks. The Menteth Limestone Member disconformably overlies this sequence of strata.

At Kashong Glen, the Jaycox-Tichenor-Deep Run transition is noticeably different from the section at Houston Road Gully and consists of three distinct layers. At the base, a very hard 38 cm (15 inch) thick bioturbated, Menteth-like calcareous siltstone ledge unconformably overlies the Jaycox Shale Member. This bed, in turn, is overlain by a 122 cm (48 inch) thick calcareous siltstone unit barren of fossils. The uppermost layer is characterized by a richly fossiliferous muddy encrinite. This layer traditionally has been referred to as the Tichenor; however, the present study interprets these deposits here and at Houston Road Gully to lie above the Jaycox (uppermost Ludlowville Formation) and to be localized, early phases of Tichenor (Moscow Formation) deposition. Moreover, these deposits represent partial closure of the sequence boundary unconformity that floors the Moscow Formation.

The lowermost layer of the Deep Run Shale Member is 132 cm (52 inches) thick series of silty fossiliferous layers displaying the typical fauna so characteristic of the Kipp Road Bed. The overlying Willard siltstone interval consists of 13.31 m (43.67 ft) thick barren to poorly fossiliferous unit with a few shell-rich horizons. Similar to Houston Road Gully, the uppermost strata is 33 cm (13 inches) thick wavy, coarse-grained siltstone resembling ripple marks which is, in turn, overlain disconformably by the Menteth Limestone Member.

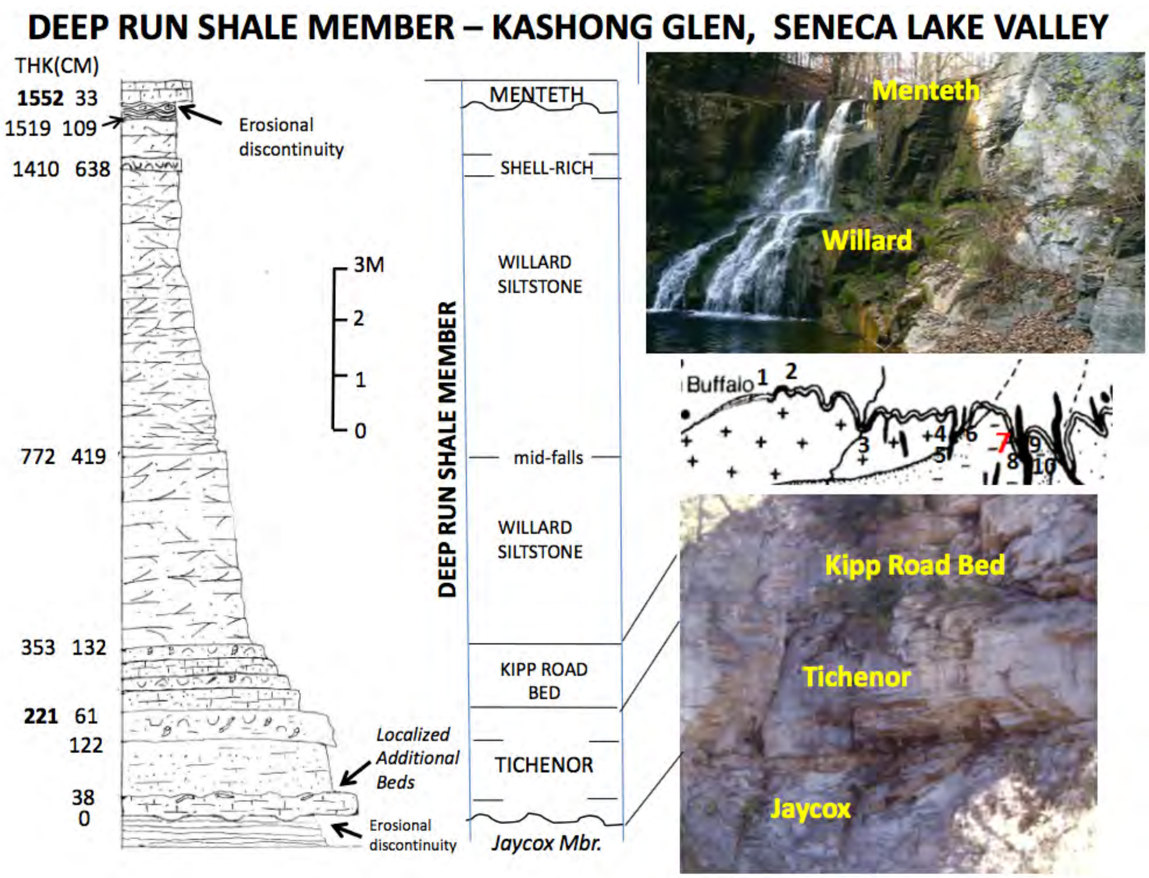

Figure 4. Generalized stratigraphic column of the Deep Run Shale Member, Kashong Glen, Seneca Lake Valley.

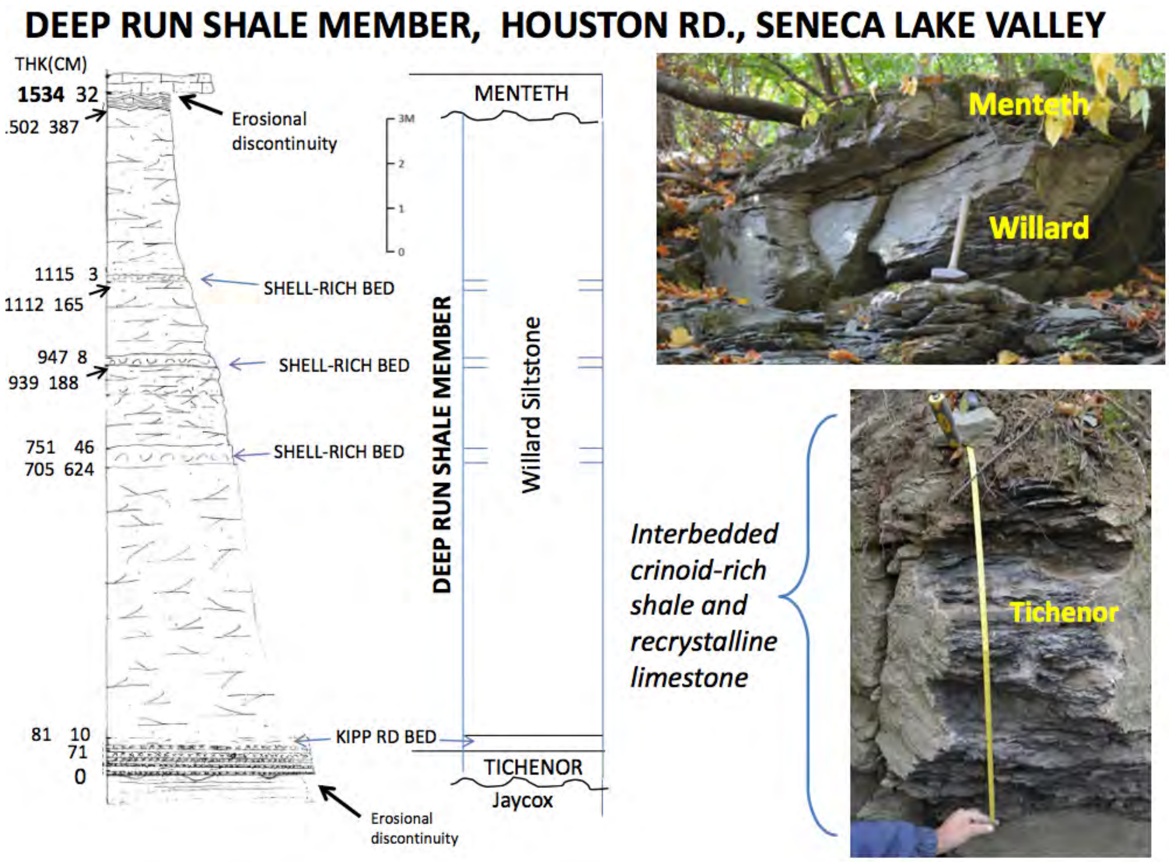

Figure 5. Generalized stratigraphic column of Deep Run Shale Member, Houston Road Gully, Seneca Lake Valley.

BIOFACIES GRADIENTS AND DEPOSITIONAL ENVIRONMENTS

The Deep Run Shale Member displays several isochronous beds, which can be directly correlated across the western and central Finger Lakes Region (Fig. 6). Moreover, several geographically widespread lithofacies and biofacies can be directly related to inferred depositional environments. Reconstructions of these depositional environments are based on the paleoecological models for the Hamilton Group presented in Brett, Baird, and Miller (1986) as well as in Brett et al (1990, 2007, 2013). The model (Fig. 7) shows the distribution of fossil associations along gradients of increasing bathymetry compared to gradients of increasing sedimentation and increasing turbidity. Furthermore, Brett et al (1994, 2013) have shown that the axis of the northern arm of the Appalachian Basin undergoes a progressive westward shift across New York State probably due to thrust loading in the Acadian Orogeny. During the time of the deposition of the Deep Run Shale Member, sediment accumulation was greatest in the central basin or depocenter now occupied by Canandaigua Lake Valley. Both to the east and west of this central trough, sediment accumulation was significantly less, as observed in the thickness of the outcrops of the Seneca Lake Valley and the Genesee River Valley. Furthermore, across the western shelf, sediment starvation played an important role in the depositional environments observed in the western localities.

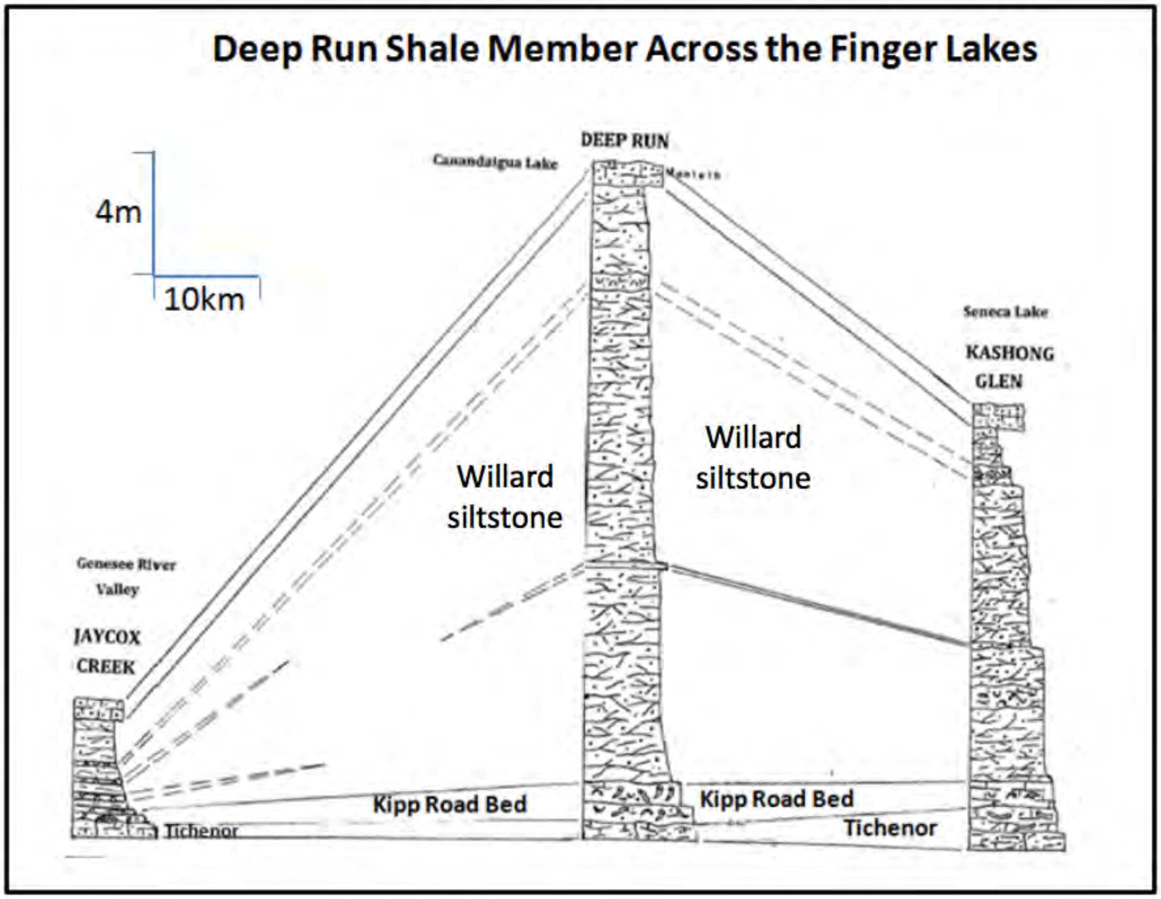

Figure 6. Correlation of the Deep Run Shale Member from the Genesee River Valley to Seneca Lake. Note schematic drawn to show emphasis on key units and not specific locality details.

Kipp Road Bed: Fossils in the western exposures of the Kipp Road Bed are representative of the *Favosites hamiltoniae* biofacies of Brett et al (2013). The fossils observed in sections at Jaycox Creek and further west are very diverse and abundant, yet this faunal assemblage may represent a time-averaged accumulation of fossils aggregated by relatively slow sedimentation. This is due to the observation of well-preserved corals *Favosites hamiltoniae* and *Heliophyllum halli* mixed in with disarticulated and/or broken shell and crinoidal debris within a condensed stratigraphic section. Furthermore, the occurrence of these corals, along with large trilobites, fenestrate bryozoans and brachiopods, is indicative of clear, warm, shallow water (Fig. 8).

As the Kipp Road Bed is traced eastward into the central depocenter, the *Favosites hamiltoniae* biofacies very gradually grades basinward into the *Spinocyrtia-Ptychopteria* biofacies of Brett et al (2013). Particularly noteworthy is the loss of the corals *Favosites* and *Heliophyllum* which are replaced by *Cystiphyllum* and Eridophyllum. However, most of the additional taxa remain similar but a few chonetid brachiopods, as well as the pteriomorph bivalve *Actinopteria,* are present to abundant as part of the *Spinocyrtia-Ptychopteria* biofacies. This indicates that the water became too deep and/or too turbid to support colonies of *Favosites* and *Heliophyllum* and taxa more tolerant of those environmental conditions were present. Moreover, on the eastern side of the central trough and the eastern shelf, corals disappear altogether.

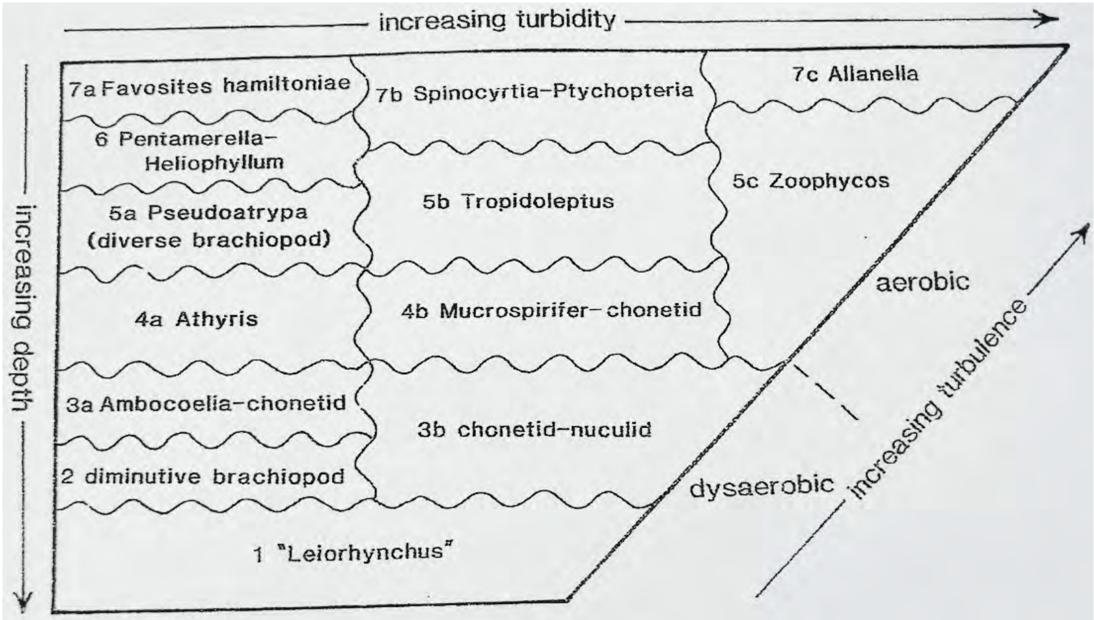

Figure 7. Paleoecological model relating Ludlowville – Moscow biofacies to inferred bathymetry, sediment accumulation rate and turbidity. Adapted from Brett et al. (1990, 2013).

These beds also seem to record a nutrient-rich, robust ecosystem. The occurrence of large trilobites with rare phyllocarids suggest a hierarchy within an active food chain. These beds are also characterized by the presence of large infaunal to semi-infaunal diverse bivalve fauna. The common occurrence of the clams, *Grammysia*, *Modiomorpha*, *Goniophora* and others are suggestive of "good times" as well as the abundance of *Zoophycos* and *Tropidoleptus* further suggests at least moderate to high nutrient presence.

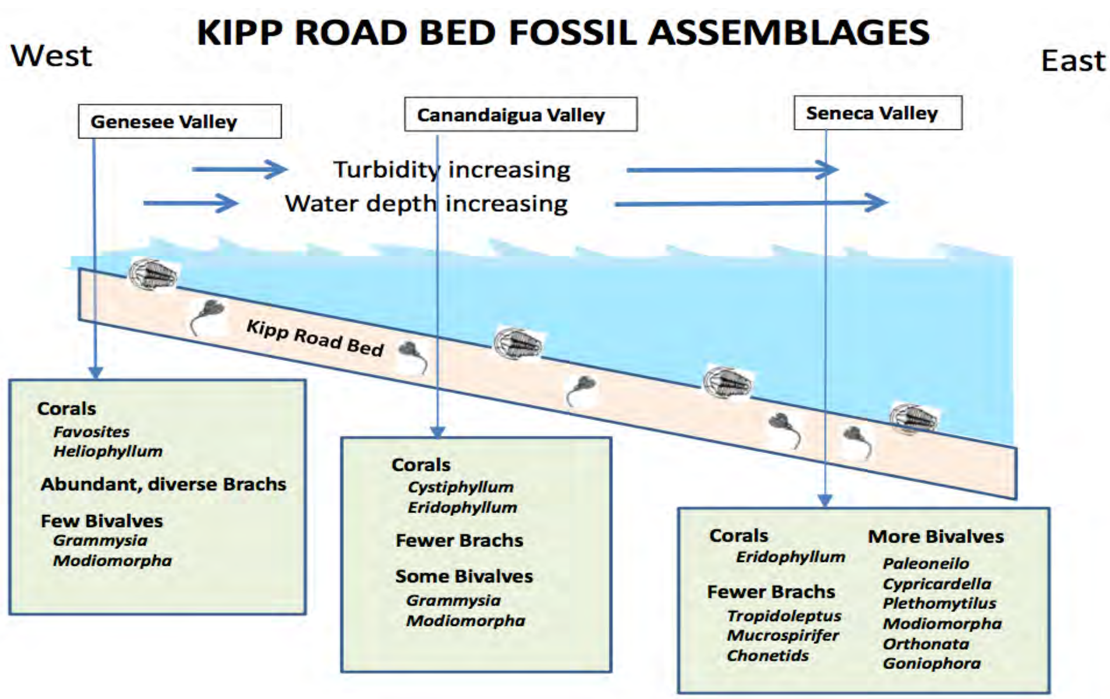

Figure 8. Schematic illustrating lateral change in Kipp Road Bed fossil assemblages from west to east across the Finger Lakes.

Willard siltstone interval: The transition from the Kipp Road Bed to the Willard siltstone interval is relatively abrupt. Water depths and rates of sedimentation must have increased significantly as siliciclastics become increasingly thick and fossils become scarce and widely scattered. Rapid burial at the onset of the deposition of the Willard siltstone interval is further indicated by the localized abundances of well-preserved fossils including articulated *Taxocrinus* crowns. Depositional environments shift in the central trough (Canandaigua Lake Valley) from the *Spinocyrtia – Ptychopteria* biofacies to the *Tropidoleptus* through the *Mucrospirifer* – chonetid to the chonetid - nuculid biofacies (Fig. 7). The presence of the brachiopods *Tropidoleptus*, *Mucrospirifer*, *Mediospirifer*, and *Devonochonetes coronatus* as well as nuculid bivalves, such as *Paleoneilo* and numerous other bivalves including *Modiomorpha*, *Cypricardella* and *Goniophora* clearly indicate muddy and or turbulent, deep water environmental conditions. Except for occasional small phacopid trilobites and crinoidal debris, the taxa of the *Favosites hamiltoniae* biofacies are gone. No tabulate or rugose corals can colonize and live on this rapidly accumulating muddy sediment substrate.

Moreover, an additional biofacies represented by the taxon *Zoophycos* is present in the silty mudstone to muddy siltstone deposits of the Willard interval (Fig. 9). Sediment mixing by the *Zoophycos* – producing animal created a seafloor too unstable for colonization by most benthos (Rhoads, 1974) resulting in a low density low diversity faunal assemblage. Within this barren to poorly fossiliferous sequence, a few scattered shell-rich horizons indicate periods when sedimentation rates temporarily slowed thereby allowing minor colonization of the seafloor by benthos. Often-times these taxa are preserved in-situ suggesting renewal of rapid burial and the return to the *Zoophycos* biofacies.

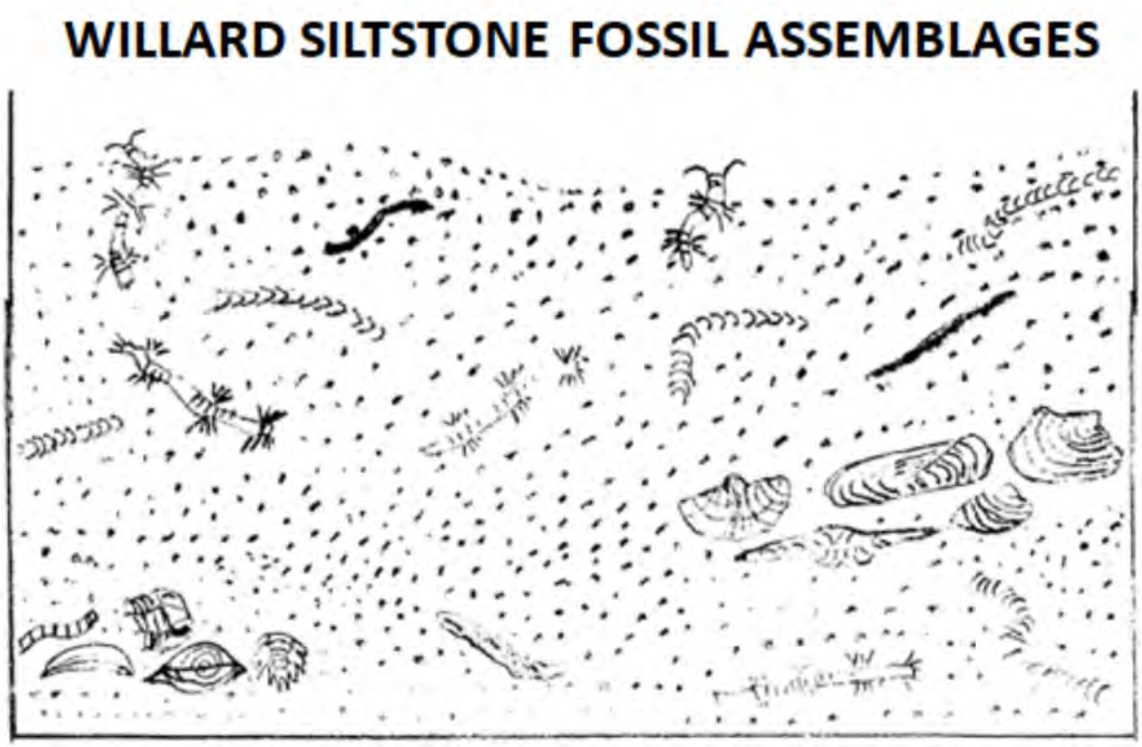

Figure 9. Schematic illustrating Willard siltstone fossil assemblages. Note substrate is barren to poorly fossiliferous with pervasive bioturbation and localized shell-rich horizons.

At some point in time, sea levels began to drop, the water became shallower, and sedimentation rates slowed due to apparent sediment bypass. At the very top of the Willard siltstone, an erosional surface developed presumably during a shallowing episode at the end of the deposition of the Deep Run Shale Member. Evidence of this surface is manifested by the wavy and irregular, very thin, less than 5 cm (2 in.) thick "stacked" ripple-like beds directly beneath the Menteth Limestone. This cryptic surface lacks fossils and may have originated at or above intertidal wave base. Additionally, well-developed scour and fill sedimentary structures form part of the base of the Menteth Limestone. This erosion removed or truncated sediments both east and west of the central trough depocenter. Coupled with sediment starvation on the western shelf, all traces of the Deep Run Shale Member have been removed in the vicinity of present-day western Erie County. On the eastern shelf, Baird (1979) showed the facies of the Deep Run Shale Member merged into the Portland Point Limestone Member east of the present-day Seneca Lake Valley.

SUMMARY

Detailed microstratigraphic study of the Deep Run Shale Member has revealed two regionally mappable units through the Finger Lakes of New York consisting of a 1 m thick lower, fossiliferous layer designated the Kipp Road Bed and an upper, barren to sparsely fossiliferous interval designated the Willard siltstone. These units were deposited across a western shallow shelf and a central basinal trough of the northern Appalachian Basin. Moreover, sections along the west shore of present-day Seneca Lake revealed more beds, which may have been deposited only in the central trough and are interpreted to be early stages of Tichenor deposition.

The Kipp Road Bed is a muddy siltstone characterized by high species diversity and abundance, which decreases basinward due to increased bathymetry and turbidity. The Willard siltstone interval is typified by low species diversity and scarcity, which reflects rapid rates of sedimentation with intense bioturbation and maximum water depths. A few widely scattered very thin, shell-rich horizons in the Willard contain many well-preserved in-situ fossils indicating a temporary slowing of sedimentation, limited short-term colonization of the substrate followed by renewed rapid burial.

Although the Deep Run Shale Member records a general deepening of sea level commencing with the deposition of the subjacent Tichenor Limestone, sea level must have dropped at some point, which allowed an erosional surface to develop near the very top of the Willard. Siliciclastics were truncated both east and west of the central trough prior to the deposition of the Menteth, thereby ending the accumulation of sediments of the Deep Run Shale Member.

ACKNOWLEDGEMENTS

I would like to thank Frederick M. Haynes (retired Petrophysicist ExxonMobil) for his assistance in measuring important stratigraphic sections of the Deep Run Shale Member at both the type locality along Canandaigua Lake as well as at the section along Houston Road. Furthermore, I would like to thank him for aiding in the preparation of many diagrams utilizing his expertise with Microsoft PowerPoint software.

I would like to thank my wife, Tammy Mayer, who assisted me in measuring the difficult stratigraphy at Kashong Glen. Not only is the ravine very steep and strenuous to gain access into and out of, she braved the heat, humidity and bugs. She untiringly listened to my ideas while not having a formal education in

geology. She helped in typing the manuscript and most importantly she has been very patient with me during this research project.

REFERENCES

Benton, M.J., 2004. The Atlas of Life on Earth. Borders Press, London, United Kingdom, 368 p.

Baird, G.C., 1979. Sedimentary relationships of Portland Point and associated Middle Devonian rocks in central and western New York. New York State Museum Bulletin No. 433, 24 p.

Baird, G.C., Brett, C.E. and S.J. Wamback, 1988. Regional, late diagenetic, color-hardness gradient in Paleozoic marine mudstone deposits, Lake Ontario region: a potential measure of basin thermal history. Society of Economic Paleontologists and Mineralogists, Mid-year Meeting, Columbus, 5:5.

Baird, G.C., Lyons, T.W. and C.E. Brett, 1991. Thermally-controlled color gradient for fossils and associated sediments: implications for paleoecology, 14. In Lidgard, S. and P.R. Crane (eds.), Fifth North American Paleontological Convention, Paleontological Society Special Publication (6).

Blakey, R.C., 2008. Gondwana paleogeography from assembly to breakup – a 500 million year odyssey, in Fielding, Christopher R., Frank, Tracy D., and Isbell, John L. (eds.), Resolving the Late Paleozoic Ice Age in Time and Space: Geological Society of America, Special Paper 441, p. 1-28.

Brett, C.E. and Baird, G.C., 1985. Carbonate-Shale cycles in the Middle Devonian of New York: An evaluation of models for the origin of limestones in terrigenous shelf sequences. Geology, v. 13, p. 324-327.

Brett, C.E. and Baird, G.C., 1986. Middle Devonian stratigraphy, facies, and depositional environments of western New York State. In Miller, M.A. (ed.). A field excursion to Trenton Group (Middle and Upper Ordovician) and Hamilton Group (Middle Devonian) localities in New York, and a survey of their Chitinozoans. American Association of Stratigraphic Palynologists Field Trip Guidebook.

Brett, C.E. and Baird, G.C., 1990. Submarine erosion and condensation in a foreland basin: Examples from the Devonian of Erie Çounty, New York. p. A1-A56. New York State Geological Association 62nd Annual Meeting, Field trip Guidebook.

Brett, C.E., and Baird, G.C., 1994. Depositional sequences, cycles, and foreland basin dynamics in the Late Middle Devonian (Givetian) of the Genesee Valley and western Finger Lakes Region, p. 505-586. In New York State Geological Association, 66th Annual Meeting Field Trip Guidebook.

Brett, C.E., Baird G.C. and Miller, K.B., 1986. Sedimentary cycles and lateral facies gradients across a Middle Devonian shelf-to-basin ramp Ludlowville Formation, Cayuga Basin, p. 81-127. In New York State Geological Association, 58th Annual Meeting, Field Trip Guidebook.

Brett, C.E., Miller, K.B., and Baird, G.C. 1990. A temporal hierarchy of paleoecological processes within a Middle Devonian epeiric sea, p. 178-209. In Miller, W., III, ed., Paleontological Society Special Paper 5.

Brett, C.E., Bartholomew, A.J. and Baird, G.C., 2007. Biofacies recurrence in the Middle Devonian of New York State: An example with implications for habitat tracking. Palaios 22, p. 306-324.

Brett, C.E., Zaffos A., Baird, G.C., and Bartholomew, A.J. 2013. Fossil beds, facies gradients and seafloor dynamics in the Middle Devonian Moscow Formation, western New York. In New York State Geological Association 85th Annual Meeting, Field Trip Guidebook. p. 68-101.

Clarke, J.M., 1903. Classification of New York Series of Geologic Formations. New York State Museum Handbook 19, 1st. ed., 28p.

Cooper, G. A., 1930. Stratigraphy of Hamilton Group of New York. American Journal Science, 5th series, v. 19, p. 116-134, 214-236.

Ettensohn, F.R., 1985. The Catskill Delta Complex and the Acadian Orogeny: A model. In Woodrow, D.L. and Sevon, W.D., eds., The Catskill Delta. Geological Society of America Special Paper 201, p. 39-49.

Grabau, A.W., 1898-1899. Geology and Paleontology of Eighteen-Mile Creek and the Lakeshore Sections of Erie County, New York. Buffalo Soc. Nat. Sci. Bull. 6 (Pts. 1,2), 403 p.

Grasso, T.X., 1973. A comparison of environments: The Middle Devonian Hamilton Group in the Genesee Valley: faunal analysis, Jaycox Run. In New York State Geological Association 45th Annual Meeting Field Trip Guidebook, p. B1-B24.

Hall, J., 1843. Geology of New York, Part IV, Comprising the Survey of the Fourth Geological District, 525 p. Albany, 1843.

Mayer, S.M., 1989. Stratigraphy and paleontology of the Jaycox Shale Member, Hamilton Group of the Finger Lakes region of New York State: Unpub. MS thesis, State University of New York at Fredonia, 120 p.

Mayer, S.M., 1994. Field studies of the Middle Devonian Ludlowville - Moscow sequence in the Genesee and Seneca Valleys, New York State. In New York State Geological Association 66th Annual Meeting, Field Trip Guidebook.

Mayer, S.M., Baird, G.C., and Brett, C.E., 1994. Correlation of facies divisions in the uppermost Ludlowville Formation (Givetian) across western and central New York State, in Studies in Stratigraphy and Paleontology in Honor of Donald W. Fisher, New York State Museum Bulletin 481, p.229-264.

Miller, K.B. 1991. High-resolution correlation within a storm-dominated muddy epeiric sea: Taphofacies of the Middle Devonian Wanakah Member, western New York, p. 129-152. In E. Landing and C. E. Brett (eds.), Dynamic Stratigraphy and Depositional Environments of the Hamilton Group (Middle Devonian) in New York State, Part II. New York State Museum Bulletin 469, 171 p.

Rhoads, D.C., 1974. Sediment-animal relationships on the muddy seafloor. Annual Review of Marine Biology. Volume 12, p 263-300.

Van der Voo, R., 1983. Paleomagnetic constraints on the assembly of the Old Red Continent. Tectonophysics, V.91, p. 271-283.

Van der Voo, R. 1988. Paleozoic paleogeography of North America, Gondwana, and intervening displaced terranes: Comparisons of paleomagnetism with paleoclimatology and biogeographical patterns. Geological Society of America Bulletin, V. 100, p. 311-324.

ROAD LOG AND STOP DESCRIPTIONS

Cumulative Miles	Incremental Miles	Route Description
0	0	Leave Alfred University
0.8	0.8	proceed on North Main Street
2.1	1.3	Continue straight on NY-244E

6.1	4.0	left onto NY-21 N
6.3	0.2	Turn left onto Karrdale St
6.6	0.3	Turn right to merge onto I-86 E/NY- 17 E
11.5	4.9	Take Exit 34 N to merge onto NY- 36 N
25.5	14.0	Turn left onto I-390 N ramp
25.7	0.2	Merge onto I- 390 N
41.2	15.5	Take Exit 7 toward Geneseo
41.6	0.4	Turn right onto NY-408 N
41.7	0.1	Continue straight on NY–63 N
45.0	3.3	Continue straight on US-20A E
45.7	0.7	Turn left onto Main Street
46.1	0.4	Proceed onto Rt. 39 Avon Road
48.5	2.4	Continue north, past Nations Road, site on left across field Must obtain permission from Genesee River Conservancy Research Reserve.

STOP 1: Jaycox Creek – The Rest of The Story

Location Coordinates: (42.829^0 N, 77.790^0 W)

Jaycox Creek is a classic exposure of the Ludlowville and Moscow Formations within the Hamilton Group. This is the type locality for the Jaycox Shale Member, which contains 2 prominent mappable coral beds, the lower Green's Landing Coral Bed and the upper Cottage City Coral Beds separated by variably fossiliferous shales and calcareous mudstones. Although many studies have examined the stratigraphy and paleontology of the Jaycox Shale Member, (Grasso, 1973, Baird, 1979, Brett and Baird, 1994, Mayer, 1989, Mayer, 1994), most people have not scrutinized the overlying Tichenor Limestone and the Deep Run Shale Members.

The Deep Run Shale Member is well exposed here from the base of the Kipp Road Bed through the upper Willard siltstone (Fig 3). The bluish-gray calcareous mudstones of the Kipp Road Bed are observable in the creek floor and banks and exhibit great faunal diversity and abundance. Moreover, the Willard interval, characterized by barren to poorly fossiliferous bioturbated siltstones also contains three distinct shell-rich lenses. Whereas the transition from the Tichenor Limestone to the Deep Run Shale Member is relatively gradational, the uppermost contact of the Willard is abrupt with the overlying Menteth. Sediments of the Deep Run Shale Member are observed to be much thinner in the Genesee Valley than in the Canandaigua Valley due to apparent sediment bypass on the western shelf of the Appalachian Basin and from erosional overstep by the Menteth Limestone Member.

Cumulative Miles	Incremental Miles	Route Description
54.9	6.4	Proceed north on Rt. 39 to Avon
55.7	0.8	Turn right onto West Main Street (Routes 5 & 20) proceed around traffic circle to east Main Street continue to McDonald's on left.
		This is a Lunch/Restroom stop.

82.1	26.4	Proceed east on Routes 5 & 20 to NY-364 S.
85.6	3.5	Turn right onto NY-364 S (East Lake Road)
85.7	0.1	Pass Kipp Road
		Park in Deep Run Beach area. Walk across road to creek.

Stop 2: Deep Run Gully

Location Coordinates: (42.821^0 N, 77.259^0 W)

This creek not only is the type locality for the Deep Run Shale Member but also provides an excellent view of the upper Wanakah, Spafford and Jaycox Members. Of interest in the small falls at the base of the overall section is the Limerick Road Bed of the Spafford Shale Member. Moreover, in the Jaycox Shale Member the lower Green's Landing Coral Bed and the upper Cottage City Coral Beds are observed in the floor and banks of the creek. The top of the first major waterfall is capped by the Tichenor Limestone, which disconformably overlies sediments of the Jaycox Shale Member.

Above the falls and in the floor of the creek, the transition from the Tichenor Limestone to the Kipp Road Bed is again relatively gradational. Here in the Canandaigua Valley, the Deep Run Shale Member obtains its maximum thickness within the central depocenter of the Appalachian Basin. The Kipp Road Bed exhibits decreased species diversity apparently due to increased water depths and turbidity. Also, the Willard siltstone interval contains a few shell-rich lenses within a predominately barren to sparsely fossiliferous siltstone indicating overall rapid sedimentation rates punctuated by a few periods of quiescence allowing colonization of the substrate. The Menteth Limestone tops this sequence of siltstones forming an erosionally resistant ledge to a second large waterfall at Deep Run Gully.

This field trip will not observe the Deep Run Shale Member at Kashong Glen due to the inherent steep sides of the ravine. Similarly, the sections along the west shore of Seneca Lake will also not be examined due to their inaccessibility. However, just one-half mile north of Deep Run Gully on Canandaigua Lake is an exceptional exposure of the Jaycox Shale Member at Green's Landing. This will be our last stop.

Cumulative Miles	Incremental Miles	Route Description
86.2	0.5	Proceed north on East Lake Road to Tamberlane Farms
		Must ask permission to enter property.

Stop 3: Green's Landing

Location Coordinates: (42.830^0 N, 77.257^0 W)

Approximately 1600 ft. east of Rt 364, this small stream cuts through the Jaycox Shale Member as well as the Kipp Road Bed of the Deep Run Shale Member. The only slight falls along this creek is created by the cap of the Tichenor Limestone, otherwise, the locality is generally ramped upstream and provides an accessible view of these units.

Here, the lower coral bed of the Jaycox derives its name because of its remarkable development in this creek. The Green's Landing Coral Bed is an argillaceous mudstone containing an abundance of tabulate and rugose corals as well as brachiopods, bryozoans, crinoids, gastropods, and trilobites. Although recognizable in many localities, this mass of rock is a distinctly bedded biostrome built by and composed mainly of the remains of sedentary organisms.

Additionally, the Cottage City Coral Beds as well as the other units of the Jaycox are observable in outcrop in the floor and banks of the creek. These strata are, in turn, disconformably overlain by the Tichenor Limestone Member which gradually grades upward into the Kipp Road Bed.

The Kipp Road Bed is the only bed of the Deep Run Shale Member exposed at Green's Landing. The medium gray, silty mudstone to calcareous siltstone contains a moderately abundant fauna of large phacopid trilobites as well as camerate crinoids, which have facilitated correlation of this unit across the Finger Lakes. Moreover, the Willard siltstone interval and Menteth Limestone Member are both covered at this site.

End of Trip: Head south on NY-364 S toward Middlesex;
Turn right onto NY-245 S toward Naples;
Turn left onto NY–21 S toward North Hornell;
Turn right onto NY-66 W;
Turn right onto NY-21 S toward Alfred Station;
Turn right onto NY-244 W toward Alfred University.

A2 AND B2: UPPER DEVONIAN KELLWASSER EXTINCTION EVENTS IN NEW YORK AND PENNSYLVANIA: OFFSHORE TO ONSHORE TRANSECT ACROSS THE FRASNIAN-FAMENNIAN BOUNDARY ON THE EASTERN MARGIN OF THE APPALACHIAN BASIN

ANDREW M. BUSH AND J. ANDREW BEARD
Geosciences & Ecology and Evolutionary Biology, University of Connecticut, Storrs, CT 06269

GORDON BAIRD
Department of Geosciences, SUNY Fredonia, Fredonia, NY 14063

D. JEFFREY OVER
Department of Geological Sciences, SUNY Geneseo, Geneseo, NY 14454

with contributions by

KATHERINE TUSKES
Department of Geological Sciences, Atmospheric, Ocean, and Earth Science, George Mason University, Manassas, VA 20110

SARAH K. BRISSON AND JALEIGH Q. PIER
Geosciences & Ecology and Evolutionary Biology, University of Connecticut, Storrs, CT 06269

INTRODUCTION

Earth-system perturbations caused a series of mass extinction events during the Devonian Period, including the Taghanic event in the Givetian, the Lower and Upper Kellwasser events in the Frasnian, and the Hangenberg event in the Famennian (House, 2002; Bambach, 2006). These extinctions occurred against the backdrop of orbitally forced sea-level fluctuations, the Acadian Orogeny (Averbuch et al., 2005), the expansion of plants and animals on land (Algeo et al., 1995), and ecological changes in the marine biosphere (Signor and Brett, 1984; Bambach, 1999). The Frasnian-Famennian boundary in particular represents a significant global crisis, considered one of the "big five" mass extinctions (Raup and Sepkoski, 1982) that led to the demise of the widespread and diverse Devonian reef community (Copper, 2002).

The Appalachian Basin preserves a tremendous record of Devonian stratigraphy, and these rocks have been studied for about 200 years (Aldrich, 2000). They have been, in whole or in part, the inspiration for numerous advances and theories in geology and paleontology, including the concepts of facies (Chadwick, 1935), punctuated equilibrium (Eldredge, 1971), coordinated stasis (Brett and Baird, 1995), and considerable work on paleoecology (Sutton et al., 1970; Bowen et al., 1974; Thayer, 1974; McGhee, 1976; McGhee and Sutton, 1981; 1983; 1985; Sutton and McGhee, 1985; Stigall Rode and Lieberman, 2005). Critical faunas and floras document the invasion of land (Daeschler et al., 1994; Daeschler, 2000; VanAller Hernick, 2003).

In particular, foreland basin sediments provide an exceptionally thick and complete record of the Upper Devonian, and thus the opportunity to examine Late Devonian extinction events. Studies of the late-Frasnian Kellwasser events have been concentrated in the more offshore settings of western New York, where geochronology is well constrained by conodont biostratigraphy and carbon isotope chemostratigraphy (Over, 1997; Murphy et al., 2000; Over, 2002; Tuite and Macko, 2013; Lash, 2017). Specifically, the Pipe Creek Formation is temporally equivalent to the Lower Kellwasser Event (LKW), and a thin black shale bed in the upper Hanover Formation is equivalent to the Upper Kellwasser Event (UKW) (Over, 1997; 2002). Baird, Bush, and students have been investigating the Kellwasser events in shallower-water paleoenvironments further to the east, primarily in Steuben County, New York, and adjacent areas of Pennsylvania (Bush et al., 2015; Beard et al., 2017) (Fig. 1).

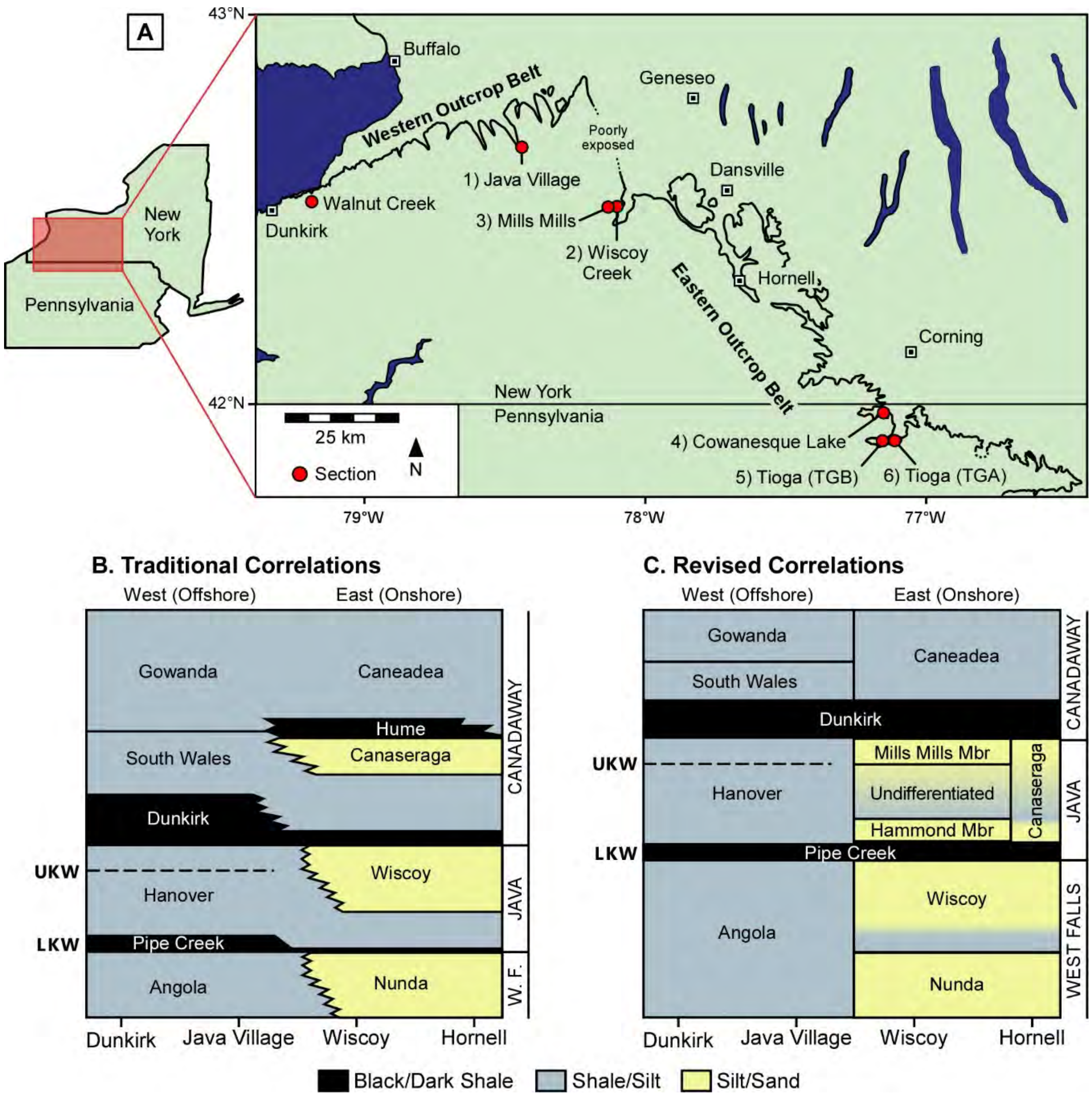

Fig. 1. A. Map of study area. The black line marks the Pipe Creek Formation, as currently correlated. **B.** Traditional stratigraphic correlations between the western and eastern portions of the outcrop belt (Pepper and de Witt, 1950; 1951; Smith and Jacobi, 2000). **C.** Revised correlations (Bush et al., 2015; Beard et al., 2017). "LKW" and "UKW" indicate the positions of the Lower and Upper Kellwasser events, and "W. F." stands for WEST FALLS. Stratigraphic groups are indicated in capital letters. B-C slightly modified from Bush et al. (2015), with permission from Elsevier.

The Java Group-through-Dunkirk Formation, in which the Lower and Upper Kellwasser events are developed, consist of interbedded organic-rich shales, gray shales, and thin nodular carbonates in the western outcrop area in Chautauqua, Erie, and Wyoming counties (Fig. 1). Eastward in Allegany, Steuben, and Tioga (PA) counties, the Java Group and equivalents become thicker and coarser, consisting of gray shales, siltstones, and sandstones with more abundant benthic faunas. The Java Group overlies the West Falls Group, where the Pipe Creek Formation rests on the Angola to the west and the Wiscoy (revised correlations, Fig. 1C) or Nunda (traditional correlations, Fig. 1B) to the east. The Hanover or the eastern equivalent Canaseraga Formation (revised correlations, Fig. 1C) overlies the Pipe Creek. The Java Group is overlain by the Canadaway Group, which is marked by the Dunkirk Formation at the base, the highest extensive organic-rich shale in the New York Upper Devonian.

Inferred paleoenvironments are variable and include (1) nearly anoxic for portions of black shale units, (2) more broadly dysoxic for the gray facies in the offshore realm characterized by depauperate benthic faunas and rare to common pelagic faunas, and (3) well-oxygenated for the interbedded sandstones, siltstones, and light-colored shales in more nearshore settings that are highly bioturbated and contain a shelly fauna (see Boyer et al., 2011; Boyer et al., 2014; Haddad et al., 2016). The closing of the Frasnian age was marked by two major episodes of ecological disruption and faunal extinction, the LKW and UKW. The second of these, marking the Frasnian-Famennian boundary and associated mass extinction, was the greater crisis globally. This extinction, in part, probably explains the lower diversity and more generalized ecological character of Famennian neritic faunas seen higher in the Devonian succession in Chautauqua and Cattaraugus counties. In Europe, North Africa, and elsewhere, the two extinction events are marked by black shale or black limestone beds within slope and basin successions (e.g., Schindler, 1993).

DAY 1 - FRASNIAN-FAMENNIAN BOUNDARY INTERVAL IN CHAUTAUQUA, ERIE, WYOMING, AND ALLEGANY COUNTIES, NEW YORK

(Over, Baird, Tuskes, Beard, Bush)

Stratigraphy and Geochronology in Western New York

Walnut Creek and Silver Creek in Chautauqua County (Fig. 1A) expose a complete section of the Java Group in the banks and stream bed (Fig. 2). The Pipe Creek Formation is a persistent black petroliferous shale that is recognized in the subsurface from eastern Kentucky to New York State by a high positive shift on gamma ray logs (de Witt and Roen, 1985). These shales represent dysoxic and anoxic benthic conditions that developed as the result of deepening in the Appalachian Basin. This deepening is the IId2 transgression of Johnson et al. (1985) and Day et al. (1996). At Walnut Creek, the Pipe Creek is a 0.6 meter-thick, very hard, black shale that abruptly overlies the softer, gray Angola Formation (Fig. 2). The laminated microfacies of the Pipe Creek contrasts dramatically with a subjacent zone of gray, pyritic Angola mudstone. The Pipe Creek can be traced regionally southwestward through Chautauqua County where it is approximately 0.6 meters thick in its westernmost section (Tesmer, 1963). To the east, it thickens to about 6 or 7 meters near Warsaw, then becomes more depositionally complicated and interbedded with turbiditic silts and sands of the underlying Nunda Formation (Baird and Jacobi, 1999, Stop 1) (which the correlations in Fig. 1C suggest might actually correlate with the Wiscoy).

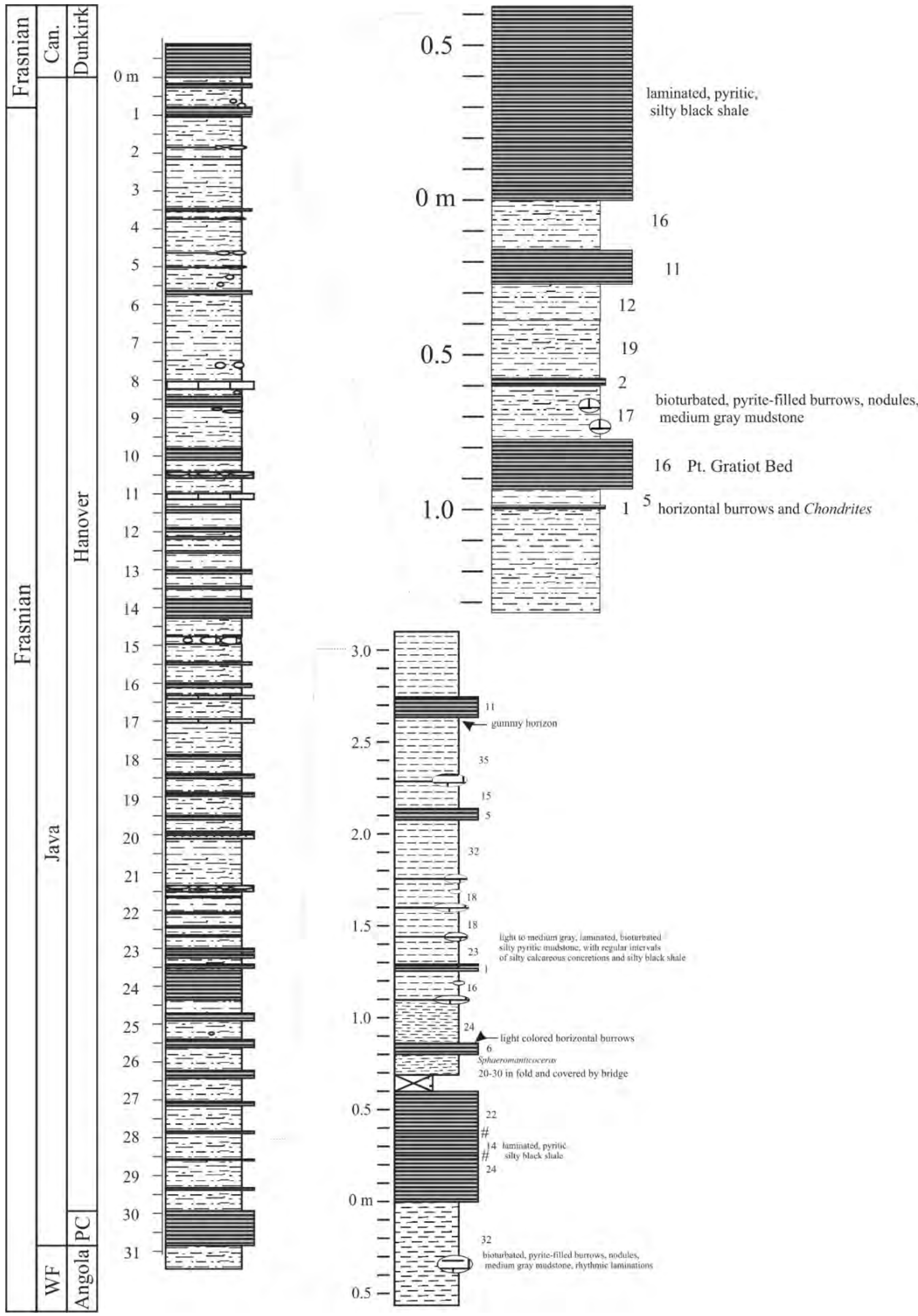

Fig. 2. Schematic stratigraphic section of Java Group exposed along bed and banks of Walnut Creek upstream and downstream from US 20 bridge in Silver Creek, NY, with details of lower and upper Java Group strata. See Fig. 4 for key to lithologic symbols. Frasnian-Famennian boundary is at the top of the Pt. Gratiot Bed. Can. = Canadaway Group; PC = Pipe Creek Formation; WF = West Falls Group.

The Hanover Formation at Walnut Creek is 30 m thick and shows a distinct near-meter-scale cyclicity of alternating thin organic-rich shales and/or nodular carbonate-rich beds with thicker gray shales which are superimposed on larger scale cycles of more organic-rich and less organic rich strata that are also evident in geochemical analysis (Lash, 2017). Dates derived from zircons in tephra horizons within the Kellwasser interval at quarry Benner in Germany yielded a calculated date of 372.55 $\pm$ 0.15 Ma for the Lower Kellwasser Bed and 371.85 $\pm$ 0.11 Ma for the Upper Kellwasser Bed. The Center Hill Tephra at Hurricane Bridge, TN ,which is in the highest Frasnian strata in the Chattanooga Shale, was dated at 371.91 $\pm$ 0.15 (Schmitz, 2014, pers. comm.). Thus the duration for deposition of the Pipe Creek and Hanover formations was approximately 800,000 years.

Bulk magnetic susceptibility data collected at 5-cm intervals through the Walnut Creek section were used to assess sea level fluctuations. The amount of magnetic minerals contained in marine sedimentary rocks varies with the amount of detrital minerals contributed from continents, which varies during eustatic, climatic, and tectonic changes (Tuskes et al., 2014). Therefore, the magnetic susceptibility curve increases during a sea level regression when base level is lowered and heightened erosion increases the detrital contribution into the marine system. A decrease in the magnetic susceptibility signature occurs during transgressions, when detrital minerals are not being weathered, eroded, and dispersed as heavily. Constant values demonstrate an aggradational phase, and increasing values demonstrate a regressive phase. The variation in magnetic susceptibility curve can then be used to document changes in sea level (Da Silva and Boulvain, 2006).

Data were analyzed using the astrochron package for the r program (Meyers, 2014) for orbital frequencies, bandpass, and the sedimentation rate, and all calculations were done through pre-programed analyses in the package. Six different cycles were identified as a frequency, and then calculated as cycles in terms of ka. The shortest two frequencies are representative of the two precession cycles that are 16.9 and 20.0 ka respectively. The middle two frequencies correlate to the two obliquity cycles of 32.25 and 40.0 ka, and the last two frequencies correlate with the eccentricity cycles of 100 and 416 ka. The MS data was then put through multiple bandpass filters in order to better understand the location of the cycles within the strata. The six cycles coalesce into three, with the small and large cycles modulating each other, and the values given by the analysis being the extreme values in the cycle. The eccentricity shows eight short eccentricity cycles and two long eccentricity cycles. In the lower 14 m of the Hanover the eccentricity curve fluctuates much more than the upper 16 m. In the lithology, this is associated with the deposition of black shales. The obliquity shows about 18 cycles, where the lower half of the Hanover experiences much more exaggeration than the upper half. The obliquity is associated with limestone or strata that are representative of a shallowing environment due to the obliquity's effect on the tides and influence in the deposition over lower latitudes.

The precession cycle shows about 34 cycles, which occur in an approximate 5:1 ratio with the eccentricity, and are associated with the occurrence of black shale beds as well. Much like the eccentricity, the precession varies much more in the lower half of the Hanover then becomes less exaggerated in the upper half. It is clear that the ~20 ka cycle corresponds to the 60 cm lithologic cycles in the lower half of the Hanover. This cycle is not as clear in the lithology of the upper portion of the section, although the signal is clear throughout the entire column based on the MS data (Fig. 3).

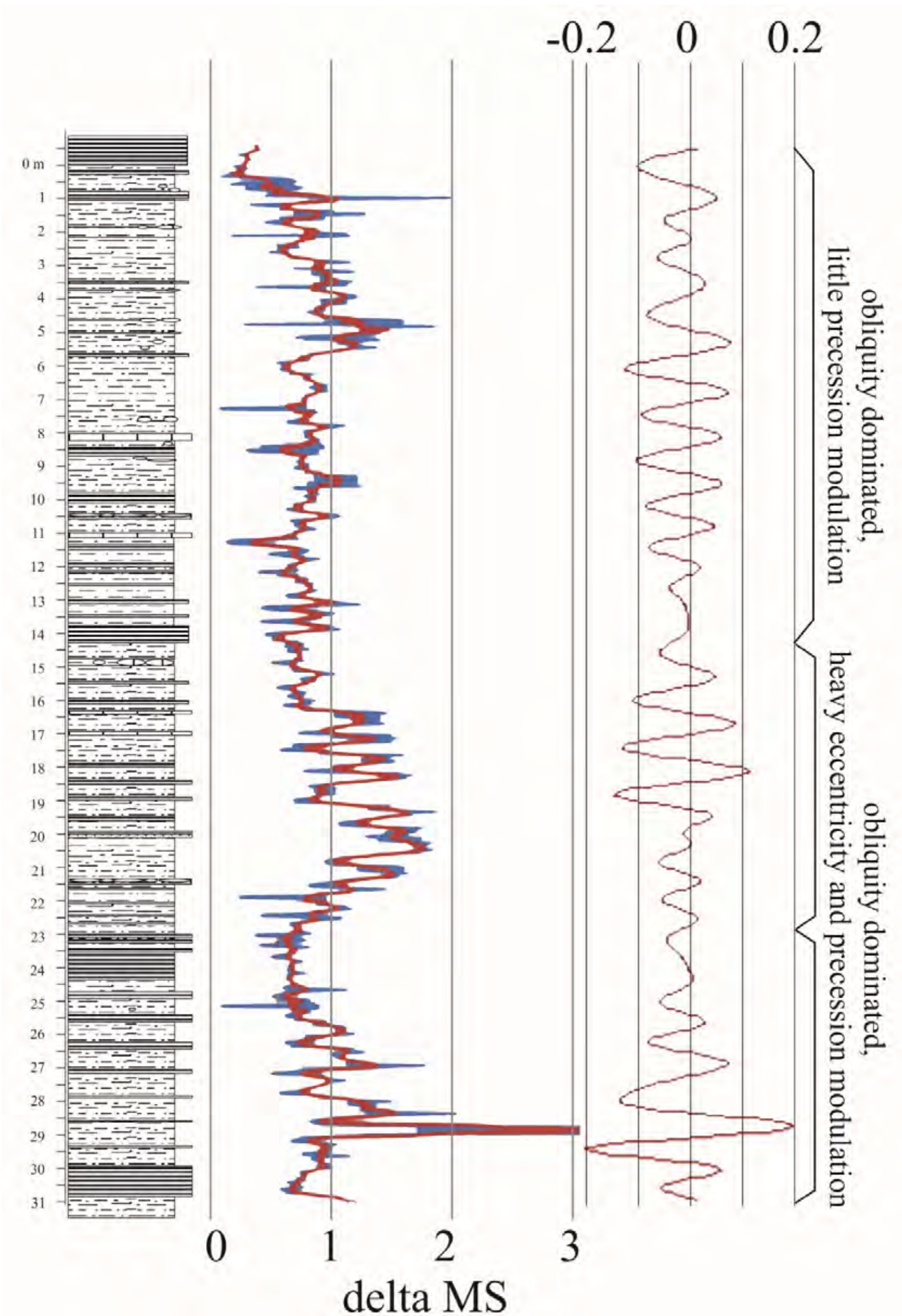

Fig. 3. Magnetic susceptibility values plotted as δMS (blue is data, red is spline of 5 values) and combined bandpassed signal of frequency analysis of three recognized cycles showing obliquity dominated cycles modulated by precession and eccentricity next to lithologic succession at Walnut Creek (see Fig. 2).

When the three cyclic frequencies are filtered together, it becomes apparent that the cycles not only modulate themselves, but also can dramatically affect each other. Again, the lower half of the Hanover is much more exaggerated compared to the upper, which implies that while the obliquity seems to be the metronome of the cycles according to the bandpass signal analysis, the depositional area was actually under significant influence from the precession and eccentricity cycles. The obliquity cycle is most apparent and unaffected in the lower Hanover, while in the upper half the obliquity may have been muted by the effects of the other two cycles. This is more apparent in the strata where there are more carbonate beds as compared to the alternating black and gray shales (Fig. 3).

The Upper Kellwasser Bed is expressed as a fissile black shale unit with some silty laminations in the upper part. This bed was designated the Point Gratiot Bed for the excellent exposure along Lake Erie at Point Gratiot at the southwest edge of Dunkirk, Chautauqua County (Over et al., 2013). This layer, which is 18 cm-thick along Walnut Creek, is traceable eastward to the vicinity of Hornell and Canisteo in Steuben County where it is approximately 2 meters-thick (Over, 1997; 2002). At Point Gratiot and at Beaver Meadow Creek at Java Village (Stop 1) the upper part of this layer has yielded articulated fish remains, including part of an arthrodire carcass (*Dunkleosteus*?) at Point Gratiot. At Beaver Meadow Creek, *Spathiocaris*, a probable cephalopod aptychus, are common. It is important to note that the Point Gratiot Bed does not mark the base of the Dunkirk Formation of the Canadaway Group as was indicated by Baird and Lash (1990) and Baird and Brett (1991); the Point Gratiot Bed marks an apparent change to finer grained, more basinal facies within the upper part of the Hanover Formation. Between Point Gratiot and Java Village the interval between the Upper Kellwasser Bed and the overlying Dunkirk thickens from 0.15 to 7 meters with addition of numerous alternating black and gray-green shale beds. At Walnut Creek the Point Gratiot Bed is 0.72 m below the base of the Dunkirk. The occurrence of reworked pyrite in the form of wire-like detrital burrow fragments at the bases of the black Dunkirk Shale and underlying upper Hanover black bands indicates that these contacts are of erosional character; some of the southwestward thinning of the upper Hanover is apparently due to collective overstep at such contacts (Baird and Lash, 1990).

The upper Frasnian Zone 13 (*linguiformis*)/*subperlobata-triangularis* chronozonal conodont boundary and inferred Frasnian-Famennian contact is crossed near or at the top of the Upper Kellwasser Bed based on work at Point Gratiot in Dunkirk, Irish Gulf, and at Beaver Meadow Creek in Java Village (see Over, 1997; 2002). Again, the major extinction event, observed globally at this level, is cryptic in the black shale facies except for the microfossil changes. A bed containing shelly taxa of earliest Famennian brachiopods and bivalves, in a thin, anomalous layer only one meter above the extinction horizon near Java Village, was described by Day and Over (2002). This "recovery layer" sheds important clues as to the nature of macrofossil changes in western New York following the mass extinction.

The Dunkirk Shale, which marks the base of the Canadaway Group, represents a significant deepening in the Appalachian Basin. The base of the Dunkirk is within the *Palmatolepis delicatula platys* (= Middle *triangularis*) conodont zone and corresponds to the base of the Huron Member of the Ohio, Gassaway Member of the Chattanooga, and Morgan Trail Member of the New Albany as well as other organic-rich shale units in North America. This extensive black shale body is the IIe transgression of Johnson et al. (1985). At Walnut Creek the lower Dunkirk black shale is on the order of 12 m thick.

Offshore-Onshore Correlations

Detailed correlation of shallow-water Upper Devonian strata in New York has been difficult due to the limited number exposed stratigraphic sections and their shortness relative to the thickness of the entire package. In addition, there is considerable variation in facies across the outcrop belt, with shales in the west and an increasing proportion of sandstones to the east. The history of correlation in this region is described in more detail by Pepper and deWitt (1950; 1951), Pepper et al. (1956), Smith and Jacobi (2000; 2001; 2006), and Bush et al. (2015).

There is a relatively continuous outcrop belt for the upper Frasnian and lower Famennian in Chautauqua, Erie, and western Wyoming counties in western New York ("western outcrop belt"; Fig. 1A), and geochronology is based on many methods, including lithostratigraphy (Pepper and de Witt, 1950; 1951; Pepper et al., 1956), conodont biostratigraphy (Over, 1997; 2002), goniatite biostratigraphy (House and Kirchgasser, 2008), carbon isotopes (Murphy et al., 2000; Tuite and Macko, 2013; Lash, 2017), and magnetic susceptibility (Tuskes et al., 2014).

After an interval of poor exposure, there is good exposure from the Genesee River Valley southeastward towards Tioga, PA ("eastern outcrop belt"; Fig. 1A). The proportion of coarse siltstone and sandstone increases greatly in the eastern outcrop belt, and several new formation names are applied to these intervals (Pepper and de Witt, 1950; 1951) (Fig. 1B,C). Unfortunately, conodonts and goniatites are less common in the shallower-water paleoenvironments of the eastern outcrop belt, where, until recently, geochronology has been based largely on lithostratigraphic correlations with the western outcrop belt. Traditionally, the Pipe Creek Formation of western New York was correlated with a dark gray shale unit directly on top of the Nunda Formation in the eastern outcrop belt (Pepper and de Witt, 1950; Rickard, 1964). Likewise, the Dunkirk Formation of western New York was often correlated with a dark gray shale above the Wiscoy Formation (Pepper and de Witt, 1950; 1951; Rickard, 1964), although Rickard (1975) and Roe (1975) presented alternate correlations (see discussion in Bush et al., 2015). Based on these correlations, the LKW should be located on top of the Nunda Formation and the UKW should be located near the top of the Wiscoy Formation (Fig. 1B).

Based on several lines of evidence, Bush et al. (2015) argued that these traditional correlations between offshore and onshore formations in New York were incorrect, and they presented revised correlations (Fig. 1C). Specifically, the Pipe Creek Formation was correlated with a dark shale above the Wiscoy Formation (not the Nunda Formation). The Dunkirk was correlated with a dark shale interval above the Canaseraga Formation, which was previously called the Hume Shale; this correlation had previously been suggested by Rickard (1975) and Roe (1975). These correlations suggest that the Kellwasser events occur higher in the section in the eastern outcrop belt than has been commonly suspected: the LKW-equivalent Pipe Creek Formation sits atop the Wiscoy Formation, and the UKW-equivalent Point Gratiot Bed (Over et al., 2013) should have an equivalent in the Canaseraga Formation (Fig. 1C).

Several lines of evidence supported the revised correlations (Bush et al., 2015):

1. The conodont *Palmatolepis winchelli* was found in the shale above the Wiscoy, indicating it was late Frasnian in age, not Famennian. Thus, it is unlikely to correlate with the Dunkirk Formation. The lower Famennian conodont *Ancyrognathus symmetricus* was found in the "Hume" Shale, which is consistent with a Dunkirk-Hume correlation.
2. The brachiopod *Spinatrypa planosulcata* commonly occurs in the lower parts of the Canaseraga Formation. Atrypid brachiopods are generally considered to have gone completely extinct in the Kellwasser extinctions, suggesting that the lower Canaseraga is Frasnian in age.
3. Correlating the Dunkirk with the shale above the Wiscoy implies that the Hume black shale exists only at the shallower end of the outcrop belt, which is odd because black shales are typically interpreted as the deepest-water facies in the basin.
4. The Dunkirk Shale is thicker than the Pipe Creek in western New York. Correlating the Dunkirk with the shale above the Wiscoy implies that it becomes much thinner in the eastern outcrop belt.
5. According to Pepper (1954), there is not actually a black shale of note above the Nunda in the Hornell area and eastward, despite depictions in summary diagrams.

The correlations shown in Fig. 1C solve these problems. All fossils considered to be markers for the Frasnian are in Frasnian strata; there is no black shale in the eastern outcrop best that lacks a correlative black shale in the deeper water to the west; and the eastward extensions of the Dunkirk and Pipe Creek are relatively similar in thickness to what is seen in the west.

Beard et al. (2017) proposed several additional changes to stratigraphic terminology. First, they suggested that the lower boundary of the Canaseraga Formation be extended downward to the top of the Pipe Creek. This solved two problems: first, Bush et al.'s (2015) correlations had left the rocks immediately above the Pipe Creek without a name, and second, the lower boundary of the Canaseraga had been placed at different horizons by different workers. The placement suggested by Beard et al. (2017) should be easier to recognize reliably across the basin. Beard et al. (2017) also began dividing the Canaseraga Formation into members (Fig. 1C).

In northern Pennsylvania, shallow-marine strata have been referred to the Lock Haven Formation (equivalent to the Chemung of New York) (Faill and Wells, 1977). In other words, all of the formations in the eastern end of the outcrop belt in New York are mapped one large formation (Berg et al., 1980), making it more difficult to identify and study Late Devonian bioevents. To make it easier to identify and discuss these events, Beard et al. (2017) proposed raising the Lock Haven to group status and dividing it into formations that match those present in New York. In the Tioga area, they recognized the Wiscoy, Pipe Creek, Canaseraga, Dunkirk, and Caneadea formations. In addition, Woodrow (1968) mapped Bradford County, Pennsylvania (to the east of Tioga) using many of the New York formation names.

FIELD GUIDE AND ROAD LOG: DAY 1

Meeting Point: Beaver Meadow Creek, Java Village, NY

Meeting Point Coordinates: N 42°40.33' W 78°26.15'

Meeting Time: 10:00 AM

Stop 1: Beaver Meadow Creek (Baird, Over)

Location Coordinates: N 42°40.33' W 78°26.15'

The strata exposed in Beaver Meadow Creek at Java Village (which are on private land) include the uppermost Angola and Nunda formations of the West Falls Group, the type locality of the Java Group (Pipe Creek Formation, including an anomalous "Nunda" facies, and Hanover Formation, including the initial coarser clastic strata that thicken to the east), and the lower portion of the Dunkirk Formation of the Canadaway Group. Approximately 50 m of strata are exposed along the bank, bed, and in several waterfalls. (Note that Fig. 1C suggests that these Nunda beds may actually correlate with the Wiscoy; until this question is examined in more detail, however, we continue to refer to them as Nunda.)

Two thick-bedded sandstone units are visible in Angel Falls in Java Village (Fig. 4). This is the uppermost part of the greater Nunda Sandstone succession characterized by light gray thin to thick bedded cross-laminated and bioturbated (*Planolites* and *Skolithos*) coarse silt–very-fine quartz sand. The gray sandstones and silty mudstones at the base of the falls are separated from the upper sandstone that forms the top of the falls by a thin (10 cm-thick) black shale that marks the base of the Pipe Creek Shale, the basal unit of the Java Group. The lower and medial part of the Nunda Formation interfingers and grades westward into the Angola Shale. The upper sand is stratigraphically distinct, designated "Nunda," as it interfingers and toes out westward within the Pipe Creek Shale (Baird and Jacobi, 1999) (Fig. 5). The base of the "Nunda" sharply overlies the thin basal black shale bed; the top is interbedded and mixed with black shale.

The brownish lumpy sandstone of the topmost "Nunda" and superajacent Pipe Creek Shale show chaotic bedding, irregular sandstone masses, and complex swirly interlayering of micaceous sandstone and sandy black shale. Diffuse breccia clasts of black shale within brown sandstone matrix suggests emplacement of fluidized sand into variable water-rich, surficial black mud deposits. The thick "Nunda" sandstone seems to be a major fan lobe sand unit (Jacobi et al., 1994; Baird and Jacobi, 1999). The "Nunda" flow event scoured the lowest Pipe Creek Shale as indicated by olistoliths of Pipe Creek Shale within the massive unit at several localities. The uppermost chaotic and diffuse "Nunda" Sandstone may represent later, smaller flow events. These sands were also reworked by storm waves as indicated by hummocky cross-stratification.

At Beaver Meadow Creek the Pipe Creek Formation is 6.2 m of organic-rich shale and the underlying 3 m of fine quartz sand of the "Nunda." A deep recessive bed at ~1.1 m is a possible tephra bed; a tephra was also described from the upper Pipe Creek at Eighteenmile Creek, as well as the upper Pipe Creek along PA 287 (Ver Straeten et al., in revision). The Pipe Creek has a limited benthic fauna consisting mainly of inarticulate brachiopods. Nektic fauna/flora consists of dacryoconarids, cephalopods, and algal spores; conodonts are uncommon, consisting of *Ancyrodella, Palmatolepis*, and *Polygnathus* indicative of FZ 12 (Over, 1997).

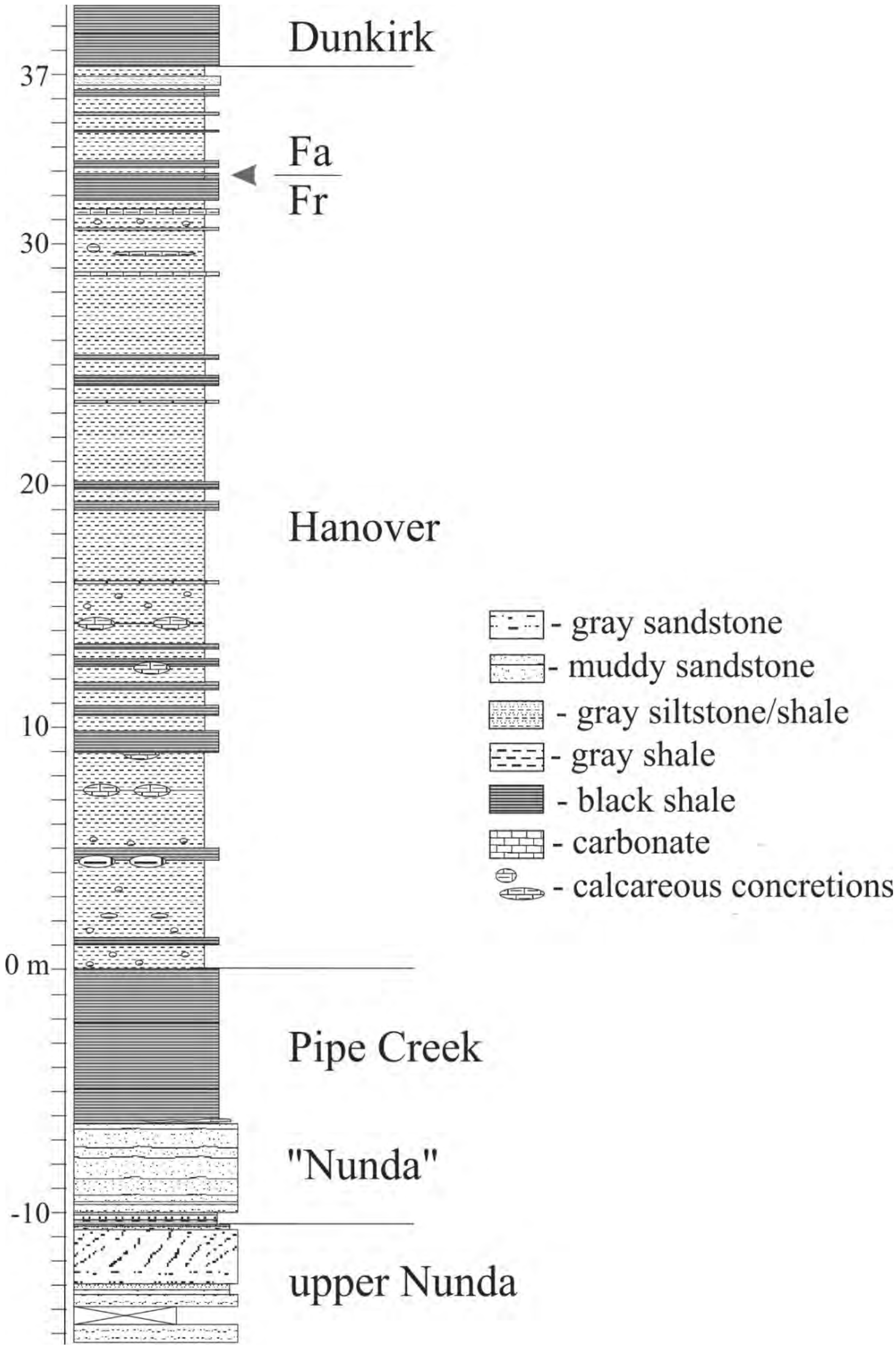

Fig. 4. Schematic diagram of the Java Group and adjacent strata exposed in the bed and banks of Beaver Meadow Creek at and upstream from NY 78 in Java Village. Fa = Famennian; Fr = Frasnian.

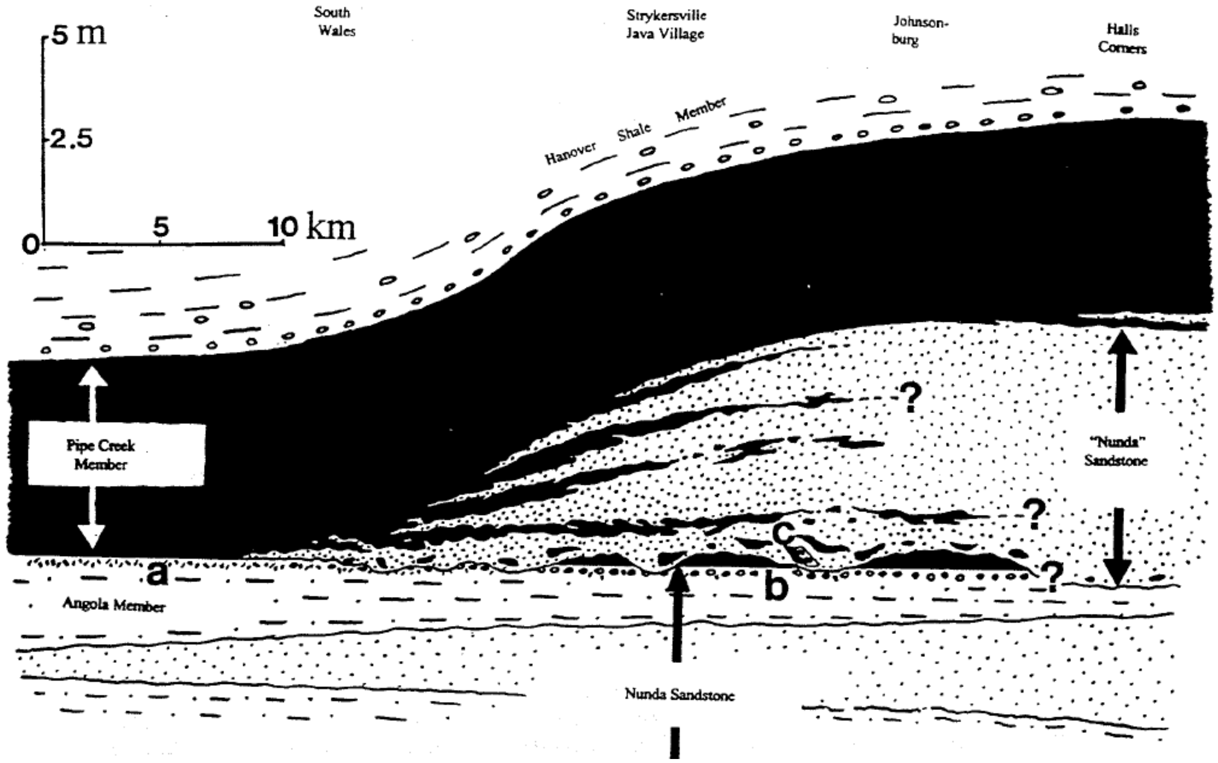

Fig. 5. Generalized east-west cross-section of the Pipe Creek Formation and associated stratigraphic units in the "western" outcrop region in Erie and Wyoming counties. Lettered features include: a, pyrite-rich zone of the Angola Shale below Pipe Creek Formation in eastern Erie County; b, carbonate nodule-rich zone below lower contact of Pipe Creek shale in non-eroded inlier below "Nunda" sandstone; c, olistolith showing exhumed Angola-Pipe Creek contact. Question marks denote uncertainty as to the position southwest of Warsaw, NY, and as to whether discrete "Nunda" beds within Pipe Creek in the Strykersville area amalgamate eastward to give the impression of a single massive flow event or whether the massive bed in the Johnsonburg-Halls Corners area is truly a single event (from Baird and Jacobi, 1999).

The Hanover Formation along Beaver Meadow Creek is 37.5 m thick consisting of intensely bioturbated gray shale interbedded with argillaceous nodular carbonate beds, calcareous nodules, and organic-rich laminated shales (Fig. 4). Concretion horizons, some with concretions ranging up to 0.7 m in diameter, are common in the lower half of the section. Similar to Walnut Creek strata, gray shale and thinner black shales and carbonates occur in near-meter scale cycles. These correspond to ~20 ka precession cycles as seen at Walnut Creek; the longer scale cycles are also evident in the organic- and less-organic-rich strata packages.

Calcareous concretions in the lowermost Hanover contain a diverse nektic and low-diversity benthic fauna of acrotretid brachiopods, ostracodes, tentaculitids, the goniatites *Delphinites cataphractus* and *Sphaeromanticoceras*, and notably the conodont *Palmatolepis bogartensis* which indicates the base of FZ 13, the highest Frasnian conodont zone. The overlying gray shales contain a pyritized molluscan fauna dominated by gastropods. The middle Hanover is notably siltier, both in the gray shales and organic-rich shales, indicative of a more proximal source area compared to Walnut Creek. A thin carbonate bed at 24.5 m in the section yielded abundant conodonts, including *Pa. hassi* s.s. and *Pa. juntianenesis*. Other carbonate horizons contain crinoid debris and the small solitary rugose coral

Metriophyllum. The Point Gratiot Bed rests on a long platform above the last waterfall. The base of the Dunkirk Formation is 4.5 m higher.

The Frasnian-Famennian boundary horizon is at or just below the top of a 10-cm organic-rich black shale bed that has distinct 1-2 cm wide light colored horizontal *Thalassinoides* burrows (cf. Boyer et al., 2014). This bed rests on a 0.7 m thick organic-rich black shale—the Pt. Gratiot Bed—that has a recessive weathering lamination at the base that is possibly equivalent to the Center Hill Tephra in Tennessee (Fig. 6). The top of the Pt. Gratiot Bed is a disconformable surface that yields abundant coalified wood and fish material, including an articulated skeleton of the placoderm *Coccosetus*? (similarly, part of an arthrodire carcass, possibly *Dunkleosteus*, was excavated from the Pt. Gratiot Bed at Point Gratiot in the 1980s). The nowakiid *Homoctenus* is relatively common to abundant on bedding planes, and has been recovered above the boundary in several places. These are some of the last dacryoconarids documented.

The Hanover Formation above the Pt. Gratiot Bed consists of bioturbated gray shales with thin interbeds of black shale, siltstones, and fine sandstones. Approximately 1.5 m above the Frasnian-Famennian boundary is a thin shell-rich bed that contains abundant articulate brachiopods, notably *Retichonetes, Tylothyris*, and *Praewaagenoconchia,* as well as the lingulid *Barroisella* (Day and Over, 2002). A thin sand just below the Dunkirk represents a bed of Canaseraga facies before the IIe deepening.

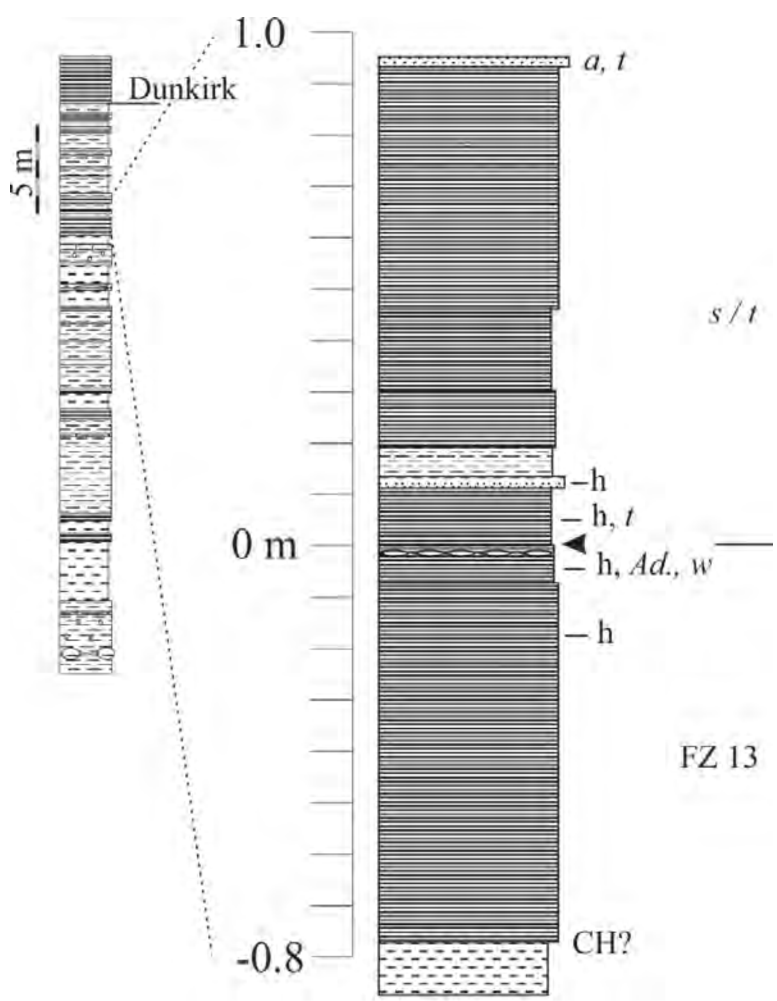

Fig. 6. Schematic diagram of Pt. Gratiot Bed and adjacent strata in the upper Hanover Formation along Beaver Meadow Creek. Frasnian-Famennian boundary is marked by arrow. a = *Icriodus alternatus*; Ad. = *Ancyrodella curvata*; CH = Center Hill Tephra; FZ = Frasnian conodont Zone; h = dacryoconarids (mostly *Homoctenus*); s = *Palmatolepis subperlobata*; t = *Pa. triangularis*; w = *Pa. winchelli*.

STOP 2: Wiscoy Creek

Location Coordinates: N 42°30.280’ W 78°5.014’

Wiscoy Creek is the type location of the Wiscoy Formation, and the section has been illustrated and discussed by many authors (e.g., Pepper and de Witt, 1950; Pepper and de Witt, 1951; Smith and Jacobi, 2000; 2001; 2006; Bush et al., 2015). Overlying the Wiscoy Formation is a black shale unit that has often been correlated with the Dunkirk Formation (Pepper and de Witt, 1950; 1951; Smith and Jacobi, 2000; 2001; 2006), but that Bush et al. (2015) correlated with the Pipe Creek Formation (Fig. 7).

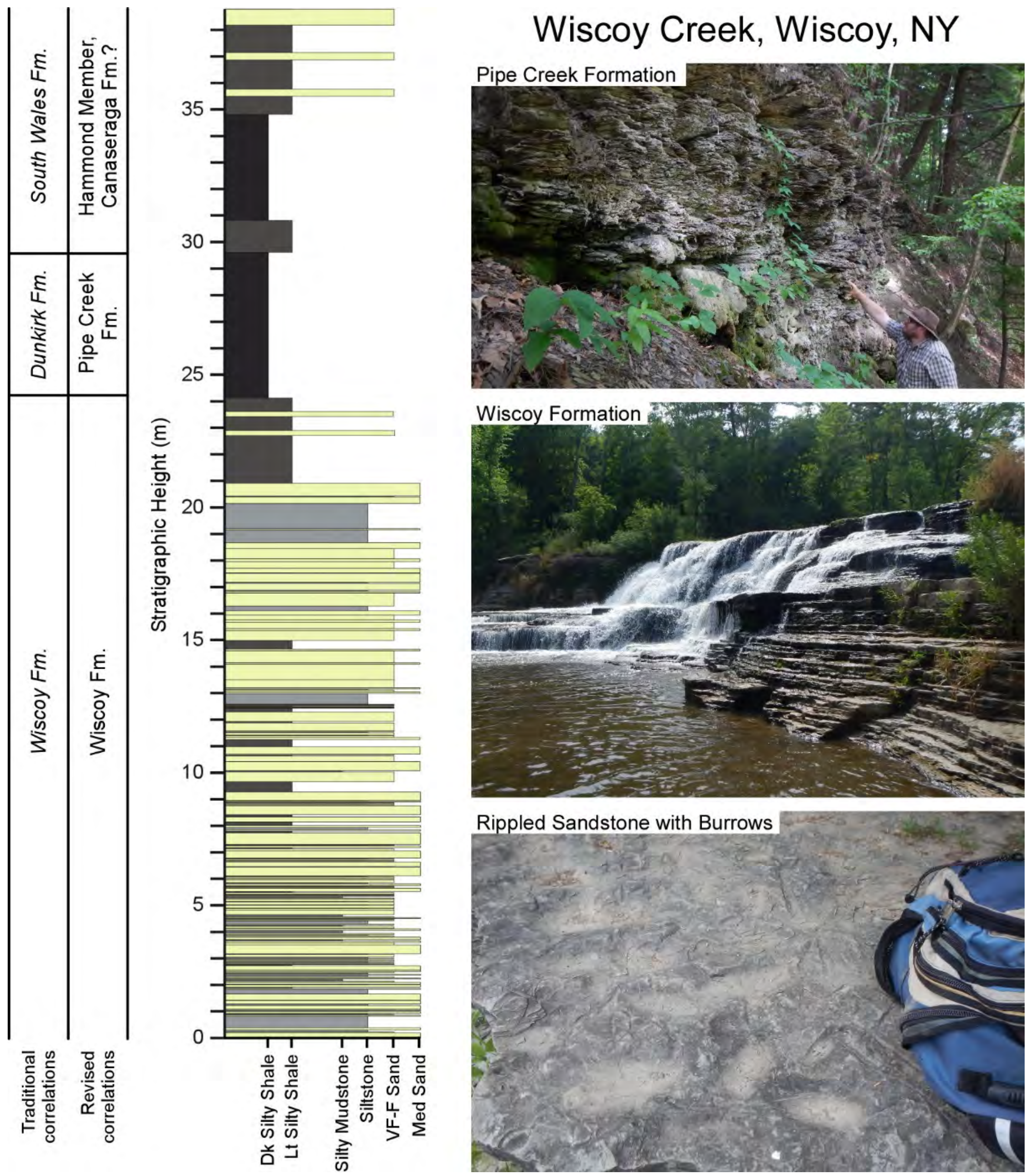

Fig. 7. Wiscoy Creek, Wiscoy, NY. Stratigraphic section based on Pepper and de Witt (1950), Smith and Jacobi (2001), and our own observations. Traditional correlations from Pepper and De Witt (1950, 1951), and revised correlations from Bush et al. (2015) and Beard et al. (2017) (see Fig. 1B, C).

Smith and Jacobi (2001) interpreted the depositional environment of the Wiscoy as lower shoreface, transitioning to more offshore environments in the upper part of the formation. (They also suggested a lagoon or bay as a possibility, but given our observations of the Wiscoy in more proximal settings, that is less likely.) Body fossils are scarce, but trace fossils are abundant in the Wiscoy; Smith and Jacobi (2001) noted the presence of *Skolithos*, *Arenicolites*, *Teichichnus*, *Planolites*, *Rhizocorallium*, and *Zoophycos*.

The dark shale that we correlate with the Pipe Creek Formation, and that previous authors have correlated with the Dunkirk Formation, is visible on the north bank by the dam. It consists of dark, silty shale interpreted as an offshore environment, possibly with low oxygen levels (Smith and Jacobi, 2001). It is overlain by sandstones or siltstones, visible above the dam, that could be correlative with the Hammond Member of the Canaseraga Formation, as defined by Beard et al. (2017).

STOP 3: Mills Mills, Wiscoy Creek

Location Coordinates: N 42°30.12' W 78°07.18'

The Mills Mills locality (Fig. 8) is also located along Wiscoy Creek, upstream from Location 2. The upper part of the Canaseraga Formation is exposed along the creek on private land, downstream from the parking area, and the Dunkirk Formation ("Hume Shale") is exposed along Pond Road and adjacent roads. Smith and Jacobi (2001) indicated that there is approximately 30 m of section between the Pipe Creek and the base of the exposure at Mills Mills.

A meter or two of sandstone and siltstone are exposed at the base of the Mills Mills outcrop, followed by a dark silty shale with interbedded siltstones (Fig. 8). This is overlain abruptly by a thick amalgamated sandstone. Smith and Jacobi (2001, 2006) defined this sandstone as the base of the Mills-Mills Formation, and Beard et al. (2017) treated it as the base of the Mills Mills Member of the Canaseraga Formation. Smith and Jacobi (2001) interpreted these sandstone beds as "TA/B starting turbidites (proximal) that represent channel deposits" in "a channel-levee complex in a prograding deep sea fan. The interbedded shales and siltstones may represent interchannel deposits." An additional sandstone bed at the top of the Mills Mills was interpreted similarly. Much of the remainder of the Mills Mills consists of gray and black shales, interpreted as representing the beginnings of the deepening that culminated in the Dunkirk ("Hume") Shale.

Given the correlations proposed by Bush et al. (2015) (Fig. 1C), the UKW plausibly is exposed at the Mills Mills section, somewhere within the upper Canaseraga Formation. There are numerous intervals of black or dark gray shale that could be correlative with the Point Gratiot Bed. Carbon isotope analysis (in progress) may resolve this question.

Below the top of the Beaver Meadow Creek section is a thick, falls-capping bundle of turbiditic beds, followed by a major transgressive kick to black shale approximately 25 - 30 m above the top of the UKW. If the turbiditic bundle and highest black shale interval on Beaver Meadow Creek are respectively correlative to the Mills Mills and Hume divisions, then this should provide a clue as to the best interval along Wiscoy Creek for searching for the UKW on Wiscoy Creek, knowing the aggregate thickness of the Canaseraga interval at that locality. Moreover, the conspicuous lithologic change from intensely bioturbated, nodular, gray mudrock (lower–middle Hanover interval) below the F-F transition into variably turbiditic, dark shale facies above it at Beaver Meadow Creek, should still be quite findable on Wiscoy Creek, given the modest 25 km distance between the two sections. The shell-rich "recovery bed" above the UKW, noted by Jeff Over at Glade and Beaver Meadow creeks, might also be similarly present above the UKW on Wiscoy Creek and better developed in this upslope setting.

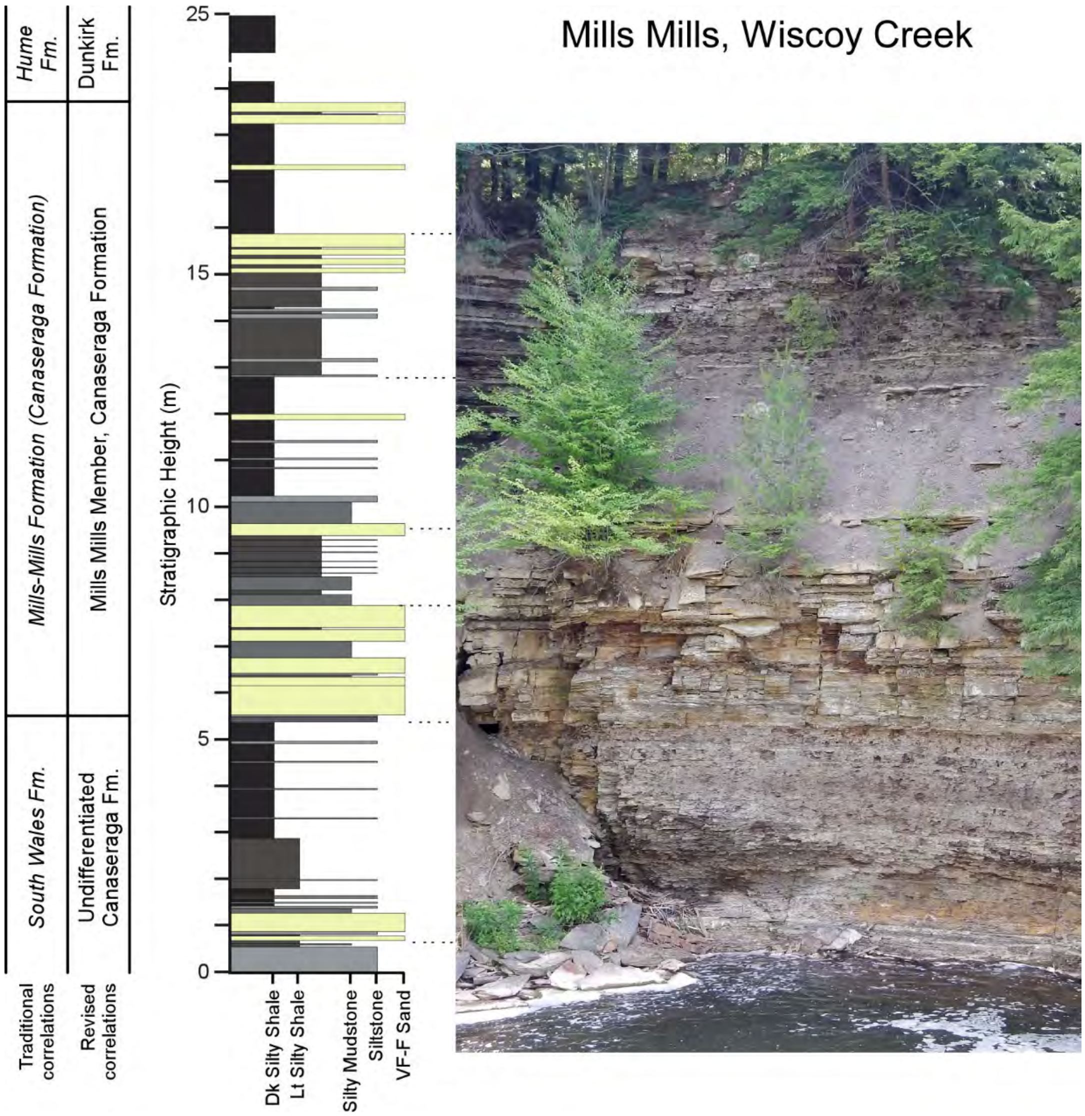

Fig. 8. Mills Mills, Wiscoy Creek, NY. Stratigraphic section based on our own observations. Traditional correlations from Smith and Jacobi (2001); revised correlations from Bush et al. (2015) and Beard et al. (2017) (see Fig. 1B, C).

DAY 2 - FRASNIAN-FAMENNIAN BOUNDARY INTERVAL IN TIOGA COUNTY, PENNSYLVANIA

(Bush, Beard, Brisson, Pier, Over, Baird)

Brachiopod Biostratigraphy

Macrofossil biostatigraphy has long been essential in establishing correlations in the Upper Devonian of the Appalachian Basin (e.g., Chadwick, 1935; Dutro, 1981; Warne and McGhee, 1991; Rossbach, 1992; Brame, 2001), and we present a revised stratigraphic range chart for biostratigraphically important brachiopod species (Table 1) along with photographs of species from the Wiscoy-Candeadea formations (Figs. 9-49). The range chart expands on the one presented by Bush et al. (2015). We expect to add more species to the range chart, but for now we include only those that we are reasonably certain can serve as stratigraphic markers—other species either ranged from the Wiscoy through Caneadea formations, or their range is uncertain. Some ranges may be extended as collecting continues.

The greatest turnover of species occurs from the Wiscoy to the Canaseraga—that is, across the Pipe Creek Formation/Lower Kellwasser equivalent according to revised correlations (Bush et al., 2015). The turnover across the Upper Kellwasser is much less pronounced, although additional work may pinpoint additional species that go extinct in the Upper Kellwasser event or first occur shortly thereafter.

Table 1. Stratigraphic ranges of biostratigraphically useful brachiopod species. The two species marked by asterisks only occur in the lowermost Canaseraga (Hammond Member).

	Wiscoy	Lower Canaseraga	Upper Canaseraga-Caneadea
	pre-LKW	LKW-UKW	post-UKW
Douvillina arcuata	X		
Douvillina cayuta	X		
Strophonelloides coelata	X		
Nervostrophia nervosa	X		
Orthid sp. A	X		
Stainbrookia infera	X		
Pseudoatrypa devoniana	X		
"Spirifer" williamsi	X		
Cyrtina cf. *hamiltonensis*	X		
Schizophoria amanaensis	X	*	
Spinatrypa cf. *hystrix*	X	*	
Cyrtospirifer chemungensis	X	X	
Spinatrypa planosulcata		X	
"Productella" rectispina		X	?
Semiproductus onustus		X	X
"Productella" stigmata		X	X
"Thiemella" leonensis		X	X
Jacoburbirostrum duplicatus		X	X
"Athyris" angelica		X	X

Many of the species documented here are in need of taxonomic revision; some have not been examined in detail since the various work of James Hall (e.g., Hall, 1867; Hall and Clarke, 1892; 1894). Here, we merely seek to provide photographs of the fossils, since standard guidebooks (Linsley, 1994; Wilson, 2014) only contain reprints of Hall's lithographs, and some species are not included. We make no attempt at taxonomic revision—for continuity with existing literature, we use previously applied genus names, often from Linsley (1994). Our identifications are based on comparisons with published works and, in many cases, type specimens. Locality information is provided in Table 2, after the figures. In a few cases, we have photographed fossils from other Upper Devonian formations in order to show better specimens. This work is still in progress, so additional species may be recognized in the future.

Lingulates

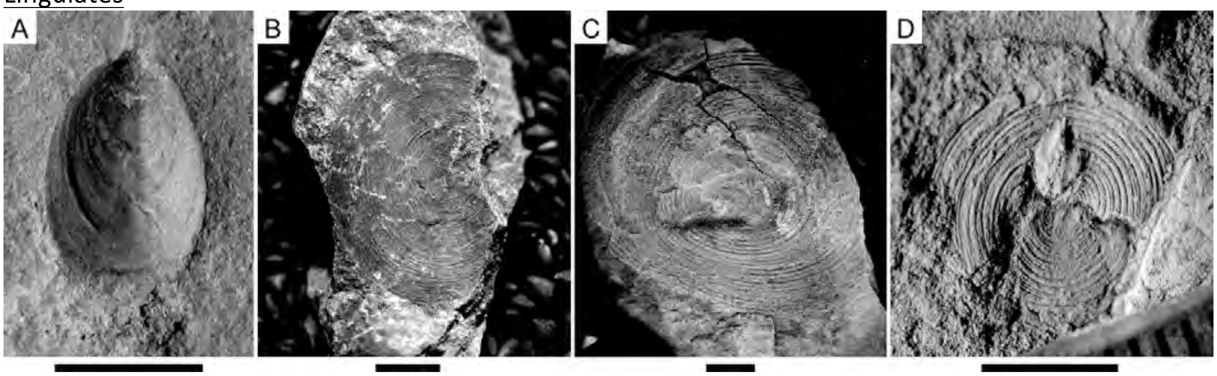

Fig. 9. **Lingulate brachiopods**. We have not attempted to identify these in detail, but both linduloids (**A**) and discinoids (**B-D**) are present. A. Sample ERC-1. B. Sample TGA 20. C. Location ERC. D. Sample CAM 160. Canaseraga Formation. Scale bars = 5 mm.

Strophomenids

Fig. 10. ***Douvillina arcuata***. **A**. Ventral internal mold, sample BCP 106. **B**. Dorsal internal mold, sample CAM 43. **C**. Dorsal external mold, CAM 43. Wiscoy Formation. A-B reprinted from Bush et al. (2015), with permission from Elsevier.

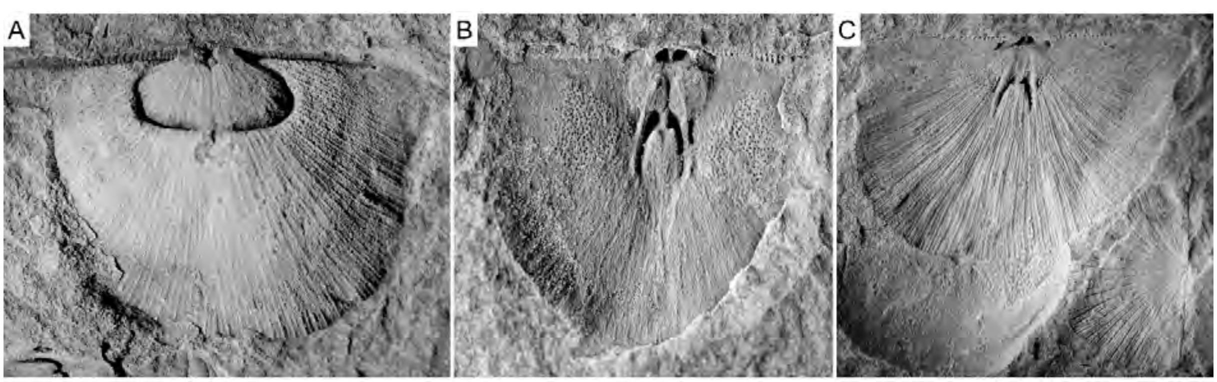

Fig. 11. ***Douvillina cayuta***. **A**. Ventral internal mold. **B**. Dorsal internal mold. **C**. Dorsal internal mold (upper) and exterior mold (bottom right). Location WEL, Gardeau Formation. Scale bars = 5 mm.

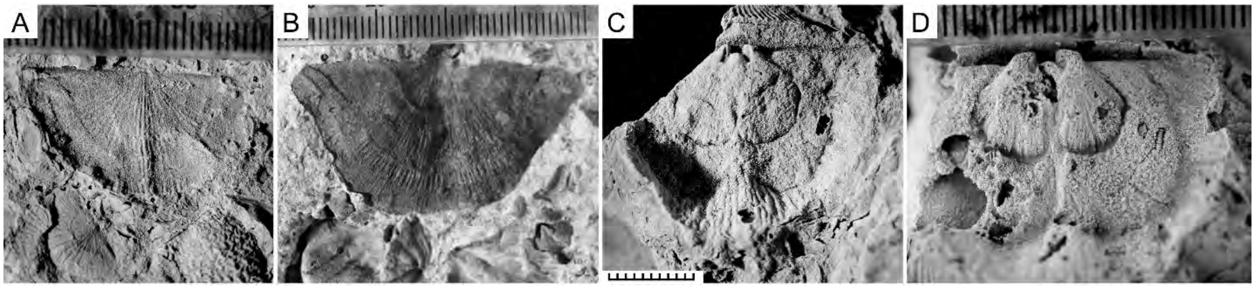

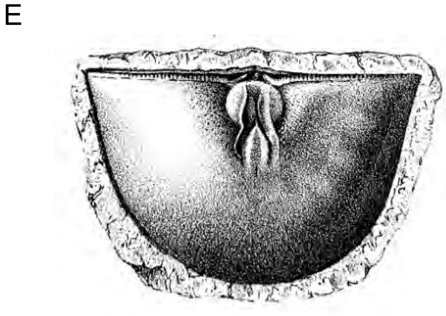

Fig. 12. ***Strophonelloides coelata***. **A**. Ventral external mold, location CRR. **B**. Dorsal external mold, location ADR. **C**. Ventral internal mold, sample TGB 5. **D**. Ventral internal mold, sample CAM 12. **E**. Dorsal internal mold, from Hall (1867, plate 19, fig. 7). Panel A from the Nunda Formation, B-D from the Wiscoy Formation. Scale bars in mm. C reprinted from Bush et al. (2015), with permission from Elsevier.

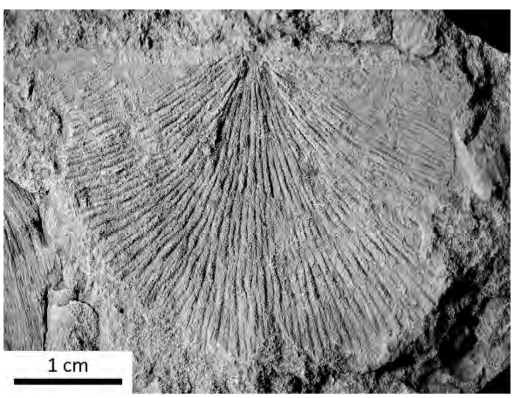

Fig. 13. ***Nervostrophia nervosa***. Mold, location BPH. Wiscoy Formation. Reprinted from Bush et al. (2015), with permission from Elsevier.

Chonetids

Fig. 14. **Chonetid brachiopods**. The small forms are not always well preserved, and we have not tried to identify them in detail. **A**. Ventral external mold, location CRR, Nunda Formation. **B**. Sample CAM 108, Canaseraga Formation. **C**. Sample CAM 106, Canaseraga Formation.

Productids

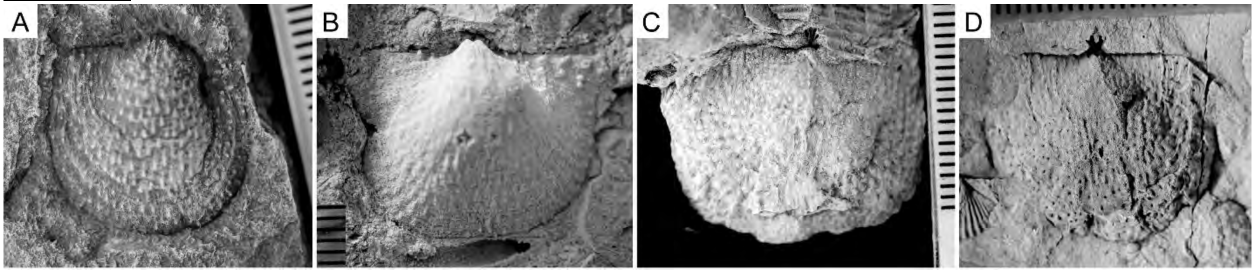

Fig. 15. ***Praewaagenoconcha speciosa***. **A-B**. Ventral molds, CAM 152 and TGA 35, Canaseraga Formation. **C**. Dorsal valve, mold, CAM 148, Canaseraga Formation. **D**. Dorsal valve, mold, Rt. 119 north of Cameron, NY, Wiscoy Formation.

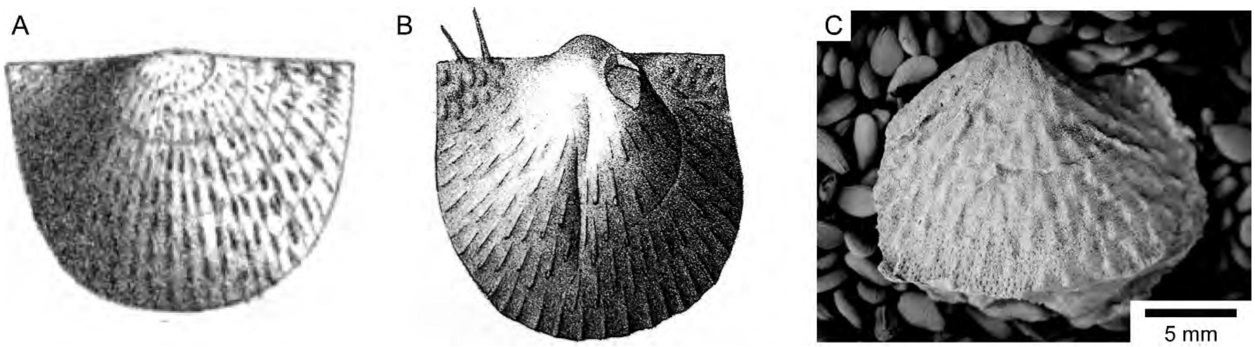

Fig. 16. ***Praewaagenoconcha lachrymosa***. **A-B**. Ventral valves from Conrad (1842) and Hall (1867). Chemung Narrows, Gardeau Formation, the type locality. **C**. Possible *P. lachrymosa*, CAM 132, Canaseraga Formation. Hall (1867) also illustrated fossils from well into the Famennian as *P. lachrymosa*, some of which do not greatly resemble the Chemung Narrows forms. We suspect that some of these belong to a different species. Leighton (2000) felt that *P. lachrymosa* and *P. speciosa* from the late Frasnian were conspecific, representing a morphological gradient.

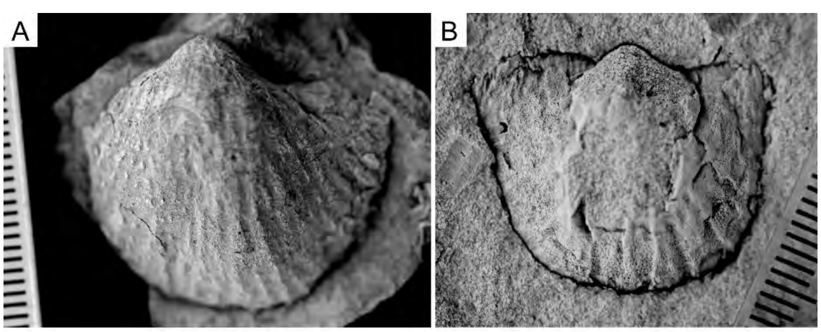

Fig. 17. Productid with ridges. Possibly *Spinulicosta arctirostrata*, or poorly preserved *P. lachrymosa*? **A**. Ventral valve, location TGA, base of section. **B**. Ventral valve, location SWA. Canaseraga Formation. Scale in mm.

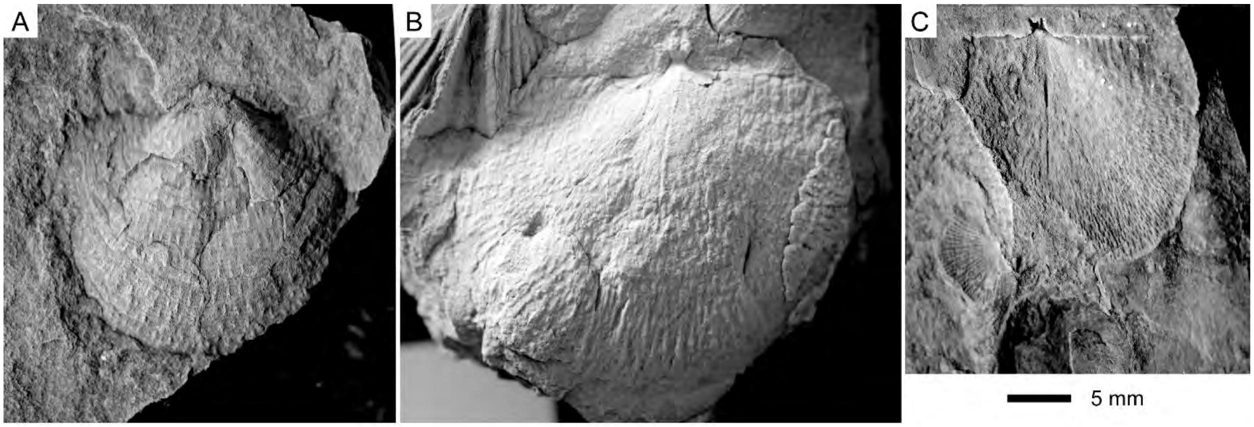

Fig. 18. ***Semiproductus onustus***. **A**. Ventral exterior, location TGA, float, Canaseraga or Caneadea formation. **B**. Dorsal interior, sample TGA 45, Canaseraga Formation. **C**. Dorsal interior mold, sample CAM 108, Canaseraga Formation.

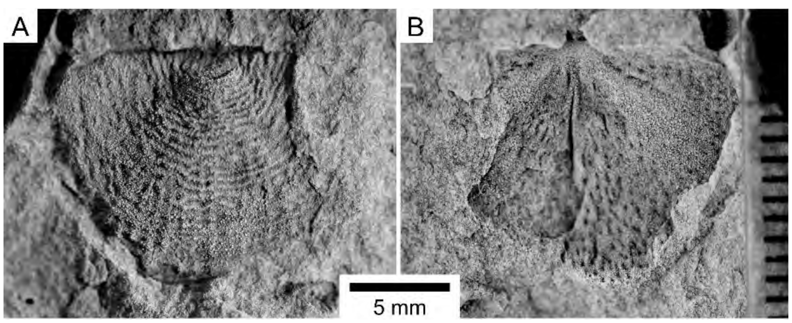

F **Fig. 19**. ***Devonoproductus* cf. *walcotti***. **A-B**. Dorsal external and internal mold, sample BCP 106. Wiscoy Formation.

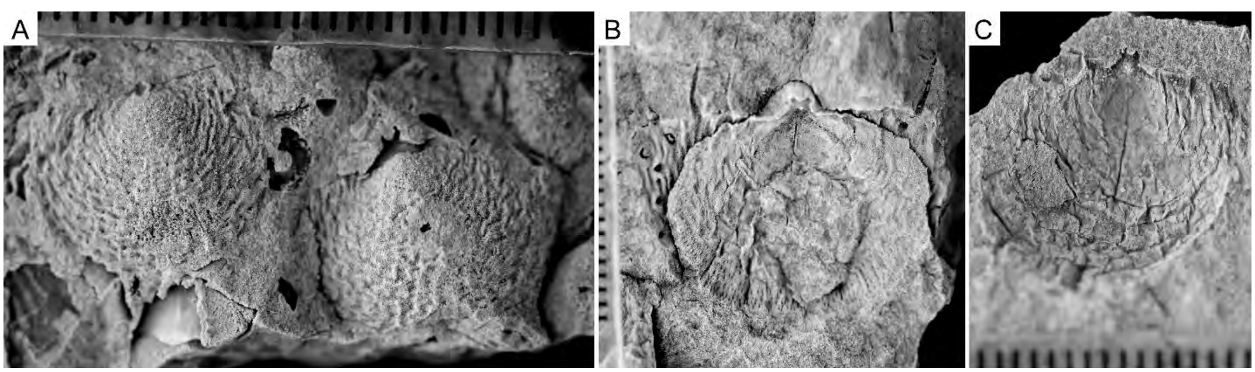

Fig. 20. ***Whidbornella hirsuta***. **A**. Sample CAM 20, Wiscoy Formation. **B**. Dorsal interior mold overlying ventral exterior mold, sample BCP 22, Wiscoy Formation. **C**. Dorsal internal mold, location EHR, base of section, Canaseraga Formation. Scale in mm.

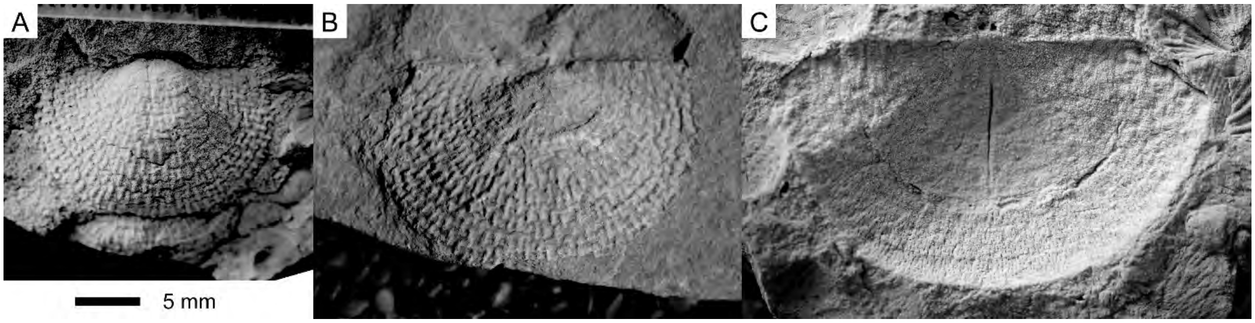

Fig. 21. ***"Productella" rectispina***. **A**. Ventral, location CSA. **B**. Dorsal, sample CAM 79F. **C**. Dorsal internal mold, sample CAM 110. Canaseraga Formation.

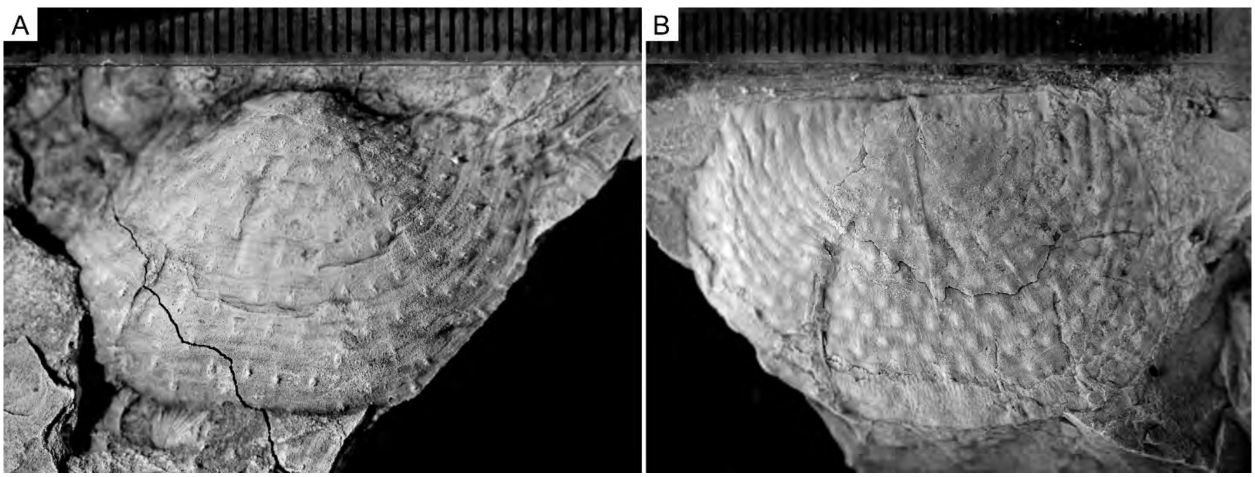

Fig. 22. "*Productella*" *stigmata*. **A-B**, Ventral and dorsal, location PD. Mapped as the Towanda Formation (Woodrow, 1968) or Lock Haven Formation (Berg et al., 1980); these fossils are from strata that are probably equivalent to the Caneadea Formation. This species resembles *Productella lachrymosa* var. *stigmata* Hall (1867), although some fossils that he described as *P. lachrymosa* may belong to this species as well. Scale bars in mm.

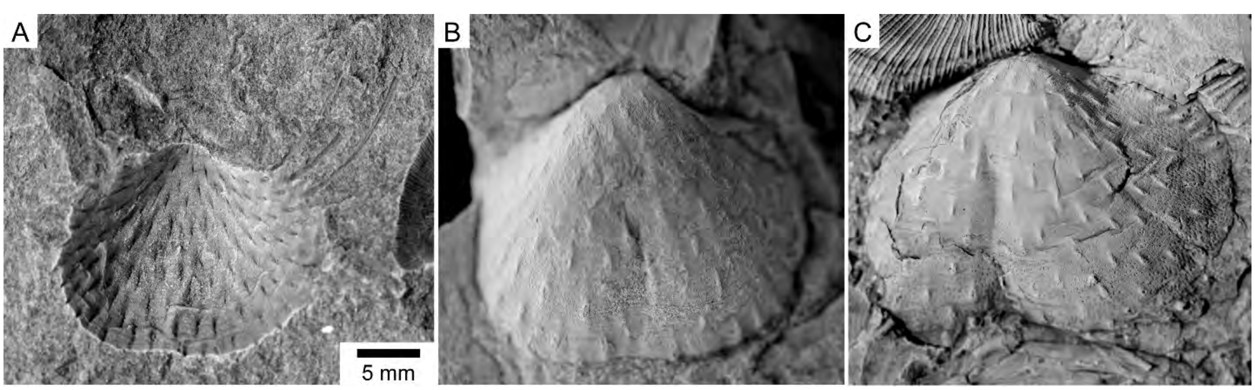

Fig. 23. **"*Productella*" *boydii***. **A**. Ventral external mold, location USA. **B**. Ventral, sample TGA 16R. C. Ventral, location TGB. Canaseraga Formation.

Orthotetids

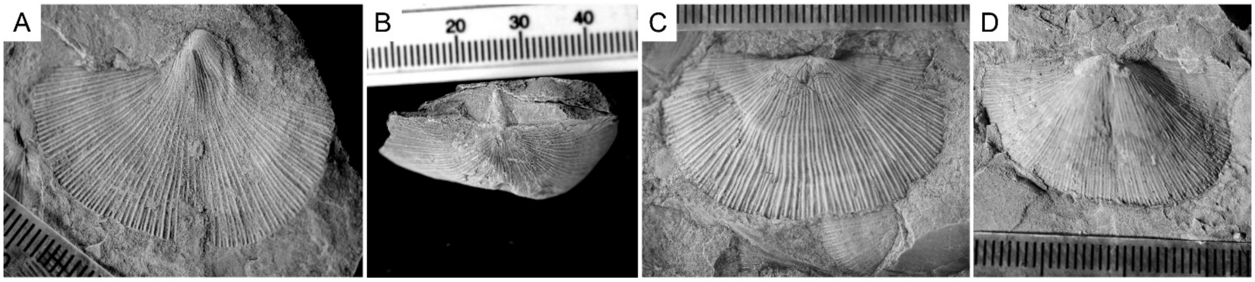

Fig. 24. ***Floweria chemungensis***. **A**. Location TGA, float, Canaseraga or Caneadea. **B**. Ventral exterior, oblique view showing delthyrium, location TGA, base of section, Canaseraga Formation. **C**. Location TGA, float, Canaseraga or Caneadea. **D**. Ventral exterior, location CAM, float, Wiscoy or Canaseraga. All scale bars in mm. See Stigall Rode (2005) for more information on the genus.

Orthids

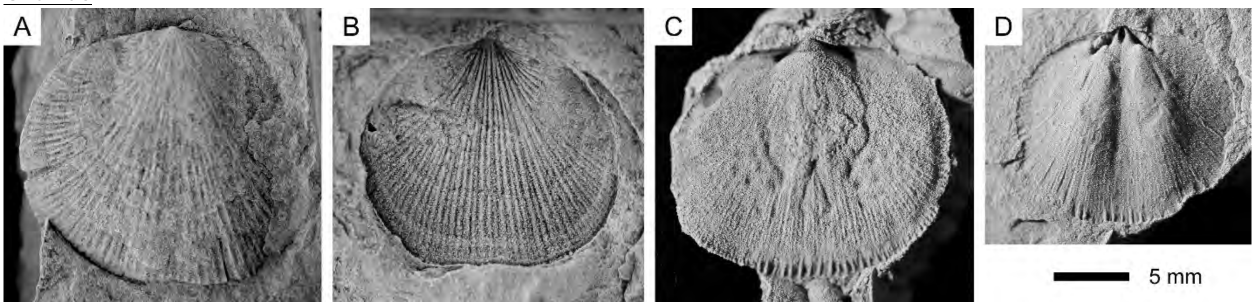

Fig. 25. "*Thiemella*" *leonensis*. **A**. Exterior, sample SLD-2013. **B**. Exterior mold, location unknown. **C**. Ventral internal mold, sample CAM 132. **D**. Dorsal internal mold, float from above the Pipe Creek Formation, location BCP. Canaseraga Formation. C-D reprinted from Bush et al. (2015), with permission from Elsevier.

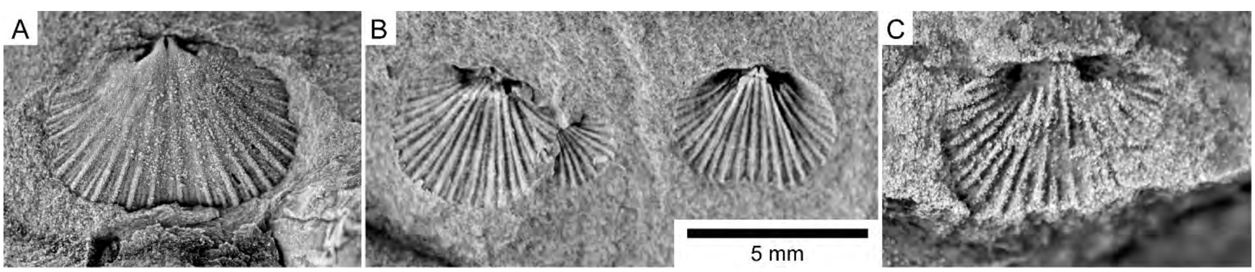

Fig. 26. **"*Dalmanella" allegania* (?)** of Williams (1908). **A**. Dorsal internal mold, location BCP, float, above the Pipe Creek Formation, thus presumably Canaseraga Formation. **B**. Same location. **C**. Location PCR, Canaseraga Formation.

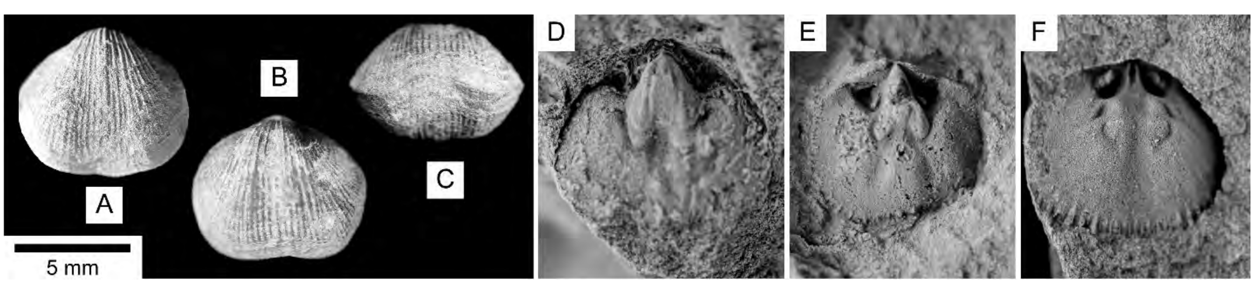

Fig. 27. ***Stainbrookia infera***. **A-C**. Ventral, dorsal, and anterior views, location HNS. **D**. Ventral internal mold, sample BCP 125. **E**. Ventral internal mold, location DAN. **F**. Dorsal internal mold, location BRC. Wiscoy Formation. A-C reprinted from Bush et al. (2015), with permission from Elsevier.

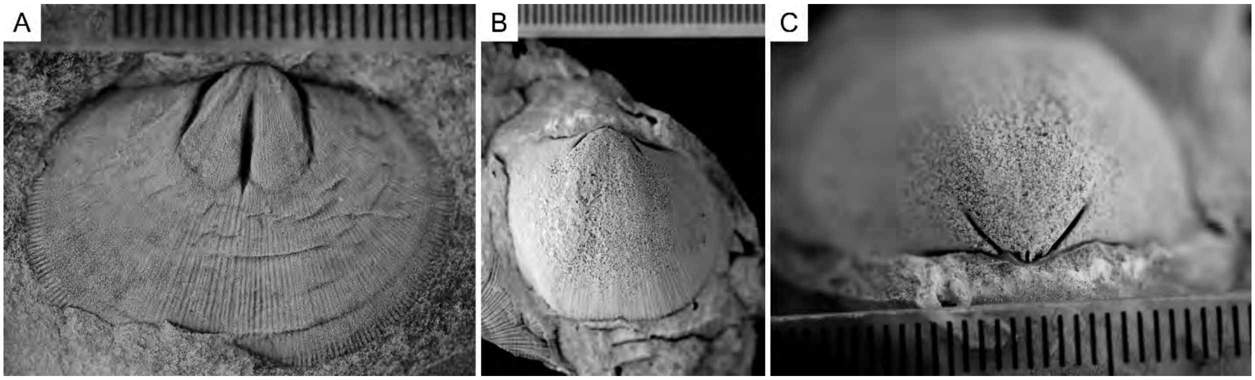

Fig. 28. ***Schizophoria impressa*****, “small” morphotype. A**. Ventral internal mold, sample PCE-1. **B-C**. Dorsal internal mold, sample TGA 1. Scale bars in mm. Canaseraga Formation. See Stigall Rode (2005) for more information on the genus. As defined by Hall (1867), *Schizophora impressa* appears to encompass two forms, referred to here as “small” and “large”.

Fig. 29. ***Schizophoria impressa*****, “large” morphotype**, ventral internal mold, location SGU. Scale in mm. Canaseraga Formation.

Fig. 30. ***Schizophoria*** **sp.?** Ventral internal mold, sample TGA 27. Scale in mm. Canaseraga Formation.

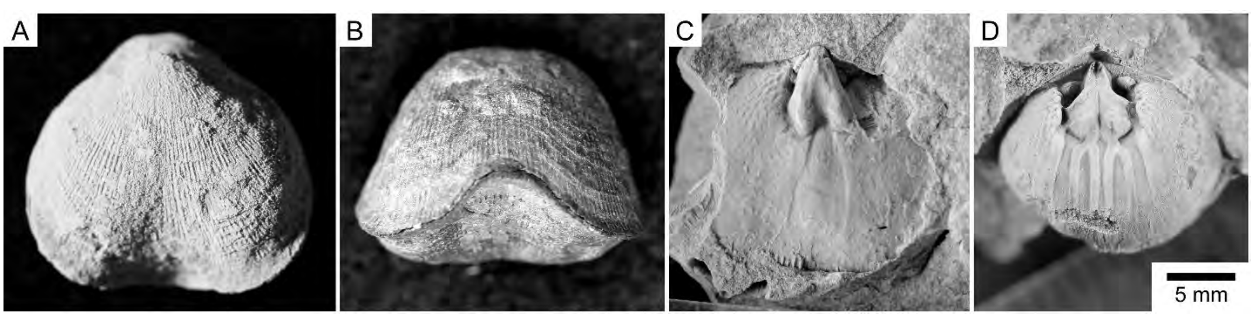

Fig. 31. ***Schizophoria amanaensis***. **A-B**. Ventral and anterior views, location HNS. **C**. Ventral internal mold, sample DAN 30. **D**. Dorsal internal mold, sample BCP 134. Wiscoy Formation. A, B, and D reprinted from Bush et al. (2015), with permission from Elsevier.

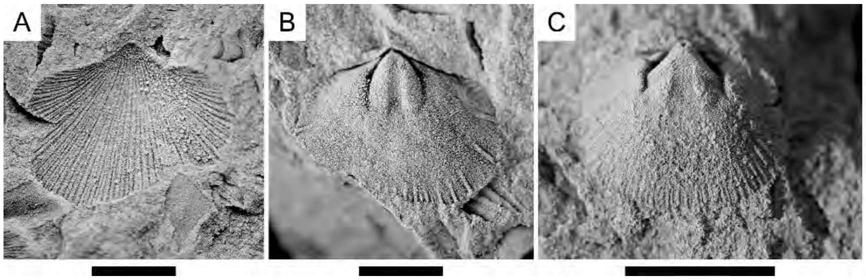

Fig. 32. **Orthid sp. A** (Bush et al. 2015). **A-B**. Ventral external and internal molds, sample CAM 23. **C**. Dorsal internal mold, sample BCP 53. Scale bars = 5 mm. Wiscoy Formation. Reprinted from Bush et al. (2015), with permission from Elsevier.

Rhynchonellids

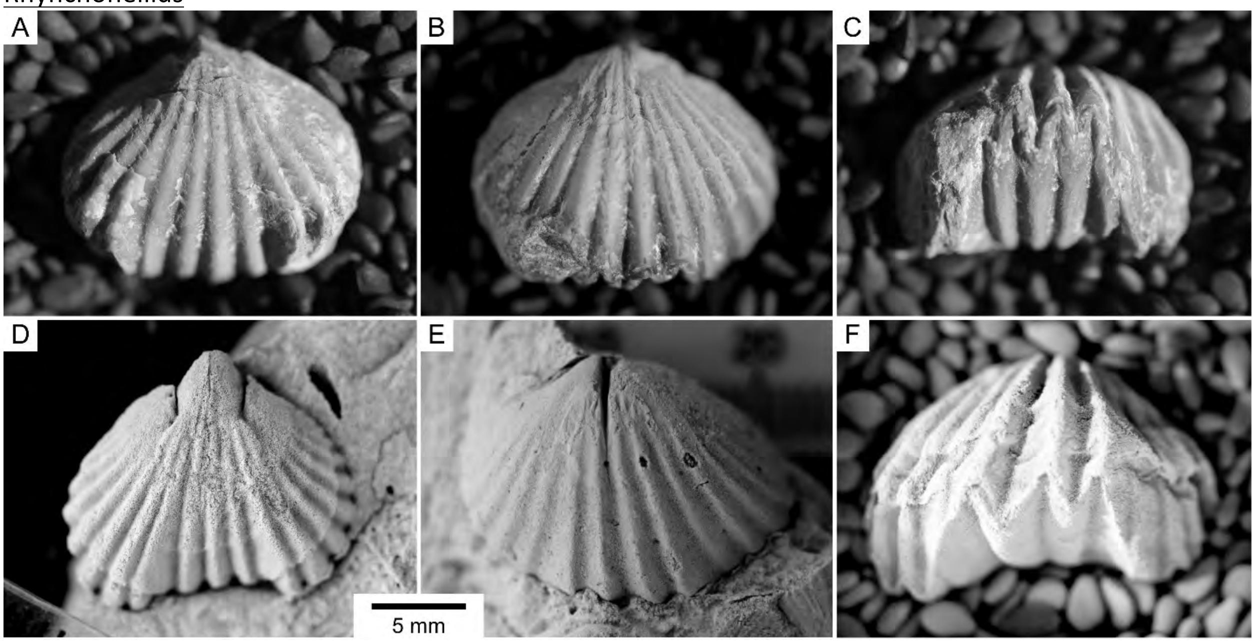

Fig. 33. **"*Cupularostrum*" *contractum.* A-C**. Ventral, dorsal, and anterior views, sample TGA 22, Canaseraga Formation. **D**. Ventral internal mold, Rt. 119 north of Cameron, NY, Wiscoy Formation. **E**. Dorsal internal mold, sample TGB 49, Canaseraga Formation. **F**. Anterior view, location unknown.

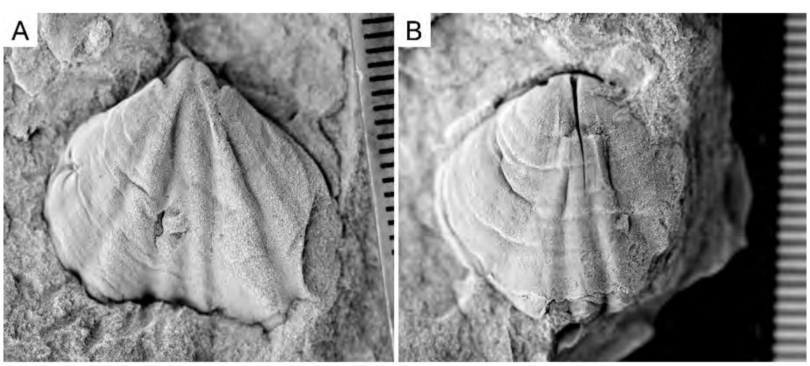

Fig. 34. ***Jacoburbirostrum duplicatus*. A-B**. Ventral and dorsal internal molds, location PCR. Canaseraga Formation. Scale in mm. See Sartenaer (2014) for redescription.

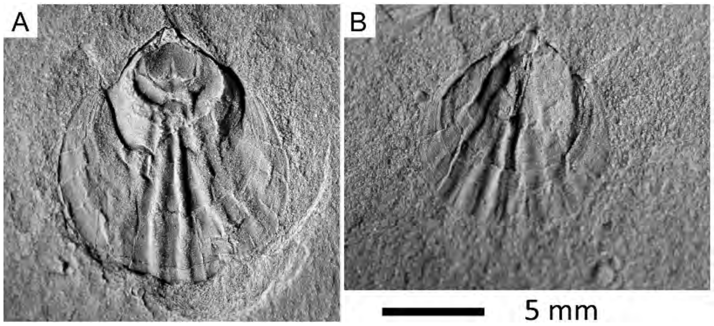

Fig. 35. ***Camarotoechia mesacostalis***. **A-B**. Compressed specimens. Sample BCP 149. Pipe Creek or Canaseraga Formation, pending exact placement of the boundary.

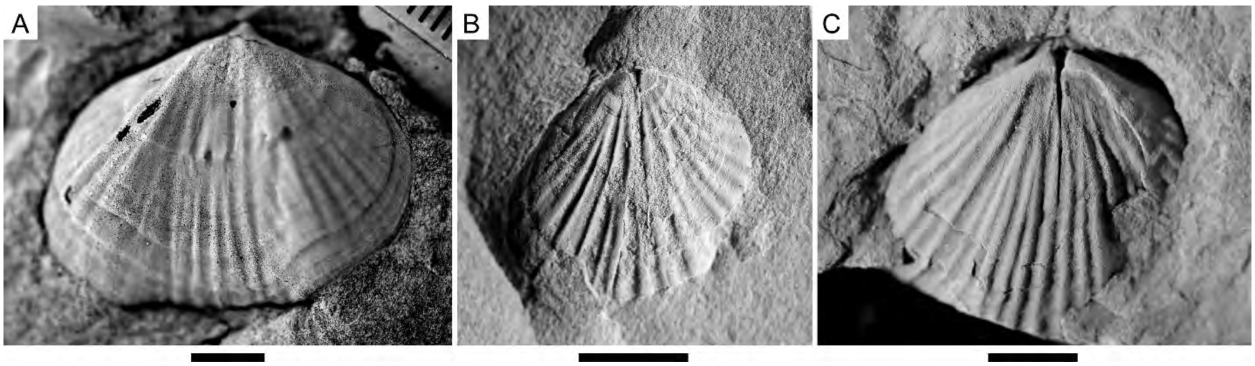

Fig. 36. ***Eumetabolatoechia multicostata***. **A**. Ventral internal mold, location SWA. **B**. Dorsal mold, sample BCP 150. **C**. Dorsal internal mold, location PCR. Canaseraga Formation. Scale = 5 mm.

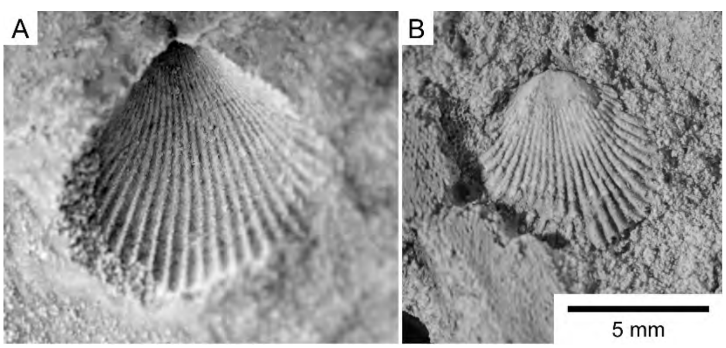

Fig. 37. **Small rynchonellids?** Location TF. Mapped as the Wiscoy Formation (Woodrow, 1968) or Lock Haven Formation (Berg et al., 1980).

Atrypids

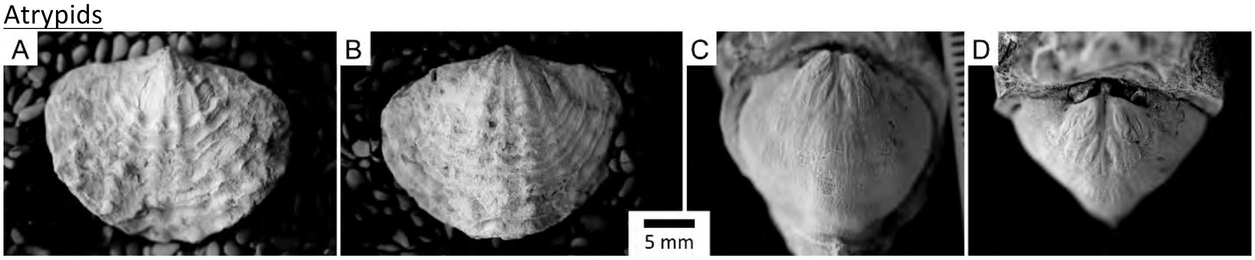

Fig. 38. ***Spinatrypa* cf. *hystrix*, "small" morphotype**. **A-B**. Ventral and dorsal views. **C-D**. Dorsal internal mold. Location HNS, Wiscoy Formation. Coarse-ribbed *Spinatrypa* in the Wiscoy Fm. have often been identified as *S. hystrix*. We suspect that there may be two species in the Wiscoy ("small" and "large" morphotypes). Further work is needed.

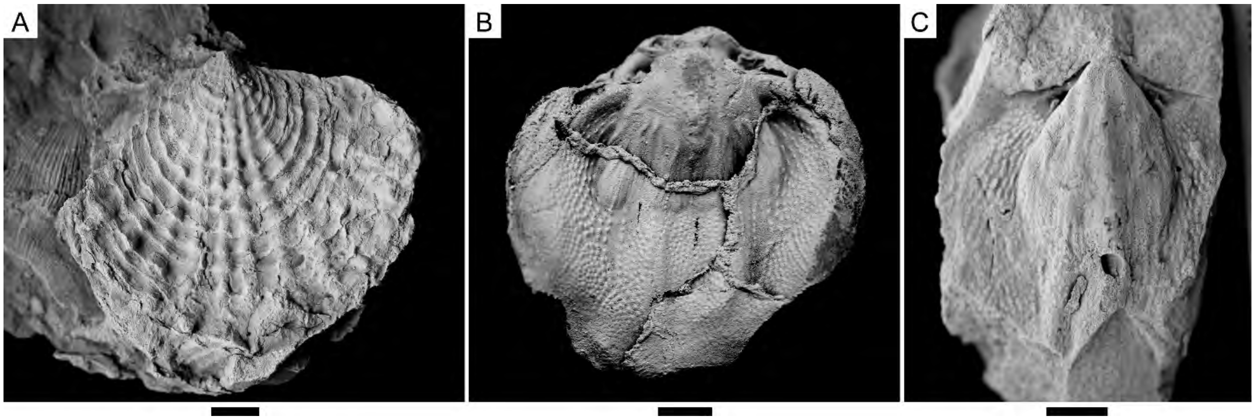

Fig. 39. ***Spinatrypa* cf. *hystrix*, "large" morphotype**. **A**. Ventral views, location TGB, Hammond Member. **B**. Ventral internal mold, Wiscoy Formation. **C**. Ventral internal mold, sample BCP 7, Wiscoy Formation. Scale bars = 5 mm.

Fig. 40. *Spinatrypa planosulcata*. External molds. Location CAM, float, Canaseraga Formation. Scale in mm. See Day and Copper (1998) for illustration of material from Iowa.

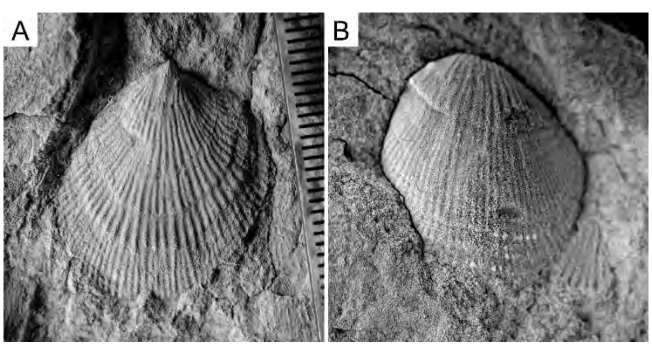

Fig. 41. ***Pseudoatrypa devoniana***. **A**. Ventral valve. **B**. Dorsal valve. Sample BPH 2, Wiscoy Formation. See Day and Copper (1998) for illustration of material from Iowa.

Athyrids

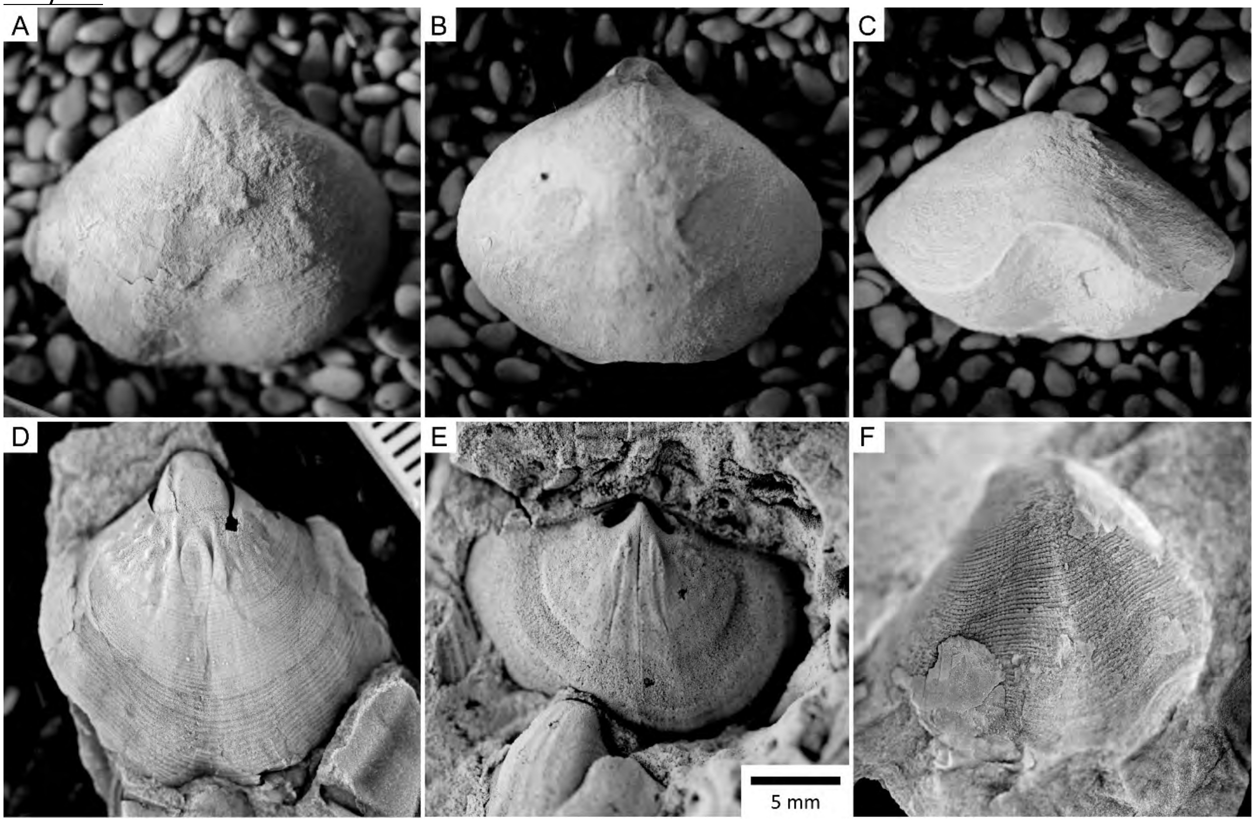

Fig. 42. "*Athyris*" *angelica*. A-C. Ventral, dorsal, and anterior views, sample TGA 13R. **D**. Ventral internal mold, sample showing growth lines, CAM 120. **E**. Dorsal internal mold, sample CAM 145. **F**. Ventral external mold showing growth lines and surface texture, location TGB. All from the Canaseraga Formation.

Spiriferids

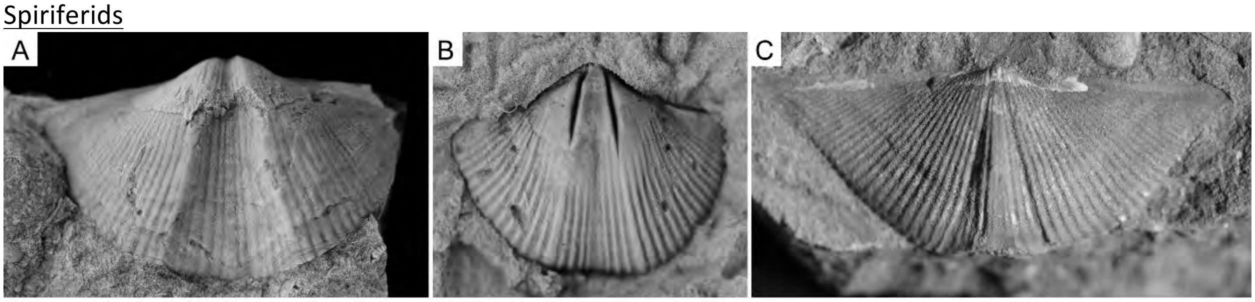

Fig. 43. ***Cyrtospirifer inermis***. **A**. Ventral valve, sample CAM 155. **B**. Ventral internal mold, sample SKI 4. **C**. Dorsal internal mold, sample CAM 155. Scale = 5 mm. Canaseraga Formation. Fossils resembling Greiner's (1957) *C. hornellensis* seem to grade into *C. inermis*; the former is typically smaller but could just represent earlier growth stages.

Fig. 44. ***Cyrtospirifer* cf. *angusticardinalis*** or ***preshoensis***. Sample CAM 159, Canaseraga Formation. Scale in mm.

Fig. 45. ***Cyrtospirifer chemungensis***. Poorly preserved specimen from sample CAM 135, Canaseraga Formation. Scale in mm.

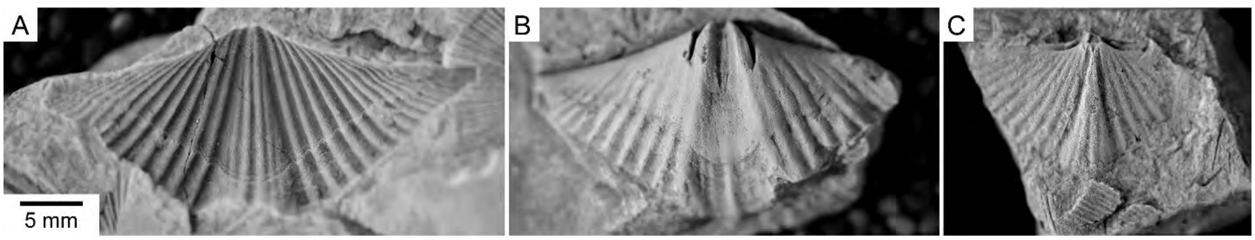

Fig. 46. **"*Spirifer*" *williamsi***. **A**. Ventral external mold. **B**. Ventral internal mold. **C**. Dorsal internal mold. Sample BCP 16, Wiscoy Formation.

Fig. 47. ***Tylothyris mesacostalis***. **A**. Ventral internal mold showing growth lines, location PCR. **B**. Ventral internal mold, CAM 150. **C**. Dorsal internal mold, location PCR. Canaseraga Formation. Scale in mm.

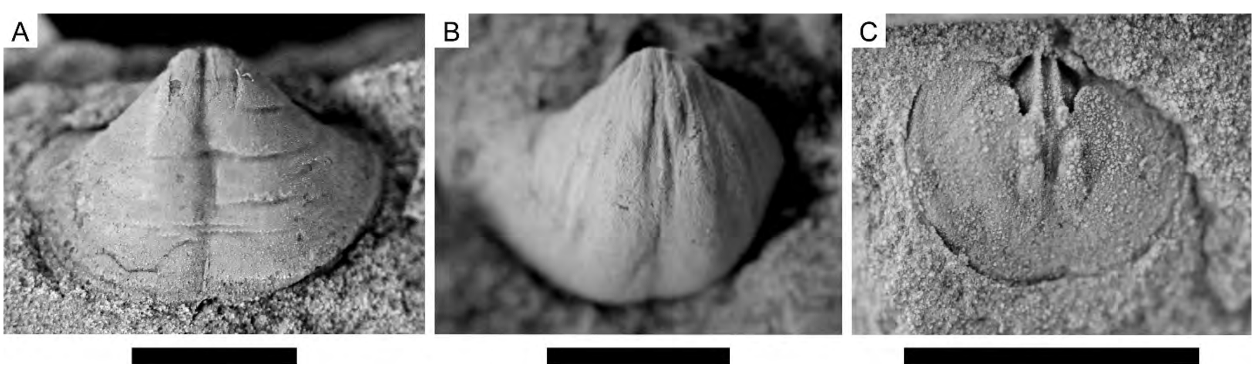

Fig. 48. ***Ambocoelia gregaria***. **A**. Ventral exterior, BCP 141. **B**. Ventral internal mold, BCP 35. **C**. Dorsal internal mold, sample BCP 106. A from Pipe Creek or Canaseraga, depending on placement of boundary. B-C from Wiscoy Formation. Scale = 5 mm. See Zambito and Schemm-Gregory (2013) for redescription.

Spiriferinids

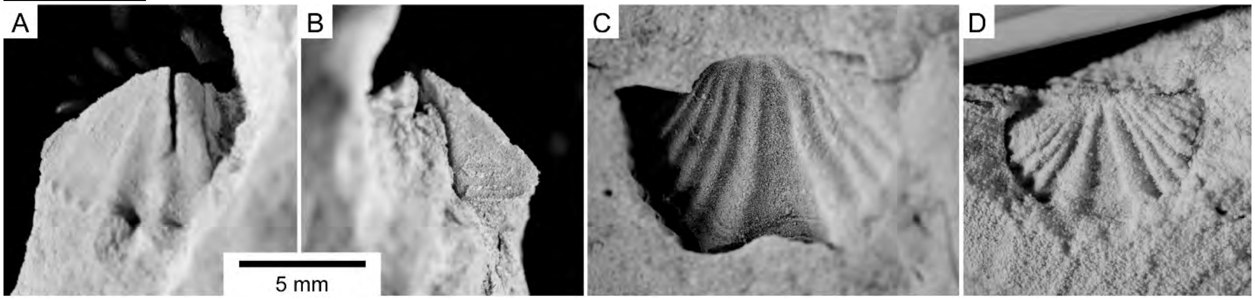

Fig. 49. ***Cyrtina* cf. *hamiltonensis***. **A-B**. Ventral internal mold, broken near the umbo, BCP 106. In B, one side of the delthyrium is visible. **C**. Dorsal external mold, sample BCP 49A. **D**. Dorsal external mold, sample BCP 8. Wiscoy Formation.

Table 2. Locality information for illustrated fossils.

	State	Latitude N	Longitude W		State	Latitude N	Longitude W
ADR	NY	42° 15.430'	77° 32.156'	PCR	NY	42° 15.584'	77° 38.852'
BCP	NY	42° 21.810′	77° 38.675′	PD	PA	41° 42.055'	76° 32.211'
BPH	NY	42° 04.394'	77° 17.953'	SGU	NY	42° 18.135'	77° 32.559'
BRC	NY	42° 23.325'	77° 43.643'	SKI	NY	42° 28.609'	77° 51.441'
CAM	NY	42° 12.008′	77° 26.219′	SLD	NY	42° 25.871'	77° 46.985'
CRR	NY	42° 09.076'	77° 18.792'	SWA	NY	42° 28.731'	77° 50.919'
CSA	NY	42° 16.123'	77° 32.201'	TF	PA	41° 48.734'	76° 30.134'
DAN	NY	42° 29.615'	77° 39.920'	TGA	PA	41° 54.690'	77° 07.446'
HER	NY	42° 28.545′	77° 50.612′	TGB	PA	41° 54.233'	77° 09.949'
ERC	NY	42° 15.303′	77° 40.773′	USA	PA	41° 49.752'	77° 05.289'
HNS	NY	42° 17.649'	77° 38.678'	WEL	NY	42° 00.998'	76° 43.492'
PCE	NY	42° 15.398'	77° 38.011'				

FIELD GUIDE AND ROAD LOG: DAY 2

Meeting Point: Cowanesque Lake Outcrop, Route 49, west of Lawrenceville, PA

Meeting Point Coordinates: N 41° 58.896' W 77° 08.951'

Meeting Time: 10:00 AM

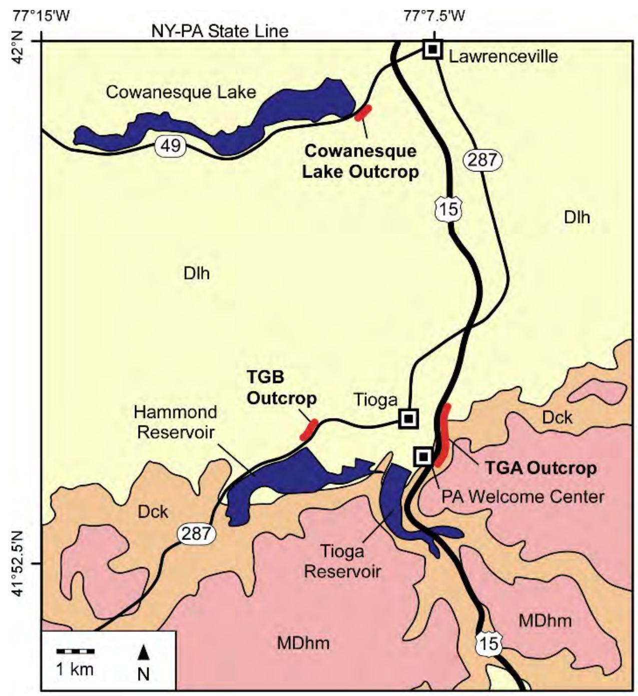

Fig. 50. Geologic map of Tioga, PA area showing the locations of field trip stops. Modified from Beard et al. (2017). Based on Berg et al. (1980). Dlh: Lock Haven Group. Dck: Catskill Formation. MDhm: Huntley Mountain Formation.

STOP 4: Route 49, Cowanesque Lake, PA

Location Coordinates: N 41° 58.896' W 77° 08.951'

This outcrop of the Wiscoy Formation (Figs. 50-51) is similar to the numerous outcrops along I-99/Rt. 15 on either side of the New York-Pennsylvania border, but it is easier to access. The strata display hummocky and swaley cross-stratification, and appear similar to facies S2-S3 of Beard et al. (2017) (see Table 3). Facies S2 indicates medium- to thick-bedded, fine-grained sandstone with < 20% interbedded mudstones with abundant swales, and was interpreted as middle shoreface, and S3 is similar but with thin to medium beds and 20-50% interbedded mud, and was interpreted as lower shoreface.

Fossils are abundant and are easy to find in the float, particularly brachiopods, bivalves, and trace fossils. Brachiopods include *Strophonelloides coelata*, *Whidbornella hirsuta*, *Spinatrypa* cf. *hystrix*, "*Cupularostrum*" *contractum*, and chonetids.

Fig. 51. Outcrop along Rt. 49, Cowanesque Lake, PA.

Table 3. Descriptions and interpretations of sedimentary facies from Tioga, PA, summarized from Beard et al. (2017).

Sand-dominated facies			
	Lithology	**Features**	**Interpretation**
S1	Medium-bedded sandstone with discontinuous coarser laminations	Mud rip-up clasts, swales, dune/ripple cross-stratification	Middle Shoreface
S2	Medium- to thick-bedded, fine-grained sandstone, < 20% mudstone	Swales, hummocks, oscillatory or combined flow ripples	Middle Shoreface
S3	Thin- to medium-bedded, fine-grained sandstone with 20–50% mudstone	Swales, hummocks, oscillatory or combined flow ripples	Lower Shoreface
S4	Very fine-grained, muddy sandstone, medium- to thick-bedded	Structureless, dewatering structures, concretions, increasing mud upwards	Shoreface, rapid deposition
S5	Scour-based, medium- to thick-bedded fine-grained sandstone	Plane-laminated or cross-stratified assoc. with 3D dunes, plant debris with iron staining, wave-ripples	Shelf Channel
Mud-dominated facies			
M1	Gray–brown mudstones with thin beds of siltstone to fine-grained sandstone	Plane-laminations, oscillatory or combined flow ripples (sandstones)	Inner Shelf
M2	Gray, fissile, silty mudstone	May have regularly spaced bedding-parallel red banding	Outer Shelf
M3	Dark gray, fissile silty mudstone	May have regularly spaced bedding-parallel red banding	Outer Shelf, dysoxic–anoxic

STOP 5: Route 287, Tioga, PA

Location Coordinates: N41° 54.423′ W 77° 09.715′

Outcrop of Wiscoy, Pipe Creek, and Canaseraga formations (Fig. 52). Location TGB of Bush et al. (2015) and Beard et al. (2017), and type section of the Hammond Member of the Canaseraga Formation.

Beard et al. (2017) provided a facies description of the Tioga sections, which is summarized below by stratigraphic interval (see Fig. 52 for section and Table 3 for facies descriptions). For other descriptions and interpretations of these sections, see Berg et al. (1981, pp. 153-158), Castle (2000), and Bush et al. (2015).

Wiscoy Formation: The lowermost portion of the TGB section consists of swaley, fine-grained sandstones with various amounts of interbedded mudstone, interpreted as lower to middle shoreface (facies S2-S3). The upper several meters of the Wiscoy are finer grained, consisting of interbedded mudstone and thin siltstone/sandstone beds, interpreted as inner shelf. Fossils include *Strophonelloides coelata*, *Schizophoria amanaensis*, *Spinatrypa* cf. *hystrix*, *Douvillina arcuata*, *Cyrtospirifer inermis*, rugose corals, other invertebrates, and trace fossils.

Pipe Creek Formation: Dark gray, silty shale, interpreted as a low-oxygen, offshore setting. However, depositional conditions could not have been permanently anoxic, because Beard et al. (2017) noted the presence of occasional trace fossils, small bivalves, and lingulid brachiopods.

Hammond Member, Canaseraga Formation: Beard et al. (2017) defined the Hammond Member at the TGB section as the basal portion of the Canaseraga Formation that directly overlies the Pipe Creek. It is considerably coarser-grained than the Pipe Creek and the overlying part of the Canaseraga, and Beard et al. (2017) interpreted it as represented a middle shoreface environment. At Tioga, the base is covered by large burrows, possibly *Teichichnus* isp. and *Thalassinoides* isp., which appear to have been mining the organic-rich sediments of the Pipe Creek once fully oxygenated conditions returned. Other beds of the Hammond at Tioga also contain abundant trace fossils. The coarsest sandstone beds at the base of the Hammond are capped by granule-rich, rippled bedform (Beard et al., 2017, fig. 6A,B) similar to those interpreted in the Appalachian Basin and elsewhere as transgressive ravinement surfaces (Castle, 2000; Plint, 2010; McClung et al., 2013).

The brachiopod *Floweria chemungensis* is extremely common in the Hammond Member, forming pavements at some horizons. The Hammond also contains the last representatives of a couple species that elsewhere have not been found above the Wiscoy, including *Spinatrypa* cf. *hystrix* and *Schizophoria amanaensis*. Trace fossils are also abundant, as well as the large bivalve *Grammysia*, as noted by Berg et al. (1981).

Undifferentiated Canaseraga Formation: The transition from the Hammond to the overlying undifferentiated portion of the Canaseraga represents a deepening. The remainder of this interval generally coarsens upward from primarily facies S3 (lower shoreface; approximately 20 to 30 m) to largely S2 (middle shoreface). The lower, slightly deeper portion of the undifferentiated Canaseraga has a diverse fauna, including several brachiopod species that first appear in this formation ("*Thiemella*" *leonensis*, "*Athyris*" *angelica*, and *Spinatrypa planosulcata*), but the upper reaches of the outcrop are dominated by *Cyrtospirifer inermis*. Glass sponges have also been found in the lower portion of the undifferentiated Canaseraga (Fig. 53).

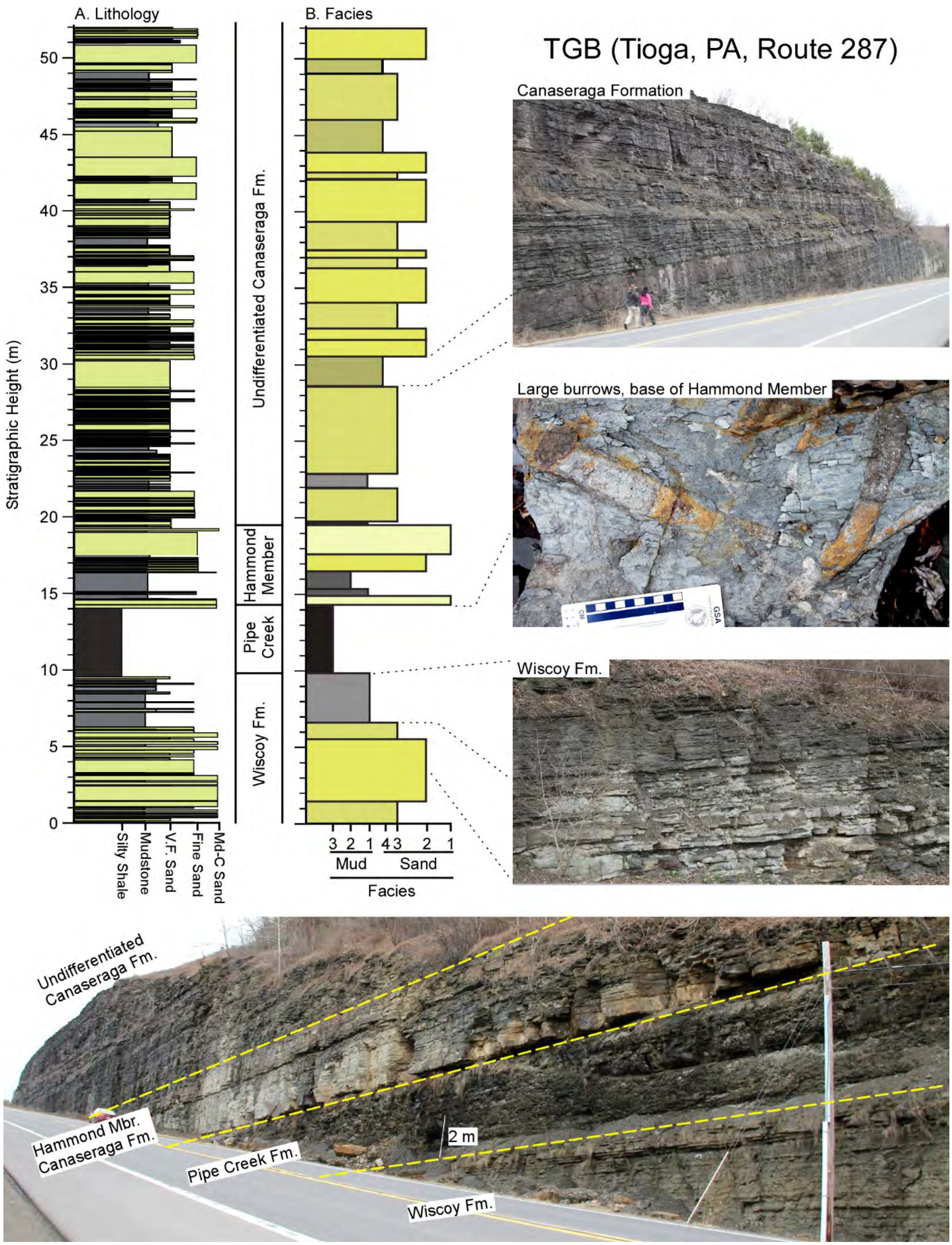

Fig. 52. TGB section, Route 287, Tioga, PA. **A.** Lithology. **B.** Facies analysis (see Table 3). Portions modified from Beard et al. (2017).

Several noteworthy beds are marked in Fig. 52 as facies S4, which consists of muddy, fine grained sand characterized by dewatering structures and convoluted bedding. Beard et al. (2017) interpreted these beds as representing the rapid deposition of mud and sand that were loaded prior to dewatering. Brachiopods are often present in these layers.

The lower 10 m of the TGB section represent an increase in water depth from the swaley sediments of the Wiscoy Formation to the offshore paleonvironments of the Pipe Creek. The transition from the Pipe Creek to the middle shoreface sediments of the base of the Hammond is abrupt, suggesting a forced regression. Additional large changes in water depth are suggested by the rippled bedform atop this basal sandstone, similar to transgressive ravinement surfaces (Castle, 2000; Plint, 2010; McClung et al., 2013), followed by mudstone, then the middle shoreface sediments of the upper Hammond Member. Facies changes are more subdued in the rest of the section, which generally coarsens upward. These patterns appear similar to those seen in the magnetic susceptibility data from further offshore shown in Fig. 3: large facies changes above the Pipe Creek, followed by smaller fluctuations.

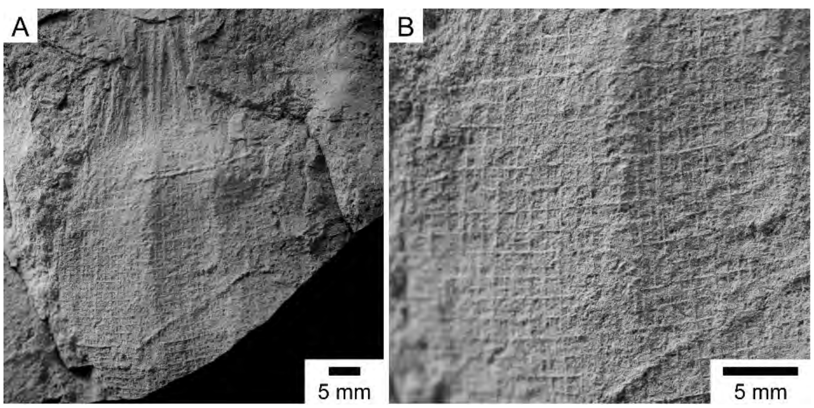

Fig. 53. A. Glass sponge, sample TGB 44, Canaseraga Formation. **B.** Close-up of specimen in panel A.

STOP 6: Route 15, Tioga, PA

Location Coordinates: N 41° 54.690' W 77° 07.446'

Location TGA of Bush et al. (2015) and Beard et al. (2017). Upper Canaseraga (Mills Mills Member), Dunkirk, Candeadea, and Catskill formations. Stratigraphic units are described below in ascending order (Fig. 54; see Table 3 for facies descriptions). Also see Berg et al. (1981, pp. 148-152), Woodrow et al. (1989), Castle (2000), Oest et al. (2013), Bush et al. (2015).

Mills Mills Member, Canaseraga Formation: 10 m of the Mills Mills is exposed at the base of the section. It fines from facies S2 and S3 (middle to lower shoreface) to M1 (inner shelf). Fossils are abundant and include "*Athyris*" *angelica*, *Tylothyris mesacostalis*, *Praewaagenoconcha* sp., *Floweria chemungensis*, *Schizophoria impressa*, and "*Cupularostrum*". Bivalves are also abundant. No Frasnian taxa have been found (e.g., *Spinatrypa* sp., *Cyrtospirifer chemungensis*), consistent with placement above the UKW event.

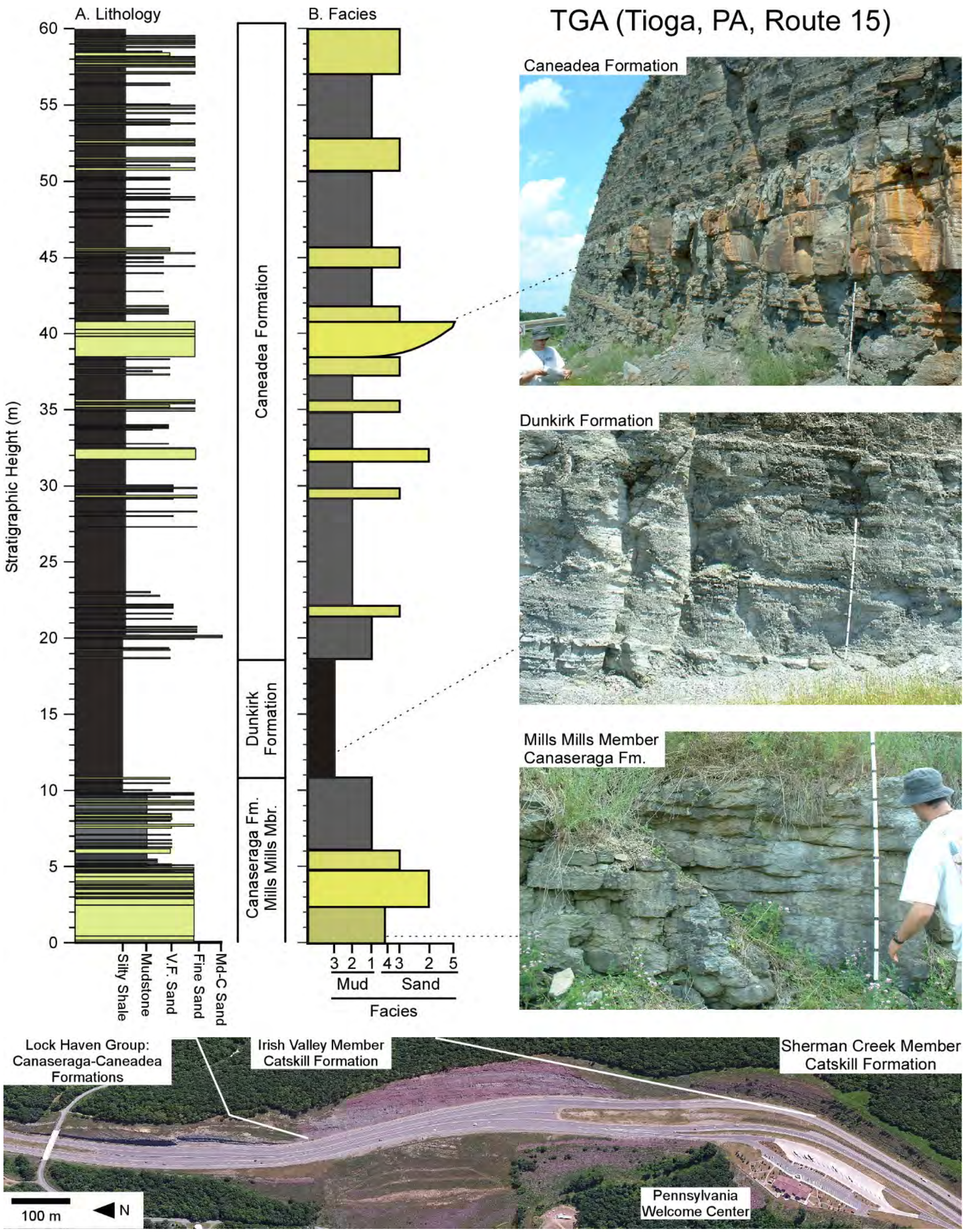

Fig. 54. TGA section, Rt. 15 (future I-99), Tioga, PA. **A.** Lithology. **B.** Facies analysis (see Table 3). Portions modified from Beard et al. (2017). Bottom panel: Imagery ©2017 Google, Map data ©2017 Google. Staff = 2 m with 20 cm divisions.

Dunkirk Formation: The Dunkirk Formation is the uppermost thick black shale unit in the Devonian of New York. At Tioga, it consists of a dark gray, silty shale, and we place the top of the unit at a package of silty-sandy interbeds. Fossils similar to those in the Mills Mills Member are found in the lowermost Dunkirk, although it becomes less fossiliferous above that. Beard et al. (2017) interpreted it as an offshore paleoenvironment, perhaps dysoxic, although the fossils near the base may indicate a gradual decrease in oxygen.

Caneadea Formation: The Caneadea is a thick interval of gray shale overlying the Dunkirk. At Tioga, there are frequent silty-sandy interbeds. It generally coarsens upward from the top of the Dunkirk to the base of the Catskill Formation. Beard et al. (2017) interpreted it mostly as facies M2 and M1 (outer and inner shelf), with increasing S3 (lower shoreface) toward the top. At 40 m, there is a thick sandstone interval with a scoured base, plane laminations, cross beds, ripples, and abundant plant material that Beard et al. (2017) interpreted as a shallow shelf channel. Fossils are generally similar to those in the Mills Mills Member, although above ~40 m, *Cyrtospirifer*, "*Cupularostrum*", and *Floweria* become the dominant brachiopods.

Catskill Formation: We have not examined the Catskill Formation in detail. The lowermost Catskill consists of alternating red and gray strata that are similar to the Irish Valley Member described elsewhere in Pennsylvania, and the overlying strata are similar to the Sherman Creek Member (McLaurin, 2010) (Fig. 54, lower panel). Cotter and Driese (1998) discussed the depositional environments of these units at an outcrop further to the south in Selinsgrove, PA. Lingulids and *Cyrtospirifer* are occasionally present in the lower portion of the Catskill, and trace fossils are abundant in the float. Fish remains are also present, and tetrapods have been found in the Fammenian of the region (Daeschler et al., 1994; Daeschler, 2000).

The lower 10 m of the TGA outcrop represent an increase in water depth from the uppermost Canaseraga Formation into the offshore environments of the Dunkirk. Overall, the section coarsens upward from the Dunkirk into the Candeadea, although it remains mostly mudrock dominated. The transition to the lower Catskill Formation represents further decrease in water depth, culminating in the transition to terrestrial sedimentation.

ACKNOWLEDGEMENTS

Thanks to Kurt Schwenk for the use of lab facilities, to the conference organizers for the invitation to participate, and to the many other people who have helped in this work over many years.

REFERENCES CITED

Aldrich, M.L., 2000, New York Natural History Survey 1836-1842: A Chapter in the History of American Science: Paleontological Research Institution, Ithaca, New York.

Algeo, T.J., Berner, R.A., Maynard, J.B., and Scheckler, S.E., 1995, Late Devonian oceanic anoxic events and biotic crises: 'rooted' in the evolution of vascular land plants?: GSA Today, v. 5, p. 64–66.

Averbuch, O., Tribovillard, N., Devleeschouwer, X., Riquier, L., Mistiaen, B., and Vliet-Lanoe, V., 2005, Mountain building-enhanced continental weathering and organic carbon burial as major causes for climatic cooling at the Frasnian–Famennian boundary (c. 376 Ma)?: Terra Nova, v. 17, p. 25-34.

Baird, G.C., and Brett, C.E., 1991, Submarine erosion on the anoxic seafloor: paleoenvironmental and temporal significance of reworked pyrite-bone deposits, *in* Tyson, R.V., and Pearson, T.H., eds., Modern and Ancient Continental Shelf Anoxia. Geological Society of London Special Publication 58, p. 223–257.

Baird, G.C., and Jacobi, R.D., 1999, "Nunda Sandstone" depositional event in the Pipe Creek Black Shale, South Wales - Varysburg area, New York: Field Trip Guidebook, New York State Geological Association 71st Annual Meeting, p. Sun B1-Sun B7.

Baird, G.C., and Lash, G.G., 1990, Devonian strata and environments: Chautauqua County region, New York State Geological Association, 62nd Annual Meeting Guidebook, p. A1-A46.

Bambach, R.K., 1999, Energetics in the global marine fauna: a connection between terrestrial diversification and change in the marine biosphere: Geobios, v. 32, p. 131-144.

Bambach, R.K., 2006, Phanerozoic biodiversity mass extinctions: Annu. Rev. Earth Planet. Sci., v. 34, p. 127–55.

Beard, J.A., Bush, A.M., Fernandes, A.M., Getty, P.R., and Hren, M.T., 2017, Stratigraphy and paleoenvironmental analysis of the Frasnian-Famennian (Upper Devonian) boundary interval in Tioga, north-central Pennsylvania: Palaeogeography, Palaeoclimatology, Palaeoecology, v. 478, p. 67–79, doi: doi: 10.1016/j.palaeo.2016.12.001.

Berg, T.M., Crowl, G.H., Edmunds, W.E., Luce, P.B., Sevon, W.D., Wilshusen, J.P., and Woodrow, D.L., 1981, Geology of Tioga and Bradford Counties, Pennsylvania, Guidebook for the 46th Annual Field Conference of Pennsylvania Geologists: Pennsylvania Geological Survey, Harrisburg, Pennsylvania.

Berg, T.M., Edmunds, W.E., Geyer, A.R., Glover, A.D., Hoskins, D.M., MacLachlan, D.B., Root, S.I., Sevon, W.D., Socolow, A.A., Miles, C.E., and Kuchinski, J.G., 1980, Geologic map of Pennsylvania: Pennsylvania Geological Survey, 4th ser.

Bowen, Z.P., Rhoads, D.C., and McAlester, A.L., 1974, Marine benthic communities in the Upper Devonian of New York: Lethaia, v. 7, p. 93-120.

Boyer, D.L., Haddad, E.E., and Seeger, E.S., 2014, The last gasp: trace fossils track deoxygenation leading into the Frasnian-Famennian extinction event: Palaios, v. 29, p. 646–651, doi: 10.2110/palo.2014.049.

Boyer, D.L., Owens, J.D., Lyons, T.W., and Droser, M.L., 2011, Joining forces: Combined biological and geochemical proxies reveal a complex but refined high-resolution palaeo-oxygen history in Devonian epeiric seas: Palaeogeography, Palaeoclimatology, Palaeoecology, v. 306, p. 134–146.

Brame, R.I., 2001, Revision of the Upper Devonian in the Central-Southern Appalachian Basin: biostratigraphy and lithostratigraphyPh.D., Virginia Tech, Blacksburg, Va.

Brett, C.E., and Baird, G.C., 1995, Coordinated stasis and evolutionary ecology of Silurian to Middle Devonian faunas in the Appalachian Basin, *in* Erwin, D.H., and Anstey, R.L., eds., New Approaches to Speciation in the Fossil Record: Columbia University Press, New York, p. 285-315.

Bush, A.M., Csonka, J.D., DiRenzo, G.V., Over, D.J., and Beard, J.A., 2015, Revised correlation of the Frasnian-Famennian boundary and Kellwasser events (Upper Devonian) in shallow marine paleoenvironments of New York State: Palaeogeography, Palaeoclimatology, Palaeoecology, v. 433, p. 233-246.

Castle, J.W., 2000, Recognition of facies, bounding surfaces, and stratigraphic patterns in foreland-ramp successions: an example from the Upper Devonian, Appalachian Basin, U.S.A.: Journal of Sedimentary Research, v. 70, p. 896-912.

Chadwick, G.H., 1935, Chemung is Portage: Geological Society of America Bulletin, v. 46, p. 343-354.

Conrad, T.A., 1842, Observations on the Silurian and Devonian systems of the United States with descriptions of new organic remains: Journal of the Academy of Natural Sciences of Philadelphia, v. 8, p. 228–280.

Copper, P., 2002, Reef development at the Frasnian/Famennian mass extinction boundary: Palaeogeography, Palaeoclimatology, Palaeoecology, v. 181, p. 27-65.

Cotter, E., and Driese, S.G., 1998, Incised-valley fills and other evidence of sea-level fluctuations affecting deposition of the Catskill Formation (Upper Devonian), Appalachian foreland basin, Pennsylvania: Journal of Sedimentary Research, v. 68, p. 347–361.

Da Silva, A., and Boulvain, F., 2006, Upper Devonian carbonate platform correlations and sea level variations recorded in magnetic suseptibility: Palaeogeography, Palaeoclimatology, Palaeoecology, v. 240, p. 373-388.

Daeschler, E.B., 2000, Early tetrapod jaws from the Late Devonian of Pennsylvania, USA: Journal of Paleontology, v. 74, p. 301-308.

Daeschler, E.B., Shubin, N.H., Thomson, K.S., and Amaral, W.W., 1994, A Devonian tetrapod from North America: Science, v. 265, p. 639-643.

Day, J., and Copper, P., 1998, Revision of latest Givetian-Frasnian Atrypida (Brachiopoda) from central North America: Acta Palaeontologica Polonica, v. 43, p. 155-204.

Day, J., and Over, D.J., 2002, Post-extinction survivor fauna from the lowermost Famennian of eastern North America: Acta Palaeontologica Polonica, v. 47, p. 189–202.

Day, J., Uyeno, T.T., Norris, A.W., Witzke, B.J., and Bunker, B.J., 1996, Middle–Upper Devonian relative sea-level histories of North American cratonic interior basins, *in* Witzke, B.J., Ludvigson, G.A., and Day, J., eds., Paleozoic Sequence Stratigraphy: Views from the North American Craton, Geological Society of America, Special Paper 306, p. 259–276.

de Witt, W., Jr., and Roen, J.B., 1985, Correlation and geographic extent of some Middle and Upper Devonian and Lower Mississippian black shales in the Appalachian Basin: U. S. Geological Survey Bulletin, v. 1605-A, p. A45-A57.

Dutro, J.T., 1981, Devonian brachiopod biostratigraphy of New York state, *in* W. A. Oliver, J., and Klapper, G., eds., Devonian Biostratigraphy of New York: Subcommission on Devonian Stratigraphy, Washington, D.C., p. 67-82.

Eldredge, N., 1971, The allopatric model and phylogeny in Paleozoic invertebrates: Evolution, v. 25, p. 156-167.

Faill, R.T., and Wells, R.B., 1977, Bedrock geology and mineral resources of the Salladasburg and Cogan Station Quadrangles, Lycoming County, Pennsylvania: Pennsylvania Geological Survey, Fourth Series, Atlas 133cd.

Greiner, H., 1957, “Spirifer disjunctus”: its evolution and paleoecology in the Catskill Delta: Peabody Museum of Natural History Bulletin, v. 11.

Haddad, E.E., Tuite, M.L., Martinez, A.M., Williford, K., Boyer, D.L., Droser, M.L., and Love, G.D., 2016, Lipid biomarker stratigraphic records through the Late Devonian Frasnian/Famennian boundary: Comparison of high- and low-latitude epicontinental marine settings: Organic Geochemistry, v. 98, p. 38-53, doi: http://dx.doi.org/10.1016/j.orggeochem.2016.05.007.

Hall, J., 1867, Descriptions and figures of the fossil Brachiopoda of the upper Helderberg, Hamilton, Portage, and Chemung Groups: New York Geological Survey, Paleontology, v. 4, p. 428 p.

Hall, J., and Clarke, J.C., 1892, An introduction to the study of the genera of Palaeozoic Brachiopoda, Part I. Natural History of New York, Palaeontology VIII: Geological Survey of New York, Albany, New York.

Hall, J., and Clarke, J.C., 1894, An introduction to the study of the genera of Palaeozoic Brachiopoda, Part II. Natural History of New York, Palaeontology VIII: Geological Survey of New York, Albany, New York.

House, M.R., 2002, Strength, timing, setting and cause of mid-Palaeozoic extinctions: Palaeogeography, Palaeoclimatology, Palaeoecology, v. 181, p. 5–25.

House, M.R., and Kirchgasser, W.T., 2008, Late Devonian Goniatites (Cephalopoda, Ammonoidea) from New York State: Bulletins of American Paleontology, v. 374, p. 1-288.

Jacobi, R., Gutmann, M., Piechocki, A., Singer, J., O'Connell, S., and Mitchell, C., 1994, Upper Devonian turbidites in western New York: preliminary observations and implications, *in* Landing, E., ed., Studies in Stratigraphy and Paleontology in Honor of Donald W. Fisher. New York State Museum Bulletin 481, p. 101-115.

Johnson, J.G., Klapper, G., and Sandberg, C.A., 1985, Devonian eustatic fluctuations in Euramerica: Geological Society of America Bulletin, v. 96, p. 567–587.

Lash, G.G., 2017, A multiproxy analysis of the Frasnian-Famennian transition in western New York State, USA: Palaeogeography, Palaeoclimatology, Palaeoecology, v. 473, p. 108-122.

Leighton, L.R., 2000, Environmental distribution of spinose brachiopods from the Devonian of New York: test of the soft-substrate hypothesis: Palaios, v. 15, p. 184-193.

Linsley, D.M., 1994, Devonian paleontology of New York: Paleontological Research Institute, Special Publication, v. 21.

McClung, W.S., Eriksson, K.A., Terry, D.O., Jr., and Cuffey, C.A., 2013, Sequence stratigraphic hierarchy of the Upper Devonian Foreknobs Formation, central Appalachian Basin, USA: Evidence for transitional greenhouse to icehouse conditions: Palaeogeography, Palaeoclimatology, Palaeoecology, v. 387, p. 104–125.

McGhee, G.R., Jr., 1976, Late Devonian benthic marine communities of the central Appalachian Allegheny Front: Lethaia, v. 9, p. 111-136.

McGhee, G.R., Jr., and Sutton, R.G., 1981, Late Devonian marine ecology and zoogeography of the central Appalachians and New York: Lethaia, v. 14, p. 27-43.

McGhee, G.R., Jr., and Sutton, R.G., 1983, Evolution of late Frasnian (Late Devonian) marine environments in New York and the central Appalachians: Alcheringa, v. 7, p. 9-21.

McGhee, G.R., Jr., and Sutton, R.G., 1985, Late Devonian marine ecosystems of the lower West Falls Group in New York, *in* Woodrow, J.W., and Sevon, W.D., eds., The Catskill Delta: Geological Society of America Special Paper 201, p. 199–209.

McLaurin, B.T., 2010, Bedrock geologic map of the Mansfield Quadrangle, Tioga County, Pennsylvania: Pennsylvania Geological Survey, 4th Series,Open-File Bedrock Geologic Map Report, v. 10–03.0.

2014, Astrochron: An R package for Astrochronology (Version 0.3.1). Available from http://www.geology.wisc.edu/~smeyers.

Murphy, A.E., Sageman, B.B., and Hollander, D.J., 2000, Eutrophication by decoupling of the marine biogeochemical cycles of C, N, and P: a mechanism for the Late Devonian mass extinction: Geology, v. 28, p. 427-430.

Oest, C., Fleeger, G.M., Schmid, K., and Anthony, R., 2013, Upper Devonian terrestrial-marine transition along Rt. 15, Tioga Coutny, Pennsylvania.: The 78th Field Conference of Pennsylvania Geologists: The Nippenose Valley and the Route 15 corridor: A Tale of Two Provinces, p. 37–42.

Over, D.J., 1997, Conodont biostratigraphy of the Java Formation (Upper Devonian) and the Frasnian-Famennian boundary in western New York State: Geological Society Special Paper, v. 321, p. 161-177.

Over, D.J., 2002, The Frasnian/Famennian boundary in central and eastern United States: Palaeogeography, Palaeoclimatology, Palaeoecology, v. 181, p. 153-169.

Over, D.J., Baird, G.C., and Kirchgasser, W.T., 2013, Middle-Upper Devonian strata along the Lake Erie Shore, Western New York: New York State Geological Association Field Trip Guidebook, v. 85th annual meeting, p. 182–219.

Pepper, J.F., 1954, Bedrock geology of the Hornell quadrangle, New York: USGS Geologic Quadrangle Map, v. GQ 37.

Pepper, J.F., and de Witt, W., Jr., 1950, Stratigraphy of the Upper Devonian Wiscoy Sandstone and the equivalent Hanover Shale in western and central New York: U. S. Geological Survey Oil and Gas Investigations Chart, v. OC 37.

Pepper, J.F., and de Witt, W., Jr., 1951, Stratigraphy of the Late Devonian Perrysburg Formation in western and west-central New York: U. S. Geological Survey Oil and Gas Investigations Chart, v. OC 45.

Pepper, J.F., deWitt, W., Jr., and Colton, G.W., 1956, Stratigraphy of the West Falls Formation of Late Devonian age in western and west-central New York: USGS Oil and Gas Investigations Chart, v. OC 55.

Plint, A.G., 2010, Wave- and storm-dominated shoreline and shallow-marine systems, *in* James, N.P., and Dalrymple, R.W., eds., Facies Models 4: Geological Association of Canada GEOText 6.

Raup, D.M., and Sepkoski, J.J., Jr., 1982, Mass extinctions in the marine fossil record: Science, v. 215, p. 1501-1503.

Rickard, L.V., 1964, Correlation of the Devonian rocks in New York State: New York State Museum Map and Chart Series, v. 4.

Rickard, L.V., 1975, Correlation of the Devonian rocks in New York State: New York Museum and Science Service Map and Chart Series, v. 24.

Roe, L.M., II, 1975, Sedimentary environments of the Java Group (Upper Devonian) - a three dimensional study: Ph.D. Dissertation, University of Rochester, Rochester, New York.

Rossbach, T.J., 1992, Biostratigraphy of the Greenland Gap Group in Virginia and West Virginia: Ph.D. Dissertation, University of North Carolina, Chapel Hill, North Carolina.

Sartenaer, P., 2014, *Jacoburbirostrum*, a new middle Famennian rhynchonellid (brachiopod) genus from southwestern New York State: Bulletin of Geosciences, v. 89, p. 607–616.

Schindler, E., 1993, Event-stratigraphic markers within the Kellwasser crisis near the Frasnian/Famennian boundary (Upper Devonian) in Germany: Palaeogeography, Palaeoclimatology, Palaeoecology, v. 104, p. 115-125.

Signor, P.W., and Brett, C.E., 1984, The mid-Paleozoic precursor to the Mesozoic marine revolution: Paleobiology, v. 10, p. 229-245.

Smith, G.J., and Jacobi, R.D., 2000, Re-evaluating the Canadaway Group: a revised stratigraphic correlation chart for the Upper Devonian of southwestern New York State: Northeastern Geology and Environmental Sciences, v. 22, p. 173-201.

Smith, G.J., and Jacobi, R.D., 2001, Tectonic and eustatic signals in the sequence stratigraphy of the Upper Devonian Canadaway Group, New York state: AAPG Bulletin, v. 85, p. 325-357.

Smith, G.J., and Jacobi, R.D., 2006, Depositional and tectonic models for Upper Devonian sandstones in western New York state: New York Sate Geological Association Guidebook, v. 78, p. 54-115.

Stigall Rode, A.L., 2005, Systematic revision of the Middle and Late Devonian brachiopods *Schizophoria* (*Schizophoria*) and '*Schuchertella'* from North America: Journal of Systematic Palaeontology, v. 3, p. 133-167.

Stigall Rode, A.L., and Lieberman, B.S., 2005, Using environmental niche modeling to study the Late Devonian biodiversity crisis, *in* Over, D.J., Morrow, J.R., and Wignall, P.B., eds., Understanding Late Devonian and Permian-Triassic Biotic and Climatic Events: Towards an Integrated Approach: Elsevier, Amsterdam, p. 93–180.

Sutton, R.G., Bowen, Z.P., and McAlester, A.L., 1970, Marine shelf environments of the Upper Devonian Sonyea Group of New York: Geological Society of America Bulletin, v. 81, p. 2975-2992.

Sutton, R.G., and McGhee, G.R., Jr., 1985, The evolution of Frasnian marine "community-types" of south-central New York: Geological Society of America Special Papers, v. 201, p. 211-224.

Tesmer, I.H., 1963, Geology of Chautauqua County, New York, Part I, Stratigraphy and Paleontology: N. Y. State Museum Bulletin, v. 391.

Thayer, C.W., 1974, Marine paleoecology in the Upper Devonian of New York: Lethaia, v. 7, p. 121-155.

Tuite, M.L., Jr., and Macko, S.A., 2013, Basinward nitrogen limitation demonstrates role of terrestrial nitrogen and redox control of $\delta^{15}N$ in a Late Devonian black shale: Geology, v. 41, p. 1079–1082.

Tuskes, K., Over, D.J., Hartvigsen, G., Schmitz, M.D., and Davydov, V.I., 2014, Orbital cyclostratigraphy within the Late Devonian Kellwasser crisis indicated by magnetic susceptibility in western New York State – preliminary results: Geological Society of America Abstracts with Programs, v. 46, p. 322-7.

VanAller Hernick, L., 2003, The Gilboa Fossils: The University of the State of New York, Albany, New York.

Warne, A.G., and McGhee, G.R., Jr., 1991, Stratigraphic subdivisions of the Upper Devonian Scherr, Foreknobs, and Lock Haven formations near the Allegheny Front of central Pennsylvania: Northeastern Geology, v. 13, p. 96-109.

Wilson, K.A., 2014, Field Guide to the Devonian Fossils of New York: Paleontological Research Institution Special Publication 44.

Woodrow, D.L., 1968, Stratigraphy, structure, and sedimentary patterns in the Upper Devonian of Bradford County, Pennsylvania. General Geology Report G 54: Pennsylvania Geological Survey, Harrisburg, Pa

Woodrow, D.L., Brett, C.E., Selleck, B., and Baird, G.C., 1989, Sedimentary sequences in a foreland basin: the New York system, 28th International Geological Congress, Field Trip Guidebook, T156: American Geophysical Union, Washington, D.C.

Zambito, J.J., IV, and Schemm-Gregory, M., 2013, Revised taxonomy and autecology for the brachiopod genus *Ambocoelia* in the Middle and Late Devonian Northern Appalachian Basin (USA): Journal of Paleontology, v. 87, p. 277-288.

A3 AND B3: SALAMANCA ("LITTLE ROCK CITY") CONGLOMERATE TIDE-DOMINATED & WAVE-INFLUENCED DELTAIC/COASTAL DEPOSITS UPPER DEVONIAN (LATE FAMMENIAN) CATTARAUGUS FORMATION

JAMES H. CRAFT
Engineering Geologist (retired), New York State Department of Environmental Conservation

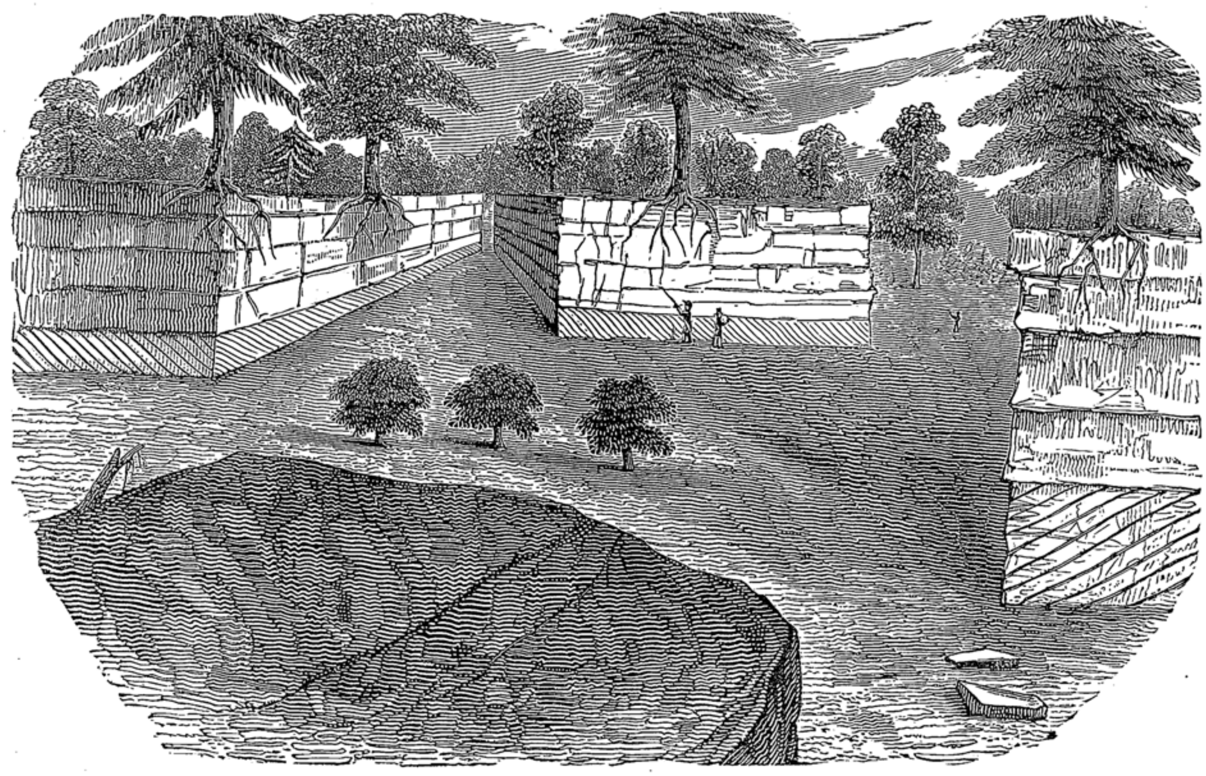

View in Rock city, seven miles south of Ellicottville. From a sketch by Mr. E. N. Horsford.

(*Geology of New York*, 1843)

INTRODUCTION

On a hilltop in Rock City State Forest, three miles north of Salamanca, New York, the Salamanca Conglomerate outcrops in spectacular fashion. Part of the Upper Devonian (late Fammenian) Cattaraugus formation, the quartz-pebble conglomerate forms a five to ten-meter high escarpment and topographic bench at ~ 2200 feet elevation amid a mature cherry-maple-oak forest. In places, house-sized blocks have separated from the escarpment along orthogonal joint sets and variably "crept" downhill. Where concentrated, a maze of blocks and passageways may form so-called "rock cities", an impressive example of which is Little Rock City. The well-cemented blocks permit extraordinary 3-D views of diverse and ubiquitous sedimentary structures and features.

Six outcrop areas with the most significant exposures were logged over a four-kilometer north-south traverse. The traverse largely follows the east-facing hillside which roughly parallels the presumed paleoshore of the Devonian Catskill Sea. Extensive "bookend" outcrops at the north face (off the Rim Trail) and at the southeast perimeter ("Little Rock City" along the North Country-Finger Lakes Trail) and vertical (caprock) control allow a nearly continuous look at spatial and temporal changes in sedimentary deposits along a four-kilometer stretch of inferred late Devonian seacoast.

We'll examine several outcrops which reflect a high-energy and varied coastline as summarized below.

Summary of Findings

Three major depositional environments are interpreted from north to south:

Shoreface to foreshore (beach) coarsening-upward sequence - ("north face" **Outcrops #2 & 3** from base)

- ~ 1 m of thin-bedded (5-10 cm) wave cross-laminated strata; mostly buff, medium sand with some coarse sand, granules, and a few fine pebbles.
- ~ 3 m of amalgamated coarse-grained, large (10-20 cm x 50-100 cm), smooth-crested wave ripples with abundant pebbles (some apparent 3-D forms seem without analogues), interbedded in places w/thin fine-grained (rolling-grain) wave ripples; some trough/planar cross-beds near top.
- ~ 3 m of parallel/low-angle strata of gray interbedded coarse sand and pebbles.

Prograding tide-dominated delta (w/coarse-grained distributaries, tidal channels, bars, and shoals) **(Outcrops # 4, 5, & 6)**

- abundant channels (abundant pebbles, meters to tens of meters wide, ~1-2 m deep) and channel point bars (coarse sand to pebble lateral-accretion deposits of tidal, delta distributary/fluvial channels). One channel complex directly overlies fine-grained wave ripple-laminated (marine) sandstones.
- cross-bedded strata of various dimensions (~ 0.05 m to +1 m) commonly arranged in cosets, some bidirectional.
- current indicators mainly directed shoreward (E-SE) but bi-directional cross-beds common; some truncation surfaces show wave influence.

Sub-aqueous tidal dune field – **Outcrop area # 7** ("Little Rock City")

- very large scale (up to 5+ m thick) planar 2-D cross-beds with fine-to-coarse sand and abundant granule/fine pebble concentrations and occasional larger pebbles; dune foresets mostly inclined 20-30^{o} and ~ 5-10 cm thick; granule layers usually thicker; some dunes are traceable up to 150 m across several blocks.

- foreset azimuths (50^{o} to 150^{o}) show dunes migrated parallel with and toward the paleoshore with no major reactivation surfaces; most toesets are tangential; planar truncation surface at the top of the dunes shows wave influence.
- a complete 2-3 m dune bedform ("form-set": foreset, topset, stoss preserved); core shows directionally-opposed cross-strata which aggraded vertically until one flow direction (100^{o} – apparent flood tides) prevailed and the ~ 3 m dune began to migrate by periodic foreset deposition.

The entire sequence is overridden by ~ 2-3 m thick channel/lateral accretion deposits with some reddish, well-oxidized strata and plant remains. The caprock varies spatially and is generally similar to the underlying deposits with some reworking evident. Within the deltaic sequence, the uppermost caprock contains large (average 2-4 cm; up to 7 cm) densely/randomly-packed flat-lying vein-quartz pebbles (and some red and brown sandstone, a jasper? clast w/quartz veins, and red mudstone rip-up clasts not seen elsewhere) with abundant aligned plant remains. And finally, with diligent search, wave-ripple laminated buff-colored sandstones with abundant marine fossils (not seen elsewhere) can be found draping the caprock in this area.

The orthoquartzitic Salamanca conglomerate evidently records a high-energy Upper Devonian seacoast, with at least meso-tidal range, as indicated by a pebbly beach, a tide-dominated delta prograding over marine wave-rippled fine sands, and a sub-aqueous large-scale dune field formed by strong flood tides. Most of the sequence records delta progradation and sediment transport/redistribution along shore to dunes and beaches by tides and waves. Well-exposed channel deposits at the top (which overlie wave-truncated dunes and beach deposits at a similar elevation) suggest either expansion of the delta/delta plain or a transition to a coastal plain terrestrial environment (perhaps including a major flood event as suggested by localized large clasts of quartz, sandstone, mud rip-up clasts, and abundant plant fossils) followed by an apparent abrupt rise in relative sea level and a transgression as indicated by subsequent fine-grained wave-formed strata with an abundant marine fossil fauna.

Location and Physiographic Setting

The conglomerate beds of southwestern New York have long been a source of wonder. Appearing in widely-scattered and limited outcrops and more often, as isolated "float" blocks, these beds may more rarely form accumulations of large joint-separated blocks ("buildings") and passages ("streets") dubbed "rock cities". Examples include "Rock City Park" south of Olean (Pennsylvanian age), "Thunder Rocks" (Mississippian? age) atop Allegany State Park, "Panama Rocks" (Upper Devonian age) and "Little Rock City" (the Upper Devonian Salamanca Conglomerate), the subject of this study and perhaps the finest example of a rock city in an unrivaled and freely-accessible setting.

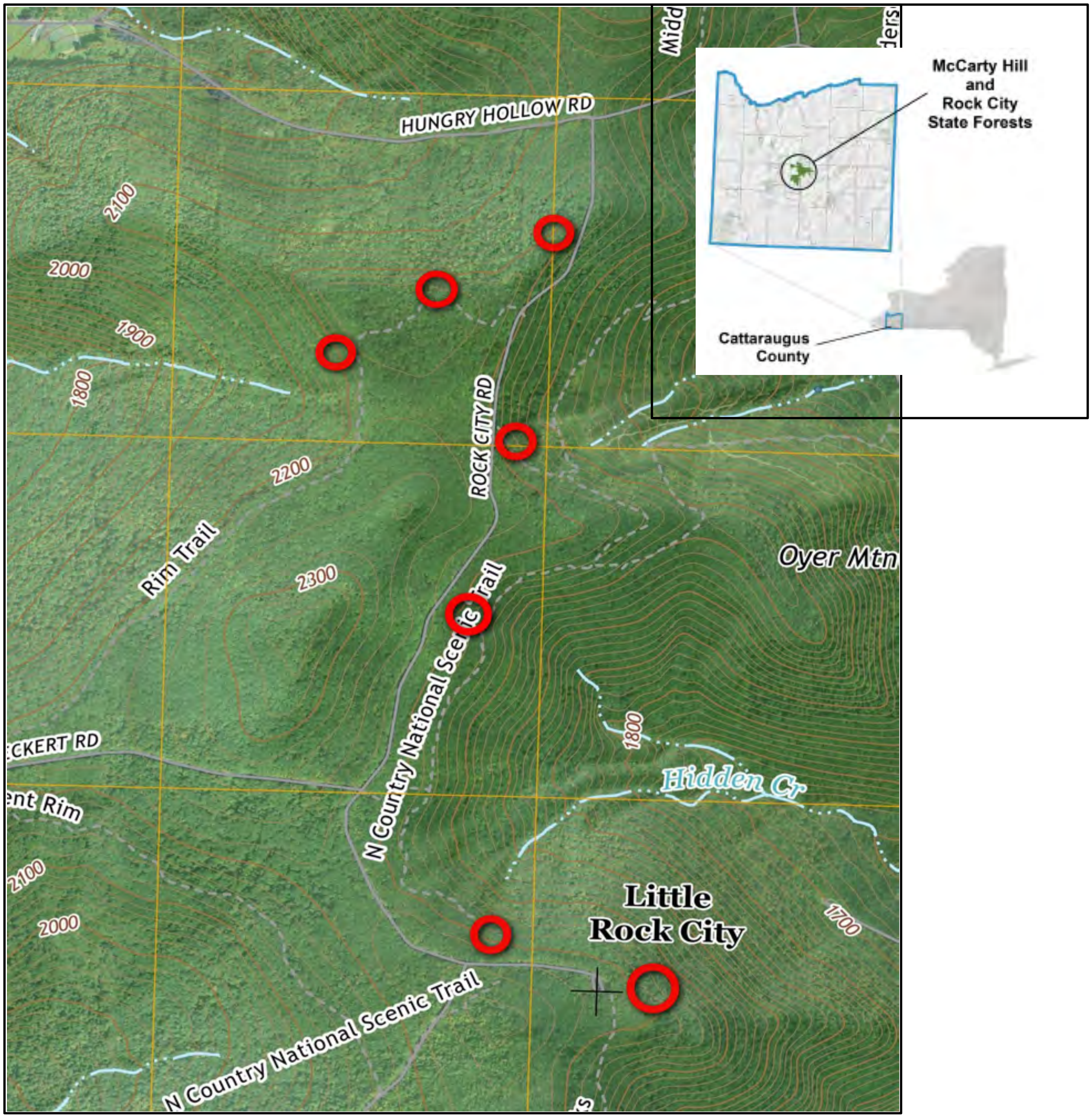

Figure 1. Location Map – Outcrops in Red (#1 - #7 - North to South)

Scale: 1 cm = 200 m Source: USGS – Salamanca Quadrangle (2016)

The Salamanca Conglomerate outcrops prominently (up to a 10m escarpment) and forms a locally-widespread plateau (~ 2200 feet elevation) in Rock City State Forest and adjacent McCarty Hill State Forest (http://www.dec.ny.gov/lands/77184.html). This mature forest of cherry, maple, and oak blankets nearly ten square miles of Appalachian Plateau uplands between Ellicottville and Salamanca, NY. "Little Rock City" (LRC - outcrop #7) at the southeast outcrop perimeter is the type locality (Tesmer, 1975). With perhaps the most exquisite exposures, LRC has been an attraction since the early 1800s (e.g., Hall, 1843). Much of the outcrop belt is partially obscured by vegetation, rubble, and in places, glacially-deposited debris but it is readily traceable around the entire hill perimeter as facilitated by a network of hiking trails such as the North Country National Scenic Trail, the Finger Lakes Trail, and the Rim Trail. The outcrop and separated "blocks" are also readily visible with online orthoimagery (https://orthos.dhses.ny.gov/) and can be traced to nearby hillsides.

Glaciation – Evidence and Effects

The study area is mapped within the Salamanca Re-entrant, which is part of the unglaciated Appalachian Plateau and northernmost unglaciated area in the eastern United States. Muller (1977) placed an "uncertain" glacier margin at about 1800 feet elevation at roughly one to five kilometers north of the outcrop belt. However, evidence of glaciation in the study area includes: (1) "drab" glacial till (chaotically-oriented thin-bedded sandstone in a gray clay matrix) exposed in a small ephemeral stream east of Eckert Road at 2200 feet AMSL (the only stream found at this elevation), (2) some large quartz clasts which appear shattered and sheared-off level with the top surface of caprock, and (3) a stretch of outcrops disrupted and largely "buried" with float that includes, in places, abundant slabs of thin-bedded wave-rippled fossiliferous sandstone. This evidence is clustered in the area of subdued outcrops (limited exposures of ~ 2m), from Outcrop #5 to Salamanca Road that includes a topographic col/saddle which may have focused ice movement albeit in east-west directions. In addition, Smith and Jacobi (2006) reported an upside-down house-sized block atop another block as evidence of glacial activity.

Other areas appear largely unaffected such as the isolated and well-weathered "sentinel" blocks (outcrop #1) and the isolated erosional remnants (~ 3m "cubes") perched on the escarpment at outcrop #4 and some extensive block "fields" at the NW and SE corners; outcrops #3 and #6). It appears then that direct glaciation affected this area variably but periglacial effects such as permafrost, prolonged freeze-thaw cycles, and ice wedging were likely intense. Such conditions likely enhanced block separation, undermining/slump, and downslope movement due to solifluction ("soil flow"/creep due to saturated conditions) and genifluction, (creep in contact with ice/permafrost; e.g., Millar & Nelson, 2001). And the general process of soil creep continues, typically the slowest (~ mm/year on average) but geologically the most significant mass movement process (Allen, 1982).

Structural Geology

The regional dip is gently southward (about 30 feet/mile – S/SW; Glenn, 1902 and 20-50 feet/mile – South; Tesmer, 1963). No surface expression of folds or faults were observed but Glenn (1902) reported small folds in Cattaraugus County and the Clarendon-Linden fault complex is nearby in Allegany County (Smith and Jacobi, 2006). Jointing is the most obvious structural feature as it controls the similar block dimensions and the extraordinary rock exposures on the sides of the blocks. The vertical joint sets are generally orthogonal, spaced ~ 10-20 meters apart, and trend NE-SW (30^o-45^o) and NW-SE (125^o-140^o). Per Engelder (1986), the NW-oriented "cross-fold" joints are extension fractures formed by abnormal pore pressures in response to NW-directed tectonic compression during the Alleghanian Orogeny. The orthogonal strike ("release") joints are thought to develop later during regional uplift aligned with NE-oriented residual compressive fabric. The NE strike-joint set may not be as well developed and may waver more in direction and linearity as seen in the gentle sinuous patterns at outcrop #5 and along the “streets” of Little Rock City. Joints can also be affected by changes in lithology and bedding as suggested by the frequent overhangs of the upper channel deposits at the top of the blocks. Apparently these joints either did not readily propagate through the more varied (more permeable?) channel bedding in places or did so at a different spacing and/or direction. Similar effects are can be seen in shale/siltstone/sandstone sequences elsewhere (Engelder, 1986).

An interesting observation during collection of paleocurrent data was the frequent alignment (within a few degrees) of the true (maximum) dip of cross-bedding with the trend of the main joint set. What seemed like a helpful coincidence can be explained by the alignment of the NW joint set and its formative compressive stress field (as noted above). Tectonic strike (NE trend of plate boundaries/orogeny/mountains) would be roughly normal (like strike joints) to the maximum tectonic compression as should the corresponding paleoshoreline/basin. Fluvial/tidal channels and deposits generally trend normal to shore (down-paleoslope) and are often exposed in cross-section on NE-oriented strike joint surfaces. Marine (tidal and wave) deposits usually trend toward shore, generally SE which is a dominant flow direction as often displayed by cross-beds on cross-fold joint surfaces in this sequence.

While these Upper Devonian joint sets formed during the Pennsylvanian Period, similarly-oriented tectonic plate collisions (e.g., Taconic and Acadian orogenies) earlier in the Paleozoic yielded similar tectonic strikes/mountain ranges, alluvial plains, shoreline strikes, and depositional basins. Pettijohn (1975; p. 520) noted the stability of many paleocurrent systems through time and in particular, from Ordovician to Pennsylvanian time in the Appalachian basin. Numerous paleogeographic studies document fairly consistent paleocurrent directions and paleoslopes, generally NW-oriented as first recorded by Hall (1843) in the Ordovician Medina sandstone. In pioneering paleogeographic work, Hall deduced beach deposition, strandline orientation (NE-SW as noted is common throughout most of the Paleozoic Appalachian basin), and ocean/wave direction (NW) from oriented fossils, current scours, heavy mineral “clouds”, ripple marks, and swash marks on bedding planes in a building stone quarry (once great “outcrops” but all but extinct) near Lockport.

Iron Seams

The “iron ore” (hematite) seams of Hall (1843) are red to black in color, 1-3 cm thick, usually sub-horizontal but often smoothly contorted and commonly crosscut bedding. The seams appear most common higher in the sequence and in close association with fluvial/deltaic channels/redbeds and plant remains (Fig. 2 - outcrop #1). In the dune field (outcrop #7), iron seams cover several vertical joint surfaces (Fig. 3). And rare cylindrical shapes (10-20 cm in diameter) are suggestive of hollow logs.

With terrestrial input of iron via streams, precipitation of hematite where reduced iron-rich porewater mixed with oxygenated water might account for some seam occurrences such as in redbeds. The joint plane seam occurrences must have formed during or after joint formation. Jointing involves extension fracturing via abnormal pore pressure generated by tectonic compression (Engelder, 1986). Iron-rich porewater seems possible but the source of large amounts of reduced iron is unknown. However, the high porosity and permeability of this conglomerate could have facilitated later fluid migration. Together with hematite replacement of quartz cement in places, iron seam formation at depth after lithification, and during or after joint formation is indicated.

Iron Seams (Fig. 2 - many sub-horizontal seams in redbeds; Fig. 3 - vertical on joint planes in dune field)

Decaying plants provide localized reducing environments in sediments where dissolved metals such as iron may precipitate. Berner (1980) noted that whereas fresh/brackish waters (e.g., estuaries/deltas) are low in sulfur, plants are a source of sulfur for pyrite precipitation. Klein (2017; pers. comm.) noted that Devonian plant remains are typically pyritized and upon weathering, yield limonite/goethite and hematite as seen at several outcrops. Since pyrite is stable under reducing conditions at depth and oxidized iron (Fe^{+3}) is not readily reduced or mobilized, a direct iron source from plants appears unlikely. However, iron-rich solutions are evident; iron was sequestered as pyritized (FeS_2) plants and at some point, as hematite seams (Fe_2O_3) formed perhaps in response to undefined chemical and/or pressure gradients. In somewhat similar but more varied occurrences in Jurassic sandstones, Chan et al. (2000) thoroughly reviewed iron mobility and reactions (including Fe reduction reactions with hydrocarbons) and proposed that mixing of fault-related saline brines with shallow, oxygenated groundwater accounted for the precipitation of iron and manganese. With the Salamanca iron seams, the apparent formation at depth after lithification suggests unusual conditions perhaps related to tectonic stresses, faulting, and/or brine migration. Careful mapping and petrographic, chemical, and x-ray analyses of the iron seams may provide clues on their origin.

Previous Work and Stratigraphy

James Hall provided the first scientific descriptions of these rocks ("the conglomerate") as part of the multi-year Geologic Survey of New York (1839-1843). Working in western and central NY (the 4th district), Hall's descriptions and interpretations of some sedimentary structures (e.g., "diagonal lamination" and "ripple marks") and depositional environments (e.g., Medina Sandstone beach) were among the earliest recorded in scientific literature.

Hall's (1843; p. 285-290) conglomerate description (which is difficult to improve upon other than adding "well-rounded" to pebbles) of what at the time was apparently the premier rock city (and perhaps still is) follows below:

> *"The conglomerate consists of a mixture of coarse sand and white quartz pebbles, varying from the size of a pin's head to the diameter of two inches. They are generally oblong, or a flattened egg shape. Some of these are of a rose tint when broken, but white upon the exposed surface. Pebbles of other kinds are very rare in the mass, though red and dark colored jasper are sometimes found.*
>
> *This rock in the Fourth District occurs in outliers of limited extent, capping the summits of the high hills toward the southern margin of the State…From its position, it has been much undermined; and*

separating into huge blocks, by vertical joints, which are often many feet apart, the places have received the name of ruined cities, Rock city, etc.

There are several points in Cattaraugus County where the conglomerate is very well exposed upon the tops of the hills. The best known of these is the "Rock City," about seven miles south of Ellicottville (present-day Rock City State Forest)*….The sketch* (shown above on the title page) *represents a few of the immense blocks at this place, with the passages between them. The large trees which stand upon the top, have often sent their roots down the sides, where they are sustained in the deep soil, supporting the huge growth above upon an almost barren rock.*

The masses present the same features as before described, and offer fine exhibitions of the diagonal lamination and contorted seams of iron ore. The rectangular blocks are from thirty to thirty-five feet in thickness, and standing regularly arranged along the line of outcrop, present an imposing appearance, and justify the application of the name it has received."

The Salamanca Conglomerate is one of several conglomerate members of the Cattaraugus Formation of the Upper Devonian (late Fammenian) Conewango Group (Tesmer, 1963, 1975). First described by Hall (1843) as a single widespread unit, "the conglomerate", Carll (1880) named the Salamanca conglomerate and proposed correlation of several similar beds. Glenn (1902) likewise correlated several conglomerate beds and traced the Wolf Creek conglomerate (a very similar cross-bedded unit of sand and discoidal pebbles overlying "Chemung" beds) and the Salamanca conglomerate from the Portville/Olean area into the Salamanca quadrangle. Clarke (in Glenn, 1902) in a very prescient interpretation, cautioned Glenn about unconformities that rings true today: *"...these sand reefs constantly display indications of deep decapitation due to shifting of bars and change of directions of currents, or a modification by heavy tidal flow on a shelving coast."* Other stratigraphic work (e.g., Caster, 1934) was summarized comprehensively by Tesmer (1975) who concluded that conglomerate correlation is difficult and uncertain due to limited and separated outcrops, glacially-derived cover, probable facies changes, and possible structural complications (e.g., slight dip changes/folding/faulting). Tesmer (1975) tentatively placed the Salamanca member in the middle of the Cattaraugus formation, following Glenn (1902) who had mapped the Salamanca member well above (~ 60-70 m) the basal Wolf Creek member in the Olean area.

Baird and Lash (1990) noted some progress with correlation of the Panama Conglomerate member with the LeBeouf Sandstone in Chatauqua County and also the need to locate and observe the upper and lower contacts of these conglomerate units in order to place them in geological context (this study offers glimpses). Smith and Jacobi (2006) placed the Salamanca conglomerate at the base of the Conewango Group which puts it between the Wolf Creek conglomerate (type section near Olean, NY) and the westernmost Panama conglomerate (type section at Panama, NY). Collectively then, these units may represent the furthest preserved shoreline advance into the Devonian Catskill Sea of New York.

<u>Discussion</u> - Considering another ~ 200 meters of mostly marine Cattaraugus sedimentation above the basal conglomerate(s) (e.g., Wolf Creek), and the repetitive oscillating lithofacies (apparent shorelines) of Tesmer (1963), and the repeated T-R cycles of Smith and Jacobi (2001) in the Canadaway Group, and general observations at LRC, perhaps Tesmer's (1975) caution over conglomerate correlation is well-founded. If these very coarse, relatively thin (5-10 m, except for Panama; up to 20-25 m) units with sharp contacts represent the main transporters of sediment to the aggrading basin (e.g., as rapidly prograding deltaic complexes), one might expect these units to be vertically staggered throughout the section due to fluctuating sea levels. Larger more stable deltaic systems from larger streams (e.g., the deltas of the Cretaceous seaway – vanChappelle et al., 2016) would likely be much thicker and less influenced by small-scale relative sea level changes and more correlatable. But it seems likely that these conglomerate units scale with the streams/distributaries that formed them (fairly small channels; tens

of meters wide and at most a few meters deep) and offer glimpses of the shoreline as it oscillated through time and space with changes in relative sea level and sediment supply. Rapid progradation, evident in this study, moved the shoreline west-northwest which was followed by a marine transgression and shoreline retreat. Thick marine deposits appear to sandwich the Salamanca as glimpsed at LRC and in scattered marine outcrops nearby. Shoreline re-advance, if it occurred/reached this area after the inferred marine transgression, would likely have been well-separated vertically from the Salamanca.

By some estimates (e.g., Dennsion, 1985), the Catskill Sea shoreline beat a transgressive retreat back toward the Olean area by the close of the Devonian perhaps completing a halting but largely continuous loop through late Devonian time. Glenn (1902 map) depicts the Wolf Creek (first apparent Cattaraugus shoreline advance; type section near Portville) and the Salamanca placed about 60 - 70 m above it and overlain by the Oswayo shale (the uppermost Conewango Group/last Devonian formation) and the Olean conglomerate (Lower Pennsylvanian; w/larger, more spheroidal quartz pebbles (wider quartz veins unroofed?...a story for another day). Glenn (1902) described the Salamanca here as a hard gray sandstone (10-15 feet thick) which becomes coarser and thicker and passes westward into a massive conglomerate (such as at LRC). Once quarried extensively near Olean ("Mt. Hermon Sandstone"), it is a medium to coarse-grained buff to gray sandstone with occasional small quartz pebbles, medium-bedded (20 – 40 cm) with some layers speckled with oxidized iron (pyrite?) and pierced by many prominent vertical "fucoid" trace fossils. Given such a drastic facies change (and opposite trend to that of the prograding Wolf Creek which is usually very coarse and massive in this vicinity), the Salamanca here may represent a retrograding/stalled shoreline, perhaps the last Devonian shoreline in New York. Ongoing work will attempt to elucidate the relationship of these Devonian conglomerates and the paleoshoreline through time.

Relative Sea Level Changes – Gradual & Abrupt Examples

Tesmer (1963; Fig. 16) portrayed a coarsening-upward Cattaraugus formation with about six alternating repetitions of lithofacies (gray siltstones - buff sandstones – conglomerates). While generalized, his lithofacies curve suggests small-scale oscillations in relative sea level (T-R cycles) that are more pronounced and frequent than in underlying formations. Smith and Jacobi (2001), with detailed sedimentological work at 1200 outcrops, refined parts of the Upper Devonian T-R curve based largely on shoreface occurrences in the Canadaway Group of Allegany County. They were able to show small-scale sea-level fluctuations resulting from the separate effects of eustasy, syndepositional faulting within the Clarenden-Linden fault complex, and general tectonic subsidence with the conclusion that sea level curves inferred from local foreland basins may have a stronger tectonic signal than previously understood.

The Salamanca shows an apparent abrupt deepening at the top of the caprock. At outcrop #5, very coarse (up to 60+ mm) fluvial/deltaic-deposited pebbles are overlain by fossiliferous wave-rippled thin-bedded sandstones (the first fossil occurrences in the sequence; molds of *Productella sp., Camarotechcia sp., and Crytospirifer sp.*). Whereas wave/tidal ravinement (largely limited to reworking) along the caprock is evident in places, mud rip-up clasts (a terrestrial/fluvial source-the only mud observed in the sequence) within the matrix of some of the largest clasts (including some large sandstone and metamorphic clasts; their first significant appearance) observed within the caprock precluded significant disturbance. Given then the absence of a preserved transgressive foreshore/shoreface sequence, a fairly rapid depth change of at least 10 m is interpreted. Subsidence was likely the main cause especially in light of the copious sediment supply/vigorous fluvial input (which appeared to be expanding at the top of the sequence), energetic marine processes (tides and waves), and active progadation which could likely keep pace with relatively small-scale and slow eustatic fluctuations. Bishuk et al (2003) noted a similar abrupt deepening (with inferred 10-15 m of subsidence) in a Sonyea Group (Frasnian) coastal sequence where shallow-marine hummocky cross strata overlie terrestrial paleosols. Other examples of inferred rapid subsidence include abrupt transitions of hummocky cross strata (upper shoreface) to interbedded mudstones/thin siltstones (offshore) in the Frasnian West Falls Group (Craft and Bridge, 1987) and stacked shorefaces in the Canadaway Group (Smith and Jacobi, 2001, 2006).

PALEOGEOGRAPHY - GEOLOGIC SETTING

A paleolatitude of 25-30 degrees south (Fig.4) and a warm, seasonally wet-dry climate has been posited for the Upper Devonian of New York (e.g., Woodrow et al., 1973; Scotese, 2000). Southeast trade winds likely prevailed but the Acadian highlands presented a rain shadow (Woodrow, 1985). However, abundant rainfall would be expected from postulated monsoonal circulation (Witzke, 1990, Streel et al., 2000, Smith and Jacobi, 2006) perhaps similar to the present-day Indian Ocean/Indian subcontinent. Climate is a primary control on source-to-basin sediment flux and in warm climates, siliciclastic flux is greatest under highly seasonal rainfall (Cecil, 1990).

Given the likelihood of monsoonal rainfall, frequent floods, episodic hurricanes (Duke, 1985; Craft and Bridge, 1987; Baird and Lash, 1990; Smith and Jacobi, 2006) with possible storm-flood (Collins et al., 2016) and storm-tide coupling, and evolving plants which paradoxically may have increased weathering rates in places (Berner, 1997), significant weathering and transport of sediment to the Catskill Sea would be expected. In addition, pulsed orogenesis in the source area (the third collisional tectophase of the Acadian Orogeny; Ettensohn, 1985) likely increased stream/erosional gradients, significant fluxes of sediment into the basin, and basin subsidence in response to tectonic/sediment loading on the crust.

Figure 4. Late Devonian paleogeographic map – study area highlighted (modified from Blakey, 2017 and Zambito, 2011; shoreline extended into western NY; all boundaries approximate)

Basin Subsidence/Deposition Rates

The average subsidence rate in the Catskill foreland basin was nearly an order of magnitude higher in the upper Devonian than the middle Devonian (Faill, 1985) with deposits as thick as ~ 2000-3000 m over the ~ 14 million year duration of the Upper Devonian. In western New York, Faill (1985; Fig. 7) showed an estimated subsidence/deposition rate of ~ 100 m/million years (or roughly 2 million years to deposit the ~200 m Cattaraugus Formation). Coupling that rate with an average shoreline advance of ~ 30 km/million years (Dennison, 1985; Fig. 4), gives a rough volumetric deposition rate of three million cubic meters per million years per linear meter of prograding shoreline (or 3 cubic meters of sediment/meter of prograding shore/year). Very approximately then, for a 4 km swath of paleo-coast (such as at LRC), an average of 12000 cubic meters of sediment might be deposited per year. Sediment influx was likely much greater, on average, at prograding deltas which was then partly or mostly redistributed along and offshore by marine processes.

Shoreline

The coastal zone of the Devonian Catskill Sea varied in space and time as shown by the varied interpretations of shoreline deposits. Coastal paleoenvironments included deltas, distributary channels/mouth bars, tidal channels/flats, mud flats, and beaches (e.g., compilation in Sevon, 1985). Despite a number of early tidal interpretations, an assumption persisted that the probable tidal range/energy was low. But seminal work such as Johnson and Friedman (1969; tidal channels/flats) and Rahmanian (1979; tide-dominated delta) and tidal modeling by Slingerland (1986) and Ericksen et al. (1990) which suggested at least mesotidal (2 m -4 m) range, recognition of tidal coastal deposits increased over time (e.g., Bridge and Droser, 1985; Bridge and Willis, 1988; Bishuk et al., 1991, 2003; Duke at al., 1991; Willis & Bridge, 1994; Prave et al., 1996).

In a study with specific applicability to LRC, Slingerland and Loule (1988) documented a tide-dominated shoreline (tidal channels/flats/shoals/estuaries) with a wave-dominated (sand ridges) offshore in a shore-parallel, time-equivalent (mid-Frasnian) transect through central Pennsylvania. They posited that nearshore circulation was to the SW (clockwise), estimated tidal range was high mesotidal, and that three major clastic dispersal systems (drainage basins) existed across Pennsylvania. They also noted that meandering fluvial deposits capped all sections studied and that a lack of mouth bars and levees was attributed to strong tidal currents (like at LRC).

In a comprehensive synthesis of Devonian Catskill alluvial and coastal deposits, Bridge (2000) noted several coastal features in common: *"(1) sandy, tide-influenced channels; (2) shallow bays and tidal flats where mud and sand were deposited; (3) rarity of beaches; (4) storm-wave domination of the marine shelf. Much of the variability in the deposits across the area could be explained within the context of a wave- and tide-influenced deltaic coastline with a tidal range that varied in time and space."*

Regarding variations in tidal ranges, Reynaud and Dalrymple (2012) noted that since tides interact strongly with shelf and coastline morphology, changes in relative sea level can have a profound effect on tidal currents and deposits. Tidal resonance (amplitude strength) varies with shelf width (i.e., highest at increments of one-quarter of the tidal wavelength) and is directly affected by changing sea levels. They stated that: *"The increase in tidal influence can be geologically instantaneous in situations where the geomorphology changes rapidly. This was the case in the Gulf of Maine-Bay of Fundy system, which changed from microtidal to extreme macrotidal over a period on only a few thousand years."* Short-term changes then (e.g., tectonic or climate-driven sea-level variations) can bring about rapid change, *"potentially causing an alternation between tidal and non-tidal deposits"* and *"different parts of the transgressing sea can become resonant at different times"*. Also, once tidal resonance has been reached, further increases in sea level often result in a decrease in tidal influence. They suggested, as possible examples, abandoned tidal dune fields preserved beneath North Sea muds and tidal sandbodies in the Devonian Castkill Sea. They cited Ericksen et al. (1990) for the latter, who did not provide specific examples but the Salamanca tidal dune field at LRC is a possible example of decreasing tidal influence with wave-truncated dune tops overlain by channel deposits.

Sediment Sources & Dispersal Systems

Based on the inferred position of the Acadian orogen (Faill, 1985), source areas were likely located about 400 km to the southeast (cf. Pelletier, 1958) during Fammenian time. Weathering and erosion of actively-rising mountains produced detritus (including tabular vein quartz gravel) that was conveyed by streams to the foreland basin. As the shoreline advanced, drainage networks continually expanded and likely interacted to varying degrees. Sevon (1985) depicted up to six "sediment dispersal systems" which could have affected western NY, Slingerland and Loule (1988) noted three major drainage systems, and Boswell and Donaldson (1988) posited five stable drainage systems with large trunk streams for the Fammenian of West Virginia. The size of these drainage basins and streams are difficult to gauge but given an alluvial plain of at most 400 km, these were not the large continental rivers and deltas of today. Bridge (2000) noted that Catskill river channels were smaller near the coast (i.e., sinuous, single-channel rivers, tens of meters wide, maximum depths of 4 - 5 m, sinuosity of 1.1-1.3, mean bank-full flow velocity of 0.4 - 0.7 m/s) and perhaps distributive (delta-related). With increasing distance from the coast, slopes increased, rivers became wider (up to hundreds of meters), deeper (up to 15 m), coarser grained, and possibly braided.

Sediment - Sand & Pebbles

Other than localized rip-up clasts, no mud-sized sediment was observed. Quartz sand ranges in size from fine to very coarse, is sub-rounded to sub-angular, and composed largely of clear monocrystalline quartz. Clear quartz is mainly derived from intrusive plutonic rocks such as granite; such crystals are generally < 1 mm and are the source of most quartz sand. Cloudy polycrystalline quartz (the stuff of pebbles) predominates in coarser (1-2 mm) grains. Sand lithology is +95% quartz with occasional opaque grains including magnetite. Fine-grained magnetite comprises a very minor overall component (<<1%) of sand but it may concentrate locally along laminations in places. Bagged samples of disaggregated sand obtained from nearshore marine, beach transition, and channel deposits were magnetically-separated; all showed trace amounts of magnetite with channel deposits containing somewhat higher amounts. Since the specific gravity of magnetite (5.18 g/cm^3) is nearly double that of quartz, fine (0.125-0.25 mm) grained magnetite sand is roughly the hydraulic equivalent of medium (0.25-0.5 mm) quartz sand. At the shoreface/foreshore transition and in foresets of some dunes, dark-colored laminations and streaks occur. However, where samples could be obtained (e.g., moss-weathered outcrops), magnetite was rare. Magnetic separation showed partial black coatings on quartz grains and separated black flakes (magnetic attraction varied but mostly slight; possible hematite?).

Cross-stratified medium to very coarse sand dominates much of the sequence and is frequently interbedded with single or multiple layers of discoidal pebbles which usually conform to bedding and accentuate sedimentary structures.

PEBBLES

Perhaps the most interesting geological feature of the Salamanca conglomerate (in addition to cross-bedded monoliths the size of houses) are the ubiquitous well-rounded discoidal vein-quartz pebbles. The Salamanca is classified as an orthoquartitic conglomerate since the pebbles are lithologically and texturally mature. The milky polycrystalline quartz pebbles range from ~ 2 mm to 60+ mm (very fine to very coarse pebbles), average ~ 8-10 mm in size and are oblate ("flattened") ellipsoids in shape. Pebble lithologies are +98% quartz with minor amounts of red jasper and rock fragments. Shallow pits and fracture traces are evident on the surface of many pebbles. Most pitting is likely related to point-contact pressure solution upon burial which probably provided much dissolved silica for this well-cemented unit. Some surface ornamentation may be impact-related such as possible percussion marks on beach clasts (Allen, 1970) and V-shaped pits. The milky/cloudy nature of the polycrystalline quartz pebbles derives from microscopic fluid inclusions which disperse light. Fluid inclusions are consistent with a hydrothermal origin where silica-rich fluids were likely emplaced under pressure and crystallized rapidly in fractures of an active orogen source zone. Uplifted older vein quartz deposits, formed in the same fashion, are also possible.

Pebbles often conform with and accentuate sandy stratification and hence are very helpful in defining sedimentary structures and paleoflow directions, and assessing paleohydraulics. However, in beds where pebbles dominate (e.g., minor sand matrix, clast-supported "open framework gravels" such as common in channel bars and fills), stratification may be crudely developed and difficult to interpret. Pebble imbrication can be helpful such as the common orientation of oblong pebbles transverse to flow but pebble inclination may be ambiguous. Jumbled/chaotic/unstable pebble orientations are common especially in channel deposits which suggests disequilibrium with waning, rapidly depositing flows ("unsteady" tidal currents) and sediment-choked channels.

Pebble Shape/Origin

The origin of the distinctive discoidal pebble shape has been ascribed to beach-shoreface abrasion since the Salamanca was named (Carll, 1880) and accepted over time by Glenn, 1902, Tesmer, 1975, and Miller, 1974, as cited by Baird and Lash 1990). While appealing, it is not clear how an entire population (billions?) of extremely durable quartz pebbles could be systematically and symmetrically abraded/flattened to yield co-planar sides and with a probable concomitant mass loss of up to 80-90%. Prolonged abrasion experiments show little mass loss for quartz pebbles after initial edge rounding (e.g., Krumbein, 1941; Keunen, 1956; Attal and Lave, 2009; Domokos, 2012). Also, at this locality the majority of Salamanca pebbles are found in channel deposits; beach deposits are not common. It seems clear then that the cloudy pebbles of vein-quartz derived their tabular shape from their origin in tabular quartz-filled fractures (veins) in the source area and rounding/smoothing during stream transport. As Pettijohn (1975) noted, the end-shape of sedimentary quartz is an expression of its initial shape.

Pebble Dimensions - Fractures/Fragmentation

Clast thickness is largely determined by the dimensions of tabular quartz veins in the source area. Caliper triaxial measurements of ~ 100 pebbles spanning the available size range yielded a C-axis (the short ellipsoidal axis) range of 1.5 mm to 16 mm which suggests veins of that size range in the source area. And that rather restricted thickness range suggests a rather consistent source area of narrow tabular veins of quartz (no rogue spheroidal clasts; other lithologies are less durable). And hydraulic (size) sorting during extended fluvial transport likely restricted the upper size limit (the majority of pebbles are < 15 mm; large clasts are sequentially sorted out; Pelletier 1958 showed an exponential decline in the Pocono Group). The sudden appearance of some very coarse pebbles (up to 60 mm and 25% different lithologies; sandstone and metamorphic clasts) at the top of the caprock suggests an unusual event or process.

The triaxial pebble measurements yielded axial ratios (B/A and C/B) that plot, for the most part as expected, within the Disc zone of the Zingg shape diagram (1935; in Pettijohn, 1975) (Fig. 5). However, smaller size ranges (< 8 mm) trend toward, and in particular, many 2-4 mm ("granules") pebbles, plot within the Sphere zone. The C-axes, while thin (1.5 mm – 3 mm), are still recognizable as parallel which suggests the same vein origin. These more equant shapes result when the A - B axes approach the C-axis in dimension.

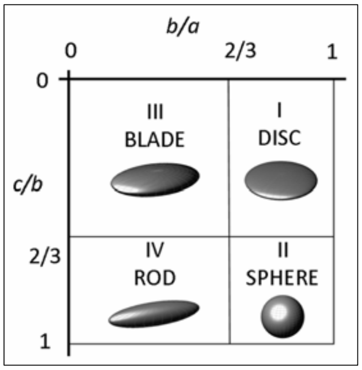

← Figure 5

Figure 6 →

So the C-axis is essentially fixed (vein-pebble thickness = lowest common diameter); the A and B axes can get smaller due to breakage normal to C. The suggested mechanism is the greater susceptibility of thinner veins and clasts to weathering and fragmentation at the outcrop and in early transport in high-gradient streams. Fracture traces, often outlined by iron-oxide staining, are common and are generally normal to the two co-planar sides (A & B axes). Some pebbles show smoothing/rounding of fracture-parallel edges (missing chunks) which suggests fragmentation/smoothing occurred during transport (Fig. 6). Other pebbles show sharp-edged breaks which, if natural, suggest little transport after fragmentation. So planes of weakness would tend to focus breakage along the short "C" axis and the thinner the veins/pebbles, the higher the expected rate of disintegration (lots of thin veins/pebbles = lots of milky granules and odd shapes, e.g, irregular or roughly triangular, appear more common in small pebbles). The highest fragmentation rates during transport would be expected in near-source high-gradient streams where strong flows, a wide size range of particles in motion, and high impact velocities which, along with existing planes of weakness, would promote fragmentation (e.g., Attal and Lave, 2009).

Rounding

Experiments have shown that lithology controls abrasion rates (e.g., Keunen, 1956, Domokos et al., 2014). Quartz pebbles are extremely durable with fairly rapid rounding (Attal and Lave, 2009; Domokos et al, 2012) but little overall change in clast diameter ("virtually indestructible", Pettijohn, 1975; Southard, 2006). In an elegant series of experiments, modeling, and field studies (Domokos et al,. 2012; Miller et al. 2014) demonstrated that *"abrasion occurs in two well-separated phases: first, pebble edges rapidly round without any change in axis dimensions until the shape becomes entirely convex; and second, axis dimensions are then slowly reduced while the particle remains convex." The first phase occurs mainly in high-gradient, source-proximal streams, the second, in lower-gradient alluvial plains where size sorting due to stream hydraulics and lithologically-controlled abrasion prevails."* Coupled with the fragmentation process noted above, most sizing and shaping (fragmentation) and rounding (convex shaping) of pebbles likely occurs in near-source high-gradient streams whereas most hydraulic (size) sorting and abrasion (slight for quartz) occurs in lower gradient alluvial plain streams.

The Granule "Problem" - Pettijohn (1975) and Southard (2006) noted a general scarcity of very coarse quartz sand and granules (1 mm - 4 mm) in the rock record. The cause appears related to the fact that the most common sizes of quartz crystals in plutonic rocks, the source of most quartz sand, are mostly < 1 mm. The Salamanca and other Upper Devonian conglomerates have an abundance of coarse sand, granules, and fine pebbles likely due to an abundance of vein quartz and the processes noted above. These size ranges are more spherical than larger pebbles and readily transported by nearshore currents and are abundant in dunes and nearshore marine deposits. The general source of quartz grains can be roughly distinguished in field: Clear = monocrystalline plutonic sources vs. Milky = polycrystalline vein sources. The tannish granule/pebble layers ("grain striping") within the light gray sands of large dune foresets is a macro-example.

Paleohydraulic Estimates

By some measures, such as a simple fluid/particle force balance and frictional considerations, low-profile discoidal pebbles should be more difficult to entrain and transport. However, once entrained ("mobilized") in a current, the tabular clasts would likely settle slower as indicated by calculation of the Maximum Projection Sphericity (Sneed and Folk, 1958). Also known as Maximum Settling Sphericity, a range of pebble sizes averaged about 0.5 or equivalent to about twice the cross-sectional area of a sphere of equivalent volume which suggests slower settling of discoidal pebbles. Bradley et al. (1972) studied the effect of shape both in the field (Knik River, Alaska ; high-gradient glacial-meltwater stream) and in the laboratory. They detected downstream sorting of shapes, with platy pebbles being the most easily transported, then elongate pebbles (rollers), and more equant pebbles being the least easily transported. The different shape-sorting effects were attributed to particles moving by traction and by -suspension and hence closely related to flow strength and particle size.

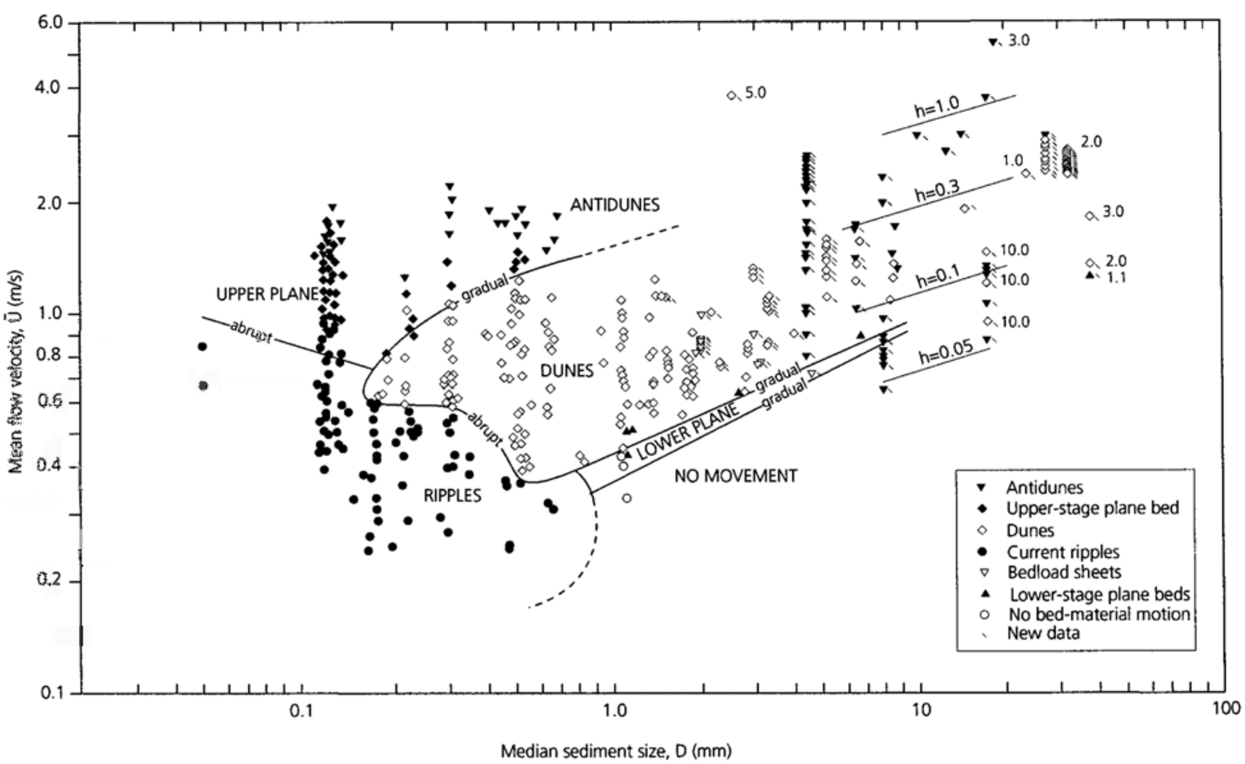

Figure 7. Bedform Existence Fields for Unidirectional Flows (Carling, 1999; redrawn after Southard and Boguchwal, 1990 and extended to gravel sizes, D ~ 33 mm). For general background, see Middleton (1977), Allen (1982), and/or Harms et al. (1982).

The bedforms most applicable to conditions at LRC are Dunes and Bedload Sheets. Dunes of various dimensions produce cross-strata which incline downcurrent and scale with depth, flow strength, and grain size. Ripples, smaller-scale (<= 4 cm) dune-like bedforms, require sand of < ~0.6 mm which is uncommon at LRC; ripples have not been observed. For sand sizes, a current of roughly 0.4 m/s to 1.0 m/s would be required to form dunes. For dunes composed of granules and fine pebbles (2 mm to 8 mm), a current of 0.6 to 1.5 m/s is indicated. Flows required for coarser pebbles (8 to 32 mm; limit of graph) are less clear given prominent disc shapes and data scarcity, but currents of 1 m/s to +2 m/s appear likely. Bedload sheets, low-amplitude bedforms which can transport a range of sediment are likely common at LRC but difficult to definitively identify; their existence field appears to coincide with dunes.

Possible Vein-Quartz Source-Area Analogues

Pettijohn (1975) and Baird and Lash (1990) noted that large vein quartz accumulations imply the destruction of large volumes of source rocks since quartz veins make up a just small percentage of normal lithosphere. However, vast amounts of vein-quartz pebbles transported within fairly limited drainage basins for at least 2 million years suggest an unusual lithosphere (an abundance of quartz veins) within areally-limited source areas. Hack's (1957) law indicates that a stream ~ 400 km long would have a drainage basin of ~ 20,000 km^2; the near-source catchment width is uncertain but likely on the order of 100 km. A similar sedimentation pattern (Olean/Pocono) continued in the Pennsylvanian Period from a similar source area (Pelletier, 1958; larger more equant pebbles suggest unroofing of thicker quartz veins).

A possible analogue for a vein-quartz source terrain is the Ouachita Mountains where more than 8000 meters of Paleozoic strata were folded during the Mid-Pennsylvanian Ouachita Orogeny. Innumerable steeply-dipping fractures, related to the major folds and faults of the region, controlled the emplacement of hydrothermal quartz (Miser, 1943; Engel, 1951). Another example and possible analogue of an abundant source area of vein-quartz as well as long distance transport of discoidal pebbles is the Miocene uplift in the southern Appalachians. As reported by Missiner and Maliva (2017), pulsed tectonism resulted in a surge in coarse siliciclastic sediment (including abundant discoidal vein-quartz pebbles of up to 40 mm in diameter) and long distance (up to 1000 km) fluvial transport. And the famous Witwatersrand gold deposit in South Africa (source of 50% of the world's gold for over a century) is a Precambrian fluvial conglomerate with discoidal vein quartz (~ 30 mm) pebbles (*let's go with this one!*).

DESCRIPTION OF CROSS-STRATA

Large-scale cross-stratification, the dominant sedimentary structure, is examined in detail and the overall depositional environments are reviewed below. But what's missing bears emphasis: unusual characteristics of this sequence are the near absence of preserved mud-sized sediment or trace fossils (perhaps small burrows in channels) or body fossils (but many fossils are present on and above the caprock). Strong currents, substrate mobility, and the apparent lack of organic matter likely presented an inhospitable environment, poor habitat, and poor preservation potential. The inferred high-energy coastal environment likely prevented deposition of fine-grained sediment which was transported offshore. Protected lower-energy coastal areas, such as back-barrier lagoons, muddy tidal flats, or fine-grained overbank fluvial/deltaic deposits, were not recognized in this sequence. Wave influence is pervasive but often subtle throughout this sequence.

Fossils – Plant remains are common in channel and associated deposits particularly within the deltaic sequence. With the exception of possible escape burrows in a channel base, trace and body fossils were not observed within the Salamanca conglomerate. However, abruptly overlying the caprock are finer-grained buff sandstones that contain an abundant brachiopod fauna and rich marine faunas are common in shallow marine deposits nearby. For example, an intact *Productella sp*. was found lying directly on the caprock seemingly in life position (Fig. 24).

Hall (1843) noted that fossils are extremely rare within the "conglomerate" citing 3 brachipod species in a sandy correlative of the Panama member. Tesmer (1975), citing the work of Butts (in Glenn, 1902) in the nearby Olean quadrangle, noted two brachiopod species in the Salamanca, Camarotoechia contracta and Crytosprifer sp? along with 13 pelecypod species, an ammoniod, and a gastropod.

Large-scale Cross-stratification

Cross-stratification, the most abundant sedimentary structure, dominates most outcrops. Individual set dimensions range over two orders of magnitude in scale (~ 0.05 m to +5 m). Most cross-strata are planar (straight- to slightly-sinuously crested = 2D type) with some trough (sinuously crested = 3D type) evident in channel deposits and upper shoreface/lower foreshore depsoits. Smaller forms may display bi-directional foresets in places (Fig. 8) but are more commonly organized in stacked co-sets (Fig. 9 ; cosets are ~ 0.75 m thick and show wave influence at the tops, e.g., centered on the 3' tape; Fig. 10 shows fine sand drapes, possible tidal influence and at the interface, wave ripples occur, then a 1 m thick cross-strata with angular toesets; small and large x-strata align shoreward; outcrop #1). Foresets are largely composed of grayish medium to coarse sand with variable interbeds of milky granules and pebbles ("grain striping" within large-scale foresets). Larger sets are generally coarser. Some channel bars and fills are composed in large part with pebbles (open framework gravel) that are crudely stratified or imbricated. The vast majority of paleocurrent data are cross-bed inclinations and range from 90°– 150° (mostly) with minor clusters at $40^{\circ} – 60^{\circ}$ and $220^{\circ} – 240^{\circ}$.


Figure 8

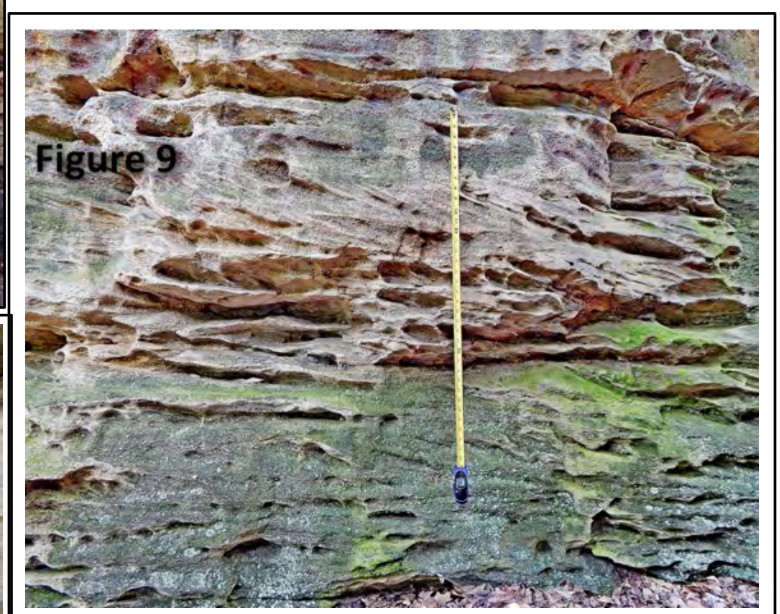
Figure 9

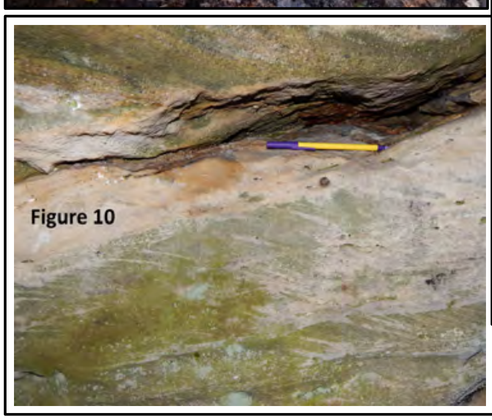
Figure 10

The largest cross-strata (0.50 – 5 m) increase in size and abundance from north to south across the outcrop belt. At the southernmost outcrops at "Little Rock City", large foresets may comprise ~ 75% of the outcrop exposures with dips of $20^{\circ} – 30^{\circ}$, no obvious or major reactivation surfaces, and most toesets are tangential (Fig. 11; largest foresets ~ 5.5 m). Some foresets are traceable for +150 m across several blocks and a planar truncation surface at the top of the dunes shows wave influence (e.g., wave ripples with crests parallel to the paleo-shore). About 1 m of low-angle stratification overlies this interface followed with about 2+ meters of gray and red low-angle strata and channels to cap the sequence (Fig. 12; foresets at base, about 1 m, then as described above; note iron seams in redbeds).

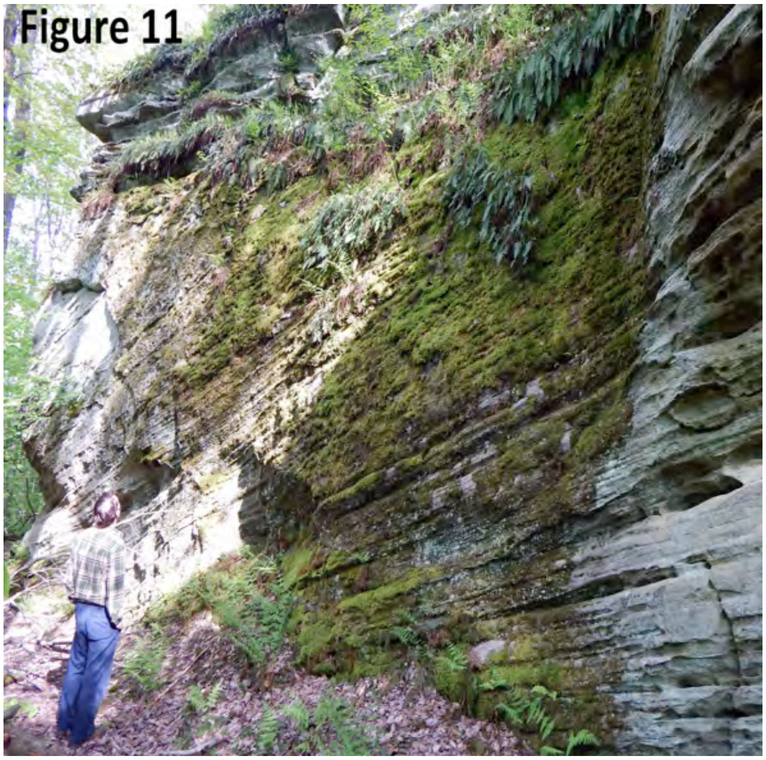

An intact 2-3 m dune bedform (a "form-set" with foreset, topset, and stoss beds preserved) is unusual at this scale (Figs. 13-15; note the connected stoss & foresets just above 6' tape in Fig. 14). This form-set informs dune genesis: a medium ebb dune forms the base with directionally-opposed cross-strata aggrading vertically until one flow direction (100^{o} – apparent flood tides, downcurrent from the deltaic" sequence) prevailed about halfway up and coincident with a 15 cm dune (18 cm yellow ruler in Fig. 15-core"photo) which formed the crest of the avalanche face at that point. The uppermost stoss beds are continuous with the topset beds; some topset beds (bedload sheets) flow continuously into foreset beds in places. A small dune is also present in the topset beds but most of its 15-20 cm thick strata appear horizontal.

Figures 13, 14, & 15

Figure 15

Another interesting occurrence in the dune field are small convex "humps" or "piles" of granules and pebbles (average 4 x 10 cm but up to 8 x 20 cm) and spaced erratically along foreset beds as exposed on a vertical joint surface; cross-section along depositional strike showing horizontal foresets ("backside") of a large dune. And two very coarse (mostly pebbles) and lower profile (~1.5 m) dunes with some opposed cross-strata were observed SE of the main southern dune field at LRC.

INTERPRETATION OF CROSS-STRATA AND DEPOSITIONAL ENVIRONMENTS

Hall's (1843) explanation of "diagonal lamination": *"...where the sand is carried on and spread over the surface, sloping off towards one side farthest from its origin. The next deposition covers this sloping side necessarily in the same manner, producing the oblique lines..."* was perhaps the first detailed account of cross-stratification (Allen, 1982); it describes the essential process of sand movement and deposition on an inclined surface. To embellish slightly, currents transport sediment along a gentle stoss slope to the bedform crest where repeated sediment avalanches down the steeper lee slope form cross-strata at or near the angle of repose. The resulting cross-strata are the depositional units formed by the migration of bedforms, dunes of various scales in this case.

Based on mostly shoreward- and some bi-directional-oriented cross-strata, the dominant currents were tidal and predominantly flood tides. Most sediment transport likely occurred during high spring tides of the bi-monthly spring-neap tidal cycle. Bedload transport rates scale roughly with the cube of the current velocity; if the flow rate doubles, bedload transport increases by a factor of roughly eight (Wang, 2012). A mesotidal range of 4 m appears to be a reasonable estimate; similar modern deposits/bedforms are produced in that range such as in the North Sea.

Based on paleohydaulic estimates noted above, the currents required to form dunes ranged from about 0.50 to 1.50 m/s. A similar velocity range (0.5 – 1 m/s) has been reported in the Dutch North Sea where very large simple dunes (like those at LRC) are actively migrating decimeters to a few meters per year (e.g., Tonnon et al., 2007; Passchier and Kleinhans, 2005; Stride, 1982). Allen (1982) reported that on the European continental shelf, sandwaves (large dunes) are found where tidal currents associated with spring tides range between 0.65 and 1.30 m/s. LRC dunes are somewhat coarser than modern examples and perhaps formed in somewhat shallower depths. A shoreface depth of ~ 10 m would conform with the dune height/depth ratio of 0.5 (Allen, 1982) for the largest (~ 5m) LRC dune (note that lower *h/d* ratios are common; Reynaud and Dalrymple suggest ~ 0.2). Tidal transport of coarse sand and pebbles at much greater depths may have been limited by the "littoral energy fence" whereby coarse particles are sequestered nearshore (Allen, 1970; Thorne and Swift, 1989). Even sand is rarely transported offshore by fair weather processes but evidence for Devonian hurricanes in the Catskill basin is strong and modern studies of sediment transport inform the past (e.g., Keen et al., 2012).

The large foresets on large "simple" dunes suggest strong very asymmetric tides. Allen (1980, 1982) depicted four general variants of "sandwaves" (what geologists now call "dunes" per Ashley, 1990) based on tidal current symmetry. Allen's conceptual "sandwave"/dune generated by the most asymmetric tides (Fig. 16; large simple foresets in bottom frame; note the velocity asymmetry of U* critical, the threshold velocity to move sediment) conforms with the large dunes at LRC. Allen (1982) also depicted superimposed smaller dunes supplying sediment to the large foresets of a larger host dune.

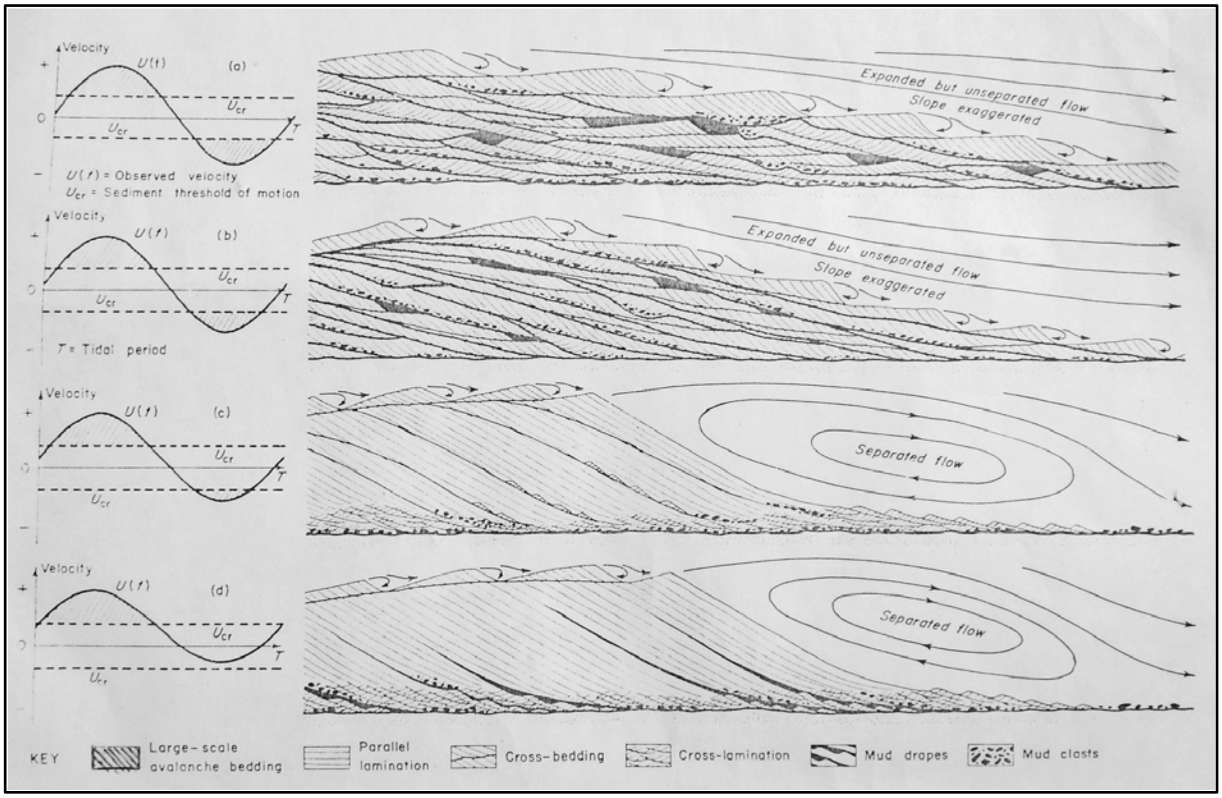

Figure 16 – Conceptual Model for generation of large dunes (Allen, 1982)

The "genesis" dune at the LRC dune field contains a small dune that appears to have "stalled" at the crest and reformed/"sharpened" it (center of Fig. 15; above 18 cm ruler); deposition continued along the aligned stoss and lee of both dunes (cf. Bridge and Demicco, 2008). Superimposed dunes pre-sort and transport sediment to and over large host dunes often in concert with bedload sheets. Pre-sorted wedges of sediment, as formed by smaller dunes ("trains") advancing over the crest ("cliff") of large host dunes, move down the flow-separated lee slopes often haltingly, by "grainflow" and finer sediment is distributed by "grainfall" from suspension (Reesink and Bridge, 2007; 2009).

One consequence is the scattered formation of lobate tongues of coarse sediment that may show inverse grading due to kinetic sieving. Otherwise known as "grain striping" (Reynaud and Dalrymple, 2012), a likely result of this process is shown in the dune cross-section along depositional strike (dune "backside") with scattered and variable convex piles of granules and pebbles along the foresets. Harms et al. (1982) described the process of foreset avalanches at high sediment concentrations as oversteepened areas which slump in places and slide down the lee slope as long "tongues". A slight scour or channelelized grainflow may form which then "debouches" with a slight positive lobe at the basal portion of the foreset. Some foresets and "grain stripes" at LRC nicely display these subtle structures in dip cross-section (Fig. 17) and the small granule "piles" on a dune backside noted above are interpreted as "grainflows" along the strike of dune foresets.

The largest cross-strata (0.50 – 5 m) increase in size and abundance from north to south across the outcrop belt which may indicate increasing water depth since dunes scale with flow depth. And the LRC dune field is downcurrent of the inferred delta complex which provided an abundant sediment supply and may partially explain the location of the dune field.

Form-set ("genesis") Dune

As shown in Figures 13-15, a medium ebb-dune formed at the base and small competing dunes aggraded vertically (or slightly in the ebb direction) until the flood (shoreward) tides began to dominate about where the small dune is perched in the middle of the bed. With an abundant up-current sediment supply, the flood tidal current began to dominate and the ~ 2–3 m dune began to migrate. In effect, the simple large dune has compound small dunes at its core/start and other superimposed dunes supplying and presorting sediment along with bedload sheets. In addition to a small dune in the topset bed, at least 2 topset locations show continuous strata between inferred bedload sheets and foreset beds. In a review of dune preservation, Reesink et al., (2015) noted that dune sets may climb due to local dominance of deposition over dune migration which generally fits this situation. But more specifically in this case, it appears that the localized balance between ebb and flood dune deposition aggraded a vertical core until the more dominant flood current and sediment supply tipped the balance toward large dune migration.

Wave-truncated Dunes

All of the largest dune (> 3 m) foresets at LRC appear to have been truncated ("beheaded dunes") horizontally at similar elevations (~ 3 m from the top of the sequence). Evidence of waves at this interface is common which suggests storm wave action which is well documented in the North Sea (e.g.,Terwindt,1971; Reynaud and Dalrymple, 2012). The overlying ~ 1 m of low-angle bedding is somewhat cryptic but the scale suggests lateral-accretion deposits of migrating tidal point bars.

Fluvial Channels/Bars

The final 2+ m of outcrop in the dune field contains robust channels and lateral-accretion w/some well-oxidized redbed deposits (Fig. 12) and some seaward-directed paleocurrents which are interpreted as fluvial meandering stream channels and point bars (Slingerland and Loule, 1988) noted a similar transition). This upper sequence appears to have shallowed upward probably from both lowered relative sea level (the beheading appears unique and the dunes never recovered) and active progradation. This upper channel sequence also overrode the rest of the sequence; the top of the beach at the north face and the tidal point bars are at similar elevation. If the beach deposits were largely preserved, then mean sea level should have been about ~1.5 m below the channels (~ half the foreshore) and roughly the same for the inferred tidal channels in the dune field. Other than crisscrossing channels within the delta sequence, surprisingly little incision is evident anywhere in this sequence but basal exposures are limited).

The remaining facies associations/depositional environments are summarized briefly with mention of outstanding issues/ongoing work:

Shoreface to Foreshore (beach) to Deltaic/Fluvial Sequence

coarsening-upward sequence - ("north face" Outcrops #2 & 3 from base)

- ~ 1 m of thin-bedded (5-10 cm) wave cross-laminated strata; mostly buff, medium sand with some coarse sand, granules, and a few fine pebbles.
- ~ 3 m of amalgamated coarse-grained, large (10-20 cm x 50-100 cm), smooth-crested wave ripples with abundant pebbles (some apparent 3-D forms seem without analogues), interbedded in places w/thin fine-grained (rolling-grain) wave ripples; some trough/planar cross-beds near top.
- ~ 3 m of parallel/low-angle strata of gray interbedded coarse sand and pebbles (a mixed gravel/sand beach, Komar, 1998; shape sorting is common whereby flatter clasts are left higher on the beachface. Not observed here but ongoing work will evaluate). Bed inclinations vary somewhat due to tilted blocks but some ~ 5^{o} are seaward (a few degrees is expected). A fairly thick beach sequence and a coarse shoreface have been suggested as indicators of significant tidal range/influence).

Figure 18 is interpreted from the top (red lines ~ 3 m): Fluvial (deltaic?) channels/bars, foreshore (beach), foreshore (wave deposits). Figure 19 is interpreted as amalgamated shoreface deposits. Figure 20 is interpreted as mainly foreshore/beach deposits (all photos from outcrop #2).

Issues: The smooth-crested ("arched") large wave ripples (noted above) probably form in a similar hydraulic regime as fine-grained hummocky cross-strata but published work (Leckie, 1988; Cummings et al., 2009) indicate such ripples should be sharp-crested in coarse sediment. Some smooth arches (10-15 cm high) weather out at some bedset boundaries at outcrop #2 and appear 3-D but not all follow strata. Perhaps sharp crests are smoothed or different bedforms arise under combined flow conditions as such with tidal interaction (e.g., Perillo et al., 2014; Passchier and Kleinhans, 2005); needs further description.

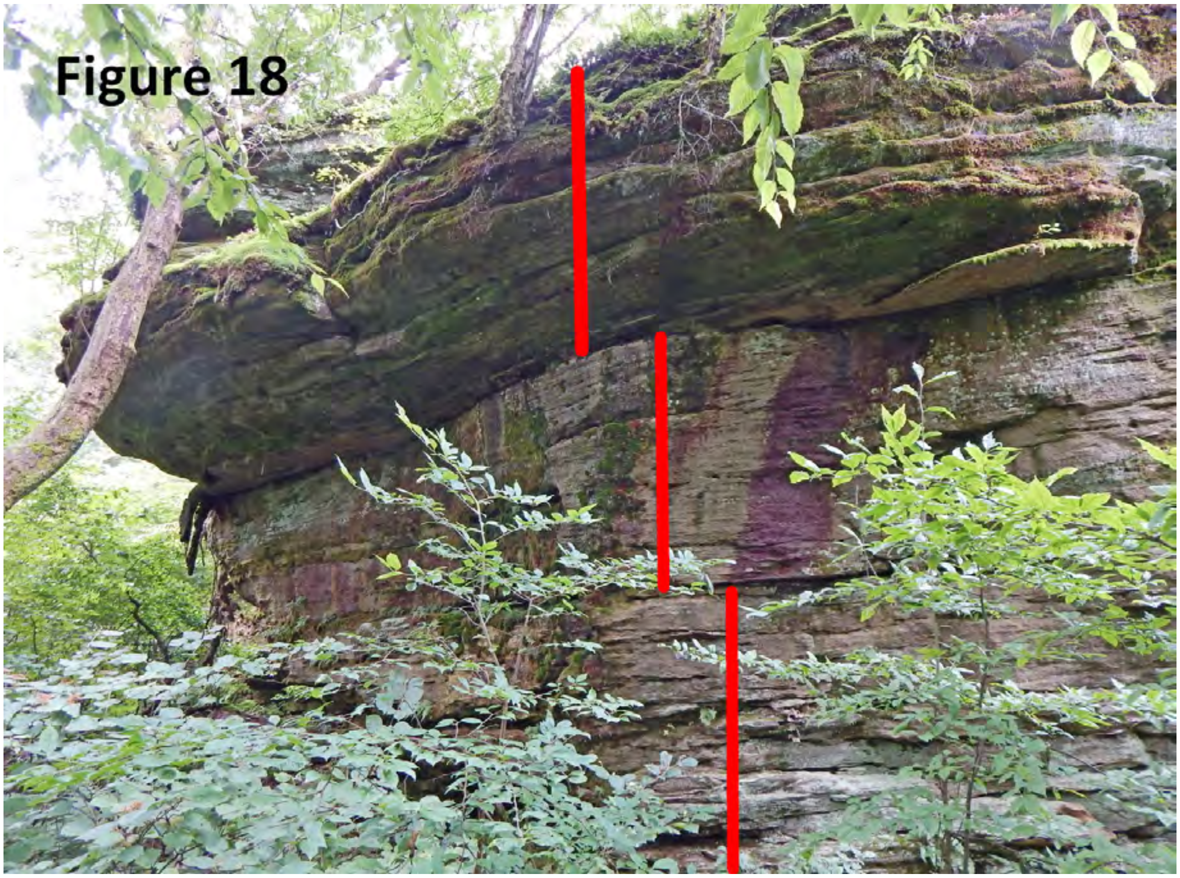
Figure 18

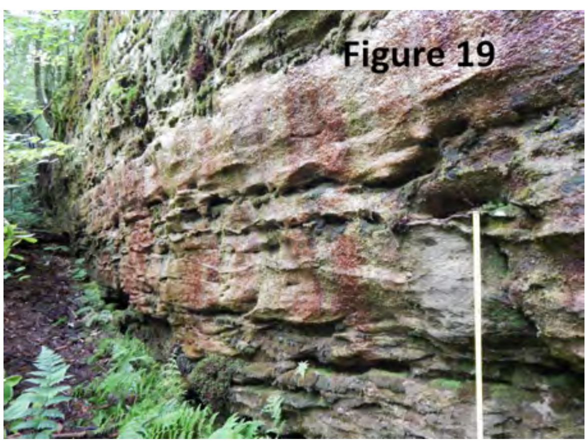
Figure 19


Figure 20

Prograding Tide-dominated Delta

Outcrops # 4, 5, & 6 - Coarse-grained distributaries, Tidal channels, Bars, and Shoals

- Outcrops #4 & 5 - abundant channels (meters to tens of meters wide, ~ 1-2 m deep) and channel point bars (coarse sand to pebble lateral-accretion deposits of tidal and delta distributary channels).
- Outcrop #6 - extraordinary exposures of channels/point bars with direct deltaic evidence (Fig. 26-27). The base of channel complex (three discrete ~ 2 m units or "storeys") directly overlies tan fine to medium-grained wave-ripple laminated sandstones which is interpreted as a distributary channel complex prograding over marine shoreface deposits.
- Cross-bedded strata of various dimensions (~ 0.05 m to +1 m) commonly arranged in cosets, some bidirectional (Fig. 21).
- Current indicators mainly directed shoreward (E-SE); some point bar tops and some truncation surfaces show wave influence (wave ripples).

As noted earlier, recognition of cross-strata in pebbly beds is difficult but most beds have crude bedding. Most of the bars appear to be point bars associated with meandering tidal channels and distributaries. The vertical dimensions of bars and channels are generally small (1-2 m) which reflect channel depths and the finer-grained bar tops may be wave-rippled suggestive of storm waves or slack tidal periods. Channel widths may approach 10+ m; an example at outcrop #5 appears to show back-and-forth lateral bar migration within a shallow channel while slowly aggrading vertically (perhaps slow subsidence due to compaction; Fig. 23).

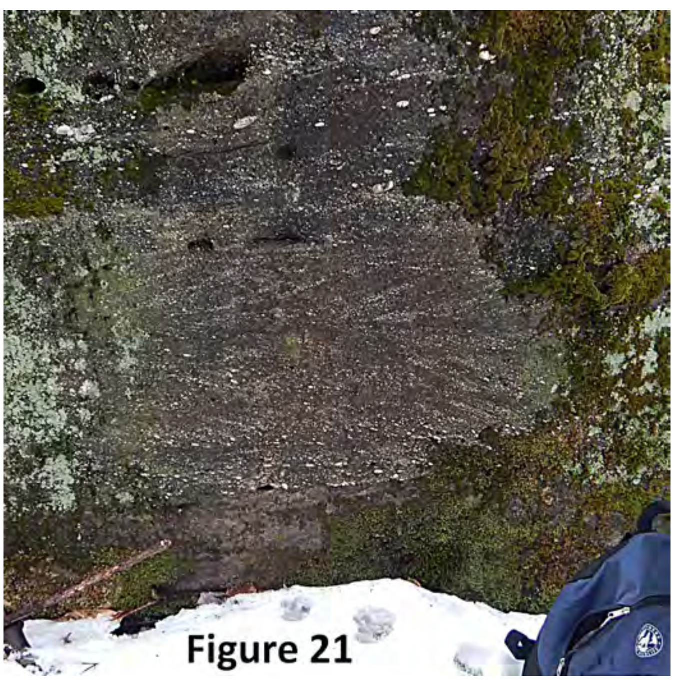

Figure 21

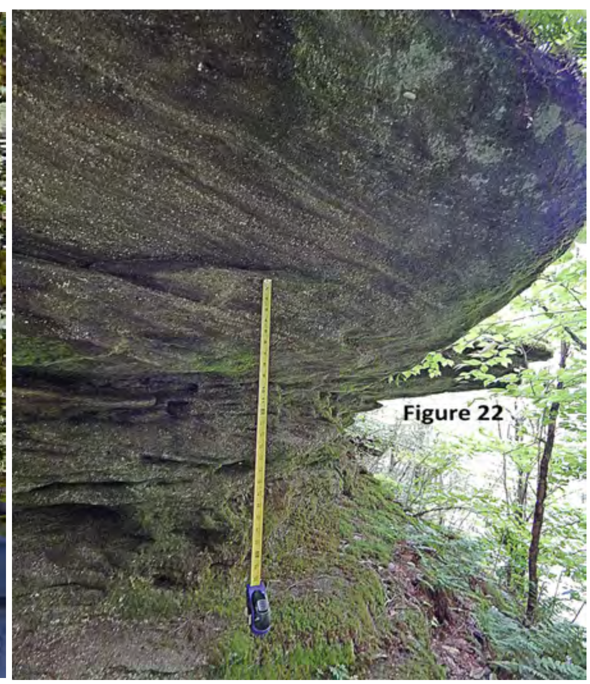

Figure 22

Figures 23 - (channels), **24** (*Productella* found on caprock), **25** (Caprock) - **Outcrop #5**

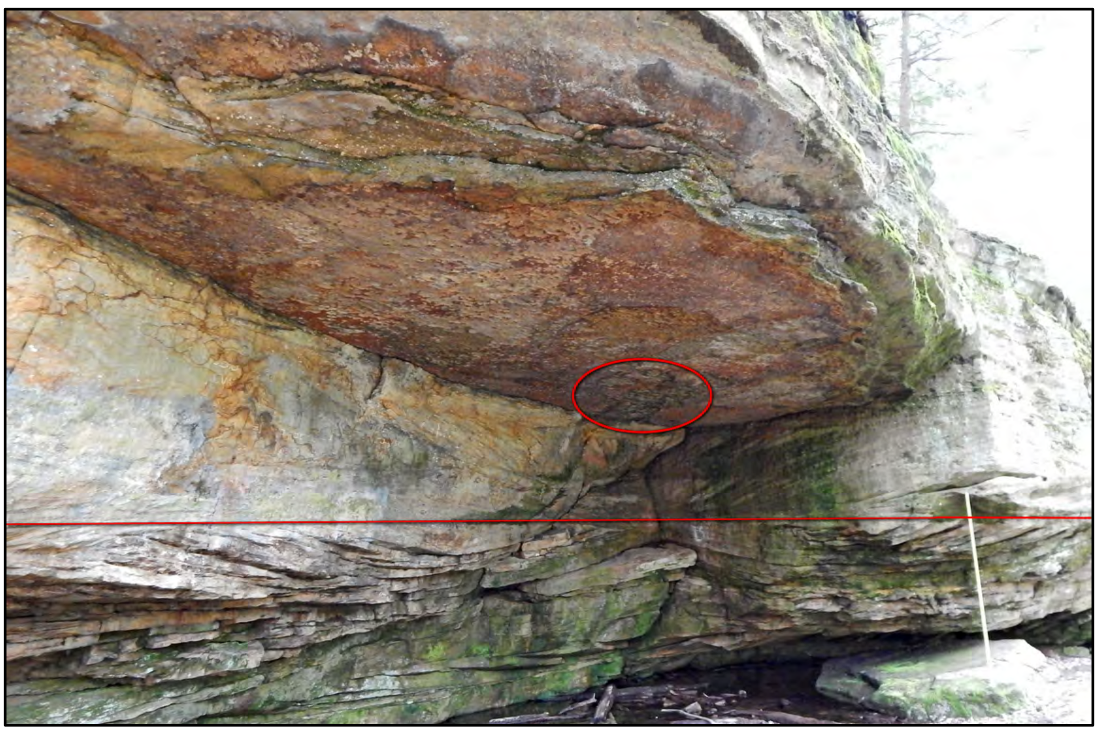

Figures 26 & 27 - – Outcrop #6 – Two westerly views of main channel complex - Multiple channels, marine deposits at base, deltaic depositional environment inferred. Figure 27 – Red line marks the truncated top of a channel missing a curved section which is defined by orthogonal joints; by length of the sides (arctan 2 m/3 m = 30^{o} tangent) yields a ~ 60^{o} bend. Large fossil "log" circled in large channel base which is much larger than the channels beneath; tape = 1 m).

Lateral Accretion Deposits vs. Cross-bedding

Point bars of a meandering steam migrate roughly perpendicular to channels in response to cut-bank erosion and deposition on the inside bends ("points") of meanders (e.g., Allen, 1982; the study of such deposits began in the 1920s on the tidal flats of the North Sea). A suite of bedforms (largely dunes in this case) may develop on the point bar surfaces in response to prevailing currents and sediment size/supply, and if preserved, form "lateral accretion deposits". As point bars migrate, the base of the depositional units may be preserved as low-angle bedding structures ("lateral accretion surfaces"; LAS) which reflect channel geometry (generally < ~ 15^o) and often display basal scour and pebble/fossil lags. So the dip direction of the larger-scale, low-angle LAS of point bars reflect channel migration direction (~ normal to channel trend) whereas the smaller-scale internal sedimentary structures (e.g., dune cross-strata) reflect current direction(s) which are generally channel-parallel. So a point bar has two scales of sedimentary structures/surfaces: usually much larger, low-angle (< 15-20^o) LAS and usually much smaller, cross-stratification (ideally 30-35^o but much less in coarse deposits and poor exposures). At LRC, the potential for overlap between LAS and foresets must be considered. Confusion is possible especially where channels are small, shallow and steep-sided and the lateral accretion deposits are thin and where coarse cross-strata can be difficult to recognize and may range into meter-scale.

Channels and point bar deposits are well exposed in places. Channel cross-sections are common at outcrops #4 and #5 as displayed on strike-joint (paleo-shore parallel) surfaces. The sense of flow direction is less clear but bi-directional cross-beds are present (Fig. 21). At outcrop #2 and #6, some channels weather out and overhang dramatically with steep (> 45^o) sides; some joint surface exposures are much less obvious. Developing criteria to distinguish tidal vs. distributary vs. fluvial channels would be useful especially for exposures on the western side of the hill yet to be studied.

Fluvial (Deltaic?) - Meandering Stream Deposits - Uppermost sequence

This sequence has been described at each outcrop; to summarize ~ 2 – 3 m thick channel/lateral accretion deposits with some reddish, well-oxidized strata and plant remains interpreted as prograding/meandering upper delta plain (beyond tidal influence) or coastal plain streams associated with the delta. No delta analogues are suggested since the exposures are not extensive and it's not clear how the three depositional sequences interrelate. However, if all of the small delta is exposed at LRC, it's at least two orders of magnitude smaller than the Niger delta (much larger drainage area and wave-dominated but with extensive tidal channels and flats; van Cappelle et al., 2016 provide an excellent review of tide-wave influenced deltas).

Figure 28 – "Caprock" at Outcrop #4

The caprock varies spatially and is generally similar to the underlying deposits with some reworking evident. The erosional remnants at outcrop #4 appear to be distinct fluvial deposits above deltaic deposits. At the base of a remnant here is an unusual deposit of large pebbles sandwiching a grayish sandstone with visible pores and abundant plant debris (Fig. 28 above). Given the position of the coarse pebble layers and possible air escape pores, rapid deposition by powerful unsteady currents is suggested; a tsunami, very large storm, or fluvial processes are possibilities. This pebble layer likely correlates with the caprock at outcrop #5 and elsewhere and needs further study. Within the deltaic sequence (outcrop #5), the uppermost caprock contains large (average 2-4 cm; up to 6+ cm) densely/randomly-packed vein-quartz pebbles (with some large red and brown sandstone and metamorphic clasts and red mudstone rip-up clasts not seen elsewhere) with abundant generally-aligned plant remains. And finally, with diligent search, wave-ripple laminated buff-colored sandstones with marine fossils (not seen insitu elsewhere) can be found draping the caprock in this area suggestive of a major flood event and a subsequent abrupt marine transgression.

CONCLUSION

The Salamanca Conglomerate records a high-energy Upper Devonian seacoast, with at least a meso-tidal range, as indicated by a pebbly beach, a tide-dominated delta prograding over marine wave-rippled fine sands, and a sub-aqueous large-scale dune field formed by strong flood tides. Most of the sequence records delta progradation and sediment transport/redistribution along shore to dunes and beaches by tides and waves. Well-exposed channel deposits at the top (which overlie wave-truncated dunes and beach deposits at a similar elevation) suggest a transition to a coastal plain environment including a major flood event as suggested by localized large clasts of quartz, sandstone, mud rip-up clasts, and abundant plant fossils followed by an apparent abrupt rise in relative sea level and a transgression as indicated by subsequent fine-grained wave-formed strata with an abundant marine fossil fauna.

ROAD LOG

Meeting Point: Rock City State Forest – Little Rock City Rd. at the DEC sign/State Forest boundary (two small parking lots; carpool if possible)

Meeting Point Coordinates: 42.225830, -78.710587

Meeting Time: 10:00 AM

Rock City State Forest is off Hungry Hollow Rd. which can be approached from US route-219 or State route-353.

All outcrops are short hikes on trail or just off the road.

Bring a lunch.

Be prepared for no facilities.

Latitude	Longitude	Stop or View Description
42.2280	-78.7092	STOP 1. The “Sentinels” - obvious from the first crest of Little Rock City Rd.; well visited but respect private property. Well-weathered, isolated blocks (two photos shown with the epilogue and Figs. 9 & 10); interpreted as tidal flats and shoals.
42.2265	-78.7137	STOP 2. The “North Face” - the highest outcrops (+10 m; which includes 3-4 m of marine strata) – shoreface/foreshore/channels; see Figs. 18, 19 & 20)..

42.2259	-78.7175	STOP 3. NW corner of outcrop belt is better exposed (sunny, less moss; "cleaner" rock faces), same interpretation as #2.
42.2217	-78.7113	STOP 4. just east of the first rise (escarpment) on Little Rock City Rd. within RCSF. A multitude of point bars (lateral accretion deposits) and channel fills. Interpreted as part of the deltaic sequence; likely mostly tidal channels and deposits.
42.2187	-78.7127	STOP 5. A few 100 meters south of #4, east side of the road, just inside treeline, extends for 100s of meters (nicely shown on as curvy strike joints on online orthoimagery (htps://orthos.dhses.ny.gov/). Outcrops appear largely filled with glacial debris – just 2 m of channel deposits exposed but with the coarsest caprock and fossiliferous sandstone.
42.2094	-78.7108	STOP 6. Follow the North Country National Scenic Trail (NCT) which enters the woods east of first campsite/shelter; perhaps the most interesting (confusing?) outcrop area. A large channel complex overlying fine-grained wave-rippled sandstone dominates the area (delta interpretation) with adjoining cross-strata of all scales.
42.2088	-78.7075	STOP 7. The NCT joins outcrop area #6 with #7 and following it south (white blazes) through Little Rock City provides a representative sampling of large scale cross-strata (tidal dune field) and overlying channel deposits (meandering streams).

EPILOGUE

Hall (1843) poetically summed up these formative geologic processes and the passage of time:

"Here was an ocean supplied with all the materials for forming rocky strata: in its deeper parts were going on the finer depositions, and on its shores were produced the sandy beaches, and the pebbly banks.

All, for aught we know, was as bright and beautiful as upon our ocean shores of the present day; the tide ebbed and flowed, its waters ruffled by the gentle breeze, and nature wrought in all her various forms as at the present time, though man was not there to say,

How Beautiful!"

REFERENCES CITED

Allen, J.R.L. ,1970, *Physical Processes of Sedimentation,* Allen and Unwin, London, 248 p.

Allen, J.R.L., 1980, Sand waves; a model of origin and internal structure: Sediment Geol. 26, p. 281–328

Allen, J.R.L., 1982, *Sedimentary Structures: Their Character and Physical Basis, Volumes I & II,* Elsevier, Oxford, 592 p./663 p**.**

Ashley, G.M.,1990, Classification of large-scale subaqueous bedforms - a new look at an old problem: Journal of Sedimentary Petrology, 60, p. 160–172.

Attal, M., and Lave, J., 2009, Pebble abrasion during fluvial transport - Experimental results and implications for the evolution of the sediment load along rivers: J. Geophys. Res., 114, F04023.

Baird, G.C. and Lash, G.G., 1990, Devonian strata and paleoenvironments - Chautauqua County region, New York State: New York State Geological Association, 62nd Annual Meeting, Field Trip Guidebook, p. A1-46.

Berner, R. A., 1970, Sedimentary pyrite formation: American Journal of Science, 268, p. 13-23.

Berner, R. A., 1997, Paleoclimate – The rise of plants and their effect on weathering and atmospheric CO_2Science, 276, p. 544–546.

Bishuk, Jr., D., Applebaum, R., and Ebert, J.R., 1991, Storm-dominated shelf and tidally-influenced foreshore sedimentation, Upper Devonian Sonyea Group, Bainbridge to Sidney Center, New York: New York State Geological Association, 63rd Annual Meeting, Oneonta, Field Trip Guidebook, p. 413-462.

Bishuk, Jr., D., Hairabedian, J., and Ebert, J.R. 2003, Coastal Margin Interfluve Paleosols and their Stratigraphic Relationships with Tidally-Influenced Deltaic Deposits in the Sonyea Group (Frasnian) of Northwestern Delaware County, New York: New York State Geological Association, 75th Annual Meeting, Hartwick/Oneonta, Field Trip Guidebook, p. 55-101.

Blakey, R., 2017. North American Paleogeography. (http://deeptimemaps.com/map-room/ ; accessed July 2017)

Boswell, R.M, and Donaldson, A.C., 1988, Depositional architecture of the Upper Devonian Catskill Delta complex: Central Appalachian basin, U.S.A.: *in* McMillan, N.J., Embry, A.F. and Glass, D.J. (eds.), Devonian Of The World, Volume II: Sedimentation, Canadian Society of Petroleum Geologists, p. 65-84.

Bradley, W.C.. Fahnestock, R.K., and Rowekamp, E.T., 1972, Coarse sediment transport by flood flows, Knik River, Alaska: Geological Society of America Bulletin, v. 83, p. 1261-1284.

Bridge, J. S., 2000, The geometry, flow patterns and sedimentary processes of Devonian rivers and coasts, New York and Pennsylvania, USA: *in* Friend, P.F., and Williams, B.P.J., (eds.), New perspectives on the Old Red Sandstone, Geological Society of London, Special Publications 180, p. 61-84.

Bridge, J. S., and Droser, M. L., 1985, Unusual marginal-marine lithofacies from the Upper Devonian Catskill clastic wedge: *in* Woodrow, D.L and Sevon, W.D. (eds.), The Catskill Delta, Geological Society of America special paper 201, p. 163-181.

Bridge, J. S., and Willis, B.J., 1994, Marine transgressions and regressions recorded in Middle Devonian shore-zone deposits of the Catskill clastic wedge: Geological Society of America Bulletin, v. 106, p. 1440-1458.

Bridge, J. S., and Demicco, R.V., 2008, Earth surface processes, landforms and sediment deposits: Cambridge University Press, Cambridge, 815 p.

Carll, J.F., 1880, The geology of the oil regions of Warren, Venango , Clarion, and Butler Counties: 2nd Penn. Geol. Survey, Rpt. 13, 58 p.

Chan, M. A., Parry, W. T., and Bowman, J. R., 2000, Diagenetic hematite and manganese oxides and fault-related fluid flow in Jurassic sandstones, Southeastern Utah: *AAPG Bulletin*, *84*(9), p. 1281-1310.

Coleman, J.M., Gagliano, S.M., and Webb, J.E., 1964, Minor sedimentary structures in a prograding distributary: Marine Geology, v. 1, p. 240-258.

Craft, J. H. and Bridge, J. S., 1987, Shallow-marine sedimentary processes in the Late Devonian Catskill Sea, New York State: Geological Society of America Bulletin, 98, p. 338-355.

Cummings, D.I., Dumas, S., and Dalrymple, R.W., 2009, Fine-grained versus coarse-grained wave ripples generated experimentally under large-scale oscillatory flow: Journal of Sedimentary Research, v. 79, p. 83–93.

Dennison, J.M., 1985. Catskill Delta shallow marine strata: *in* Woodrow, D.L., and Sevon, W.D., (eds.), *The Catskill Delta: GSA Special Paper 201*, p. 91-106.

Domokos, G., Jerolmack, D.J., Sipos, A.A., Torok, A., 2014, How river rocks round: Resolving the shape-size paradox. PLoS ONE 9(2): e88657.

Duke, W.L., 1985, Hummocky cross-stratification, tropical hurricanes, and intense winter storms: Sedimentology, 32, 167-194.

Duke, W. L. and Prave, A. R., 1991, Storm- and tide-influenced prograding shoreline sequences in the Middle Devonian Mahantango Formation, Pennsylvania, *in* Smith, D. G., Reinson, G. E., Zaitlin, B. A., and, Rahmani, R. A. (eds.), Clastic Tidal Sedimentology, Canadian Society of Petroleum Geologists, Memoirs, 16, p. 349-370.

Engel, A., 1951, Quartz Crystal Deposits of Western Arkansas: US Geological Survey Bulletin 973-E, p. 173-259.

Engelder, T., 1986, The use of joint patterns for understanding the Alleghanian Orogeny in the Upper Devonian Appalachian Basin, Finger Lakes District, New York: New York State Geological Association, 58th Annual Meeting, Field Trip Guidebook, p. 129-144.

Ericksen, M.C., Masson, D.S., Slingerland, R., Swetland, D.W., 1990, Numerical simulation of circulation and sediment transport in the late Devonian Catskill Sea, *in* Cross, T.A. (ed), *Quantitative Dynamic Stratigraphy*. Prentice-Hall, Englewood Cliffs, p. 293-305.

Ettensohn, F.R., 1985, The Catskill Delta complex and the Acadian Orogeny; a model: *in* Woodrow, D.L., and Sevon, W.D., (eds.), *The Catskill Delta: GSA Special Paper 201*, p. 39-49.

Faill, R. T., 1985, The Acadian Orogeny and the Catskill Delta, *in* Woodrow, D.L., and Sevon, W.D., (eds.), *The Catskill Delta: GSA Special Paper 201*, p. 15-37.

Glenn, L.C., 1902, Carbonic and Devonic formations of southwestern New York: NYS Musuem 56th Annual Report.

Hack, J. T.,1957, Studies of longitudinal stream profiles in Virginia and Maryland: U.S. Geol. Surv. Prof. Paper, 294-B.

Hall, J., Vanuxem, L., Emmons, E., Mather, W. Williams, 1842-43, *Geology of New York...* Carroll & Cook, Albany.

Harms, J.C., Southard, J.B.,and Walker, R.G., 1982, Structures and sequences in clastic rocks: SEPM Short Course No. 9., Society of Economic Paleontologists and Mineralogists, Tulsa, OK.

Johnson, K.G., and Friedman, G.M., 1969, The Tully clastic correlatives (Upper Devonian) of New York State: A model for recognition of alluvial, dune (?), tidal, nearshore (bar and lagoon), and offshore sedimentary environments in a tectonic delta complex, Journal of Sedimentary Petrology, v. 39, 2, p. 451-485.

Keen, T.R., Slingerland, R.L., Bentley, S.J., Furukawa, Y., Teague, W.J. and Dykes, J.D., 2012, Sediment transport on continental shelves: Storm bed formation and preservation in heterogeneous sediments, *in*: *Sediments, Morphology and Sedimentary Processes on Continental Shelves*, John Wiley & Sons, Ltd.p. 295-310

Kingsley, C.S., 1984, Dagbreek fan-delta: An alluvial placer to prodelta sequence in the Proterozoic Welkom goldfield, Witwatersrand, South Africa, *in* Koster, E.H., and Steel, R.J., (eds.), Sedimentology of gravels and conglomerates: Canadian Society of Petroleum Geologists Memoir 10, p. 321–330.

Klein, W., 2017, Personal Commications - Dr. Klein and Dr. Lisa Amati kindly fielded questions on fossil plants.

Kuenen, P.H., 1956, Experimental abrasion of pebbles, 2, rolling by current: Journal of Geology 64(4):336–368.

Krumbein, W.C., 1941, The effects of abrasion on the size, shape and roundness of rock fragments: Journal of Geology 49(5), p. 482–520.

Komar, P. D., 1998, *Beach Processes and Sedimentation: 2nd edition*, Prentice-Hall, Upper Saddle River, New Jersey, 544 p.

Leckie, D, 1988, Wave-formed, coarse-grained ripples and their relationship to hummocky cross-stratification: Journal of Sedimentary Research, 58, 4, p. 607-622

Middleton, G.V., 1977, Sedimentary processes – hydraulic interpretation of primary sedimentary structures, *SEPM Reprint Series*, *3*, 285 p.

Millar, S.W.S. and Nelson, F.E., 2001, Clast fabric in relict periglacial colluvium, Salamanca Re-entrant, southwestern NY, USA: Geogr. Ann., 83 A (3), p, 145-156.

Miller, K. L., T. Szabó, D. J. Jerolmack, and G. Domokos, 2014, Quantifying the significance of abrasion and selective transport for downstream fluvial grain size evolution: J. Geophys. Res. Earth Surf., 119, p. 2412-2429.

Miser, H.D., 1943, Quartz veins in the Quachita Mountains of Arkansas and Oklahoma, their relation to structure, metamorphism, and metalliferous deposits: Economic Geology, v. 38, i. 2, p. 91-118.

Missimer, T.M. and Maliva, R.G., 2017, Late Miocene fluvial sediment transport from the southern Appalachian Mountains to southern Florida: An example of an old mountain belt sediment production surge, Sedimentology, p. 1365-1391.

Muller, E.H., 1977, Quaternary Geology of New York, Niagara Sheet*:* NYS Museum & Science Service, Map & Chart Series #28

Passchier, S., and Kleinhans, M.G., 2005, Observations of sand waves, megaripples, and hummocks in the Dutch coastal area and their relation to currents and combined flow conditions: J. Geophys. Res., 110, F04S15, doi:10.1029/2004JF000215.

Pelletier, B. R., 1958, Pocono paleocurrents in Pennsylvania and Maryland, Geological Society of America Bulletin, v. 69, p. 1033-1064.

Perillo, M. M., Best, J. L., Yokokawa, M., Sekiguchi, T., Takagawa, T. and Garcia, M. H., 2014, A unified model for bedform development and equilibrium under unidirectional, oscillatory and combined-flows: Sedimentology, 61: p. 2063–2085.

Pettijohn, F.J., 1975, Sedimentary Rocks: 3rd edition, Harper&Row, New York, 628 p.

Prave, A. R., Duke, W. L. and Slattery, W., 1996, A depositional model for storm- and tide-influenced prograding siliciclastic shorelines in the Middle Devonian of the central Appalachian foreland basin: Sedimentology, 43, p. 611-629.

Reesink, A.J.H. and Bridge, J.S., 2007, Influence of superimposed bedforms and flow unsteadiness on formation of cross strata in dunes and unit bars: Sedimentary Geology 202, p. 281–296.

Reesink, A.J.H. and Bridge, J.S., 2009, Influence of bedform superimposition and flow unsteadiness on the formation of cross strata in dunes and unit bars – Part 2, further experiments: Sedimentary Geology, v. 222, p. 274-300.

Reesink, A.J.H., Van den Berg, J.H., Parsons, D.R., Amsler, M.L, Best,, J.L., Hardy, R.J., Orfeo, O,. , Szupiany R.N., 2015, Extremes in dune preservation: Controls on the completeness of fluvial deposits: *Earth-Science Reviews*, 150, p. 652-665.

Reynaud, J.Y. and Dalrymple, R.W., 2012, Shallow-marine tidal deposits *in* Davis, R.A., Jr. and Dalrymple, R.W., (eds.), *Principles of Tidal Sedimentology*, Springer, p. 335-370.

Scotese, C.R., 2000, Upper Devonian Paleoclimate Map (http://www.scotese.com/ldevclim.htm; accessed July 2017)
Slingerland, R.,1986, Numerical computation of co-oscillating palaeotides in the Catskill epeiric Sea of eastern North America: *Sedimentology*, *33*(4), p. 487-497.

Slingerland, R., and Loule, J. P., 1988, Wind/wave and tidal processes along the Upper Devonian Catskill shoreline in Pennsylvania, U.S.A. *in*: McMillan, N. J., Embrya, A. F., and Glass, D. J. (eds.) *Devonian of the World, Vol. II,* Canadian Society of Petroleum Geologists, Memoirs, 14, p. 125-138.

Smith, G.J., and Jacobi, R.D., 1998, Fault-influenced transgressive incised shoreface model for the Canadaway Group, Catskill Delta Complex: Journal of Sedimentary Research B, v.68, p. 668-683.

Smith, G.J., and Jacobi, R.D., 2001, Tectonic and Eustatic Signals in the Sequence Stratigraphy of the Upper Devonian Canadaway Group, New York State: American Association of Petroleum Geologists Bulletin, v. 85, no. 2, p. 325-357.

Smith, G.J., and Jacobi, R.D., 2006. Depositional and tectonic models for Upper Devonian sandstones in western New York state. Guidebook for the 35th Eastern Section AAPG Meeting and 78th NYSGA Field Trips, p. 54–115.

Sneed, E.D., and Folk, R. L., 1958, Pebbles in the lower Colorado River, Texas, a study in particle morphogenesis: Journal of Geology, 66, p. 114-50.

Southard, J., 2006, - *Introduction to Fluid Motions, Sediment Transport, and Current-Generated Sedimentary Structures,* Massachusetts Institute of Technology: *12.090* - MIT OpenCourseWare, https://ocw.mit.edu.

Streel, M., Caputo, M. V., Loboziak, S., & Melo, J. H. G., 2000, Late Frasnian–Famennian climates based on palynomorph analyses and the question of the Late Devonian glaciations: *Earth-Science Reviews*, *52*(1), p. 121-173.

Stride A.H.,1982, (ed.) Offshore tidal sands: processes and deposits, Chapman & Hall, London, 222 p.

Terwindt, J. H. J., 1971, Sand waves in the southern bight of the North Sea: Marine Geology, v. 10, 1, p. 51-67.

Terwindt, J. H. J., 2009, Origin and sequences of sedimentary structures in inshore meso-tidal deposits of the North Sea: *Holocene marine sedimentation in the North Sea Basin*, *5*, p. 4-26.

Tesmer, I. H., 1963, Geology of Chautauqua County, New York, Part I - Stratigraphy and Paleontology: N.Y. State Museum Bulletin, v. 391.

Tesmer, I. H., 1975, Geology of Cattaraugus County, New York. Buffalo Society of Natural Sciences Bulletin, 27, 105 p.

Thorne, J. A. and Swift, D. J. P., 1989, The effect of long-term sea-level changes on shelf sedimentation--the concept of sediment regime: Kansas Geological Survey, Subsurface Geology, 12, p. 19

Tonnon P.K., van Rijn L.C., Walstra D.J.R., 2007, The morphodynamic modelling of tidal sand waves on the shoreface: Coastal Engineering, 54, 4, p. 279-296.

van Cappelle, M., Stukins, S., Hampson, G. J. and Johnson, H. D., 2016, Fluvial to tidal transition in proximal, mixed tide-influenced and wave-influenced deltaic deposits: Cretaceous lower Sego Sandstone, Utah, USA: Sedimentology, 63, p. 1333–1361.

Wang, P., 2012, Principles of sediment transport applicable in tidal environments, Chp. 2 *in* Davis, R.A., Jr. and Dalrymple, R.W. (eds.), *Principles of Tidal Sedimentology*, Springer. New York, 621 p.

Willis, B.J. and Bridge, J. S., 1988, Evolution of Catskill River systems, New York State, *in*: McMillan, N. J., Embry, A.F. and Glass, D.J. (eds.), Devonian of the World, Vol. II., Canadian Society of Petroleum Geologists, Memoirs, 14, p. 85-106.

Witzke, B.J., 1990, Palaeoclimate constraints for Palaeozoic palaeolatitudes of Laurentia and Euramerica *in* McKerrow, W.S., and Scotese, C.R., (eds.), *Palaeozoic Palaeogeography and Biogeography*: Geological Society of London Memoir 12, p. 57-73.

Woodrow, D. L., 1985, Paleogeography, paleoclimate, and sedimentary processes of the Late Devonian Catskill Delta, *in* Woodrow, D.L., and Sevon, W.D., (eds.), *The Catskill Delta: GSA Special Paper 201*, p. 51-63.

Zambito, J.J., 2011, The Late Middle Devonian (Givetian) Global Taghanic Biocrisis in its Type Region (Northern Basin): Geologically Rapid Faunal Transitions Driven by Global and Local nvironmental Changes: Ph.D, Dissertation, University of Cincinnati, 231 p.

A4: PIONEER OIL MUSEUM OF NEW YORK, INC.

KELLY LOUNSBERRY
Vice President,
417 Main Street, Bolivar, NY 14715
Phone (585) 610-2038, http://www.pioneeroilmuseum.com/index.php

The Pioneer Oil Museum of New York, Inc., located in Bolivar, New York, was the creation of the New York State Oil Producers Association (NYSOPA) in the mid-1960's. The goal of the members of this organization was to "house in a readily available, central location, articles and information of historical value or interest pertaining to the New York State Oil Industry." A secondary goal was to accumulate and display artifacts related to the local petroleum industry. Also the promoters hoped to honor the men who had been pioneers in both the primary and secondary phases of oil recovery in the area.

Among the main organizers of the museum were Bill Hogan and Clarence (Mike) Schaffner, both of Bolivar. Schaffner, the mayor of the village of Bolivar, became the chairman of a NYSOPA museum committee. In 1964 at the annual NYSOPA clambake, Hogan told his fellow attendees, "If we don't do it [create a local museum], nobody will." Consequently the NYSOPA contributed $1000 toward the creation of the museum. Hogan volunteered the use of a building he owned on Main Street in the village of Bolivar. On behalf of the committee the former Colegrove and Wood Hardware Store was purchased for $2500 by the firm of Hahn and Schaffner. Previously this building had housed the McEwan Supply Store which sold oil field equipment. Other former uses of this building built in 1851 include a cigar factory, a cobbler's shop, a broom factory, a Chinese laundry, a grocery store, a dry goods store, an upstairs business in which magnetos were repaired, and a glove and mitten factory. In 1931 the large front plate glass windows were installed.

During 1965-66 further plans took place toward opening the museum. Letters were sent to potential contributors to send money and/or artifacts which would be suitable for placement in the museum. In 1965 the museum organizers petitioned the Village of Bolivar for permission to drill an oil well near the museum. The goal was to drill a real, working well which would serve as a tourist attraction as well as a possible source of revenue for the museum. Village ordinances at that time (and to this day) prevent anyone from drilling a gas or oil well in the village within 100 feet of any residence or village lot. Although no further research was found to determine the village's response, there is no exterior working well at the museum at the present time.

Also in 1966, NYSOPA agreed to increase the cost of an annual membership from $5 to $10. This increase was designed to cover the cost of the building purchase as well as other expenses the organization would incur in running the museum. During the early 1970's, the group funded two significant improvements: the addition of a vertical "board and batten" siding to restore the late-1800's original look and the installation of a large, colorful sign for the museum's front.

For the next few years artifacts, photographs, and other written documents were collected, but there was never an official grand opening of the museum. By 1973, plans were in the works for the Village of Bolivar's Sesquicentennial to be held two years later. Local residents Tom Manning, George Bradley, Art Burdick, and others decided to refurbish the museum with hopes of opening it up for visitors during the Sesquicentennial celebration. They improved the building's interior so that donated materials could be displayed. Many exhibits commemorating the area's oil story were organized, and a large number of old, irreplaceable photographs were displayed. Other aspects of local history were developed in order to tell the story of the town. The museum was a hit during the Sesquicentennial celebration, so plans were made to keep the building open on a limited full-time basis in the future.

For the rest of the decade the museum remained open on a restricted basis. Interest escalated when the original Pioneer Oil Days were held in the early 1980's. As oil prices increased, so did increased activity in the local industry. During the annual celebration numerous demonstrations and events took place. Among these were a working forge as well as bit-dressing demonstrations. A competition between "roustabout" teams entailed coupling of joints of "sucker rods" and then slinging them into the hooks of tripods.

During the 1980's, Tom Manning took over primary custodianship of the museum and helped organize staffing. Gordon (a retired oil field worker) and Ethyl Burdick were employed by the federally-sponsored Green Thumb program which utilized senior citizens in a variety of ways. They worked in the museum during the day, keeping it open for visitors. Another local resident and retired oil field worker, Max Richardson, worked with Gordon Burdick to retrieve and refurbish artifacts, as well as to maintain the property.

During the 1990's, age forced the retirement of the small staff of dedicated volunteers. To keep the museum up-and-running, each spring a new group of local retirees was assembled to help man the museum during the upcoming summer tourist season.

In the summer of 2000, Tom Manning asked several local residents if they would be interested in joining a newly-formed Board of Directors for the museum. Manning was leaving the area and wanted to place the museum in the hands of a small group of people who would perpetuate this valuable local institution. This new board, under the direction of NYSOPA President Paul Plants, included individuals with ties to area government, the local school district, and the local oil industry.

The Board of Directors attempted to stabilize the museum in terms of both its fiscal and structural viability. It made many improvements including new exhibits and displays, as well as new documentation for many of the photographs and artifacts on display. Both the interior and exterior of the building were painted. The Board conducted annual fund-drives beginning in 2001. Local citizenry, as well as members of the oil-producing industry, showed tremendous support for the museum through their support for the fund-drives. Each year NYSOPA donates to the museum one dollar from each of the approximately 1600 tickets it sells to its annual clambake and meeting.

An adjacent addition, erected in 2004 with the help of a New York State grant, enabled the museum to increase exhibition space while providing protection for equipment displayed outside in the elements. In 2008, the New York State Oil Producers' Association provided a grant to the museum that allowed the purchase of a six-acre site formerly housing the Hahn & Schaffner Pipe Supply Company. Since that time three buildings have been demolished, and five buildings have been renovated. The main store building is now another museum venue that complements the original museum on Main Street. Among other displays, this new building houses the New York State Oil Producers' Association Wall of Fame, honoring many individuals who played significant roles in the local oil and gas industry. In 2016, a new steel building was constructed for display of working oil and gas field equipment.

Each June a celebration to commemorate the heritage of the local oil industry, known as "Pioneer Oil Days," brings in hundreds of people to the museum. Local school children enjoy the tours given by museum volunteers. The number of special tours for family groups as well as organizations has grown significantly the last few years. The Pioneer Oil Museum of New York, Inc. has become a focal point for many local citizens and is dedicated to serving the people of this area for many years to come.

MUSEUM VENUES

Main Street Site

This building was constructed in 1851. Over the years it was used for a cigar factory, a cobbler's shop, a broom factory, a Chinese laundry, a grocery store, a dry goods store, an upstairs business in which magnetos were repaired, and a glove and mitten factory. Eventually it housed the McEwan Supply Store which sold oil field equipment. Before its purchase to become the Pioneer Oil Museum, its last use was for the Colegrove and Wood Hardware Store.

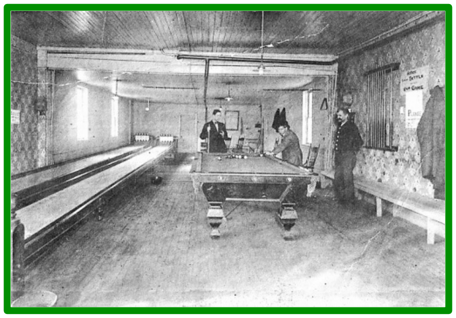

One of the more interesting uses of this building was for George Butler's Box Ball Alleys. Box ball was a modified version of bowling, using smaller balls in knocking down five pins set horizontally across a wooden alley. Lanes were portable and available in three sizes, providing for quick and easy installation in amusements parks, bars and other entertainment venues both big and small.

Hahn & Schaffner Site

The Hahn & Schaffner (H/S) site was originally the home of a pipe supply business related to the oil and gas industry. Due to the generosity of the New York State Oil Producers' Association, the six-acre site was purchased with hopes of developing it to provide an additional site for the current museum. The main store building was totally gutted and refurbished. Exhibits are in the planning stages while much of this new site is being groomed for outdoor usage. Three old dilapidated buildings were demolished while others will be refurbished to house some of these new exhibits.

Actual end of a wooden power house along with an unusual chain-drive engine; most power houses were made out of metal. and most engines were driven

One large building that has been refurbished is the Shaner Exhibition Building. Several antique oilfield engines and other equipment are already on display in that building with more to follow. Two pipe-threading buildings were totally renovated from 2016-2017. These structures were covered with board and batten to provide a rustic appearance. A steel roof and glass block windows were also added for protection and to improve the appearance. Local third-generation oil producer Joe Bucher underwrote the cost of this project which was meant to commemorate his family's legacy in the local fields.

In 2016 a new building , the "Charles H. Joyce Exhibition Building," named in honor of the president of Otis Eastern Service in Wellsville, is a 54 x 90 steel building that will be used to house antique oilfield equipment, some of it (hopefully) in working condition.

A BRIEF HISTORY OF THE BOLIVAR AREA

The early Native Americans used the Little Genesee Creek Valley over thousands of years. The creek was an important path for these people as they traversed the countryside looking for the deer which were such a staple of their diets. The Oswayo Creek joined with the Little Genesee eventually reaching the Allegheny River, a major thoroughfare for the ancient people. These early people camped along the banks of the Oswayo in nearby Ceres, while other groups built settlements nearby.

In 1819, Timothy Cowles and his two young sons arrived on the scene from eastern New York State and became the first permanent white settlers of the Bolivar valley. Soon they cleared the land, built a log house, and carved a niche for themselves in the wilderness. Each year thereafter, more and more settlers arrived, as word of the fertile soil, vastness of forests, and abundance of game, spread back home.

By 1825, enough citizens lived near the confluence of the Root Hollow and Little Genesee Creeks that they decided to form a town in newly-formed Allegany County. In February of that year, they selected the name “Bolivar” to honor the then-living liberator of South America, General Simon Bolivar.

For the next 56 years, the population of Bolivar seldom exceeded 160 hard-working residents. These people made their livings as farmers, loggers, and tanners. They continued to carve fields for their farm animals out of the ample forests as the settlement expanded.

In April 1881, a big oil gusher was struck about two miles up the road in the town of Wirt. Within ten months after this oil strike, Bolivar had become a boom town of 4500 excited oil seekers, and combined with the population of nearby Wirt, the entire valley became home to some 10,000 -12,000 fortune seekers. Business thrived in both communities, and along with the good came the bad that was so representative of any “boom town.” Oil fortunes were made or lost overnight due to gambling with the oil industry or gambling at the card tables.

Oil production slowed within a year, and the population of Bolivar dropped as suddenly. In 1920, the introduction of “flooding,” the secondary recovery of oil, brought Bolivar into a newer and longer-lasting period of prosperity. This new method of recovery caused oil and gas production to soar to undreamed-of heights, and “black gold” flowed into the coffers of a rejuvenated Bolivar. Public and private improvements in Bolivar followed, and by 1940, Bolivar (and nearby Wellsville) was one of the wealthiest communities per capita in New York State.

A BRIEF HISTORY OF OIL AND NATURAL GAS IN SOUTHWESTERN NEW YORK

New York has a long history of oil and gas production. In fact, the first natural gas well was drilled in Fredonia in 1825. For many years, townspeople had noticed that flammable natural gas was seeping out of the black shale in stream beds. After the well was drilled, pipelines were built, first out of wood coated with tar soaked rags, and then later out of lead and tin. Gas from the well was eventually used to light the streets and many buildings in Fredonia. This new source of light was hailed around the world.

Oil seeps (places where oil slowly escapes to the earth’s surface) were common in southwestern New York when the first European settlers arrived, and Native Americans were said to have used the oil for medicinal purposes. The first petroleum (oil) was “discovered” by the French at the oil spring near Cuba, New York in 1627. This was considered a sacred spot by the Seneca Indians who lived in the area. As the first settlers arrived in this area, crude oil was used to treat burns and sprains, rheumatism, and to cure horses’ saddle sores. Oil was also drunk to help with a variety of ailments.

The first commercially successful oil well in the world was drilled just south of Jamestown, NY in Titusville, Pennsylvania in 1859. The drilling boom that followed soon moved north and east to Bradford where a boom struck from 1875-76. By the 1860’s oil was known to exist in the Bolivar area. In 1879, two failed wells in nearby Allentown led to “Triangle No. 1” which was drilled by O.P. Taylor.   The boom town of Petrolia sprang up, and the southern portion of Allegany County came alive with oil fever.

On April 27, 1881, a group drilled a well in nearby Richburg. The well was shot and 70 barrels of oil soon began to flow. This was the “Richburg Discovery Well” which began oil boom which changed the Bolivar valley forever. By 1882, the Bolivar area combined with the nearby Bradford field to produce almost 23 million barrels out of a total of 27,661,000 barrels produced in the entire United States. This meant that this area produced 83% of the country’s entire output, as well as 77% of all the oil produced in the world for that year.

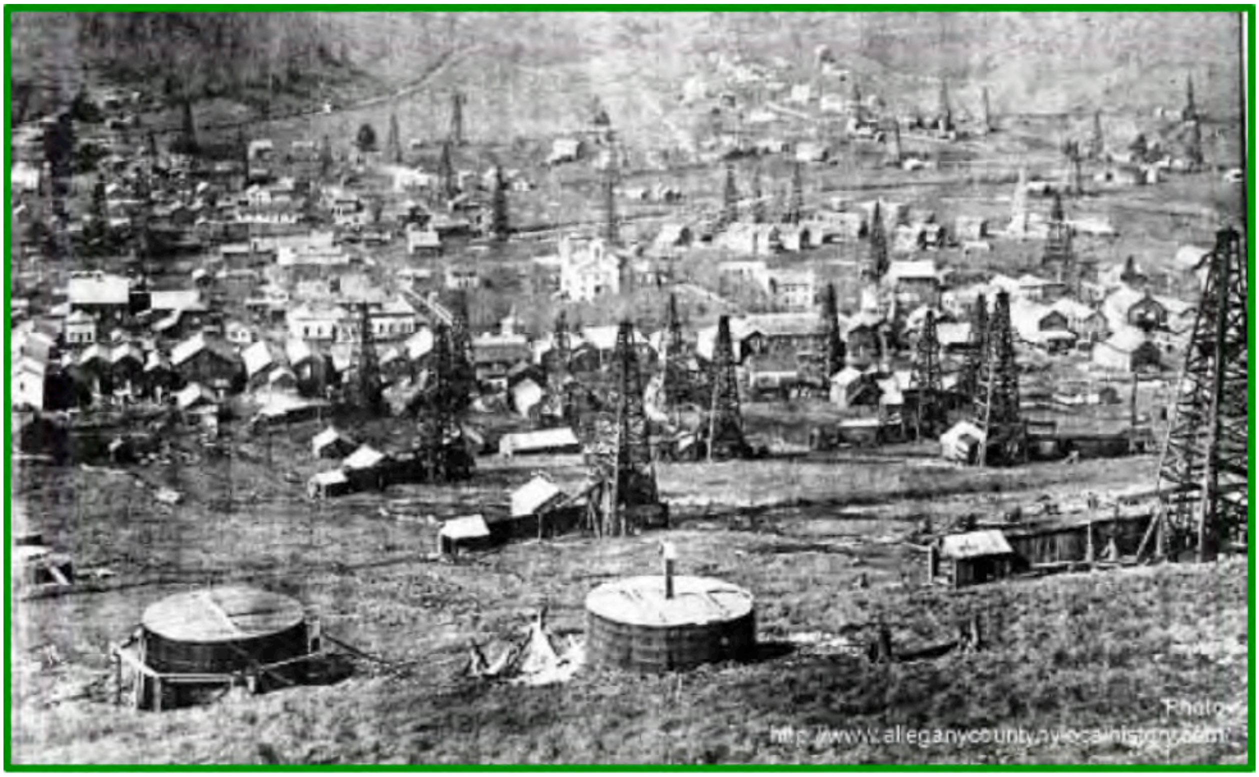

Figure 3. The heart of Richburg during the boom.

STOP DESCRIPTIONS

STOP 1. Pioneer Oil Museum Of New York, Inc.

Location Coordinates: 42.06517, -78.1681

STOP 2. Hahn & Schaffner Site   -- LUNCH

Location Coordinates: 42.06658, -78.17156

STOP 3. Former site of Bolivar Refinery, now Klein Cutlery

Location Coordinates: 42.04807, -78.18903

Allegany Refiners constructed a refinery here in 1933. It had 20 employees initially, and 52 when it closed in 1947. The site has been repurposed and currently houses Industrial Patterns, Inc., in the large building to the right, and Klein Tools in the smaller building along left edge of photo. Heritage Tools had started here in 1952, and was bought by Klein Tools in 2007. It currently employs 52 people making high quality scissors for industry.

STOP 4. Active lease with water flooding, using rod lines, etc.

Location Coordinates: 42.06379, -78.15521

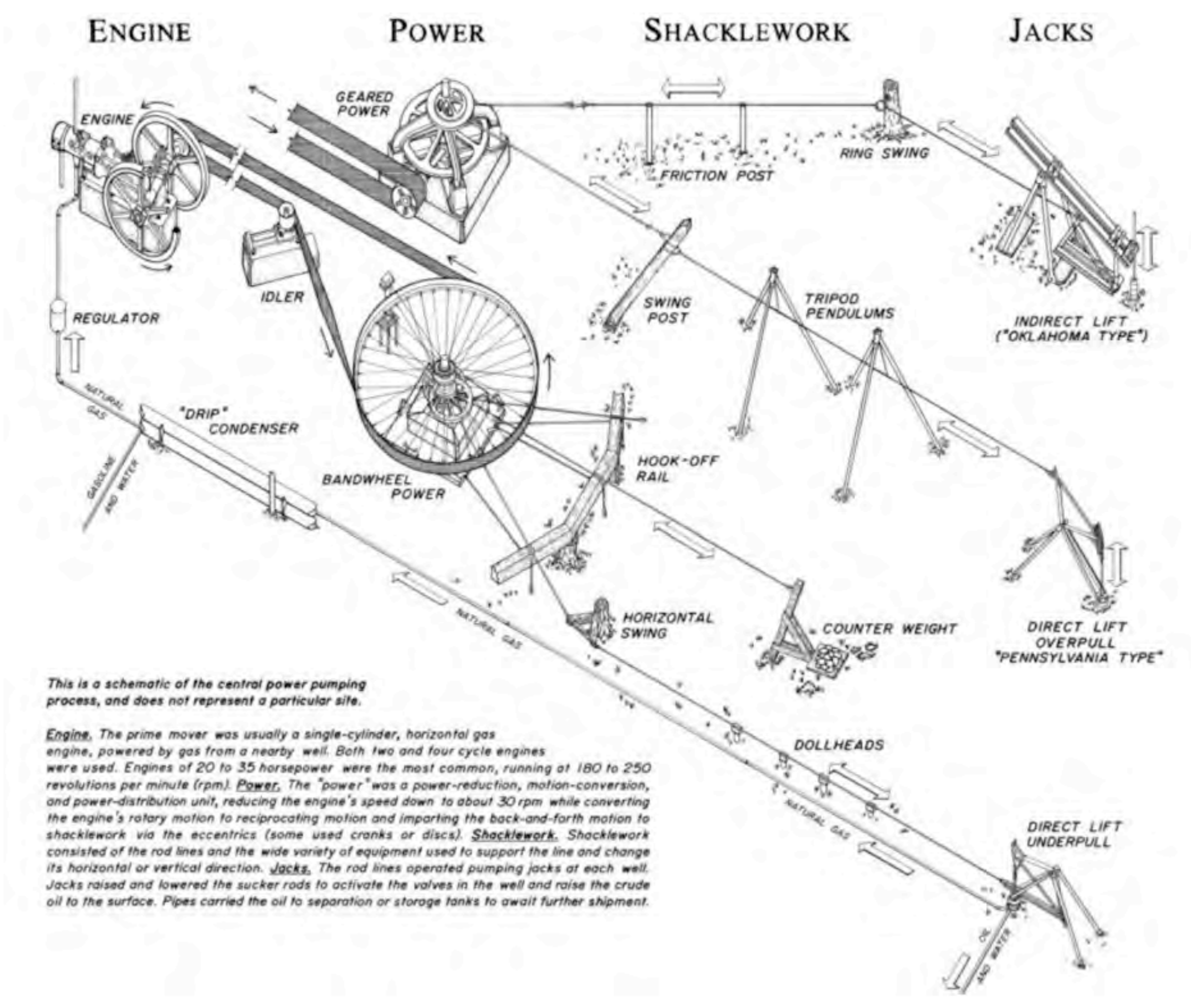

This lease is pumping water down into the oil bearing unit, to push the oil toward the well. If we are lucky it may be working at the time of our visit. The oil is collected by a local oil service company.

STOP 5. Active lease, using rod lines, etc., but without water flooding

Location Coordinates: 41.99599, -78.20132

With some rod lines stretching through the woods over 1,100 feet, this eccentric wheel can drive 12 jacks at the same time. Typically pumped for a couple hours each day, the 28 wells on this lease produce three barrels of oil every two days. The operator, David Collins, has "oil in his blood" both because his father worked the same leases as David was growing up, and because he ingests a tablespoon of crude every day, for medicinal purposes.

The oil here has some water, which is not salty, as it freezes at 32° F. The operations cease each fall as the temperatures drop, to resume the next spring.

A5: KIMBERLITES IN THE CAYUGA LAKE REGION OF CENTRAL NEW YORK: THE SIX MILE CREEK, WILLIAMS BROOK, AND TAUGHANNOCK CREEK DIKES

DAVID G. BAILEY
Geosciences Department, Hamilton College, Clinton, NY 13323

MARIAN V. LUPULESCU
New York State Museum, Research and Collections, 3140 CEC, Albany, NY 12230

JEFFREY R. CHIARENZELLI
Dept. of Geology, St. Lawrence University, Canton, NY 13617

INTRODUCTION

Diamonds in New York State? While it may be hard to believe, just over 100 years ago local residents and scientists thought that there was a very strong possibility of finding diamonds in upstate New York (Figure 1)[1]. This diamond rush lasted for the first few decades of the 20th century, but after numerous failed attempts, the diamond hunt was over and this interesting episode in New York State's history was largely forgotten.

Below we provide a chronological outline of the scientific discoveries and reports on the kimberlitic rocks of central New York, followed by detailed descriptions of the three dikes that will be visited on today's field trip. For a more detailed discussion of the ages and origins of these unusual rocks, the reader is referred to Kay et al. (1983) and Bailey & Lupulescu (2015).

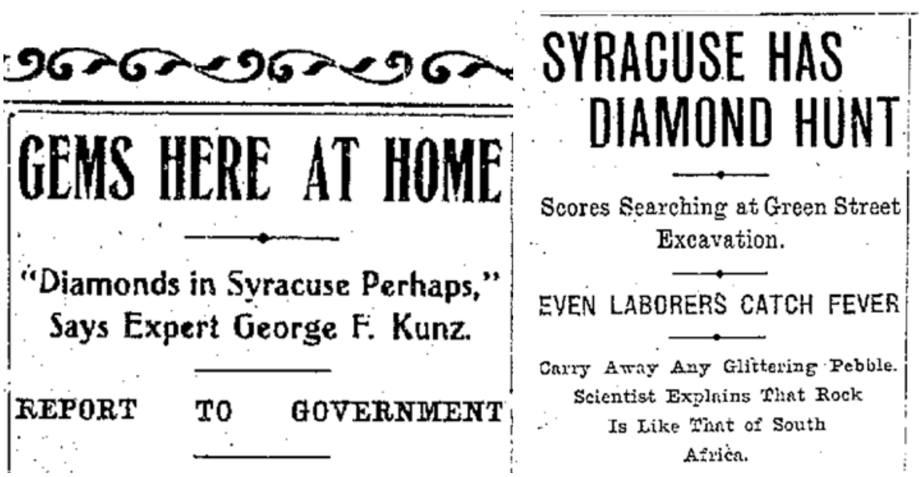
GEMS HERE AT HOME
"Diamonds in Syracuse Perhaps," Says Expert George F. Kunz.
REPORT TO GOVERNMENT

SYRACUSE HAS DIAMOND HUNT
Scores Searching at Green Street Excavation.
EVEN LABORERS CATCH FEVER
Carry Away Any Glittering Pebble. Scientist Explains That Rock Is Like That of South Africa.

Figure 1: Early 20th century newspaper articles illustrating the period of diamond exploration in central New York. Left: Syracuse Herald, July 16, 1906, p.9; Right: Syracuse Post-Standard, Nov. 28, 1905, p.14

[1] NOTE: Most of the figures in this field trip guide are available on-line, and in color, at: *http://www.nysga-online.net/nysga-2017-guidebook-maps-and-images/A5*

HISTORY OF RESEARCH ON NEW YORK STATE KIMBERLITES

What prompted the diamond rush in central NY at the turn of the 20th century? It all started in 1887 with the recognition by British geologist Henry Lewis that the diamonds in South Africa were derived from unusual mica-bearing peridotites that he named “kimberlites” (1888; Mitchell, 1986). Interestingly, the mica peridotites of upstate New York were discovered and described over fifty years prior to this, making them the first kimberlitic rocks ever described in the scientific literature (Vanuxem, 1837, 1839). In his final report for the third geological district, Vanuxem (1842) described four narrow dikes of “serpentine and limestone…trap rock” (p.169) in a ravine east of Ludlowville, a small town north of Ithaca, New York. He also noted the existence of a “dyke on East Canada creek” (p.59) in the town of Manheim, and an interesting serpentine and mica-bearing “metamorphic rock” on “Foot-street Road” in Syracuse (p.109). While these are the first published descriptions of kimberlitic rocks, local geologists clearly knew about them for some time. According to Williams (1887a) and Hopkins (1914), Oren Root, then principal of Syracuse Academy, discovered the Green Street (formerly Foot Street) dike in 1837 and reported its occurrence to Vanuxem.

After the initial reports by Vanuxem (1837, 1839, 1842) and Beck (1842), only one significant scientific study of the New York kimberlites was published over the next twenty years. In (1858), T. S. Hunt published the first extended description, and partial chemical analysis, of the “Ophiolite of Syracuse, New York”. While this study documented the ultramafic character of the rocks, their igneous origin was still not recognized; they were interpreted as “magnesian sediments which have been metamorphosed *in situ*” (p.239). In 1860, the rocks were briefly described by Geddes in a report to the New York State Agricultural Society (Geddes, 1860), and in 1874 Cornell University Professor O. Derby reported the existence of three dikes in Cascadilla Gorge and another one in Six-Mile Creek in a short paper in the Cornell Review. The Six Mile Creek dike was later described in a bit more detail by Simonds (1877). The New York “peridotites” were also mentioned in the third edition of Dana’s “Manual of Mineralogy” (Dana, 1878).

Following Lewis’s 1887 report at a meeting of the British Association for the Advancement of Science on the association of diamonds with “mica peridotites”, there was an explosion in the number of published papers on all types of peridotitic rocks, including those in New York. Between 1887 and 1909 there were over 25 separate publications on the “serpentine dikes” or “peridotites” of central New York. The first to publish extensively on these rocks, and to recognize their intrusive origins was George H. Williams of Johns Hopkins University (Williams, 1887a, b, 1890a, b).

In 1891, Professor J.F. Kemp of Columbia College revisited Vanuxem’s Ludlowville location but was able to identify only two of the four previously reported dikes. He also relocated and described the Six Mile Creek dike and the Cascadilla Creek dike in Ithaca. This paper contained a whole-rock chemical analysis of the Cascadilla Creek dike, the second published analysis of a New York peridotite.

In 1892, Professor C.H. Smyth of Hamilton College relocated Vanuxem’s dikes on East Canada Creek in the town of Manheim and described the most prominent dike as a 25cm wide dike intruding along a fault plane (striking N20E) that juxtaposed the “Utica slate” with a “calciferous sand-rock”. This was the first report relating the dikes to local structures. Smyth also noted the association of the dike with a one-inch thick vein of calcite, galena and pyrite. Smyth provided a chemical analysis and detailed petrographic description of the rock, and was the first to note the widespread occurrence of perovskite in the groundmass of the New York kimberlites (Smyth, 1892). In 1893, Smyth also reported the presence of melilite in the groundmass of the East Canada Creek dike, and on this basis, re-classified the dike as an alnoite (Smyth, 1893). (NB: Recent studies have not been able to confirm the presence of melilite in any of the New York State intrusions).

In 1895, another “dike” was discovered near Syracuse. The excavations for a new water reservoir three miles east of Syracuse in the town of Dewitt exposed large blocks of weathered peridotite (Darton and Kemp, 1895a, b). In-situ outcrop was not exposed, and the source of all available hand specimens was only the excavated material found on the banks of the reservoir. According to Darton and Kemp (1895b), the peridotite occurred as boulders buried in a greenish – yellow earthy matrix, and the size of the intrusion was estimated to be ~ 60 by 75 meters, based on the area covered by the earthy material. The intrusion was also noted to contain “many inclusions of various rocks” (p.457). A complete chemical analysis of the Dewitt intrusion was done at the United States Geological Survey and published in a number of subsequent USGS reports (Clarke, 1904; Clarke and Hillebrand, 1897; Darton and Kemp, 1895b).

At about the same time, two additional dikes were discovered in Manheim near the first dike originally reported by Vanuxem (Smyth, 1896, 1898). The largest dike, nearly 2 meters in width, was noted to be highly sheared and slickensided, and to contain long narrow “horses” of the country rock (Smyth, 1896). Smyth’s papers focused primarily on the presence or absence of melilite in the three dikes, and the mineralogical and chemical effects of weathering on the dikes.

With the expansion of the sewer system in the city of Syracuse at the close of the 19th century, additional exposures of the Green Street dike were uncovered, and described in some detail by Luther (1897), Clarke (1899) and Schneider (1902). The intrusion was described as varying in size and form along strike, from a single dike ~ 4 meters in width to a composite intrusion of multiple dikes and thin sheets with a total width of over 12 meters (Schneider, 1902). Commercial speculation heightened public and scientific interest in these rocks, resulting in multiple newspaper articles ("Gems here at home," 1906; "Serpentine rock of Onondaga rich in sparklers," 1902; "Syracuse has diamond hunt," 1905; "Would advance cash to probe stratums," 1902) and scientific publications (Kraus, 1904; Pattee, 1903; Schneider, 1902, 1903a, b; Smyth, 1902).

New dikes continued to be discovered and described in the Ithaca region (Barnett, 1905; Matson, 1905) and, at this time, Barnett concluded that a total of 25 dikes were known in New York State. This number kept increasing, as shortly after this four dikes were discovered in Clintonville (Smith, 1909), geographically in between Syracuse and Ithaca, and E. M. Kindle (in Williams et al., 1909) described five new dikes in the Ithaca area: two dikes in Indian Creek, two in Six-Mile Creek, and one east of the Central Avenue bridge.

After numerous failed attempts to find diamonds in any of the intrusions, scientific interest waned until Cornell Professor Pearl Sheldon and her students began studying the dikes in the Ithaca area (Martens, 1923a, b, 1924; Sheldon, 1921). These reports described over a dozen new dikes in the region, and Sheldon’s final publication emphasized the association of dike intrusion with faulting (Sheldon, 1927).

The next major study was conducted by Edwin Filmer (1939) who had the opportunity to conduct field work after a big storm in 1935 that washed sediment out of the ravines surrounding Ithaca, and exposed many new dikes. He also was the first to describe the large diatreme in the Poyer Orchard creek, and the small diamond washing operation that was set up here in the late 1930’s.

Over the next twenty years scientific focus moved to the Syracuse kimberlites, with Syracuse University Professor James Maynard and his students publishing the first detailed descriptions of most of the intrusions in the area (Apfel et al., 1951; Hogeboom, 1958; Maynard and Ploger, 1946; Van Tyne, 1958).

As scientific technologies advanced in the late 20th century, numerous researchers attempted to date the New York kimberlites. Zartman et al. (1967) published the first K/Ar and Rb/Sr ages on phlogopite grains extracted from two dikes, one near Ithaca and the other in the town of Manheim. The K/Ar ages ranged from 145 to 493 Ma, and the Rb/Sr ages ranged from 118 to 146 Ma. Zartman et al. recognized that the early Paleozoic ages were clearly incompatable with the known stratigraphic relationships, and attributed the old K/Ar ages to excess radiogenic argon and/or the retention of argon by old xenocrystic phlogopite. He concluded that the New York intrusions were of Late Jurassic to Early Cretaceous age. Subsequent K/Ar studies by Watson (1979) and Basu et al. (1984) confirmed the Late Jurassic to Early Cretaceous age of the New York Kimberlites with most ages between 120 and 150 Ma. The most recent radiometric dating on these rocks was done by Heaman and Kjarsgaard (2000) who extracted groundmass perovskite from two dikes northwest of Ithaca. The high precision U-Pb ages obtained on these samples ranged from 144.8 ± 3.2 to 147.5 ± 3.0 (Heaman and Kjarsgaard, 2000).

Two paleomagnetic studies were also done on dikes in the Ithaca region. The first, by Dejournett and Schmidt (1975), and the most recent and more extensive study by Van Fossen and Kent (1993). Both revealed a complex history of emplacement times and temperatures, with normal and reversed pole positions, and a previously unrecognized late Jurassic – early Cretaceous virtual geomagnetic pole position at 58^{o}N, 203^{o}E.

Foster (1970) provided an excellent and comprehensive review of the locations, mineralogy and petrology of kimberlites in the Ithaca region. Most of the subsequent work on these rocks was done by Cornell Professor S. M. Kay and her students on the macrocryst and xenolith mineralogy of the Ithaca area intrusions (Kay, 1990; Kay and Foster, 1986; Kay et al., 1983; Snedden, 1983; Snedden and Kay, 1981a, b).

Over the past twenty years, the authors, with the help of numerous colleagues and students, have compiled consistent and comprehensive data on the mineralogical and chemical compositions of all the kimberlitic intrusions in New York State. This has allowed us to identify large scale patterns and variations in Mesozoic magmatic activity across the region (Bailey and Lupulescu, 2007a; Bailey and Lupulescu, 2007b, 2009, 2015; Lupulescu et al., 2007; Lupulescu et al., 2002; MacDougall and Bailey, 2009; Rauscher et al., 2003). A general overview and summary of our current understanding of these unusual rocks is presented in the following section.

GENERAL FEATURES OF NEW YORK STATE KIMBERLITES

Geographic & Geochemical Groups

Over the past 180 years, a total of approximately 90 distinct kimberlitic intrusions have been identified in central New York State. The vast majority occur in two distinct clusters: one in the Ithaca / Cayuga Lake region, and the second in and around the city of Syracuse. A few additional dikes have been observed as far north as Ogdensburg, and as far east as "Big Nose" on the Mohawk River in Montgomery County. Most of the intrusions are thin (<30 cm wide) tabular dikes, with vertical dips and N-S strikes (± 10^{o}) (Bailey and Lupulescu, 2007b; Foster, 1970) . The widest dike is the one exposed in Williams Brook (~3.5 m) which will be our second stop on this trip. In addition to the numerous dikes, there are two fairly large and irregular intrusions that appear to be small diatremes: one in the Ithaca region (Poyer Orchard diatreme with a maximum dimension ~ 50 m)(Foster, 1970), and one in the Syracuse region (the Dewitt Reservoir diatreme with a maximum dimension of ~75 m)(Darton and Kemp, 1895b).

Each of the intrusions is, in some way, mineralogically and/or chemically distinct. Nevertheless, four broad groups of intrusions (designated Groups A, B, C & D) have been recognized, each with shared chemical and mineralogical features (Table 1; Figures 2 and 3) (Bailey and Lupulescu, 2015).

Kimberlites belonging to Groups A and B are only found in the Ithaca region. Group A dikes are only exposed along the western margin of Cayuga Lake and, in fact, very likely represent a single intrusion that crops out intermittently in en echelon segments along strike. These dikes tend to be quite wide (1-4 m), serpentine-rich, very dark green to black in color, and relatively resistant to weathering. They also are TiO_2-rich and contain abundant perovskite. Our second stop today will be to examine one the most easily accessed Group A dikes – the Williams Brook dike.

Group B dikes are the most abundant, and the most compositionally diverse. These dikes tend to be very narrow, typically < 10 cm, although dikes up to 1.5 m do occur. They also tend to be very carbonate-rich, pale tan-green in color, and highly weathered. Two of our stops today (at Six Mile Creek and Taughannock Creek) will be to examine Group B dikes.

Group C kimberlites are only found in the Syracuse Region, and appear to represent a distinct style and episode of igneous activity in central New York. The only intrusion that is still readily accessible are fragments of the Dewitt diatreme exposed along the flanks of the small water Reservoir on the LeMoyne College campus (Bailey and Lupulescu, 2012). These intrusions tend to be very dark colored, contain abundant olivine macrocrysts (usually serpentinized), and common garnet and clinopyroxene macrocrysts.

Group D kimberlites are represented by two, ~ 25 cm wide dikes exposed along the banks of East Canada Creek on the Herkimer – Montgomery County line. (NB: A third, ~ 2 m wide dike described by Smyth (1896) could not be relocated). These dikes are characterized by being extremely carbonate-rich and serpentine-poor, with large (up to 2 cm long) phlogopite macrocrysts. They are extremely TiO_2-rich, and as a result, contain abundant perovskite and secondary titanate minerals in the matrix.

Table 1. Whole-rock chemistry of Taughannock Creek (TC), Williams Brook (WB), and Six Mile Creek (SMC) kimberlite dikes (from Bailey & Lupulescu, 2015).

Dike	**TC**	**TC**	**TC**	**TC**	**TC**	**TC**	**TC**	**WB**	**WB**	**WB**	**SMC**	**SMC**
Sample	T1	T1b	T2	T5c	T6	T7a	TC-3	W1	W2	W2r	SMC-1	SMC-2A
	Major Element Oxides (XRF wt.%)											
SiO_2	27.34	24.53	19.77	29.32	17.27	15.42	28.45	35.63	32.05	32.65	7.90	23.59
TiO_2	1.53	1.85	1.50	1.63	1.60	1.33	1.61	2.73	2.42	2.41	1.58	1.25
Al_2O_3	2.89	3.50	2.80	3.41	3.38	3.16	3.94	4.16	3.09	3.17	3.01	2.86
FeO*	8.42	6.95	6.33	8.18	5.40	4.83	6.89	10.51	9.14	9.28	3.61	6.91
MnO	0.21	0.22	0.37	0.22	0.53	0.73	0.35	0.20	0.17	0.17	0.64	0.22
MgO	17.81	14.71	16.94	19.24	13.32	11.43	13.03	27.54	26.38	26.48	6.49	15.72
CaO	15.29	21.12	20.09	13.81	25.38	28.51	19.83	6.55	9.81	10.00	37.37	20.28
Na_2O	0.16	0.21	0.17	0.21	0.21	0.19	0.14	0.06	0.11	0.09	0.09	0.21
K_2O	1.37	1.49	1.31	1.70	1.57	1.28	1.37	2.40	1.94	2.00	0.89	1.63
P_2O_5	1.13	1.41	1.06	1.20	1.08	0.99	1.14	0.65	0.41	0.40	0.62	0.91
Maj.	76.50	75.98	70.67	79.49	70.04	67.86	76.74	90.44	85.51	86.65	62.21	73.57
Tr. Ox.	0.87	1.19	0.86	1.84	0.95	0.85	2.95	0.93	0.75	0.68	0.78	0.77
LOI	21.28	20.78	27.39	17.19	27.79	30.17	19.43	9.43	12.73	12.85	35.15	24.39
TOTAL	98.65	97.95	98.92	98.52	98.79	98.88	99.12	100.80	98.99	100.18	98.14	98.73
	Trace Elements (XRF ppm)											
Ni	988	913	940	945	978	672	904	1004	1013	998	790	801
Cr	1388	1627	1437	1448	1518	1215	1625	1788	1875	1769	1078	1247
Sc	24	26	20	22	23	19	19	24	17	16	15	17
V	262	313	235	313	322	293	301	320	227	215	225	238
Ba	1436	2564	1152	3333	1529	1505	20949	2198	840	860	3656	2646
Rb	50	55	51	63	58	48	58	129	80	83	41	69
Sr	1473	2153	1815	7821	1772	1783	4577	528	511	509	1062	1561
Zr	287	343	273	282	282	238	238	298	142	139	175	210
Y	22	26	25	24	27	30	22	14	11	10	28	17
Nb	183	216	172	181	173	141	178	137	110	114	146	189
Ga	9	10	8	10	8	7	9	13	8	10	6	7
Cu	68	91	63	81	72	66	74	87	63	65	57	55
Zn	74	77	61	78	83	32	85	79	66	73	59	81
Pb	10	13	17	13	15	22	10	6	8	4	17	13
La	160	222	141	144	187	117	129	84	81	84	123	164
Ce	292	428	265	280	341	222	235	151	152	153	226	266
Th	21	29	21	15	21	21	19	14	13	12	18	24
Nd	112	161	97	105	125	87	84	58	59	55	83	92
	Trace Elements (ICP-MS ppm)											
La	162.28	229.96	145.74	157.98	184.45	119.75	142.01	84.41	84.53	80.95	125.05	163.59
Ce	298.48	443.34	269.89	286.77	348.05	228.35	237.69	152.69	156.04	148.37	226.46	274.52
Pr	32.66	48.67	29.50	31.15	38.04	25.22	24.22	16.58	16.85	16.14	24.51	28.32
Nd	114.85	171.07	104.76	110.74	135.18	89.40	82.80	57.11	58.62	56.16	84.89	94.95
Sm	17.12	23.86	16.32	17.12	19.76	15.17	12.65	8.56	8.45	8.25	15.11	13.70
Eu	4.28	5.35	4.35	4.78	4.99	4.16	3.31	2.37	2.31	2.24	4.07	3.63
Gd	11.22	14.02	11.57	11.57	12.85	12.14	9.00	5.88	5.49	5.42	12.97	8.48
Tb	1.30	1.54	1.36	1.38	1.44	1.44	1.15	0.71	0.62	0.61	1.47	1.05
Dy	5.85	6.81	6.30	6.38	6.46	6.71	5.55	3.45	2.82	2.75	6.44	4.85
Ho	0.89	1.05	0.99	0.97	1.02	1.12	0.94	0.55	0.42	0.41	1.04	0.73
Er	1.86	2.17	2.09	2.04	2.14	2.55	2.12	1.24	0.85	0.83	2.32	1.55
Tm	0.22	0.26	0.24	0.24	0.26	0.31	0.27	0.14	0.10	0.10	0.29	0.18
Yb	1.14	1.33	1.24	1.24	1.28	1.79	1.49	0.77	0.52	0.50	1.57	0.98
Lu	0.16	0.19	0.17	0.17	0.18	0.26	0.21	0.11	0.07	0.07	0.23	0.13
Ba	1458	2566	1141	3367	1517	1488	20504	2231	853	834	3724	2663
Th	20.7	24.3	19.3	19.5	18.5	15.0	15.9	11.9	12.3	11.0	18.1	23.8
Nb	189.6	227.3	176.8	189.5	177.3	145.2	185.5	141.5	115.0	110.5	149.5	191.3
Y	22.0	25.6	25.4	24.0	26.6	30.0	24.7	14.1	10.1	9.8	28.2	17.9
Hf	6.3	7.7	6.0	6.5	6.2	5.2	4.9	7.3	3.5	3.4	4.2	4.7
Ta	9.6	11.7	9.4	9.6	9.1	7.5	8.1	7.7	7.9	8.4	6.4	7.0
U	4.5	5.3	4.1	4.5	4.5	3.9	4.4	3.3	2.2	2.1	4.1	5.7
Pb	10.8	14.5	13.7	12.3	11.1	11.4	13.7	7.0	5.7	4.4	16.9	13.6
Rb	49.0	54.9	49.0	63.7	56.1	45.4	52.5	125.0	76.8	76.1	40.3	66.3
Cs	2.6	1.9	2.1	1.9	1.4	1.1	3.5	2.7	2.7	2.5	1.0	4.6
Sr	1496	2186	1819	7583	1775	1793	4227	557	509	487	1075	1553
Sc	21.9	26.7	20.8	22.5	22.5	18.2	18.0	23.4	16.6	16.3	15.5	17.2
Zr	279	335	263	282	268	224	237	281	132	135	178	209

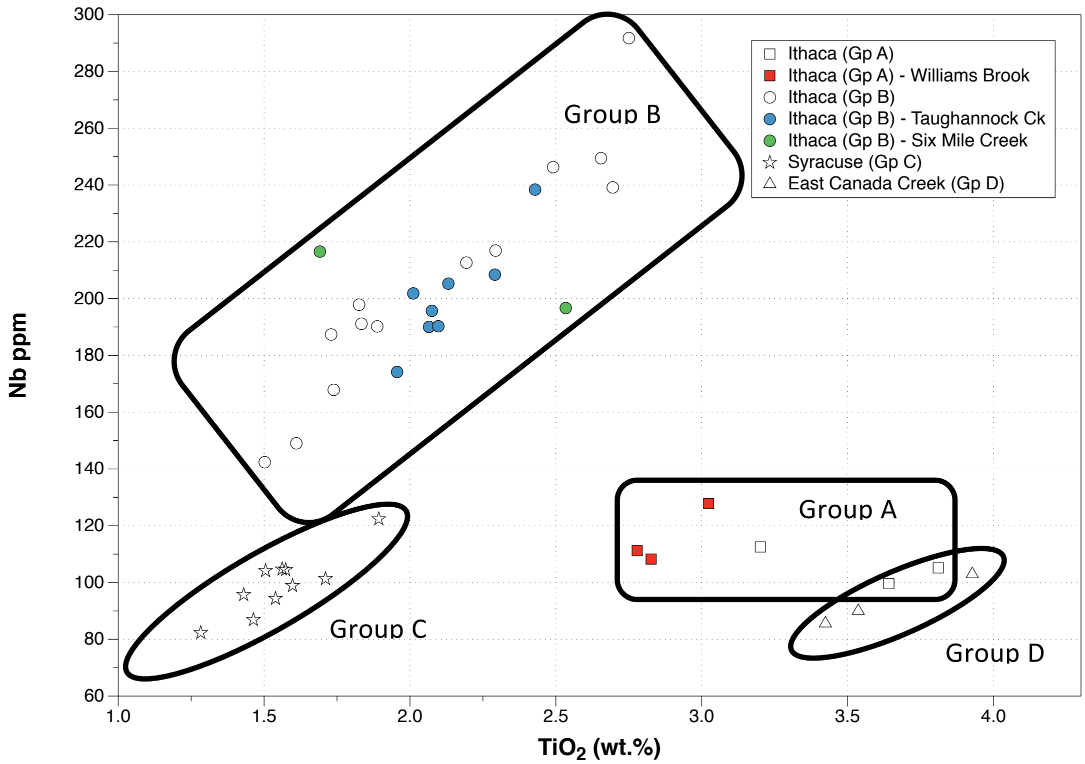

Figure 2. Nb versus TiO_2 scatter plot of New York State kimberlite whole-rock compositions showing the four major groups of intrusions.

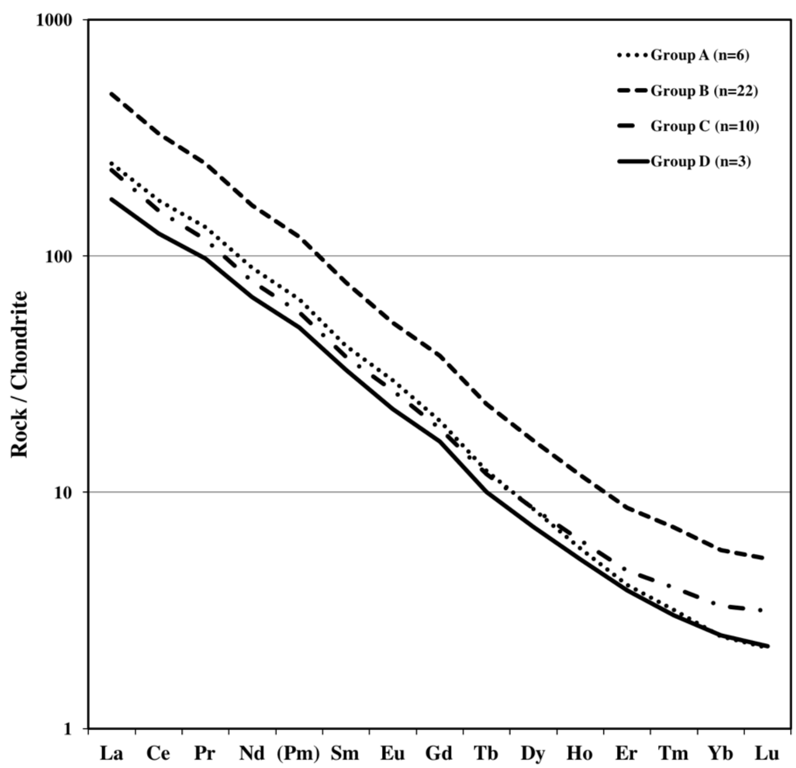

Figure 3. Average chondrite-normalized REE profile of the four groups of kimberlite intrusions in New York State (Bailey and Lupulescu, 2015).

Age and Origin

Despite many attempts, accurate emplacement ages for the kimberlites of New York have been difficult to obtain; published ages range from 500 to 110 Ma (Basu et al., 1984; Watson, 1979; Zartman, 1988; Zartman et al., 1967). Since nearly all of the kimberlites intrude Upper Devonian sedimentary units, reported ages > 400 Ma are clearly inaccurate. These ages, many of which are K-Ar ages on phlogopite macrocrysts of xenocrystic origin, do not record intrusion ages. The most accurate emplacement ages are high precision U-Pb dates of 144.8 ± 3.2, 146.7 ± 2.4, and 147.5 ± 3.0 obtained on groundmass perovskite grains from two dikes on the western margin of Cayuga Lake (Heaman and Kjarsgaard, 2000). Unfortunately, all three samples were collected from two dikes, both belonging to compositional Group A, and very likely, are part of a single intrusion. As a result, emplacement ages for most of the kimberlitic intrusions in New York State are still not well constrained. Compilation of published ages suggests that there may have been two distinct magmatic episodes: the earliest ~146 Ma (Group A and Group D intrusions), followed by emplacement of the largest number of intrusions ~125 Ma (Group B and Group C intrusions) (Bailey and Lupulescu, 2015).

We recently found and extracted a number of zircon grains from two of the intrusions we will be visiting today: The Six Mile Creek and Taughannock Creek dikes. The zircons almost certainly are derived from disaggregated xenoliths; none have been observed as discrete matrix grains in thin section. Approximately one kilogram of rock was collected from each dike, and zircons ranging in size from 25-150 microns were separated by standard techniques at the Arizona LaserChron Center at the University of Arizona. The separated zircons were imaged by scanning electron microscope including both back scattered electron (BSE) and cathodoluminscence (CL) modes, and multiple spots were selected for analyses. Interestingly, the two dikes contain very different zircon populations (Figure 4), indicating that each encountered and sampled very different lithologies on their way to the surface. Not surprisingly, most of the zircon grains found in the Six Mile Creek dike are either Mesoproterozoic (1050 to 1200 Ma) or Early Paleozoic (400-500 Ma) in age, most likely derived from the presumed Grenville age lower crust and the overlying Paleozoic platform rocks. The Proterozoic zircons are very likely inherited detrital grains also derived from the Paleozoic sedimentary sequence.

The Taughannock Creek dike, in contrast, contains a much larger population of zircons, but with a narrower range of ages, with nearly all being Neoproterozoic (550 to 1000 Ma). These are uncommon ages for basement rocks exposed to the north in the Adirondack Mountains, suggesting the possibility of previously unrecognized crustal terrane being present beneath western New York State, or having supplied detrital zircons to the overlying Paleozoic sedimentary sequence. We hope to follow up on this preliminary study with a more comprehensive survey of the zircon and perovskite populations present in New York State kimberlites, including the Hf isotopic compositions of the different zircon populations.

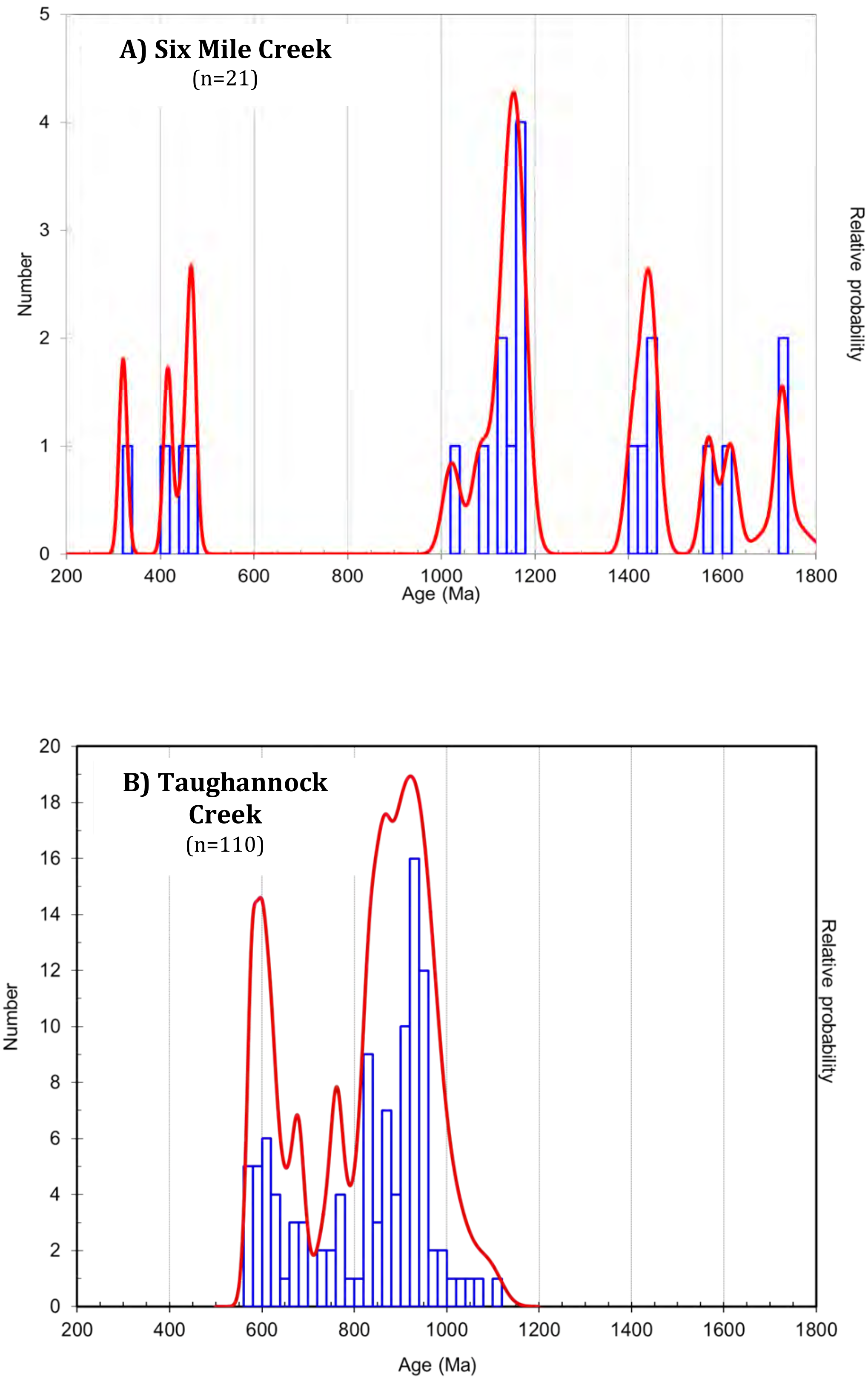

Figure 4. U-Pb ages obtained on zircons extracted from the A) Six Mile Creek, and B) Taughannock Creek kimberlite dikes. Individual analyses shown as stacked blue bars; relative age probabilities shown as red curve.

Currently, there are two theories that have been put forth to explain the origin of the kimberlitic rocks in New York State (Figure 5): 1) they are part of a chain of small, alkaline intrusions in eastern North America related to passage of the North American plate over the Great Meteor hot spot (Heaman and Kjarsgaard, 2000); or 2) they are part of a belt of kimberlitic intrusions along the western flanks of the Appalachian Mountains that were intruded along old structures that were reactivated by crustal extension related to rifting and opening of the Atlantic Basin (Parrish and Lavin, 1982). Bailey and Lupulescu (2015) concluded that the New York kimberlites have macrocryst assemblages and geochemical and isotopic characteristics consistent with derivation from a relatively shallow, asthenospheric, garnet lherzolite source. Consistent with the model of Parrish & Lavin (1982), they argued that far field stresses related to the opening of the Atlantic Ocean reactivated major crustal structures and provided pathways for small volume, volatile-rich magmas to ascend and intrude the Paleozoic sedimentary platform rocks of central New York.

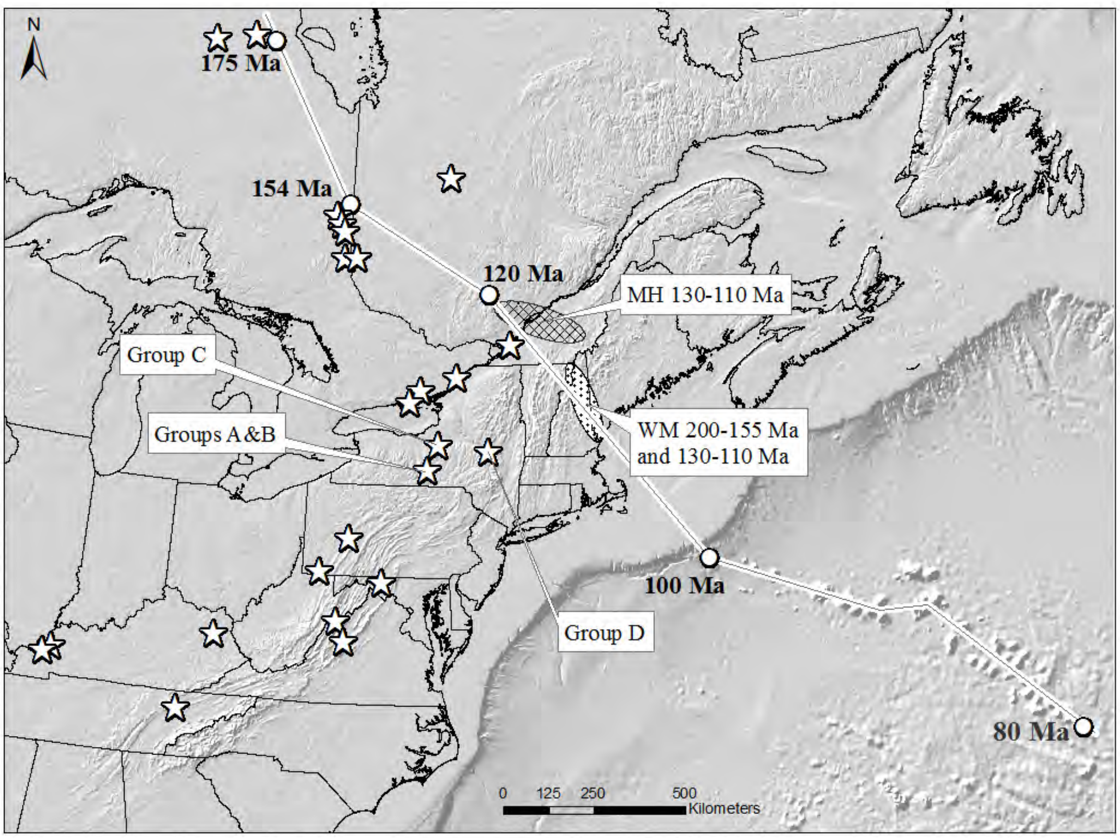

Figure 5. Map of eastern North America showing locations of kimberlitic intrusions (white stars), the path and ages of magmatism associated with the Great Meteor Hot Spot (white line and circles), and the locations of the four major groups of intrusions in central New York State (Groups A through D). MH = Monteregian Hills; WM = White Mountains.

FIELD GUIDE

Meeting Point: Wegman's Supermarket Parking Lot, southwest corner, 500 S Meadow St, Ithaca, NY

Meeting Point Coordinates: 42.43394, -76.51109

Meeting Time: 9 AM, Saturday, October 7, 2017

General Information:

All three stops will be in creeks surrounding Cayuga Lake where erosion has exposed these small intrusions. Public access is allowed in all three locations for fishing or hiking, but please respect the private property adjacent to all three sites.

Please do not collect samples of the Six Mile Creek or Taughannock Creek dikes!! The Six Mile Creek dike that we will visit is undoubtedly the best exposure of any of the New York State kimberlites. It is a beautiful exposure of a geologically and historically important rock; the outcrop should be preserved and not subjected to unnecessary sampling. The Williams Brook dike is much larger, and loose blocks can often be found in the streambed; sampling of this material for research or educational use is encouraged.

STOP #1: Six Mile Creek

Parking Location and Coordinates: Parking lot for Mulholland Wildflower Preserve, south off of Giles Street, on east side of Six Mile Creek. (42.43266, -76.48417)

Follow the nature trail on the east side of Six Mile Creek for ~600 m (~ 1/3 mile); two dikes will be exposed and clearly visible in the streambed. The largest is ~ 20 cm-wide, and stands out prominently from the surrounding shales. The second is a cluster of small, anastomosing dikelets ranging from 1 to 8 cm in width. These are two of the seven dikes that have been observed in a 4 km long stretch of the Six Mile Creek drainage southeast of Ithaca (Figure 6).

History of the Six Mile Creek (SMC) dikes

The earliest known mention of intrusive dikes along Six Mile Creek was by Cornell Professor of Geology Orville Derby in the student newspaper where he stated that the best dike for students of geology to study was one exposed in Six Mile Creek (Derby, 1874 in Kemp, 1891). Simonds (1877) noted that many of the dikes in Six Mile Creek "thin out before reaching the surface" (p.51), and Kemp (1891) was the first to prepare and describe thin sections of the dikes which he noted proved the dikes to be "eruptive rock in advanced decomposition"(p.411). Subsequent studies identified a total of seven distinct dikes, the largest being the 20 cm-wide dike we will visit on this trip (Figure 7) (Filmer, 1939; Martens, 1924; Matson, 1905; Williams et al., 1909). In addition to these dikes, one small diatreme was also identified and described as a 2.5 m by 3 m ellipsoidal mass that had been partly excavated and "washed" by earlier gem hunters (Filmer, 1939).

Other than a single petrographic report provided by Foster (1970), no modern analytical work had been done on any of the Six Mile Creek kimberlites prior to a study in 2015 by Hamilton College student Deanna Nappi. Nappi (2015) collected samples from three of the SMC dikes and presented detailed petrographic descriptions, mineral chemistry, and whole-rock analyses in her undergraduate thesis. Much of the information presented below is a summary of the results of her research.

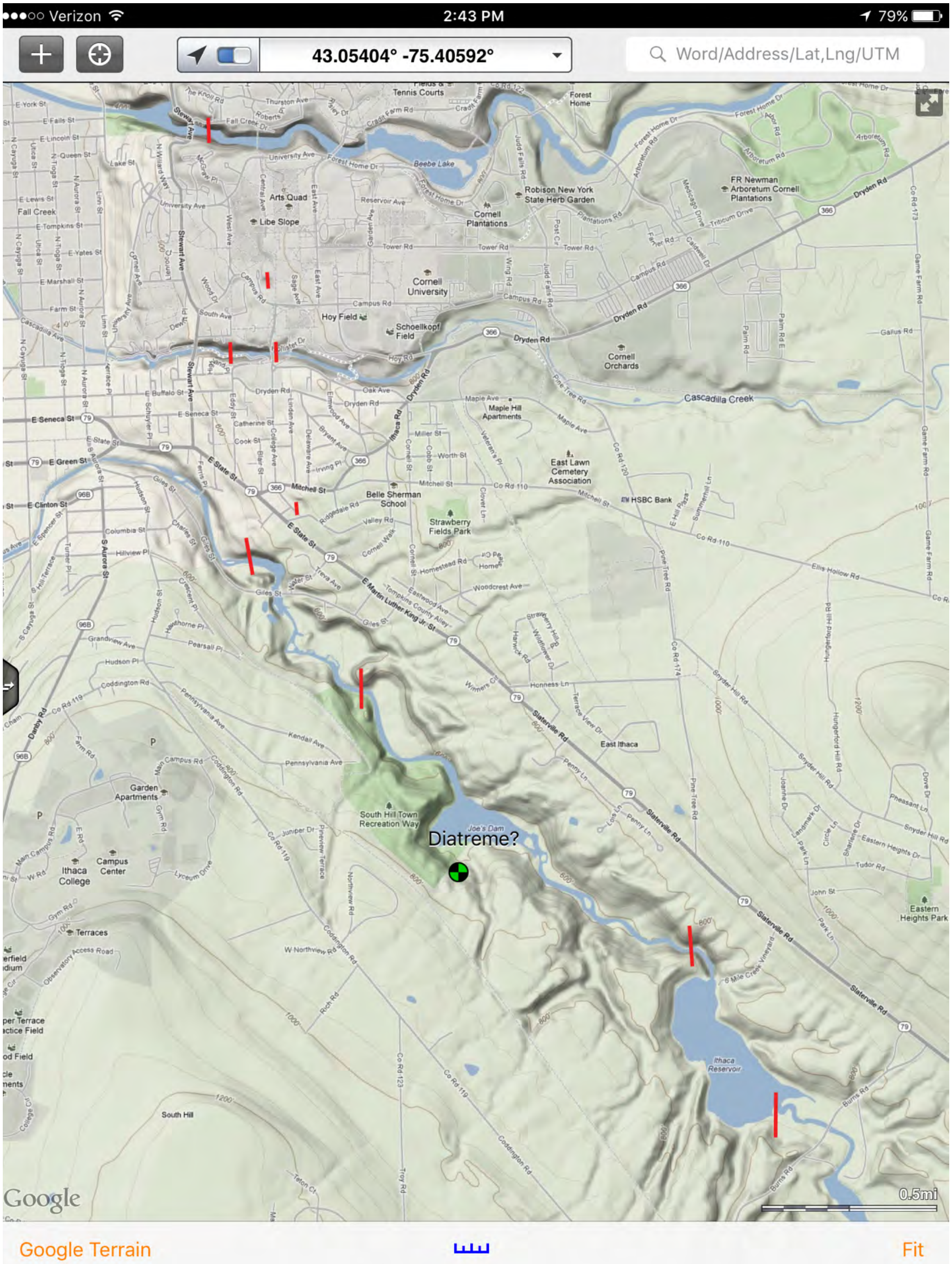

Figure 6. Shaded relief map of the Six Mile Creek drainage southeast of Ithaca, NY showing reported locations of kimberlite dikes (red lines), and one possible diatreme (green and black circle). Locations compiled (and approximated) from information in Williams et al. (1909), Martens (1924), Filmer (1939), and Foster (1970).

Figure 7. Kimberlite dike exposed at Stop #1 along Six Mile Creek. Dike is ~ 20 cm wide, and intrudes along the prominent N-S oriented fracture set in the surrounding shales.

Petrography of Six Mile Creek Kimberlites

Three Six Mile Creek dikes were sampled and 22 thin sections were made and examined using a polarized light microscope and a scanning electron microscope with an energy dispersive x-ray fluorescence spectrometer. Like all of the central New York kimberlites, the Six Mile Creek dikes are petrographically complex, with textures and phase assemblages varying from sample to sample. Overall, the SMC dikes are characterized by abundant macrocrysts of phlogopite and olivine (almost always serpentinized) in a carbonate-rich matrix, typical of the Group B kimberlites found throughout the Ithaca region (Table 2). Other observed macrocrysts include clinopyroxene (Figure 8), garnet, spinel, and orthopyroxene. While some of these macrocryst phases may actually be phenocrysts, most are clearly the remnants of disaggregated xenoliths, and most of the phases are not in equilibrium with the host magma, as evidenced by the rounded and embayed nature of most grains, and distinct reaction rims on others.

Olivine is the most abundant macrocryst in the SMC dikes, but virtually all of the grains have been replaced by a mixture of serpentine, calcite, and magnetite (Figure 8). All of the pseudomorphs are rounded and exhibit irregular morphologies; the largest grains have diameters ~ 4 mm. A few unaltered olivine grains were observed in the chilled portion of the small dike exposed at location 1; these grains have compositions ranging from $Fo_{90\text{ to }92.5}$ (Nappi, 2015).

Phlogopite is the second most abundant macrocryst phase in the SMC dikes; most grains are tabular and often flow-aligned, and individual grains can reach 5 mm in length. Larger grains tend to be rounded, and many are partly altered to serpentine and/or calcite along cleavage planes. In thin section the grains range from nearly colorless to strongly pleochroic yellow-orange in PPL, and compositionally, all are Fe-bearing phlogopites with 5-8 wt.% FeO and 1-3 wt.% TiO_2.

While scarce, garnet grains are also found as individual macrocrysts and as grains in xenoliths (Figure 9). Similar to other Group B intrusions, the garnets in the SMC dikes belong to two major compositional groups, one a Cr-bearing pyrope, the other an almandine-rich garnet (Figure 10). While the Cr-bearing pyropes are clearly of mantle origin, no garnets from any of the New York State kimberlites are "G10" garnets with compositions indicative of having come from a high diamond potential mantle source (Bailey and Lupulescu, 2015; Grutter et al., 2004).

Clinopyroxene grains are also common as discrete macrocrysts and as part of larger xenoliths (Figures 8 and 9). Most of the macrocrysts are rounded and distinctly zoned with a colorless core surrounded by a pale yellow-green rim. All are diopsides; the rims are distinctly more FeO and TiO_2-rich than the cores (up to 6 and 1.5 wt. %, respectively). In the xenoliths, the clinopyroxenes are pale green and contain up to 1 wt. % Cr_2O_3 (Nappi, 2015).

Orthopyroxene is also common as both macrocrysts and as grains within xenoliths, both with compositions ~ En_{90}. Most of the orthopyroxene grains contain thin clinopyroxene exsolution lamellae. While orthopyroxene has been reported in other New York State kimberlites (Darton and Kemp, 1895b; Jackson, 1982), we have not positively identified distinct orthopyroxene macrocrysts in any intrusion other than the dikes at Six Mile Creek.

Spinels are also common as individual anhedral, embayed macrocrysts, and as inclusions in xenoliths. Typical of kimberlitic rocks in general, a wide range of spinel compositions can be found in a single intrusion (Figure 11) (Barnes and Roeder, 2001; Roeder and Schulze, 2008). In thin section, spinel macrocrysts in the Six Mile Creek dikes range in color from opaque, to brown, to red-brown, and even to green. While individual grains are chemically homogeneous, the diversity of spinel compositions indicates that most are xenocrysts derived from a variety of disaggregated xenoliths.

The matrix of the Six Mile Creek kimberlites is very fine-grained and composed predominantly of phlogopite and carbonate (both dolomite and calcite), along with small (<50 um) grains of perovskite, chromite, apatite, ilmenite, and minor rutile.

The xenoliths found in the Six Mile Creek dikes vary from garnet pyroxenites to plagioclase and spinel bearing lherzolites, to calcareous shales, indicating that the kimberlitic magma sampled material from various depths in the mantle and crust during emplacement.

	SMC	TC	WB
Macrocrysts			
Olivine	**A**	**A**	**A**
Phlogopite	**A**	**A**	**P**
Garnet	**C**	**C**	
Clinopyroxene	**C**	**C**	**P***
Orthopyroxene	**P**		**P***
Spinel	**C**	**C**	
Chromite	**C**	**C**	
Matrix Phases			
Serpentine	**A**	**C**	**A**
Calcite	**C**	**A**	**C**
Dolomite	**C**		
Phlogopite	**A**	**C**	**A**
Clinopyroxene	**P**		**P**
Unidentified Ca-Fe Silicate			**P**
Perovskite	**P**	**P**	**C**
Ilmenite	**P**		**P**
Rutile	**P**		
Magnetite / Chromite	**C**	**C**	**C**
Apatite	**P**	**P**	**C**
Fe Sulfides and /or Fe-Ni Sulfides	**P**	**P**	
Barite / Celestine		**P**	

Table 2. Mineral phases observed in the Six Mile Creek (SMC), Taughannock Creek (TC), and Williams Brook (WB) kimberlite dikes. A = Abundant (>10%); C = Common (1-10%); P = Present (<1%); Blank = not observed; (*) = only in xenoliths.

Figure 8. Clinopyroxene, phlogopite, and serpentinized olivine macrocrysts in the Six Mile Creek kimberlite (sample SMC-2A, PPL).

Figure 9. Garnet pyroxenite xenolith in Six Mile Creek dike. Xenolith is composed of pyrope garnet (colorless), clinopyroxene (pale green), chromite (black), and amphibole (pale brown) (sample SMC-2A, PPL).

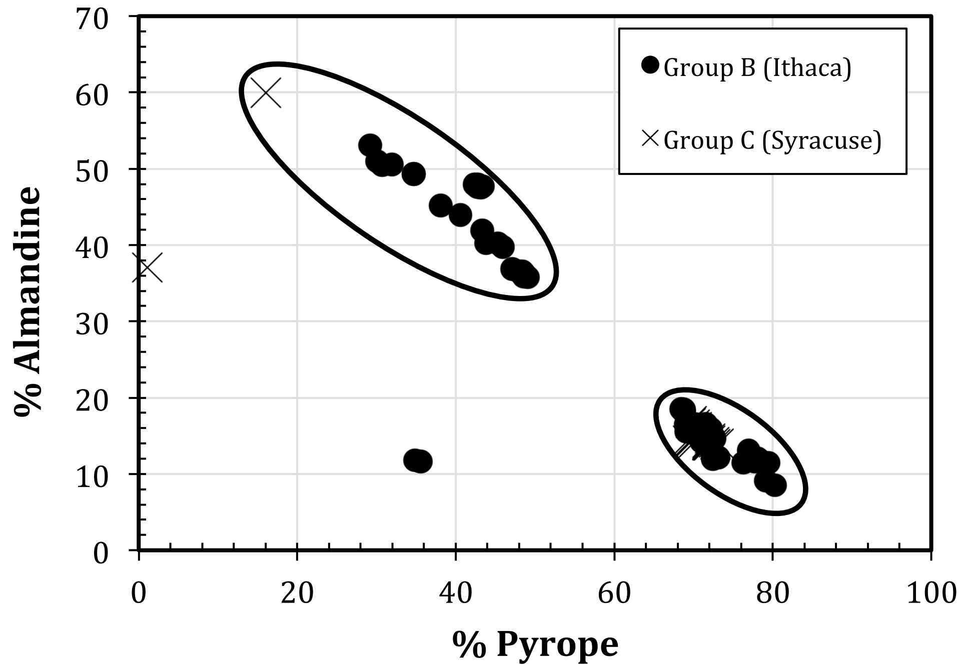

Figure 10. Garnet macrocryst compositions in New York State kimberlites.

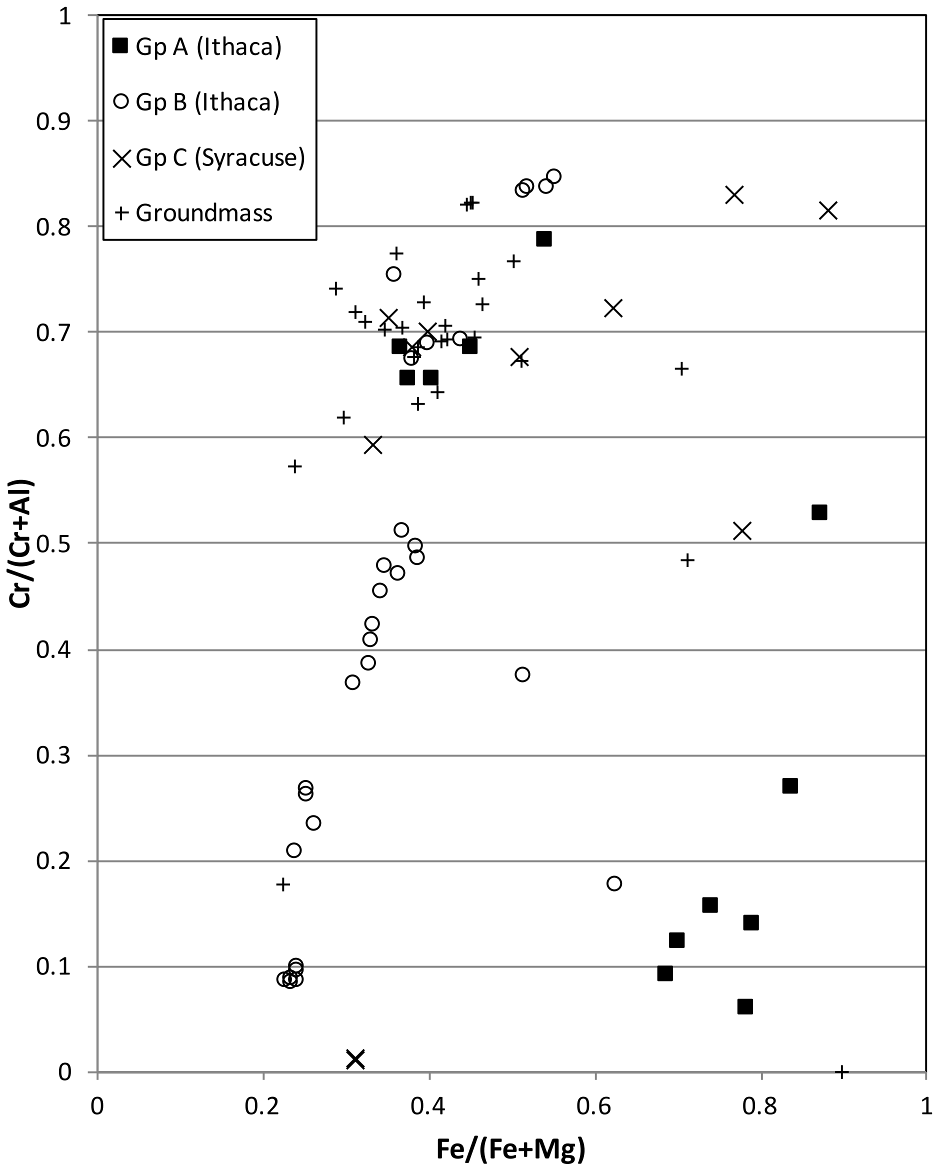

Figure 11. Molar Cr/(Cr+Al) vs. Fe/(Fe+Mg) ratios in spinel grains in New York State kimberlites.

STOP #2: Williams Brook

Parking Location and Coordinates: Small gravel turn out on west side of NY Route 96 just after turn for Hopkins Place (42.45706, -76.52462).

Just to the north of the turn out, Route 96 crosses over a small creek. Enter the creek on the west side of the road, and hike upstream for ~ 60 m. The Williams Brook kimberlite is a dark green-black dike approximately 3.5 m wide; it is best exposed on the northern bank of the creek.

History of the Williams Brook Dike

Despite being one of the largest dikes in the region, the Williams Brook dike wasn't recognized until the late 1930s, probably being first exposed by the extreme flooding that occurred in the region in July 1935 (Johnson, 1936). Filmer (1939) was the first to record the location and size of the dike; no other studies were done on the dike until a paleomagnetic study was done by a Cornell undergraduate in 1970 (DeJournett, 1970). The results of DeJournett's work indicated that the Williams Brook dike exhibited normal magnetic polarization with a pole position "reasonably consistent" with a Lower Cretaceous age of emplacement (DeJournett and Schmidt, 1975). Subsequent paleomagnetic studies of the Williams Brook and other kimberlites in the Ithaca region, however, indicated a Lower Cretaceous pole position that was not consistent with currently accepted Upper Jurassic to Lower Cretaceous pole positions for North America (Van Fossen and Kent, 1991, 1993). The interpretation of the magnetic characteristics of kimberlitic rocks is complicated by the fact that the duration of magnetization acquisition is protracted, probably occurring during serpentization following emplacement.

Basu et. al (1984) were the first to try to date the Williams Brook dike; they obtained a whole-rock K-Ar age of 139 ± 7 Ma. Because of uncertainties in how xenocrystic phlogopite and post-emplacement serpentinization impact K-Ar systematics, recent U-Pb dates obtained on groundmass perovskite grains are thought to more accurately record emplacement ages. Heaman & Kjarsgaard (2000) dated two multi-grain perovskite samples from the Williams Brook dike and obtained ages of 144.8 ± 3.2 and 146.7 ± 2.4 Ma, with a weighted average emplacement age of 146.0 ± 1.9 Ma.

Kay and Foster (1986) noted that the Williams Brook dike was petrographically distinct from most of the other dikes in the Ithaca region, containing significantly more serpentine and phlogopite, and less calcite, and lacking distinct macrocrysts of garnet, spinel, or pyroxene. These features are, in fact, shared by all of the "Group A" kimberlites, along with the presence of abundant perovskite in the matrix. The only chemical data reported for the Williams Brook dike noted its high incompatible element concentrations, and steep REE profile (Kay, 1990).

Petrography of the Williams Brook dike

The Williams Brook dike, and all Group A intrusions, are dense, dark-colored, rocks that are relatively resistant to weathering and erosion. The Williams Brook dike is fine-grained and relatively homogenous across its width; the only distinct crystalline phase visible in hand sample is phlogopite. Small (< 1cm wide) calcite-filled veins are common near the margins of the dike, probably representing cooling joints that were filled by carbonate derived from the surrounding sedimentary rocks.

In thin section, the dike is characterized by large olivine macrocrysts (up to 4 mm in diameter) that are partly to completely replaced by serpentine and magnetite (Figure 12). Electron microprobe analysis of the olivine revealed that they are relatively uniform in composition (~$Fo_{90.5}$).

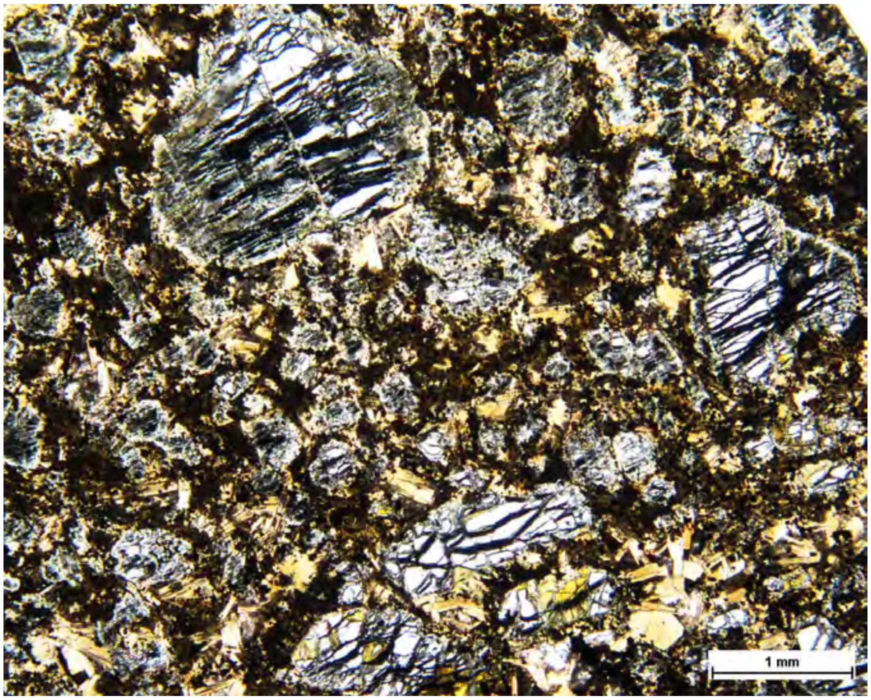

Figure 12. Photomicrograph of Williams Brook dike showing large olivine macrocrysts replaced by serpentine and magnetite (top left, right center) in a matrix of phlogopite, serpentine, calcite, magnetite, and perovskite (Sample W2; PPL).

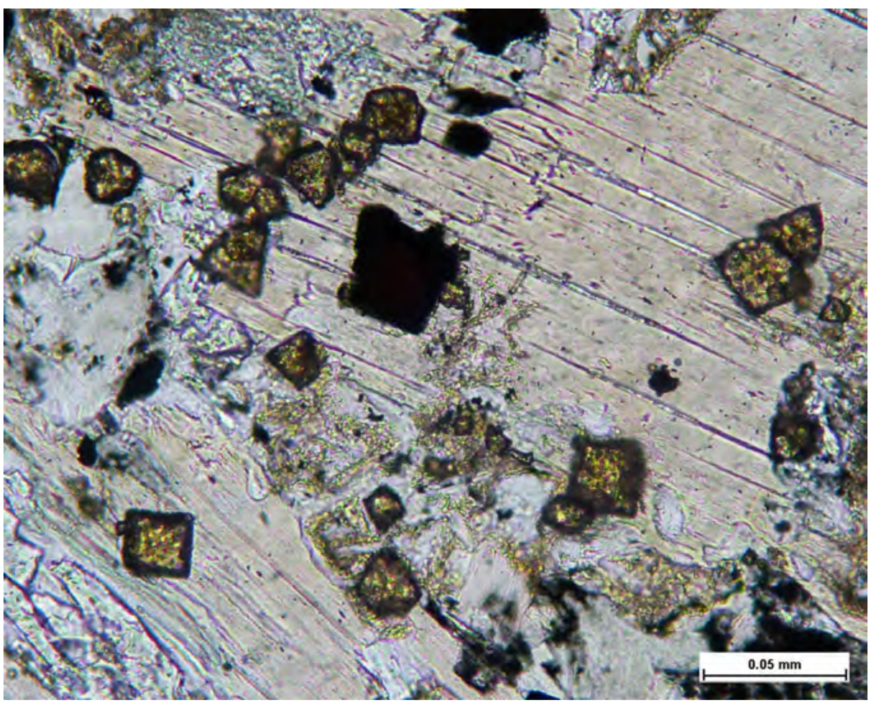

Figure 13. Photomicrograph of the matrix of the Williams Brook dike showing tabular phlogopite (pale orange), calcite (colorless, high relief), serpentine (pale green), perovskite (yellow-brown, high relief), and magnetite (opaque) (Sample W2; PPL).

Petrography of the Williams Brook dike (cont.)

While the Williams Brook dike contains abundant phlogopite in the groundmass, distinct phlogopite macrocrysts are not common. Electron microprobe and SEM/EDS analyses of the phlogopite grains reveal that they are compositionally similar to phlogopites found in the both the Group A and Group B kimberlites, with average FeO and TiO_2 concentrations of ~ 7 and 2.5 wt. %, respectively. Small amounts of barium are also present, particularly in the groundmass grains.

No other macrocryst phases were observed, and only one distinct xenolith was found. The xenolith had a maximum dimension of ~ 2 cm, and consisted of a coarse-grained aggregate of partly serpentized olivine with a few grains of bright green, Cr-bearing diopside, and pale tan enstatite (Figure 14).

The groundmass contains abundant phlogopite, and considerably less carbonate relative to Group B intrusions. The most distinguishing feature of the Williams Brook dike and related Group A intrusions exposed along the western margin of Cayuga Lake are the abundant, unaltered, relatively large (up to 75 μm diameter), euhedral perovskite grains in the groundmass (Figure 13). The abundant perovskite reflects the high TiO_2 concentrations in these intrusions (2.75 to 4.0 wt. %), and is what allowed them to be accurately dated (Heaman and Kjarsgaard, 2000). The only other New York kimberlites with high TiO_2 concentrations are the two dikes exposed along East Canada Creek (Group D intrusions). Unfortunately, the groundmass perovskite grains in these dikes have been largely replaced by rutile and a mixture of unidentified oxides and titanates.

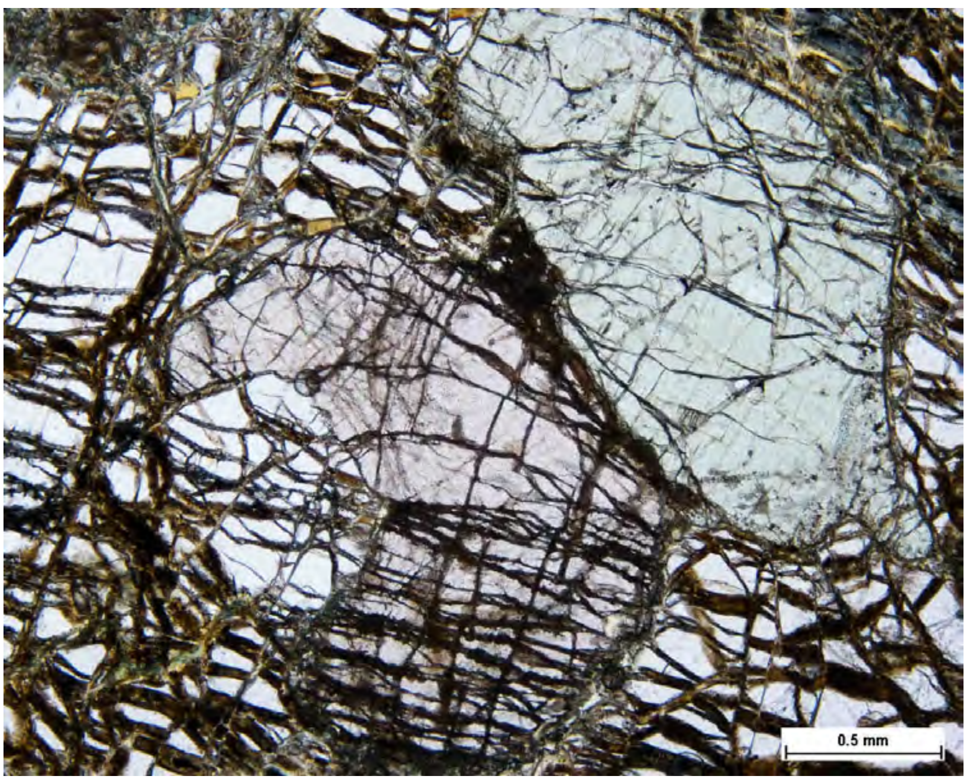

Figure 14. Photomicrograph of peridotite xenolith in Williams Brook dike. Pale green diopside (upper right), pale tan enstatite (bottom center), and olivine (colorless, with abundant serpentine along fractures). (Sample WB Inc; PPL).

STOP #3: Taughannock Creek

Parking Location and Coordinates: Small gravel turn out on south side of Taughannock Park Rd. (County Rd. 148A) (42.53054, -76.62116).

Take the short fishing access path to the nicely exposed rocks on the banks of Taughannock Creek. A total of 15 individual dikes, in five clusters, have been reported from a 1.5 km long section of Taughannock Creek (Figure 15) (Foster, 1970; Martens, 1924; Matson, 1905). Due to erosion and revegetation along the banks of the creek, few of these dikes are currently exposed. We will try to find two of the westernmost dikes in Taughannock Creek. NOTE: All of the dikes are within the confines of Taughannock Creek State Park, and sample collecting is prohibited.

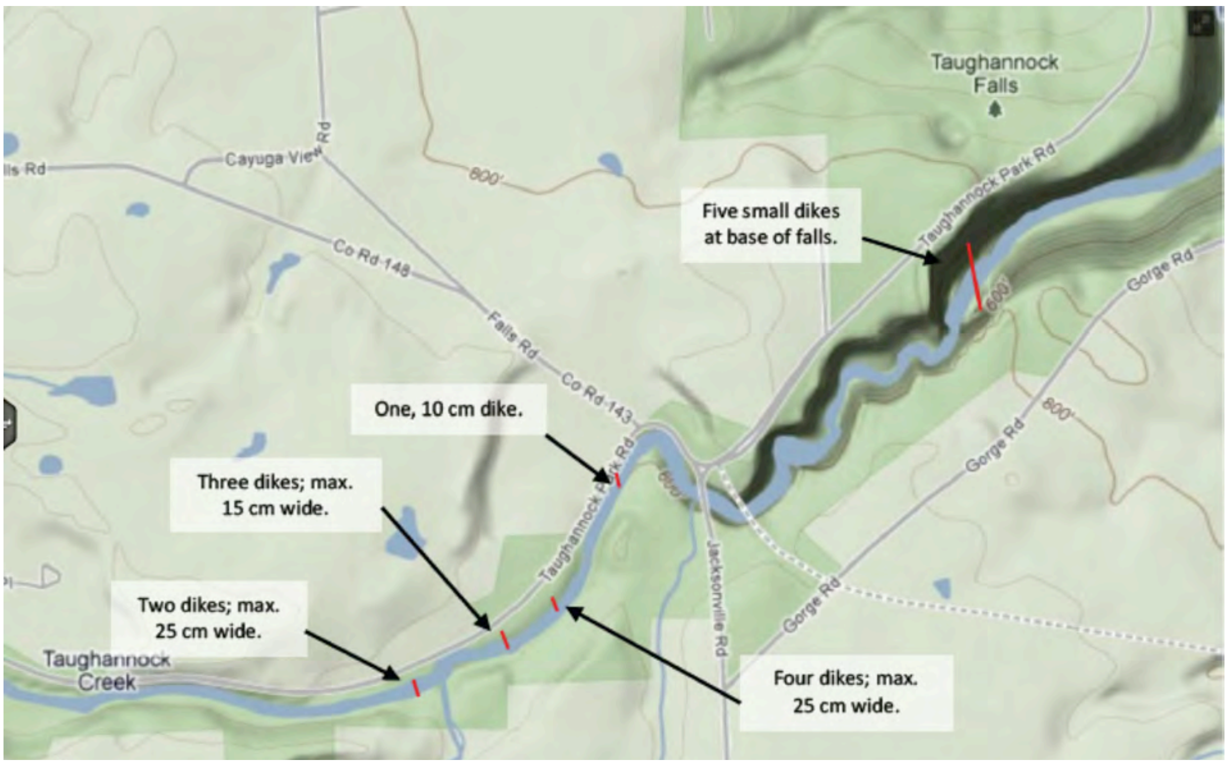

Figure 15. Approximate locations along Taughannock Creek where a total of 15 small dikes have been reported. Few are currently exposed. Modified after Foster (1970), Figure 1, p.10.

History of the Taughannock Creek Dikes

The first report of dikes exposed along Taughannock Creek was by Matson (1905) in which he described five dikes, all less than 10 cm in width, being exposed in the south wall of the gorge below Taughannock Falls, and one dike, < 5 cm wide, being exposed ~ 1 km upstream. He also noted that a thrust along a bedding plane offset the dikes exposed in the wall of the gorge by ~ 50 cm. Martens (1924) discovered one of the ~25 cm wide dikes upstream of the falls, and Foster (1970) identified and described a total of ten dikes in the section of Taughannock Creek above the high falls. Most of the dikes are < 5 cm wide, and most pinch out rapidly along strike. The lack of severe flooding in the region over the past 50 years has allowed sediment and vegetation to obscure most of these small, easily weathered dikes.

A number of petrological studies of the Taughannock Creek dikes were done in the 1980s (Jackson, 1982; Jackson et al., 1982a, b; Kay et al., 1983; Snedden, 1983; Snedden and Kay, 1981b). These were the first studies to document the multiple populations of garnet, clinopyroxene, and spinel macrocrysts that occur in these dikes, and to conclude that most are xenocrysts derived from two dominant sources: the first a shallow (< 100 km), relatively undepleted mantle peridotite, and the second a granulite facies, mafic lower crust (Kay et al., 1983). Pressure and temperature estimates of equilibration for the mantle macrocryst suite range from 28-32kb and 1020-1070^{o}C (Jackson et al., 1982a) to 15-20 kb and 850-880^{o}C (Kay et al., 1983).

Petrography of Taughannock Creek dikes

As first noted by Foster (1970), the dikes exposed along Taughannock Creek are quite variable in both hand-sample and in thin section. Overall color, texture, style of weathering, and relative abundance of macrocryst phases varies considerably from dike to dike (Figure 16). The characteristics that they share, and that define Group B intrusions, are the relative abundance of calcite in the matrix and, in addition to olivine, the presence of one or more of the following phases as macrocrysts: phlogopite, pyrope garnet, Cr-bearing diopside, and/or spinel.

Figure 16. A) Taughannock Creek dike filling N-S oriented fracture, with highly weathered chilled margins (hammer length = 33 cm). B) Polished slab of Taughannock Creek dike showing large, rounded, serpentinized olivine macrocrysts and rounded pyrope macrocryst w/ keliphytic reaction rim (width of photo = 2 mm).

Petrography of Taughannock Creek dikes (cont.)

Olivine was a common macrocryst and matrix phase in all of the Taughannock Creek dikes, but has been completely replaced by serpentine, calcite, and/or magnetite; no fresh olivine has been found in any of the specimens examined to date. In most dikes, the large olivine macrocrysts are rounded, suggesting a xenocrystic origin, however, in one dike many of the pseudomorphs retain euhedral olivine morphologies, suggesting some may have been phenocrysts in equilibrium with the host magma (Figure 17).

Phlogopite is the second most abundant macrocryst, and most of the larger grains are strongly zoned and rounded (Figure 18). Compositionally, the phlogopite macrocrysts are similar to those in other New York State kimberlites, containing up to 3 wt. % TiO_2, and 5 to 8 wt. % FeO. In many samples, the small tabular matrix grains are strongly flow-aligned.

Clinopyroxene macrocrysts are relatively common; most are < 1mm in diameter, are bright green in hand sample and colorless in thin section. Unlike the clinopyroxene macrocrysts in the Six Mile Creek dikes (Figure 7), these grains are homogeneous and do not exhibit pronounced compositional zonation. As noted by Jackson et al. (1982b) most of the grains are Cr-bearing diopsides containing 1 to 1.5 wt. % Cr_2O_3; a smaller population of Cr-poor, Al-rich diopside macrocrysts is also present.

Orthopyroxene macrocrysts were reported by Jackson et al. (1982a), but have not been observed by the authors.

Garnet macrocrysts are present in most of the Taughannock Creek dikes, but in low concentrations. Grains picked out from heavy mineral separates vary in color from pale orange to deep purple. Most grains are highly fractured and rounded, with a well-developed reaction rim (Figure 14). Three populations of garnet grains have been documented: 1) Cr-bearing pyrope (1.5 to 4.5 wt. % Cr_2O_3); 2) high-Ca pyrope-almandine; and 3) low-Ca pyrope-almandine (Figure 19). Jackson et al. (1982a) recognized the presence of both pyrope and almandine-rich garnets in the Taughannock Creek kimberlites, and attributed the pyrope garnet (and Cr-bearing diopside) macrocrysts to a shallow, upper mantle source, and the almandine-rich garnets (and Cr-poor diopside) macrocrysts to a lower crustal, eclogitic source.

Spinel macrocrysts are common; in thin section they are always anhedral, rounded, and embayed, and range in color from pale tan to dark brown, red-brown, olive green and opaque. Compositionally, spinel macrocrysts from the Group B kimberlites in the Ithaca region are the most diverse, ranging from near end-member chromite to near end-member spinel (Figure 11).

The groundmass of Group B kimberlite dikes is dominated by carbonate, serpentine and phlogopite, but in widely varying proportions between intrusions. Perovskite is also present in the matrix, but typically only as very small (< 20 µm diameter), partly altered grains, making them unsuitable for U-Pb dating. Magnetite and apatite are the only other phases commonly observed in the groundmass of Group B intrusions.

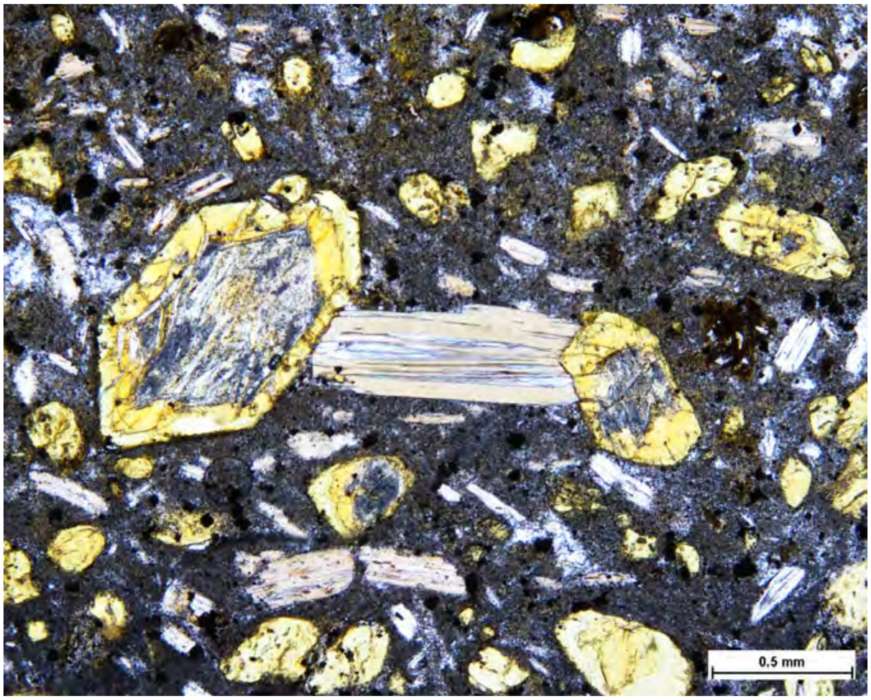

Figure 17. Photomicrograph of Taughannock Creek dike showing partly serpentized phlogopite macrocrysts (pale tan), and large euhedral olivine phenocrysts (pseudomorphed by serpentine, calcite, and magnetite) (Sample TC-3; PPL).

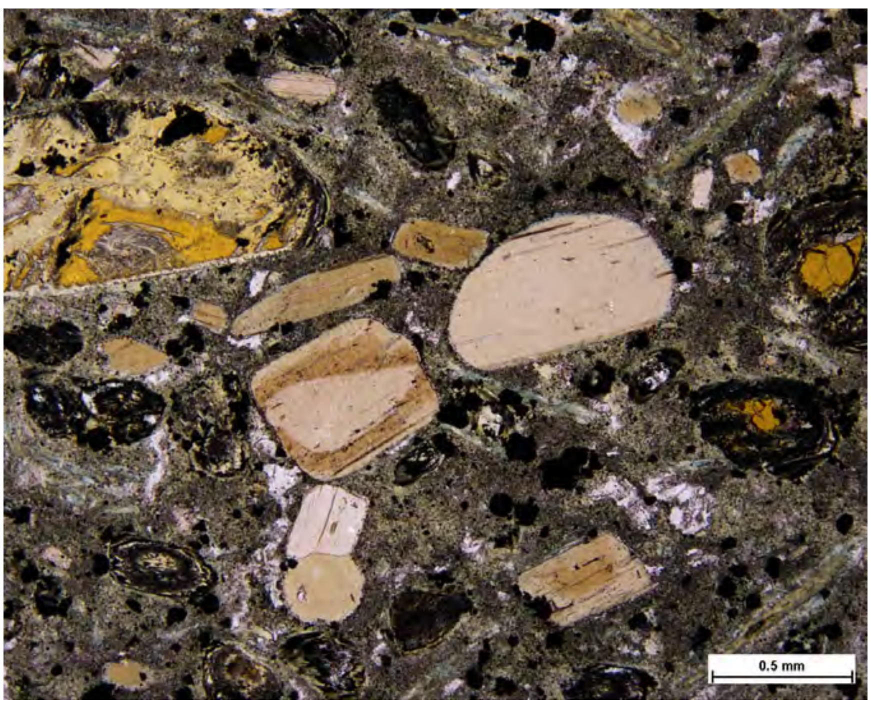

Figure 18. Photomicrograph of Taughannock Creek dike showing rounded, zoned, phlogopite macrocrysts (pale tan to brown), and large olivine macrocrysts (pseudomorphed by serpentine and magnetite) (Sample TC-1; PPL).

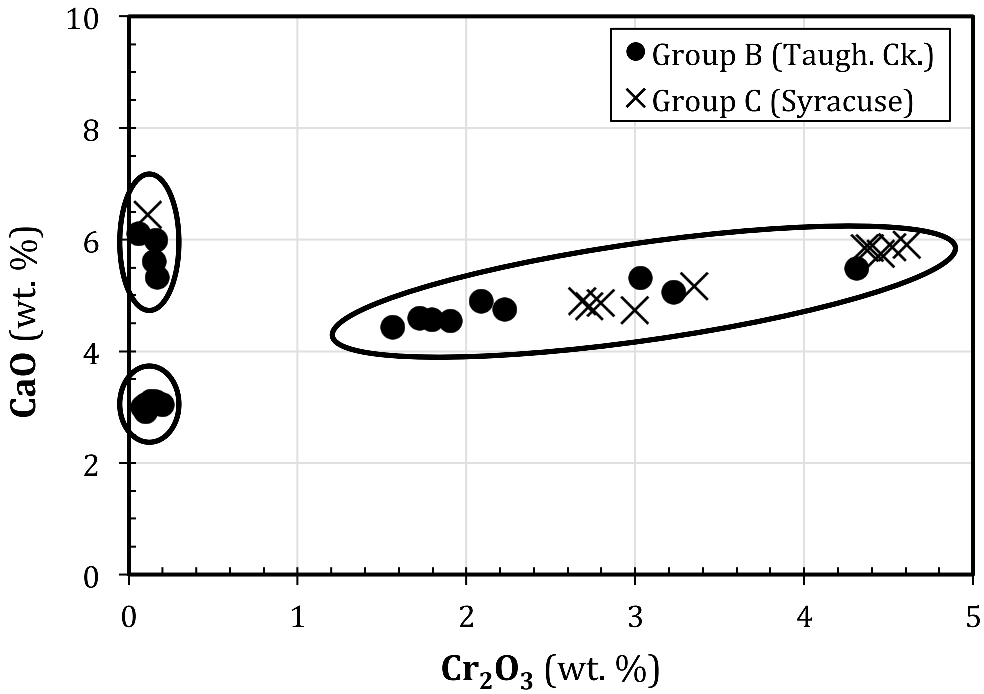

Figure 19. Compositions of garnet macrocrysts in Taughannock Creek dikes and the Dewitt Reservoir diatreme. (Data from O'Sullivan (2017) and Bailey (unpublished)).

REFERENCES:

Apfel, E. T., Maynard, J. E., and Ploger, L. W., 1951, Possible diatreme in Syracuse, New York: Geological Society of America Bulletin, v. 62, p. 1421.

Bailey, D. G., and Lupulescu, M., 2007a, Kimberlitic rocks of central New York: Guidebook - New York State Geological Association, Meeting, v. 79, p. 53-81.

-, 2012, Kimberlitic Rocks of New York: The Dewitt "Kimberlite", *in* Rayne, T. W., ed., 84th Annual Meeting, New York State Geological Association: Hamilton College, Clinton, NY, New York State Geological Association (NYSGA), p. 15.

Bailey, D. G., and Lupulescu, M. V., 2007b, Kimberlitic rocks of central New York: New York State Geological Association, Field Trip Guidebook, v. 79, p. 53-81.

-, 2009, Kimberlites of central New York State; magmatism related to Mesozoic extension and reactivation of lithospheric structures, Abstracts with Programs - Geological Society of America, Volume 41: United States, Geological Society of America (GSA) : Boulder, CO, United States, p. 337.

-, 2015, Spatial, temporal, mineralogical, and compositional variations in Mesozoic kimberlitic magmatism in New York state: Lithos [Oslo], v. 212-215, p. 298-310.

Barnes, S. J., and Roeder, P. L., 2001, The range of spinel compositions in terrestrial mafic and ultramafic rocks.: Journal of Petrology, v. 42, no. 12, p. 2279-2302.

Barnett, V. H., 1905, Notice of the discovery of a new dike at Ithaca, New York: American Journal of Science, v. 19, no. 111, p. 210.

Basu, A. R., Rubury, E., Mehnert, H. H., and Tatsumoto, M., 1984, Sm-Nd, K-Ar and petrologic study of some kimberlites from eastern United States and their implication for mantle evolution: Contributions to Mineralogy and Petrology, v. 86, no. 1, p. 35-44.

Beck, L. C., 1842, Mineralogy of New York; comprising detailed descriptions of the minerals hitherto found in the State of New York, and notices of their uses in the arts and agriculture, Albany, NY, W. and A. White, and J. Visscher, Natural History of New York, 540 p.:

Clarke, F. W., 1904, Analyses of Rocks: Bulletin - United States Gelogical Survey, v. 228, p. 46.

Clarke, F. W., and Hillebrand, W. F., 1897, Analyses of Rocks: Bulletin - United States Gelogical Survey, v. 148, p. 79.

Clarke, J. M., 1899, The peridotite on Green Street hill: New York State Museum Handbook, v. 15, p. 81.

Dana, J. D., 1878, Manual of Mineralogy, New York, 474 p.:

Darton, N. H., and Kemp, J. F., 1895a, A new intrusive rock near Syracuse: Geological Society of America Bulletin, v. 6, p. 477-478.

-, 1895b, A newly discovered dike at DeWitt, near Syracuse, New York: American Journal of Science, v. 49, p. 456-462.

DeJournett, J. D., 1970, Paleomagnetism of peridotite dikes near Ithaca, New York [B.Sc.: Cornell University, 59 p.

DeJournett, J. D., and Schmidt, V. A., 1975, Paleomagnetism of some peridotite dikes near Ithaca, New York: Eos, Transactions American Geophysical Union, v. 56, no. 6, p. 354.

Derby, O. A., 1874, Hints to Geological Students, Cornell Review, Volume 1: Ithaca, NY, Cornell University, p. 70.

Filmer, E. A., 1939, New peridotite dikes of Ithaca: Pan-American Geologist, v. 72, no. 3, p. 207-214.

Foster, B. P., 1970, Study of the kimberlite-alnoite dikes in central New York (Finger Lakes region) [M.Sc.: SUNY at Buffalo, Buffalo, NY (Master's).

Geddes, G., 1860, Geology of Onondaga County, New York: Transactions, New York State Agricultural Society, v. 19, p. 243-256.

Gems here at home, July 16, 1906, Syracuse Herald, Syracuse, NY, p. 9

Grutter, H. S., Gurney, J. J., Menzies, A. H., and Winter, F., 2004, An updated classification scheme for mantle-derived garnet, for use by diamond explorers: Lithos, v. 77, p. 841-857.

Heaman, L. M., and Kjarsgaard, B. A., 2000, Timing of eastern North American kimberlite magmatism; continental extension of the Great Meteor Hotspot track?: Earth and Planetary Science Letters, v. 178, no. 3-4, p. 253-268.

Hogeboom, W. L., 1958, The petrology of the Green Street peridotite dikes in Syracuse, New York [M.Sc. M.Sc.]: Syracuse University, 95 p.

Hopkins, T. C., 1914, The geology of the Syracuse Quadrangle [New York], Bulletin - New York State Museum, Volume 171: Albany, NY, p. 80.

Hunt, T. S., 1858, Contributions to the History of Ophiolites. Part II.: American Journal of Science, v. 26, p. 234-240.

Jackson, D. E., 1982, Petrogenesis of a shallow-level kimberlite from Taughannock Creek, New York [M.Sc. M.Sc.]: University of Tennessee at Knoxville, 70 p.

Jackson, D. E., Hunter, R. H., and Taylor, L. A., 1982a, A Mesozoic window into the sub-Appalachian mantle; kimberlite from the eastern United States: Geological Society of America, Abstracts with Programs, v. 14, no. 1-2, p. 28.

-, 1982b, Shallow-level kimberlite from the northeastern U.S.A.; an unusual mantle sample: Eos, Transactions American Geophysical Union, v. 63, no. 18, p. 463-464.

Johnson, H., 1936, The New York State Flood of 1935, *in* Interior, U. S. D. o. t., ed.: Washington, D.C., United States Government Printing Office, p. 233-268.

Kay, S. M., 1990, Central New York kimberlites; evidence for an Early Cretaceous thermal disturbance in the Appalachian Basin: Geological Society of America, Abstracts with Programs, v. 22, no. 2, p. 27.

Kay, S. M., and Foster, B. P., 1986, Kimberlites of the Finger Lakes region: New York State Geological Association, Field Trip Guidebook, v. 58, p. 219-238.

Kay, S. M., Snedden, W. T., Foster, B. P., and Kay, R. W., 1983, Upper mantle and crustal fragments in the Ithaca kimberlites: Journal of Geology, v. 91, no. 3, p. 277-290.

Kemp, J. F., 1891, Peridotite dikes in the Portage sandstones near Ithaca, New York: American Journal of Science, v. 42, p. 410-412.

Kraus, E. H., 1904, A new exposure of serpentine at Syracuse, New York: American Geologist, v. 33, p. 330-332.

Lupulescu, M. V., Bailey, D. G., and Minarik, W. G., 2007, Mineral and whole-rock chemistry of kimberlite-like rocks from New York: Abstracts with Programs - Geological Society of America, v. 39, no. 6, p. 389-389.

Lupulescu, M. V., Shaw, G. H., and Bailey, D. G., 2002, Kimberlites from the central New York; mineralogy, geochemistry, xenoliths and contact phenomena: Abstracts with Programs - Geological Society of America, v. 34, no. 6, p. 362-362.

Luther, D. D., 1897, The Economic Geology of Onondaga County, New York.

MacDougall, J. G., and Bailey, D. G., 2009, Hydrogen in pyrope garnets from New York State kimberlites: Abstracts with Programs - Geological Society of America, v. 41, no. 3, p. 109-110.

Martens, J. H. C., 1923a, A study of the basic dikes of the Ithaca region (New York) [Cornell University.

-, 1923b, Study of the igneous rocks of the Ithaca, New York, and vicinity: Geological Society of America Bulletin, v. 34, no. 1, p. 99.

-, 1924, Igneous Rocks of Ithaca, New York, and Vicinity: Geological Society of America Bulletin, v. 35, p. 305-320.

Matson, G. C., 1905, Peridotite dikes near Ithaca, New York: Journal of Geology, v. 13, p. 264-275.

Maynard, J. E., and Ploger, L. W., 1946, A study of the Salt Springs Road peridotite dike in Syracuse, New York: American Mineralogist, v. 31, no. 9-10, p. 471-485.

Nappi, D. D., 2015, Geochemical and Mineralogical Analysis of Kimberlitic Dikes Exposed along Six Mile Creek, Ithaca, NY [B.A.: Hamilton College, 75 p.

O'Sullivan, D., 2017, Major and trace element compositions of garnets from New York State kimberlites: A window into the lower crust and upper mantle [B.Sc. Undergraduate]: Hamilton College, 29 p.

Parrish, J. B., and Lavin, P. M., 1982, Tectonic model for kimberlite emplacement in the Appalachian Plateau of Pennsylvania: Geology [Boulder], v. 10, no. 7, p. 344-347.

Pattee, E. N., 1903, The Analysis of the Green Street Dike: Proceedings of the Onondaga Academy of Science, v. 1, no. 1, p. 2-3.

Rauscher, N. T., Lupulescu, M., Bailey, D. G., and Shaw, G., 2003, Mineralogy and geochemistry of kimberlite dikes from central New York, USA: Abstracts with Programs - Geological Society of America, v. 35, no. 3, p. 93-93.

Roeder, P. L., and Schulze, D. J., 2008, Crystallization of Groundmass Spinel in Kimberlite: Journal of Petrology, v. 49, no. 8, p. 1473-1495.

Schneider, P. F., 1902, New exposures of eruptive dikes in Syracuse, N Y: American Journal of Science, v. 14, no. 79, p. 24-25.

-, 1903a, The Geology of the Green Street Dikes: Proceedings of the Onondaga Academy of Science, v. 1, no. 1, p. 4.

-, 1903b, The geology of the serpentines of central New York: Proceedings of the Onondaga Academy of Science, v. 1, p. 110-117.

Serpentine rock of Onondaga rich in sparklers, April 19, 1902, Syracuse Post Standard, Syracuse, NY,

Sheldon, P. G., 1921, A new dike near Ithaca, New York: Science, New Series, v. 53, no. 1358, p. 20-21.

-, 1927, On the association of faulting with dike intrusion: Journal of Geology, v. 35, p. 353-367.

Simonds, F. W., 1877, Geology of Ithaca, NY and vicinity: American Naturalist, v. 11, p. 49.

Smith, B., 1909, Dikes in the Hamilton shale near Clintonville Onondaga County, New York: Science, v. 30, p. 724.

Smyth, C. H., 1892, A third occurrence of peridotite in central New York: American Journal of Science, v. 43, no. 256, p. 322-327.

-, 1893, Alnoite containing an uncommon variety of melilite: American Journal of Science, v. 46, no. 272, p. 104-107.

-, 1896, Note on recently discovered dikes of alnoite at Manheim, New York: American Journal of Science, v. 2, p. 290-292.

-, 1898, Weathering of alnoite in Manheim, New York: Geological Society of America Bulletin, v. 9, p. 257-268.

-, 1902, Petrography of recently discovered dikes in Syracuse, New York, with note on the presence of melilite in the Green Street dike: American Journal of Science, v. 14, no. 79, p. 26-30.

Snedden, W. T., 1983, Mineralogy and setting of the Ithaca kimberlites [M.Sc. M.Sc.]: Cornell University, 89 p.

Snedden, W. T., and Kay, S. M., 1981a, Initial stages of kimberlite eruption; evidence from mantle minerals in Ithaca kimberlites: Geological Society of America, Abstracts with Programs, v. 13, no. 7, p. 557.

-, 1981b, Mineral chemistry of kimberlite and included xenocrysts, Ithaca, New York: Geological Society of America, Abstracts with Programs, v. 13, no. 3, p. 178.

Syracuse has diamond hunt, November 28, 1905, Syracuse Post Standard, Syracuse, NY, p. 14

Van Fossen, M. C., and Kent, D. V., 1991, Paleomagnetism of Late Jurassic-Early Cretaceous kimberlite dikes from Ithaca, New York: Eos, Transactions American Geophysical Union, v. 72, no. 17, p. 99.

-, 1993, A palaeomagnetic study of 143 Ma kimberlite dikes in central New York State: Geophysical Journal International, v. 113, no. 1, p. 175-185.

Van Tyne, A. M., 1958, Petrology of the Euclid Avenue peridotite intrusiveM.Sc.]: Syracuse University, 144 p.

Vanuxem, L., 1837, First annual report of the geological survey of the third district, New York, Albany, Annual Report of the New York Geological Survey, 3rd District, 265 p.:

-, 1839, Third annual report of the geological survey of the third district, New York, Annual Report of the New York Geological Survey, 3rd District, 283 p.:

-, 1842, Geology of New York; Part III, Comprising the survey of the third geological district, Albany, NY, W. and A. White and J. Visscher, Natural History of New York, 306 p.:

Watson, K. D., 1979, Kimberlites of eastern North America, *in* Wyllie, P. J., ed., Ultramafic and related rocks, Robert E. Krieger Publ. Co., Huntington, NY, p. 312-323.

Williams, G. H., 1887a, On the serpentine (peridotite) occurring in the Onondaga salt group at Syracuse, New York: American Journal of Science, v. 34, no. 200, p. 137-145.

-, 1887b, On the serpentine of Syracuse, N.Y.: Science, v. 9, no. 214, p. 232-233.

-, 1890a, Note on the eruptive origin of the Syracuse serpentine (with discussion by James Hall and J. F. Kemp): Geological Society of America Bulletin, v. 1, p. 533-534.

-, 1890b, Origin of serpentine of Syracuse, New York: American Geologist, v. 5, no. 2, p. 118.

Williams, H. S., Tarr, R. S., and Kindle, E. M., 1909, Description of the Watkins Glen-Catatonk District, New York: U. S. Geological Survey : Reston, VA, United States.

Would advance cash to probe stratums, November 3, 1902, Syracuse Post Standard, Syracuse, NY, p. 6

Zartman, R. E., 1988, Three decades of geochronologic studies in the New England Appalachians: Geological Society of America Bulletin, v. 100, no. 8, p. 1168-1180.

Zartman, R. E., Brock, M. R., Heyl, A. V., and Thomas, H. H., 1967, K-Ar and Rb-Sr ages of some alkalic intrusive rocks from central and eastern United States: American Journal of Science, v. 265, p. 848-870.

A6: EXPLORING THE SURFICIAL GEOLOGY AND HYDROLOGY OF ALFRED NY

DAVID J. BARCLAY
Geology Department, SUNY Cortland, Cortland NY 13045
david.barclay@cortland.edu

OTTO H. MULLER
Geology Department, Alfred University, Alfred NY 14802
fmuller@alfred.edu

RICHARD A. YOUNG
Department of Geological Sciences (Emeritus), SUNY Geneseo, Geneseo, NY 14454
young@geneseo.edu

INTRODUCTION

Alfred is located in west-central New York within the Allegheny Plateau. This area is fairly close to the outer limit of glaciation, with moraines of the Last Glacial Maximum (LGM) only 43 km to the southwest (Figure 1). Nonetheless, the landscape of the Alfred area has been significantly affected by geomorphic processes associated with the Laurentide Ice Sheet (LIS) during the Quaternary (2.58 Ma to the present). These processes include localized erosion by meltwater overflowing from proglacial lakes, subglacial erosion by glacial ice, and deposition of sediment and landforms from glacial ice, meltwater streams, and in proglacial lakes. Additional landscape modification has occurred during other intervals of the Quaternary when the LIS was north of the Alfred area or entirely absent from North America.

In this field trip we will visit some of the Quaternary landforms and sedimentary deposits of the Alfred area. Although there has been a lot of research done in surrounding areas, the surficial geology and hydrology at Alfred has only seen limited reconnaissance-level work to date. Therefore, this field trip will emphasize the general picture of Quaternary landscape evolution of the glaciated Allegheny Plateau and consider how some sediments and landforms near Alfred fit within this regional context.

Background

The village of Alfred is situated between the Genesee Valley to the west and the Finger Lakes region to the northeast (Figure 1). Elevations in the area range from around 700 m (2300 feet) above sea level at the hill-tops to 350 m (1150 feet) a.s.l. in the large valley near Hornell. Canacadea Creek flows through the village and continues northeastwards to near Hornell to join the Canisteo River which, in turn, flows to the southeast to eventually join the Susquehanna River downstream of Corning. The Genesee River is separated from Alfred by a drainage divide and flows northwards to Lake Ontario.

However, in contrast to the modern rivers, the valleys of the Alfred area show an interesting arrangement (Figure 1). The valley at Hornell does not open towards the southeast; rather, it opens towards the northwest, drops 160 m (525 feet) in elevation across the Valley Heads moraine near Dansville, and merges with the Genesee Valley to continue northwards. This valley arrangement cuts through the modern drainage divide near Dansville. Furthermore, the valley southeast of Hornell becomes increasingly narrow before opening up as it nears Corning.

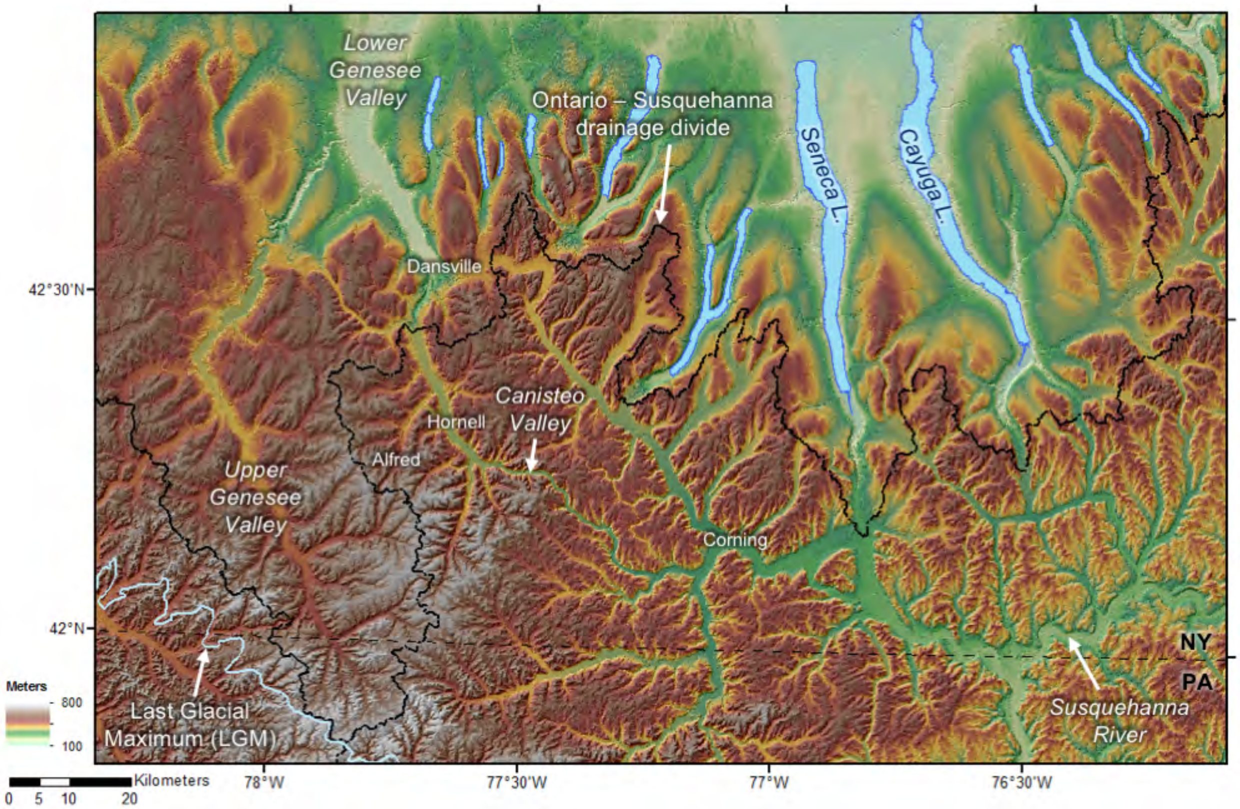

Figure 1. Shaded relief map of the Allegheny Plateau in west-central New York and Pennsylvania.

This curious mismatch of rivers and valleys in the Allegheny Plateau of New York has been the subject of numerous papers over the past century. Notable early contributions by Carney (1903), Tarr (1905), and Fairchild (1925, 1934, 1935) were based largely on inferences from topographic maps and field observations, and introduced many important ideas regarding development of major landscape features. Coates (1974) and Coates and Kirkland (1974) built on this early work and used similar methods to subdivide the Allegheny Plateau into distinct sub-regions as well as to propose a model for drainage divide incision by forced overflow from proglacial lakes.

More recent work has added critical details to understanding of the Quaternary history of this region. Radiocarbon ages tied to stratigraphic and/or paleoenvironmental analyses by Young and Burr (2006), Karrow et al. (2009), and Karig and Miller (2013) have provided chronologic control for some key pre-LGM sites in the lower Genesee Valley and around Cayuga Lake. Detailed mapping of surficial deposits by Muller et al. (1988) produced a chronology of proglacial lakes for the Genesee Valley. Seismic investigations of the stratigraphic fill of the Finger Lakes by Mullins and Hinchey (1989) and Mullins et al. (1996) revealed the subglacial erosion and deglacial stratigraphy of these deeply scoured bedrock basins. Ice flow models at both a regional (Ridky and Bindschadler, 1990) and continental (e.g. Hughes et al., 1985) scale have provided insight into the mode of ice sheet flow through the region. Regional scale modelling has also shown the time-varying pattern of glacio-isostatic rebound in the area (Lewis et al., 2005). And ongoing studies in the eastern Finger Lakes (Kozlowski and Graham, 2014) are using new dating methods (such as optically stimulated luminescence) and newly available LiDAR-based high resolution digital elevation models to further advance the understanding of these landscapes.

QUATERNARY EVOLUTION OF THE ALLEGHENY PLATEAU

These many studies provide the basis for a synthesis of the geomorphic processes that have shaped the Allegheny Plateau during the Quaternary. This synthesis is not presented here as a strict historical sequence because the details of many events remain unclear. Rather, it is intended to convey some key ideas and to facilitate interpretation of the landforms and sediments that will be seen on this field trip.

Original valley network

The original valley network of the Allegheny Plateau is pre-Quaternary in age and fluvial in origin. This drainage pattern is largely dendritic (Figure 1) and continues south of New York and Pennsylvania in the unglaciated regions of the Appalachian Plateau. It appears likely that at the start of the Quaternary the ancestral Susquehanna River drained northwards along the axis of the modern Seneca basin and that regionally the drainage divide between the Ontario and Susquehanna basins was farther south than it is today (Fairchild, 1925, 1935). Drainage divides within the plateau separated rivers that drained north from rivers that drained south (Figure 2).

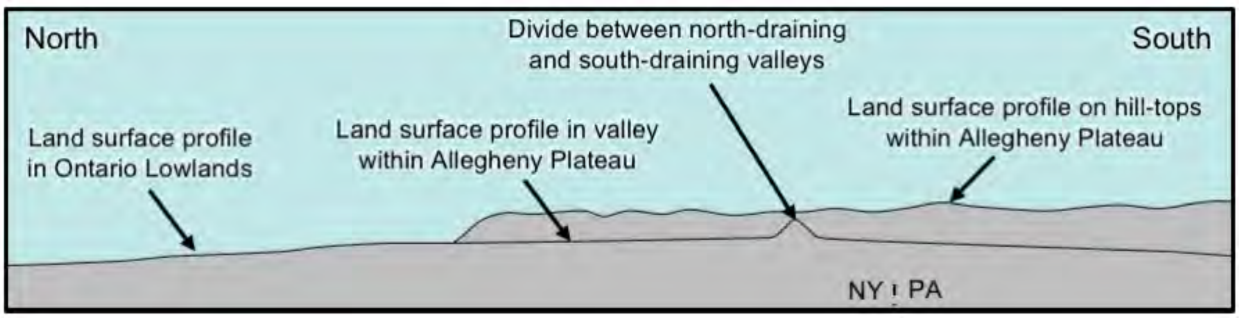

Figure 2. Schematic diagram of the northern Allegheny Plateau from Lake Ontario (left) to the LGM moraines in Pennsylvania (right). Topography is simplified from a north-south profile from Rochester NY to Galeton PA from a 10-m digital elevation model. Vertical exaggeration (VE) is 40x.

Proglacial lakes and sluiceways

Advance of the Laurentide Ice Sheet (LIS) to the northern edge of the Allegheny Plateau dammed proglacial lakes in north-draining valleys (Figure 3). Initially these lakes had low elevations as ponded water escaped through outlets along the plateau front to the west or east. However, with further advance of the ice margin these lakes were increasingly confined to valleys within the plateau and water levels were forced to rise to higher outlets draining south through the plateau.

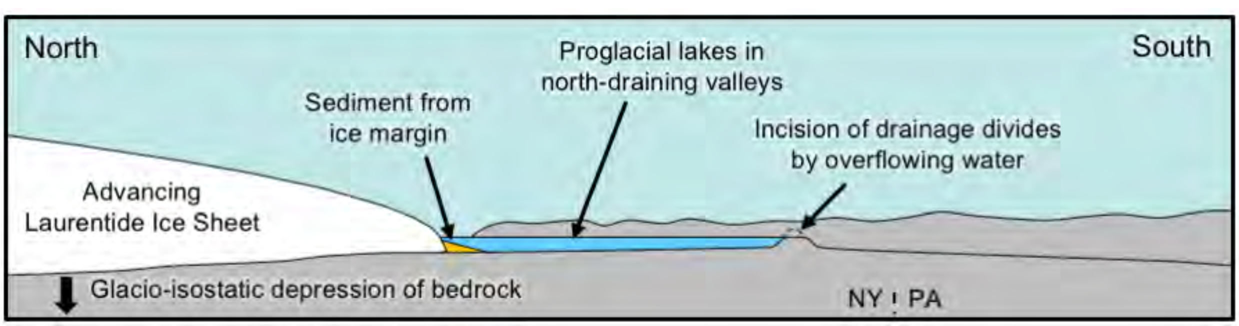

Figure 3. Schematic diagram showing the major landscape effects of advance of the LIS. Ice sheet profile assumes a basal shear stress of 100 kPa. VE is 40x.

These lake outlets would have begun as the lowest available points on the bounding drainage divides. With sustained overflow the water incised the divides and so changed the overflow points from small notches to wider, longer and lower sluiceways (Coates and Kirkland, 1974). Modern glaciers typically advance at meters per year to a few tens of meters per year and so, assuming similar advance rates and given the length of the valleys, these proglacial lakes would have likely existed for thousands of years while the LIS advanced southwards. Stillstands of the ice margin or retreats with re-advances would have extended this time for overflow incision even more. Thus, these sluiceways related to LIS advance are the result of sustained fluvial erosion over millennia rather than brief catastrophic flows.

The advancing LIS would have been a source of sediment such as clays and silts in the lakes, outwash in free-draining valleys, and till and other ice-contact sediments close to the ice margin. Although most of this sediment was eroded away during subsequent glacial over-riding, some survived in areas protected from glacial erosion. This is evidenced by the sediment sequences preserved in sections of many gorges throughout western and central New York (e.g. Von Engeln, 1931).

Glacial erosion

Subglacial erosion by the Laurentide Ice Sheet during the Quaternary has overprinted the original fluvial valley network. This erosion has been greatest in the central Finger Lakes area where the uplands between Seneca and Cayuga lakes have been substantially lowered and smoothed (Figure 1) and diminishes towards the glacial limit in Pennsylvania where the thickness and duration of ice cover was least (Figure 4) and the bedrock is generally more erosion-resistant. Erosion was also more intense at the north edge of the plateau and along the axes of the eleven finger lakes where in some cases the bedrock surface has been eroded close to or below sea level, with the bedrock bottom of Seneca Lake being the deepest at 306 m (1004 feet) below sea level (Mullins et al., 1996).

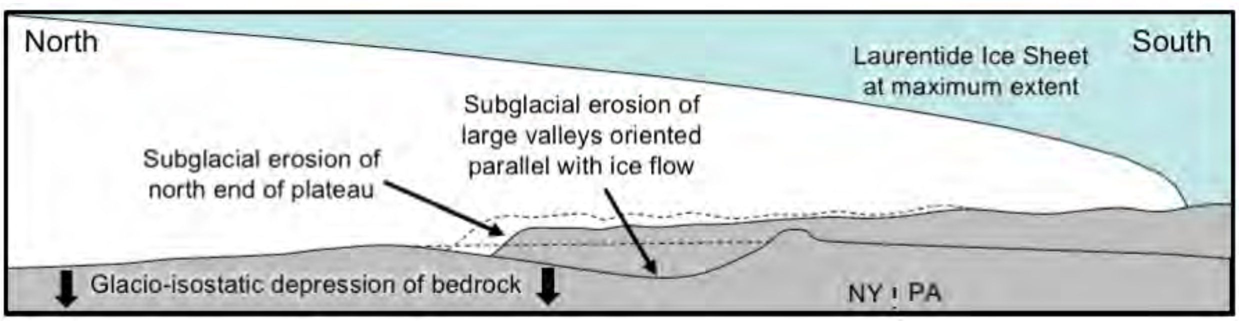

Figure 4. Schematic diagram showing the major landscape effects of the LIS while at its maximum extent. Ice sheet profile assumes a basal shear stress of 100 kPa. VE is 40x.

However, subglacial erosion was also locally selective. Sites dated to the last interglacial (c. 120 ka; Karrow et al., 2009) and the Middle Wisconsinan (c. 35 ka; Young and Burr, 2006; Karig and Miller, 2013) survived several thousand years beneath the LIS during the LGM without being eroded away. Although ice sheets can be very effective at eroding bedrock, such erosion will only happen if conditions at the base of the ice are locally favorable for erosion to occur.

The weight of the LIS also caused glacio-isostatic depression of the land surface (Lewis et al., 2005). This process would have begun to affect the area as the ice approached from the north (Figure 3) and would have continued and affected more of the area during glacial maxima (Figure 4). Total glacio-isostatic depression was greatest in the north of the region where the LIS was thickest and remained the longest.

Deglacial sediments and landforms

Sediments and landforms deposited during deglaciation are preserved at the land surface into the subsequent interglacial or ice-free interval. These include till deposits across upland areas, glacifluvial sand and gravel (outwash) in free-draining valleys, and glacilacustrine silts and clays in proglacial lake basins. These proglacial lakes (Figure 5) formed wherever drainage was blocked by the retreating ice margin and evolved from isolated high-elevation lakes into larger and lower lakes as the LIS uncovered interconnected valleys.

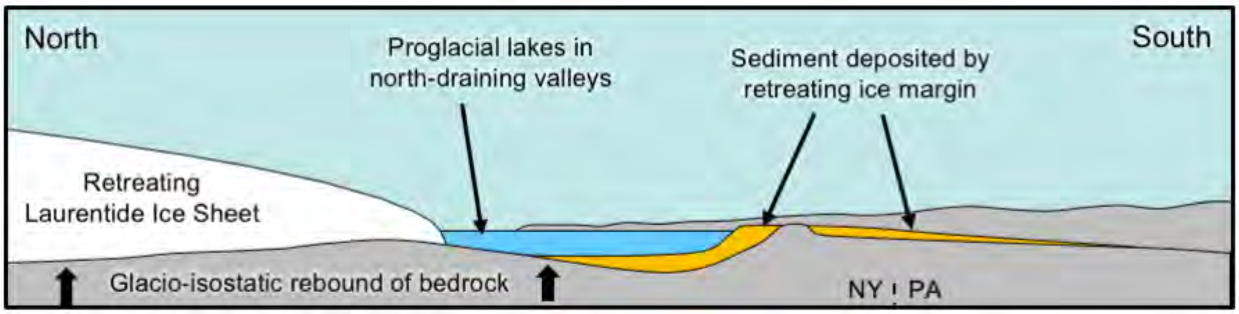

Figure 5. Schematic diagram showing the major landscape effects during deglaciation. VE is 40x.

Many outlets of these proglacial lakes during deglaciation were the same cols and sluiceways that were incised during LIS advance. Sediments deposited during advance or glacial maxima were flushed out and further incision occurred. Pulses of water from the merging of proglacial lakes caused some outflows to be briefly catastrophic and so capable of rapid outlet scouring. In addition, new lake outlet channels formed through morainal dams (e.g the Burns Outlet near Dansville) and many rivers cut new channel segments instead of re-occupying parts of their old paths (e.g. Letchworth Gorge on the Genesee River).

Deposition during deglaciation resulted in thick sediment fills in the over-deepened basins of the Finger Lakes. Seneca Lake, with a maximum sediment thickness of 270 m (885 feet), is the thickest and several others also exceed 200 meters of material (Mullins et al., 1996). Sediment also accumulated in thick deposits along the axes of large valleys throughout the Allegheny Plateau (Figure 1). Most of these valley fill deposits are capped by outwash that is graded to the Valley Heads Moraine, which today forms the modern drainage divide at the head of each large valley from Dansville to the eastern Finger Lakes.

Interglacials and other ice-free intervals

The rate of landscape change in the Allegheny Plateau is generally slower during cold or cool intervals when the LIS margin is north of the Ontario Lowlands or during interglacials when the LIS is reduced to remnant ice caps in the Arctic or completely absent. However, the formation of interglacial gorges is an exception. These developed in tributary side valleys near where larger valleys were substantially deepened during glaciation (i.e. in side valleys to the finger lakes or near drainage divides that were lowered by fluvial incision). The drop in base level in the larger valley caused headward erosion to progress upstream in the side valley, resulting in a knickpoint (i.e. bedrock-capped waterfall or cascade) at the head of erosion with a narrow gorge downstream (Figure 6).

Larger river channels, once established during deglaciation, will tend to remain in the same general location and slowly migrate through floodplain deposits. Landslides occur most often during deglaciation and become less frequent thereafter as the most unstable deposits have already failed and as the landscape becomes vegetated. Glacio-isostatic rebound, which began during deglaciation (Figure 5), also continues at a declining rate during interglacials (Figure 6).

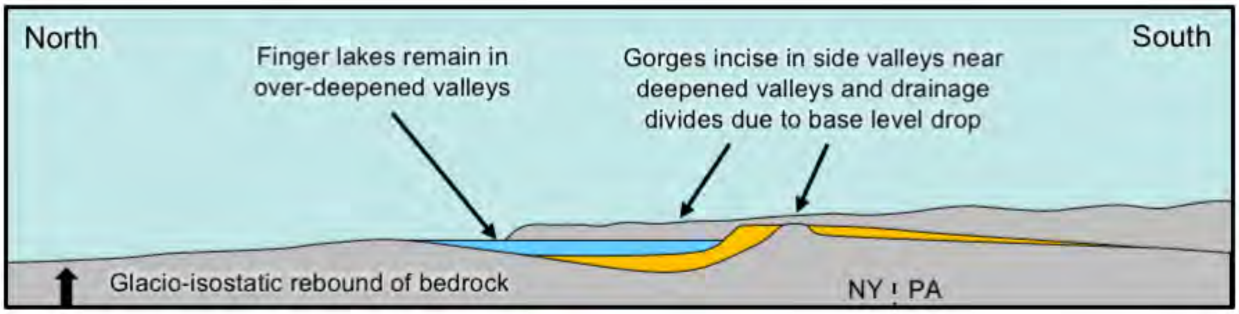

Figure 6. Schematic diagram showing the landscape during an interglacial or ice-free interval. VE is 40x.

Multiple glacial-interglacial cycles

Sediments and landforms show that the LIS has advanced into Pennsylvania at least four times during the Quaternary (Braun, 2004; Figure 7). This means that the concomitant effects on the landscape of the Allegheny Plateau from advance and retreat of the ice sheet (Figures 3-6) have also occurred at least four times. Furthermore, there may have been additional times when the LIS extended into the northern edge of the Allegheny Plateau without completely extending to Pennsylvania. Although deposits from the most recent glacial maximum and deglaciation dominate the surface and near surface sedimentary record, it is important to consider the multiple glacial-interglacial cycles of the Quaternary when interpreting landscape evolution of this region. Many deposits and landforms from prior to the LGM may currently remain unrecognized in the Allegheny Plateau.

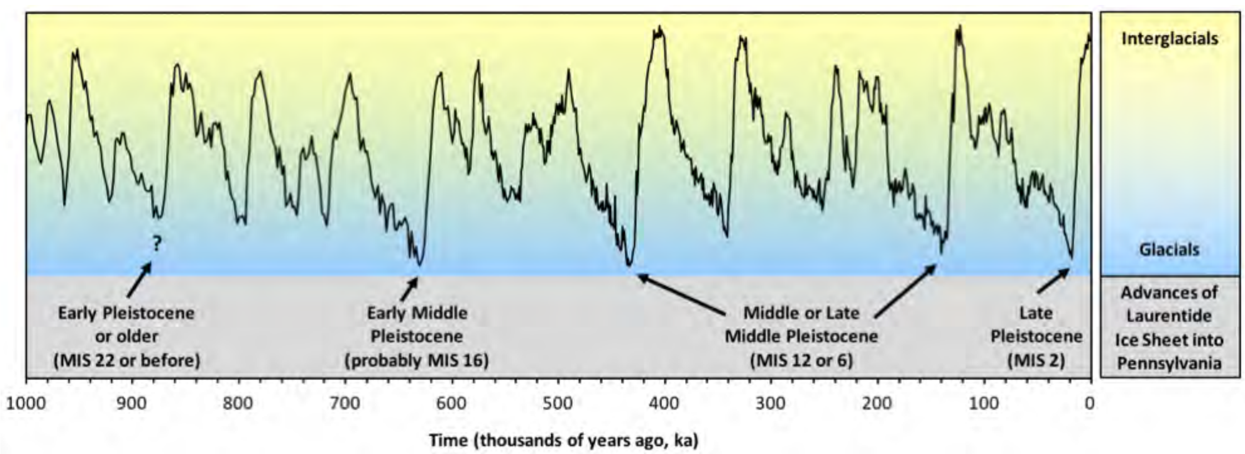

Figure 7. Deep sea oxygen isotope record, a proxy for global ice volume, with dates of LIS advances into Pennsylvania. Isotope data from Lisieki and Raymo (2005) and PA glacial data from Braun (2004).

The cumulative effect of multiple advances of the LIS through the Allegheny Plateau has been a reorganization of regional drainage. At the start of the Quaternary the Susquehanna River likely flowed north through the Seneca basin. However, incision of a pre-glacial drainage divide in northern Pennsylvania together with valley blocking glacial deposits at the south end of Seneca Lake have permanently rerouted the Susquehanna southwards. On a regional scale the drainage divide between the Susquehanna and Ontario basins has shifted northwards and, near the upper Genesee Valley, has moved westwards to leave Hornell and Alfred in the headwaters of the modern Susquehanna River.

LANDFORMS OF THE ALFRED AREA

This field trip starts at Alfred University and will follow a clockwise loop around the surrounding area (Figures 8 and 9). The route starts with sites in the Village of Alfred (stops 1-2), ascends to the uplands immediately west of the village (stops 3-4), descends the valley of McHenry Valley Creek (stops 5-7), and continues down to the western edge of the Canisteo Valley (stops 8-9). The latter part of the trip passes through Hornell to the headwaters of Bennetts Creek (stop 10) before returning to finish in the Alfred area (stops 11-12). Time will vary at each stop and we will complete as many stops as we can!

Research on the specific landforms of the Alfred area remains at a somewhat preliminary stage. Accordingly, we intend this field trip to enable participants to examine some of the most interesting features and to provide a forum for interpretation and discussion. The following pages provide some diagrams and text that we will use to during the trip to present some of the options for interpretation; please keep in mind that these are simplified and/or hypothetical and/or tentative and are not intended to be viewed as finalized explanations.

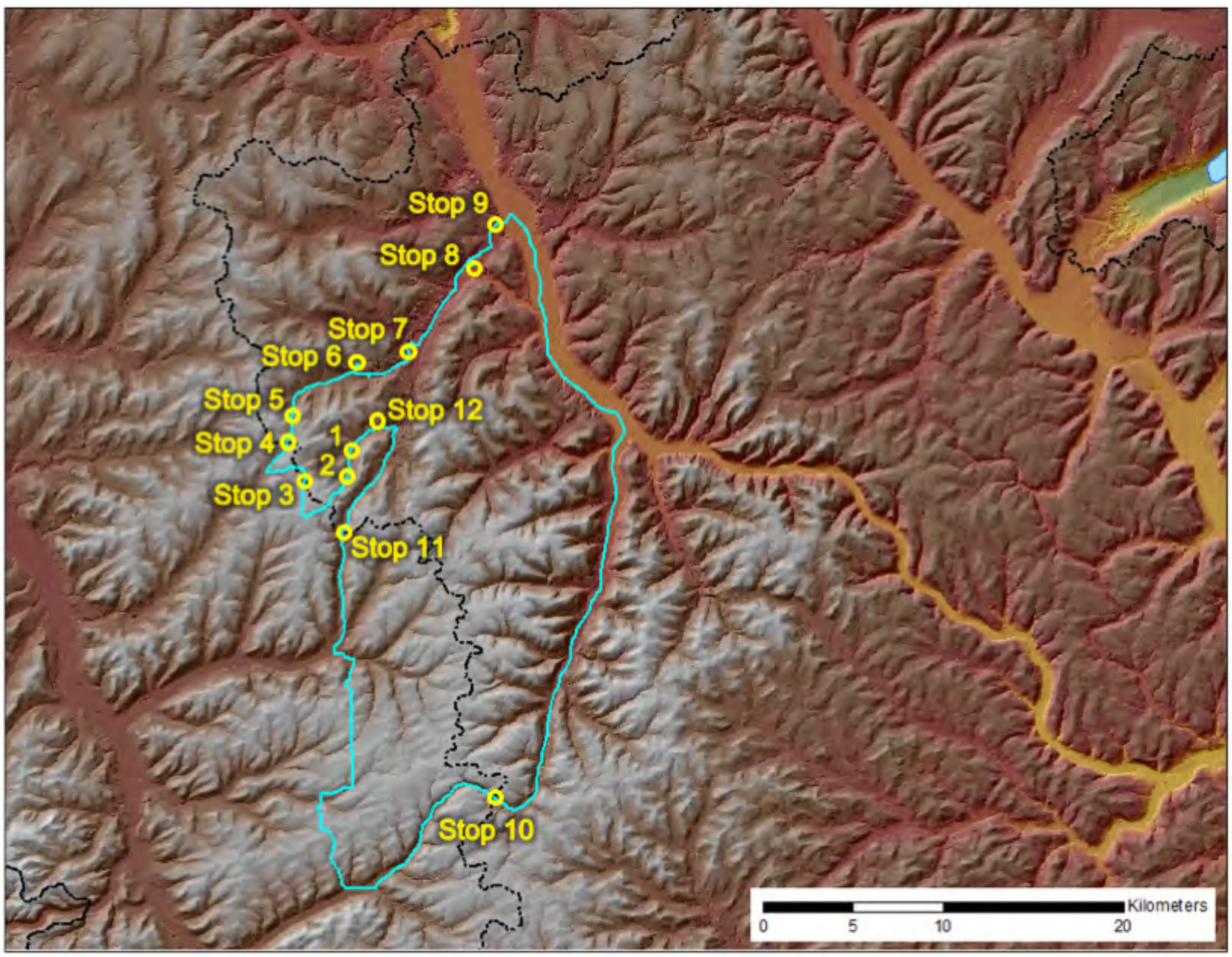

Figure 8. Field trip route. The trip begins and ends at Alfred, NY

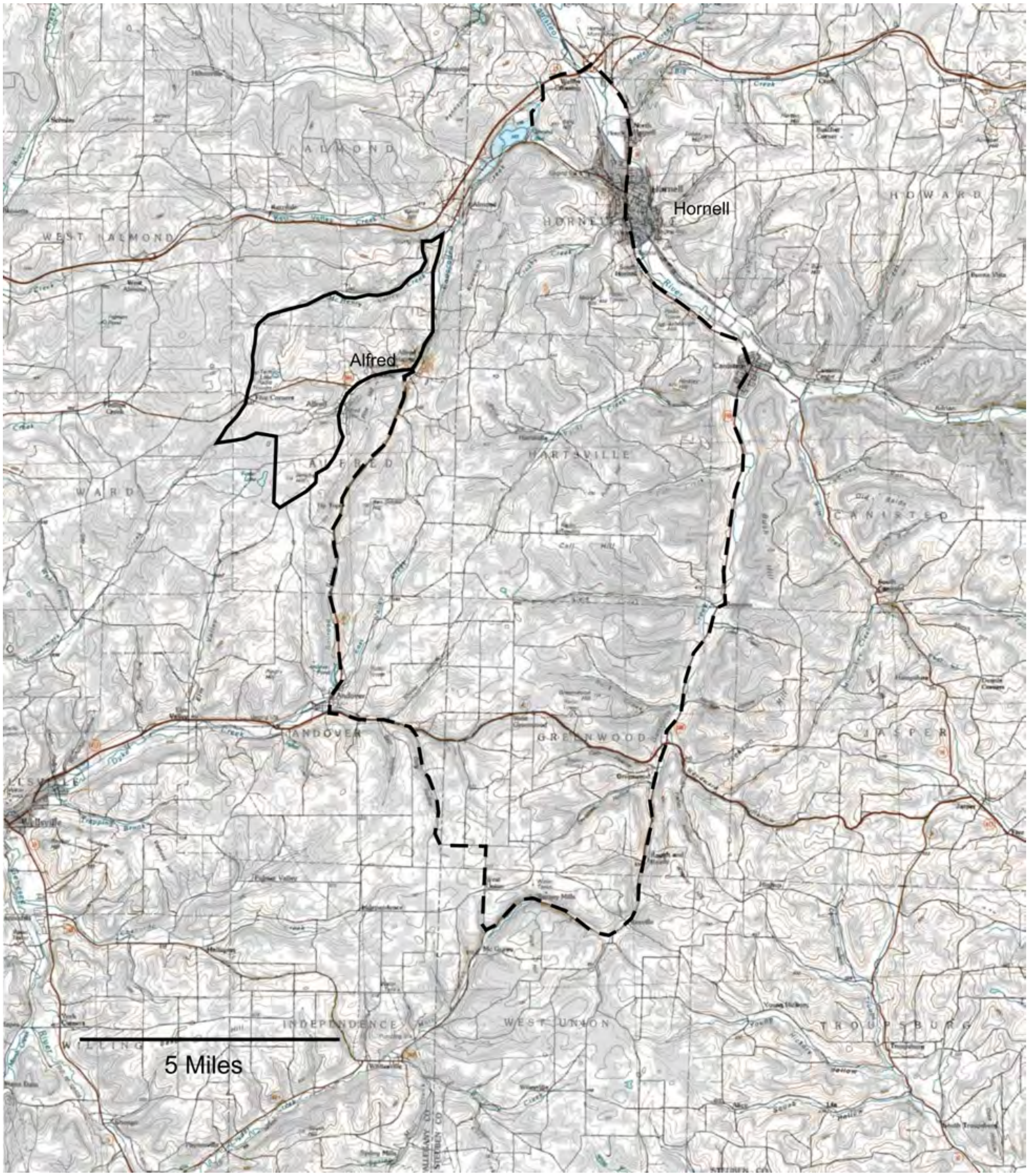

Figure 9. Field trip route, showing contours, rivers, roads, and settlements.

Col development

We have three long linear valleys occupying former cols separating the Genesee Valley from the valleys to its east: Five Corners (Stop 4), Railroad Valley at Tip Top (Stop 11), and the tail of Bennetts Creek (Stop 10). Each of these has a longitudinal profile showing the highest elevation somewhat down the valley. Figure 10 shows the actual topographic profile in Railroad Valley, and Figure 11 provides a model to explain how this profile and valley may have developed.

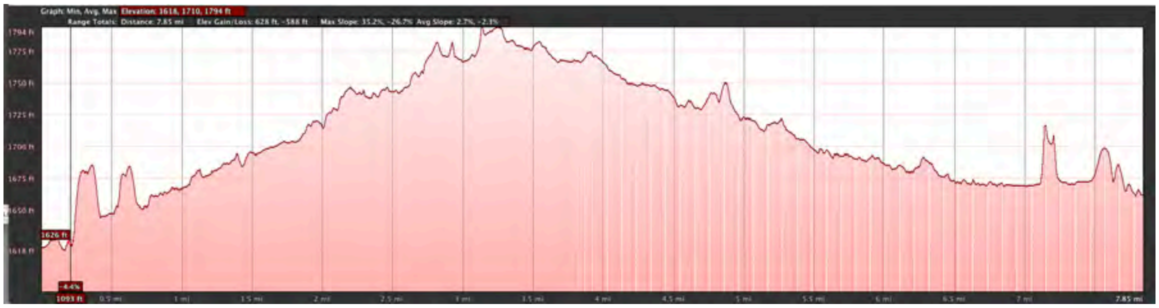

Figure 10. Topographic profile through Railroad Valley (Tip Top outlet). Profile is along the railroad track, with north (Alfred Station) to the left and south (Andover) to the right. Former lake was on the left side, where the slope is greatest and base level lowest.

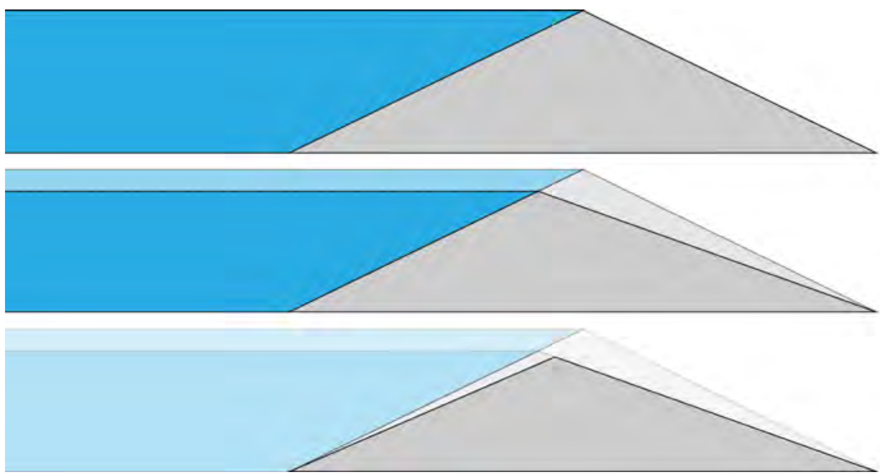

Figure 11. Model for col development.

Here is a model (Figure 11) to try and explain this:

- Top picture shows hill as it was before the lake. Slopes on both sides are equal, erosion would lower both sides at the same rate, divide would remain at the same place.
- Then the lake fills up to where it overflows the hill. Erosion now takes place on the side away from the lake, only. An outflow channel develops. This moves the divide towards the lake as the elevation of the col (at the bottom of the channel) moves down.
- Eventually the lake disappears. Now the side which had been towards the lake has a steeper gradient than the other side, so it will erode faster. It is still within the outflow channel, however. As this side erodes down, the divide will move in the direction away from where the lake had been.
- By the bottom picture the slopes on both sides are again the same, and one might imagine the divide to remain where it is as the channel continues to erode down.

Hypothetical ice margin reconstructions 1

These two maps (Figures 12 and 13) show hypothetical ice margins based on a valley tongue model (i.e. a lobe of ice extending southward from the main ice sheet that is confined to the local topography).

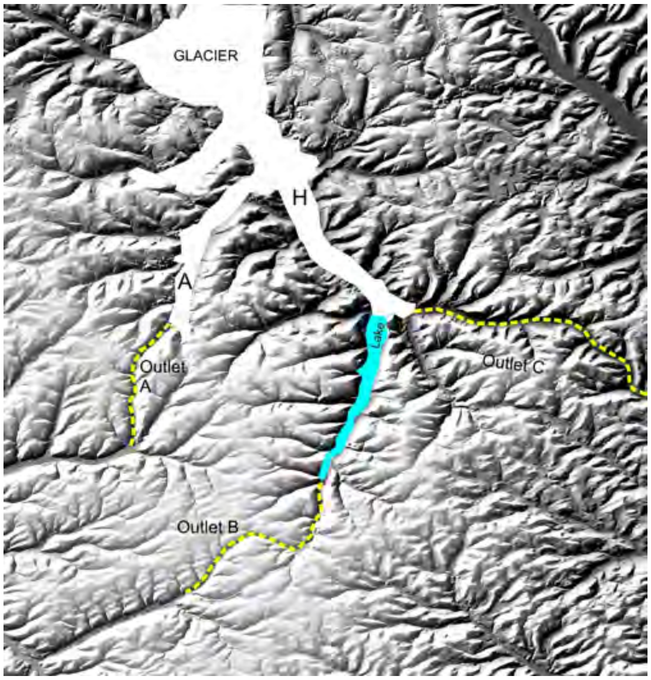

Figure 12. Hypothetical stage showing potential lobate nature of Late Wisconsin ice recession near Alfred Station (A) and Hornell (H), NY. Scale: Straight line distance from Alfred Station to Hornell (A to H) is 9.7 km (6 miles).

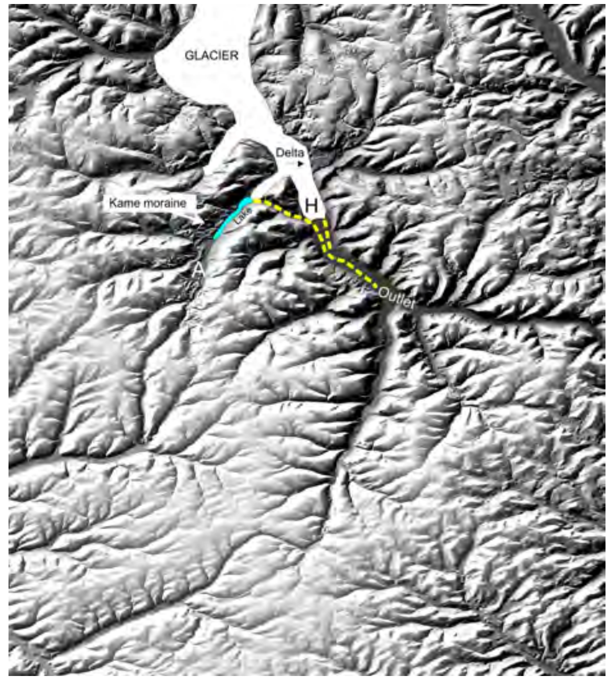

Figure 13. Hypothetical recessional ice position following earlier stage depicted in Figure 12. Scale: Straight line distance from Alfred Station to Hornell (A to H) is 9.7 km (6 miles).

Figure 12 shows a lobe of ice covering Alfred Station (A) and Hornell (H). Outlets A and B represent through-flowing meltwater discharge channels that breached local divides and joined proglacial lakes in the Upper Genesee Valley, whereas Outlet C drained southeastward toward Corning and the Chemung RIver. Lake and ice border are purely hypothetical and only are meant to be suggestive of the complexity of local conditions that might have existed during glacial recession in this area.

Figure 13 shows a subsequent stage for the same lobe of ice. Kame moraine deposits north of Alfred will be visited on field trip. Note delta abutting east side of ice depicting how depositional regimes may have varied along the ice margins, thereby producing distinctively different landforms on opposing valley walls. Outlet depicts meltwater now draining only southeastward from vicinity of Hornell to the Chemung River.

Hypothetical ice margin reconstructions 2

These two maps (Figures 14 and 15) show hypothetical ice margins for the Laurentide Ice Sheet as it receded from the Alfred (A), Hornell (H) and Canisteo (C) area.

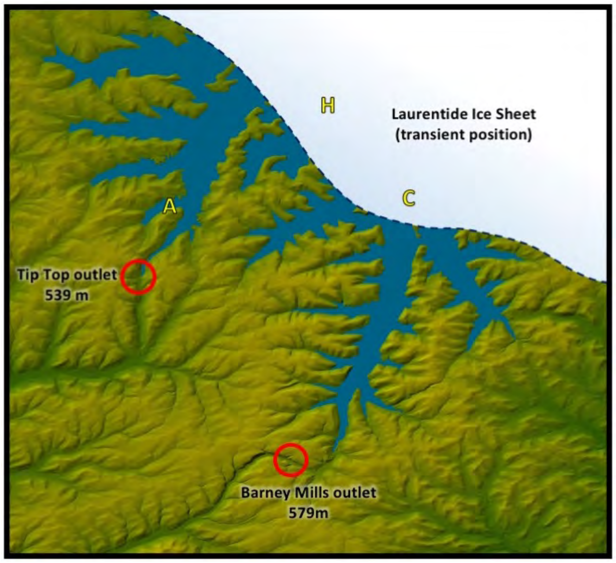

Figure 14. Transient receding ice margin impounding proglacial lakes in the Alfred area (draining through Tip Top outlet) and in Bennetts Creek valley (draining through Barney Mills outlet).

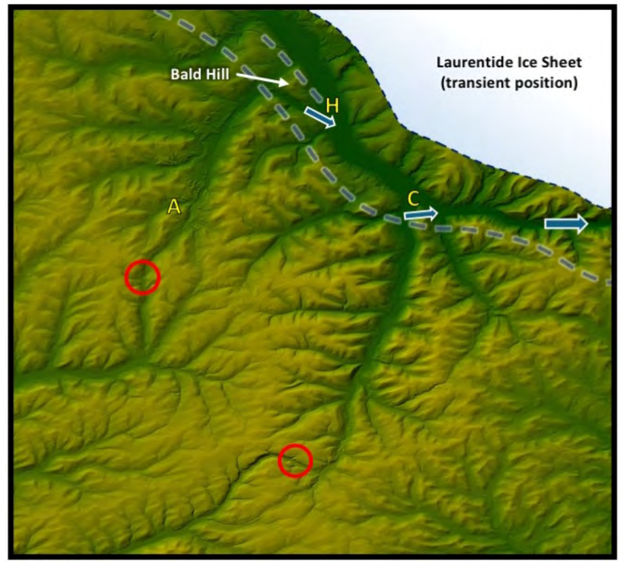

Figure 15. Further recession of the ice margin and drainage of proglacial lakes.

Figure 14 shows the Laurentide ice margin as it withdrew from the Alfred area. The general NW-to-SE trend of the margin parallels the Last Glacial Maximum (LGM) moraine farther south and the Valley Heads moraine to the north, and local topography is ignored (i.e. no attempt has been made to show ice margin lobation into valleys). Proglacial lakes in the two valleys are shown with a water surface elevation of 539 m (1768 feet) and the topography has not been adjusted for glacio-isostatic depression.

Retreat of this ice margin to Bald Hill (Figure 15) would have allowed the lake at Alfred to drain to the southeast. The floor of the sluiceway on the south side of Bald Hill is about 160-180 m (525-590 feet) lower than the Tip Top outlet and so this drainage event was very likely catastrophic. Any sediment that had been deposited in the sluiceway prior to or during the LGM was eroded out whereas sediment in another sluiceway on the west side of Bald Hill, which was protected by the ice margin, was not. This outburst flood and similar outbursts from Bennetts Creek and adjacent valleys exited the area to the southeast down the Canisteo Valley.

FIELD GUIDE AND ROAD LOG

Latitude	Longitude	Stop or View Description
42.2570	-77.7886	Walk to the new Ceramic Museum and go down to the creek where there is a strange concrete structure. Climb down into the creek and just to the north of the structure (towards the bridge) you should see a layer in the soil glistening with moisture. This is the Alfred Clay.

STOP 1. The Alfred Clay

Location Coordinates: 42.257070°, -77.788671°

Background: During the 1880's, it was discovered that the clay in the vicinity of Alfred, NY could be used to make quality terra cotta products. In 1889 the Celadon Terra Cotta Company was organized by a small group of Alfred entrepreneurs to manufacture bricks and roofing tile. The company prospered and was partially responsible for locating the New York School of Clayworking (now the New York State College of Ceramics) in Alfred. In 1906, the company was sold to the Ludowici Company of Ohio, which became the Ludowici-Celadon Company. By that time the original tile works had expanded until it covered more than an acre of ground, occupying the space where presently are located Alfred University's McLane Center and its parking lot.

The plant was completely destroyed by fire on the morning of August 26, 1909, except for the small office building which stood separately along North Main Street (and now sits at the intersection by the traffic light). While the tile factory was not rebuilt after the fire, many of its products can still be seen in town on various roof tops and on the exterior of the "Terra Cotta" building.

Observations you can make: The clays are made obvious by the water glistening on its surface. This is water which trickled down from the soil above, but hit the impermeable clay and moved along it to the stream bed. Here erosion has exposed this contact at the surface. So we see a spring at the top of the clay layer, effusing its ground water to make the clay glisten.

Dig out a bit of the clay with your finger, and note that you can roll it, mold it, make it into little sculptures. This is what artists call a "Workable Clay" and it is this property which made it valuable.

Look down the stream valley, and you will see large rocks and concrete structures, riprap, which were put in place during the reconstruction after the flood from Hurricane Agnes in 1972. Nature has disturbed many of them. This flood, which isolated Alfred for a week, caused the water to rise here to the level of the front porches of the houses across Main Street.

Other observations: In doing the foundation work for the building across the street, this clay layer was exposed. After some manipulation they put a layer of sand down on top of it, as shown below:

Figure 16. The clay layer extends from the Creek beneath the entire Ceramics Museum. Toward the right you can see it beneath the fill they put above.

Figure 17. Another view of the clay layer showing the soil above it.

Latitude	Logitude	Stop or View Description
42.2565	-77.7892	To your left, after you turn, is the Terra Cotta building referred to in the description for Stop 1. It served as a catalog for the company,

		showcasing some of their Terra Cotta tiles.
42.2548	-77.7903	The building on the east side of Main Street, Green Hall, has Terra Cotta tiles on the wall above second floor
42.2491	-77.7900	Octagon House on east, terraces on west side of the road. The houses along here were built over a century ago, and it is not likely that substantial landscape modification preceded their construction. Instead, the builders probably sought out flat spots to build on. Hence the terraces that we see here, and there are a lot of them, are probably natural. Most are separated by a foot or two difference in elevation.
42.2471	-77.7892	Downstream from this bridge are large chunks of primitive concrete which may have been part of a dam. If so, this large flat region would have been produced by the silting up of the mill pond behind the dam, and is thus anthropogenic. The terraces are visible on the right, and are at a considerably higher elevation.

STOP 2. Terraces of Lake Alfred

Location Coordinates: 42.24448, -77.78990

When the leaves are on the trees it is sometimes difficult to see the terraces which we've passed, but here there is always a clear view. The profile of the terrace is obvious, and it is dipping gently back down the valley to our north. As you continue up the hill you can view additional terraces all the way to the top, on both sides of the road.

Latitude	Longitude	Stop or View Description
42.2283	-77.8041	At the top of the hill, near the intersection with Kenyon Road, you will be at a drainage divide. The Upper Canacadea Creek watershed is behind us, and water flowing into it, towards the north, ends up in the Chesapeake Bay. Middle Dyke Creek watershed is ahead of us, and water flowing into it, towards the south, ends up in the Gulf of St. Lawrence.
42.2253	-77.8204	Shortly after turning right (west) onto Lake Road you will pass AU's Bromeley-Daggett Equestrian Center located at the Maris Cuneo Equine Park. An early director was surprised to find that many of the horse trails here, near the top of the hill, were very poorly drained.
42.2356	-77.82022	Before the intersection with Randolph Road is a turnoff to the left for AU's Foster Lake. This is a beautiful 25-acre man-made lake in a col between two hills. The lake was created by Eddy Foster in 1950 and was owned by the Foster family until 2003. Dammed at both ends, both outlets drain into the Vandermark Creek, staying within its watershed.

STOP 3. Till seen in roadside ditches

Location Coordinates: 42.24429, -77.81973

These ditches were excavated during August of 2017. Observe the angular clasts, lack of sorting, and abundant clay. Most of the clasts are sedimentary, probably derived from local bedrock.

Figure 18. Till near intersection of Lake Road and Waterwells road.

Latitude	Longitude	Stop or View Description
42.2467	-77.8249	A quarter of a mile after turning left (west) on Water Wells Road, the road reaches another high point, and drainage divide. And again, in the Upper Canacadea Creek watershed behind us, and water flows towards the north, before it turns around and ends up in the Chesapeake Bay. Whereas water in Vandermark Creek watershed ahead of us, flows towards the southwest, before it turns around and ends up in the Gulf of St. Lawrence.
42.2438	-77.8460	Make a sharp right on Vandermark Road. Proceed to the NE on this road, gaining about 60 feet in elevation as you cover 1.28 miles of road.
42.2594	-77.8321	STOP at the blinking red light at the intersection with Route 244, and when things are clear, proceed through, taking a left just beyond the intersection onto Hanneman Road, where we can park safely.

STOP 4. Five Corners

Location Coordinates: 42.259498°, -77.832163°

We are in a sizable, linear valley, having come up the Vandermark Creek and soon to go down the McHenry Valley creek - without changing direction. The valley may have formed by flow between a lake impounded at a higher elevation to the NNE, and a lake impounded in the Genesee Valley, at a lower elevation, to the SSW. This col was the lowest point between them (although originally perhaps quite a bit higher than it is now) and erosion cut it down to its current size. The processes involved, their durations and relative importance, will be discussed at this stop.

We will visit two similar valleys this afternoon.

Latitude	Longitude	Stop or View Description
42.2730	-77.8292	Cross the bridge and park at the side of the road, beyond the end of the guard rail.

STOP 5. Bridge reconstruction revealed subsurface and waterfall reveals bedrock erosion

Location Coordinates: 42.27309, -77.8292

For many years AU students measured the cross sectional areas of bridges along this road. They would often conclude that this bridge was not big enough, and they also expressed concern about how weathered the concrete was, and how erosion was undermining the wings. A StreetView image from Google Earth in 2009 shows the state of the bridge.

Figure 19. Bridge in 2009, before being rebuilt.

In the fall of 2009 major reconstruction of the bridge began. By September, when our class again visited it, much of the bridge was gone, and we got to see the material beneath the road, as shown in the figure below:

Figure 20. Subsurface beneath road a bridge under reconstruction. Area in highlighted rectangle is enlarged to the right.

About 150 feet north of the bridge, just northwest of the road, there is a waterfall in a small ravine running parallel to the road

Figure 21. Small waterfalls show active downcutting.

With the caveat, again, that much of our terrain was modified in 1972, this waterfall is cutting down through sedimentary rock, with those layers somewhat less susceptible to weathering and erosion forming a series of caprocks holding up a series of waterfalls down this stretch of the stream.

This demonstrates active down cutting and is unlike anything we saw on the other side of the col at Five Corners.

Latitude	Longitude	Stop or View Description
42.2769	-77.8285	From Five Corners we have come down about 184 feet in 1.28 miles. This is about three times as much elevation change as we saw over an equivalent distance in the Vandermark valley.
42.2984	-77.7858	After turning left at the sign for Almond Aggregates LLC, go up the hill, turn left at the sign saying, "TO PIT"

STOP 6. Almond Aggregates LLC Quarry

Location Coordinates: 42.2984, -77.7858

One of many sand and gravel quarries in the area. Note the layering, the gigantic boulders in some layers, and at least three layers of sand near the top. They are made up of fine sand and seem to be nearly horizontal. It is possible to see them in vertical sections at different azimuths, so this is a true dip, not an apparent one.

Figure 22. Quarry wall showing three sandy layers near the top.

Figure 23. Closer view of the top sandy layer from Figure 22, and boulder layer below it.

The upper levels top out at about 564 m (1850 feet) elevation. The highway beneath the quarry is at 482 m (1580 feet) suggesting a lake on the order of 82 m (270 feet) deep. The elevation of Five Corners is 631 m (2070 feet). One possibility is that the sand was deposited here before the lake had reached the Five Corners outlet elevation. Another possibility is that this deposit formed when there was a lower outlet somewhere to the NE. A third possibility is that this was formed very close to the ice front, and that various tongues of ice dammed up the lake.

There is some bedding which has steep apparent dips, and other sandy units with curious wave shaped features in some vertical sections.

That the majority of cobbles are well rounded, and there is less clay than we saw in the roadside ditches indicate that this is a fluvial deposit, perhaps a kame or kame delta.

Figure 24. Quarry wall showing steep apparent dips

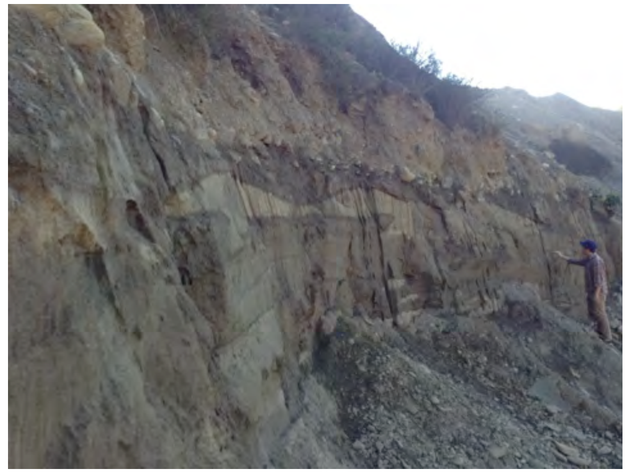

Figure 25. Wavy features in a vertical section.

STOP 7. Breached Dam (Park in road maintenance lot, to right, just before big bridge)

Location Coordinates: 42.2984, -77.7858

The higher elevations here (442 m, 1450 ft) sit on sands. We parked at about 427 m (1400 ft) suggesting that the lake responsible for those sands was about 15 m (50 feet) deep.

Beneath those sands are glacial deposits. The lake stretched up the valley we have just come down, and was prevented from draining to the north by this glacial deposit or the ice margin blocking its way. Eventually the lake broke through the dam, but the point where it did that was above bedrock, not this nice, easily eroded, glacial stuff. Still, that's where the breach was, so that is where the erosion occurred. The result is the chasm moving off to our west.

Figure 26. Old bridge, which served as a dam after debris lodged against it in 1984.

In 1984 thunderstorms brought a lot of debris down this valley, and much of it lodged against the dinky bridge, Figure 26, which was here, thus producing another dam and flooding many of the families living upstream.

STOP 8. Kanakadea Park (LUNCH)

Location Coordinates: 42.35029, -77.71071

We will take a short walk into an "old growth" forest. This has likely survived because the topography was judged too steep to farm on successfully.

The dam was built after a disastrous flood in 1935. It survived the 1972 flood, and has been used several times since then to store storm waters

STOP 9. Valley overlook at Hornell

Location Coordinates: 42.37088, -77.69656

From the vantage point of this hill, we can decipher some of the glacial history of the large valley at Hornell. Note the delta stretching towards us in the distance, and let your eye follow that elevation to the left (north). You may see homes and barns at about that elevation, suggesting a terrace there. This elevation is about 427 m (1400 feet), the same elevation that we parked at on our last stop before lunch. It isn't unreasonable to consider this the approximate base level for McHenry Valley creek. If this is true, then perhaps the breach in the dam there occurred while this delta was being formed.

Note, also, that the top of the delta is smooth, whereas similar elevations on this side of the valley are hummocky. An explanation for this might be that the delta was formed by water borne sediments, not containing any ice. This side seems to be a glacial deposit, perhaps containing chunks of ice the size of a large barn, buried at depths where they would melt only slowly. The waves of the lake originally planed off the surface on this side, so it was quite like that on the other side, but later, as that ice melted, the surface collapsed in producing all of these kettle holes.

Latitude	Longitude	Stop or View Description
42.3561	-77.6691	Bald Hill, to our right (west) is an umlaufberg, which is defined by Coates (1974) as an outlier of bedrock surrounded by (usually) glacifluvial deposits. These landforms are widespread in the glaciated Allegheny Plateau and are due to erosion from glacially forced drainage that separated the bedrock hill from the adjacent upland, and then subsequent outwash deposition around the base.
42.2780	-77.61035	Levees built after flood of 1935, rebuilt after 1972
42.2594	-77.8321	More levees and the bridge over Purdy Creek
4.2.0791	-77.6714	Road curves to the right (W) to enter the outlet valley.
42.0852	-77.6858	Watershed Boundary: Water behind us flows ESE then N in Bennetts Creek, then SE in the Canisteo River to end up in the Chesapeake Bay. Water ahead of us flows WNW before turning SW in Marsh Creek and Cryder Creek, then N in the Genesee before ending up in the Gulf of St. Lawrence.

STOP 10. Barney Mills Outlet Valley

Location Coordinates: 42.088650, -77.69327

We are in a deep valley, running about N 60 W, or WNW, and just to our south is what appears to be an incised meander. This is one of the higher cols draining to the west into the Genesee valley, at 579 m (1900 feet).

Latitude	Longitude	Stop or View Description
42.0377	-77.7628	Whitesville: Marsh Creek enters Cryder Creek
42.2151	-77.79335	Watershed Boundary: From here to the north, water ends up in the Chesapeake, whereas south of here it ends up in the St. Lawrence
42.2228	-77.7895	Tip Top. We will continue up the road a bit to where there is parking.

STOP 11. Near Tip Top

Location Coordinates: 42.2228, --77.7895

Highest point in the valley between Alfred and Andover. This valley is called "Railroad Valley" and it was an important stretch of the Erie Railroad. When the Erie Canal was built, folks in the Southern Tier feared that transportation would pass them by. They successfully lobbied for the state to authorize another railroad to take the southern route between New York and Chicago. This railroad was named the Erie Railroad, and operated from 1832 to 1960. The Erie Railroad's repair shops were Hornell's biggest employer and have since morphed into Alstom. On the route from New York to Chicago, Tip Top was the highest location at 541 m (1774 feet). Climbing to here from Hornell meant rising 622 feet in 12.24 miles, one of the steepest grades in New York. In 1877 this became famous because a train carrying strike breakers was unable to get over Tip Top, as strikers had soaped a quarter mile of the track. The strikers uncoupled the passenger cars, which removed enough weight so the locomotive and mail car could continue, thus avoiding any charges of interfering with the federal government.

In terms of the hydrology and geology, note another swamp which drains from both ends, just as we saw at Five Corners and Barney Mills.

Latitude	Longitude	Stop or View Description
42.2627	-77.7607	Alfred-Atlas Sand and Gravel Pit to the right (east)

STOP 12. New Enterprise Stone & Lime Co., Inc. Pit

Location Coordinates: 42.268687°, -77.760126°

This quarry is operated by the New Enterprise Stone & Lime Co., Inc., formerly known as Buffalo Crushed Stone. The deposits here are perhaps some kind of kames. Where exposed one can often see steep apparent dips on bedding similar to what we saw at Stop 6. Sandy layers occur, and may have apparent dips that are nearly horizontal. The deposits probably stretched across Route 21 originally, and large quarry operations on the east side of that highway, operated by Buffalo Crushed Stone as well as Alfred Atlas, at one time produced immense quantities of pea gravel, used for years for Leathers Playgrounds.

Figure 27. Wall of New Enterprise Stone & Lime Co. Pit.

These deposits may have been responsible for damming up what we call Lake Alfred, and, as at Stop 6, the glacial debris dam was at the northern end of the valley. It is often assumed that the lakes in this region were contained by ice dams to the north, and it is interesting to consider the possibility that the ice may have been far away when these lakes existed.

Much of the floor of the pit is occupied with piles of products - crushed stone at different sizes and meeting different specs, or waste material. The operation takes cobbles and crushes them, spinning the clasts against the outside wall of the crusher. This will reduce softer rocks to fine particles, which are washed away with water. The harder clasts are then sorted by size.

Figure 28. One of the crushing plants at the New Enterprise Stone & Lime Co. Pit.

REFERENCES CITED

Braun, D.D., 2004, The glaciation of Pennsylvania, USA, in, Ehlers, J. and Gibbard, P.L. (eds), Quaternary Glaciations - Extent and Chronology Part II, p. 237-242.

Carney, F., 1903, A type case in diversion of drainage, The Journal of Geography, v. 2, p. 115-124.

Coates, D.R., 1974, Reappraisal of the glaciated Appalachian Plateau, in Coates, D.R. (ed), Glacial Geomorphology, p. 205-243.

Coates, D.R. and Kirkland, J.T., 1974, Application of glacial models for large-scale terrain derangements, in Mahaney, W.C. (ed), Quaternary Environments: Proceedings of a Symposium, Geographical Monographs no. 5. p. 99-135.

Fairchild, H.L., 1925, The Susquehanna River in New York and evolution of western New York drainage, New York State Museum Bulletin, No. 256, 99 pp. with 25 plates.

Fairchild, H.L., 1934, Seneca Valley physiographic and glacial history, Bulletin of the Geological Society of America, v. 45, p. 1073-1110.

Fairchild, H.L., 1935, Genesee Valley hydrography and drainage, Proceedings of the Rochester Academy of Science, v. 7, p. 157-188.

Hughes, T., Borns, H.W. Jr., Fastook, J.L., Hyland, M.R., Kite, J.S. and Lowell, T.V., 1985, Models of glacial reconstruction and deglaciation applied to Maritime Canada and New England, Geological Society of America Special Paper 197, p. 139-150.

Karig, D.E. and Miller, N.G., 2013, Middle Wisconsin glacial advance into the Appalachian Plateau, Sixmile Creek, Tompkins Co., NY, Quaternary Research, v. 80, p. 522-533.

Karrow, P.F., Bloom, A.L., Haas, J.N., Heiss, A.G., McAndrews, J.H., Miller, B.B., Morgan, A.V. and Seymour, K.L., 2009, The Fernbank interglacial site near Ithaca, New York, USA, Quaternary Research, v. 72, p. 132-142.

Kozlowski, A. and Graham, B., 2014, Glacial geology of Cayuga County of the eastern Finger lakes: lakes, lore and landforms, Guidebook for the 77th Annual Reunion of the Northeastern Friends of the Pleistocene, Auburn, NY, 148 pp.

Lewis, C.F.M., Blasco, S.M. and Gareau, P.L., 2005, Glacial isostatic adjustment of the Laurentide Great Lakes Basin: using the empirical record of strandline deformation for reconstruction of early Holocene paleo-lakes and discovery of a hydrologically closed phase, Géographie Physique et Quaternaire, v. 59, p. 187-210.

Lisiecki, L.E. and Raymo, M.E., 2005, A Pliocene-Pleistocene stack of 57 globally distributed benthic $\delta^{18}O$ records, Paleoceanography, v. 20, doi:10.1029/2004PA001071.

Muller, E.H., Braun, D.D., Young, R.A. and Wilson, M.P., 1988, Morphogenesis of the Genesee Valley, Northeastern Geology, v. 10, p. 112-133.

Mullins, H.T. and Hinchey, E.J., 1989, Erosion and infill of New York Finger Lakes: implications for Laurentide ice sheet deglaciation, Geology, v. 17, p. 622-625.

Mullins, H.T., Hinchey, E.J., Wellner, R.W., Stephens, D.B., Anderson, W.T. Jr., Dwyer, T.R. and Hine, A.C., 1996, Seismic stratigraphy of the Finger Lakes: a continental record of Heinrich event H-1 and Laurentide ice sheet instability, Geological Society of America Special Paper 311, p. 1-35.

Ridge, J.C., 2003, The last deglaciation of the northeastern United States: a combined varve, paleomagnetic and calibrated ^{14}C chronology, New York State Museum Bulletin 497, p. 15-45.

Ridky, R.W. and Bindschadler, R.A., 1990, Reconstruction and dynamics of the Late Wisconsin “Ontario” ice dome in the Finger Lakes region, New York, Geological Society of America Bulletin, v. 102, p. 1055-1064.

Tarr, R.S., 1905, Drainage features of central New York, Bulletin of the Geological Society of America, v. 16, p. 229-242.

Von Engeln, O.D., 1931, A preglacial or interglacial gorge near Seneca Lake, New York, New York State Museum Bulletin, v. 286, p. 127-134.

Young, R.A. and Burr, G.S., 2006, Middle Wisconsinan glaciation in the Genesee Valley, NY: a stratigraphic record contemporaneous with Heinrich Event, H4, Geomorphology v. 75, p. 226-247.

B5: GLACIAL FEATURES AND THE "GREAT DIVIDE" BETWEEN WATKINS GLEN AND ITHACA

CAROL GRIGGS, CORNELL TREE-RING LAB
Cornell University Ithaca, NY cbg4@cornell.edu

Glacial features are generally studied on the large-scale, just as glaciers are naturally large. Here we look at some features in a small valley in the Finger Lakes Region of upstate New York that are interesting because they were developed by the interaction and possible collisions of ice and meltwater forces on a larger scale when the Valley Heads Moraine was formed. In this study we are looking at conditions that began in approximately 15,000 years cal BP.

The area of study starts in the Susquehanna River Valley in south-central New York State (Figure 1), to the south of the Valley Heads Moraine (VHM). A tributary to the Susquehanna from Bath to Waverly, NY, is the Cohocton River that runs along the southwest side of the VHM at the bottom of the Finger Lakes. It merges with the Tioga River into the Chemung River in Corning, which continues eastward on the south side of Elmira, and joins the Susquehanna River south of Waverly, NY. While Horseheads, NY, sits on an alluvial plain just north of the Chemung, no significant river runs through the city today. Rather the alluvium was deposited by the ice sheet runoff over time, and one of the VH lobes ended just north the city (Figure1).

Figure 1. The route from Bath, along the Cohocton and Chemung Rivers, to Horseheads in south-central New York.

Latitude	Longitude	Stop or View Description
42.17397	-76.80574	STOP 2. Gravel pit

One glacial feature (#2, Figure 1) is a gravel pit in Horseheads. A large layer of logs was uncovered when the gravel pit was excavated in the mid-1970s. A report of this finding indicated that the company could

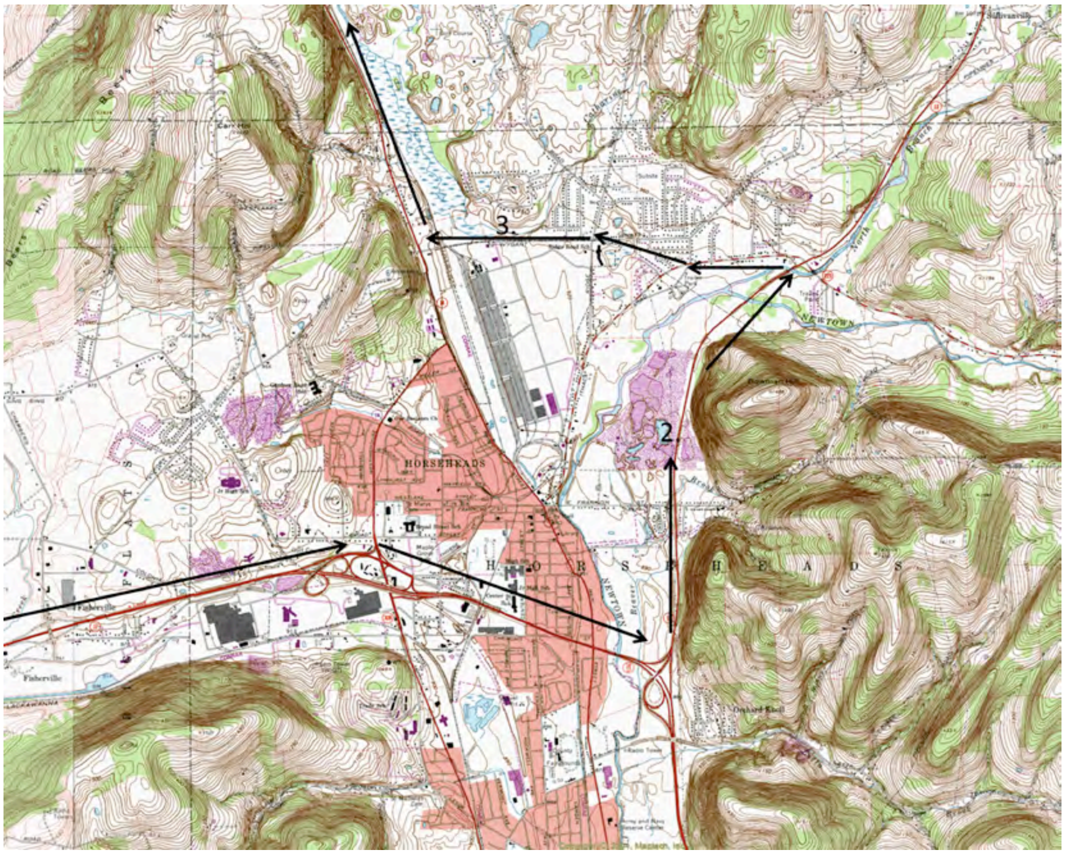

Figure 2. Horseheads, NY, where the Valley Heads Moraine is at its southernmost tip. Site 2 is a Gravel pit where many logs were found far below surface level, and are probably from before the Last Glacial Maximum. Site 3 is the southern tip of the moraine, where drainage basins meet. Streamflow to the south of the moraine goes into the Susquehanna River and north into Lake Ontario.

not dig any farther down and had tried to find someone interested in the logs, but with no response. Unfortunately that pit was no longer excavated, flooded in, and remains so to this day. The logs were most likely pushed down by ice flow, and could have been deposited before the glacier advanced over the valley, or earlier.

Latitude	Longitude	Stop or View Description
42.19017	-76.8979	STOP 3. Catherine Creek turns almost completely around

North of Wygant Rd in the same floodplain as the gravel pit is the southernmost point of Catherine Creek (#3 in Figure 2), where it does a rounded 175° turn to west, then north to drain into Seneca Lake.

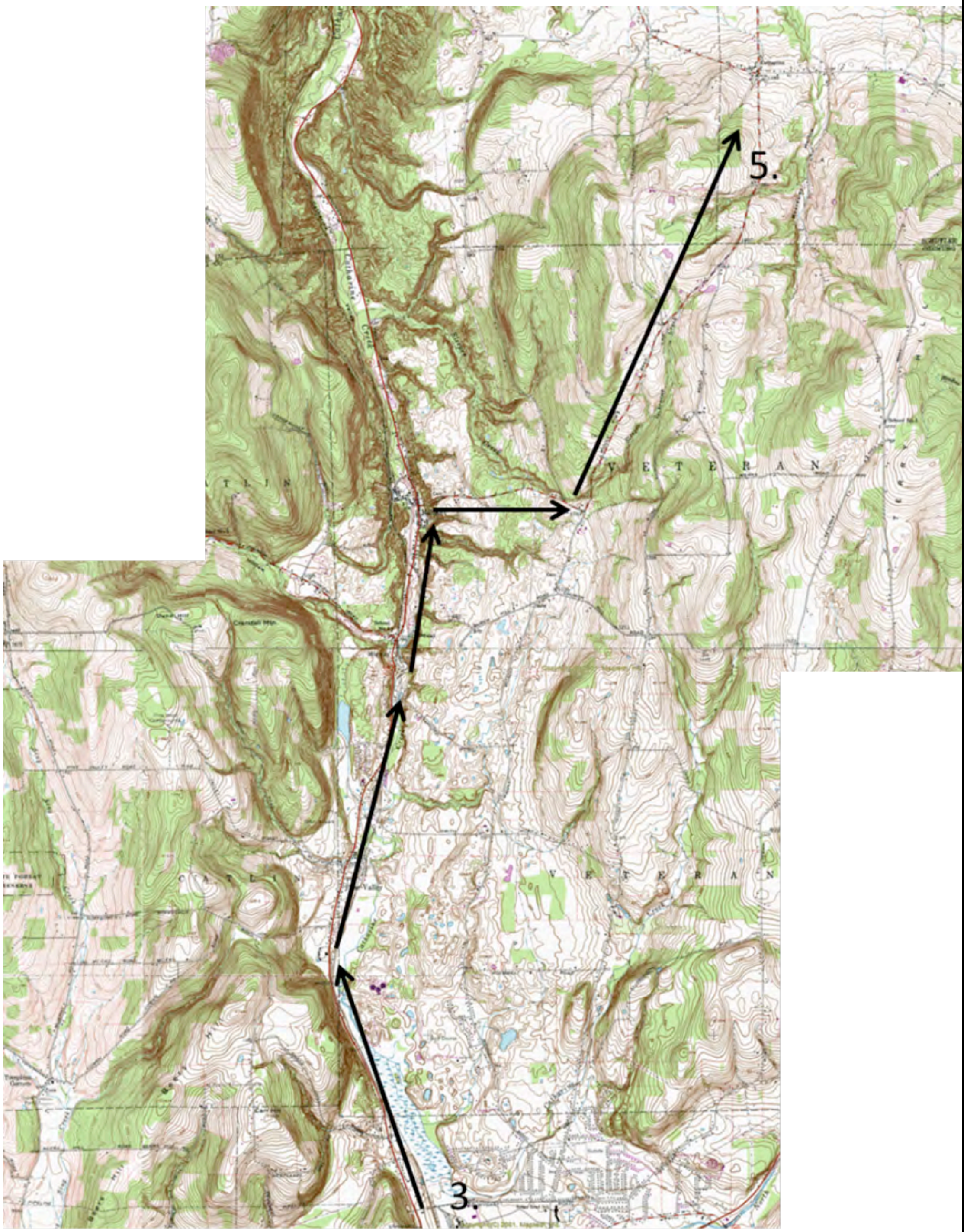

Figure 3. From the south tip of the VHM lobe (#3) to the area of mastodon site (#4) and the top of the VHM looking north (#5).

Latitude	Longitude	Stop or View Description
42.25206	-76.83596	STOP 4. Post Office near the Mastodon site

Within the Catherine Creek Valley is the Chemung mastodon site but it was not found in the creek itself, but above the valley in a small kettle pond in the vicinity of #4 (Figure 3). In general, mastodon sites in upstate New York are small kettle ponds or small-scale alluvial plains in the VHM and on the Allegheny Plateau (Griggs and Kromer 2008). Definitive sites with at least some articulated bones have not been found in larger river valleys.

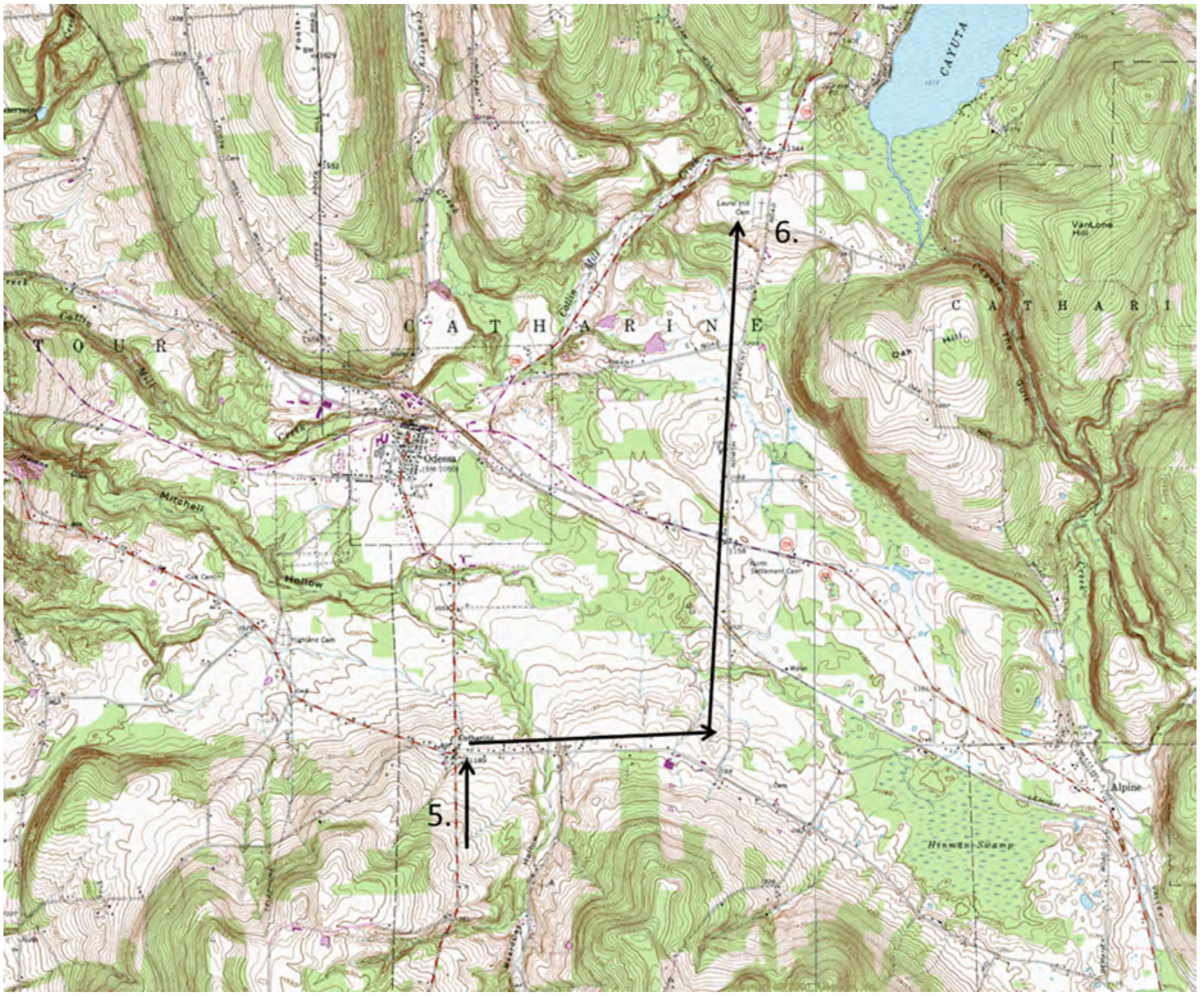

Figure 4. Locations of stops: #5 - overlook on top of VHM; #6 - dike on south side of Cayuta Lake.

Above the Catherine Creek Valley floor is the Valley Heads Moraine (#5; Figures 3, 4).

Latitude	Longitude	Stop or View Description
42.3059	-76.7847	STOP 5. Top of Valley Heads Moraine – complex

To the north is the town of Odessa, with streamflow from its immediate surroundings draining into Seneca Lake and Lake Ontario. Cayuta Lake (or "Little Lake") is in the valley beyond the two main hills to the N and NE. Going up that valley, which still drains into Lake Ontario, we come to an abrupt divide between the Lake Ontario drainage and the Susquehanna/Chesapeake Bay system. The divide is a dike (#6; Figure 5), formed by a moraine at the south end of the Cayuta Lake basin, and north side of the basin is essentially where the ice sheet split into two lobes (addendum, other map?).

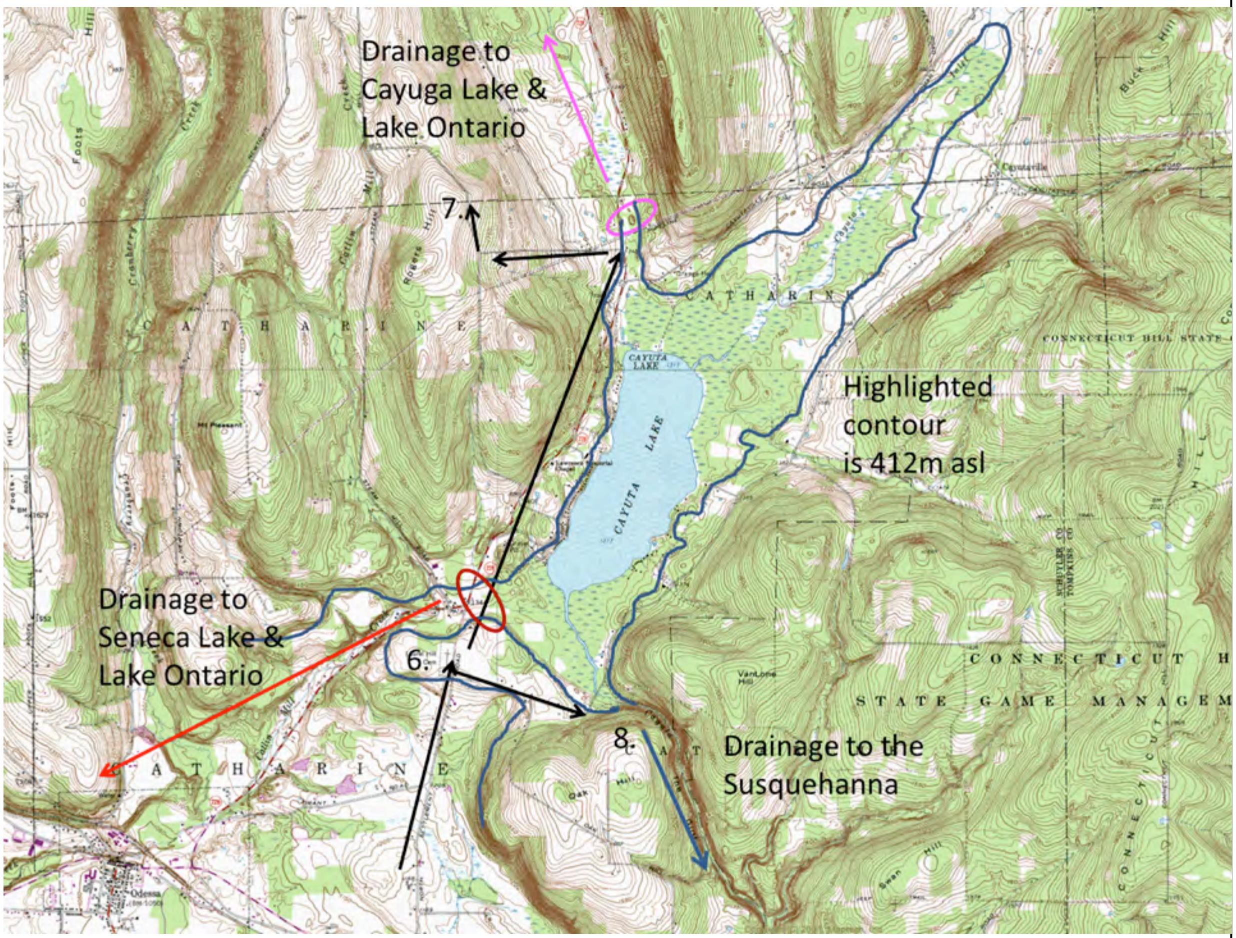

Figure 5. The Cayuta Lake basin. Stop #6 is on the dike. The valley to the SW drains into Seneca Lake with the divide at the oval shape, and the valley to the north is the headwater of Taughannock Creek into Cayuga Lake. Both of the Finger Lakes join and drain into Lake Ontario. Cayuta Lake drains SSE into the Susquehanna River and into the Chesapeake Bay. Stop #7 is an overview of the Cayuta Lake Basin and the swamp and headwater of Taughannock Creek.

Latitude	Longitude	Stop or View Description
42.35285	-76.754867	STOP 6. Dike (park in the cemetery)
42.38826	-76.76354	STOP 7. Potato Hill Overview of Cayuta Valley
42.38805	-76.72242	STOP 8. Middle of Valley
42.37636	-76.73298	STOP 9. North Shore of Cayuta Lake
42.34911	-76.73733	STOP 10. Cayuta Lake outlet - Barton Dam

The valley floor is relatively flat, but all except the northeastern sector has relatively steep valley walls (Figure 5). The ancestral lake bed sediments across the valley have a large variety of glacial clays to pure pea-size gravel, both sorted and unsorted.

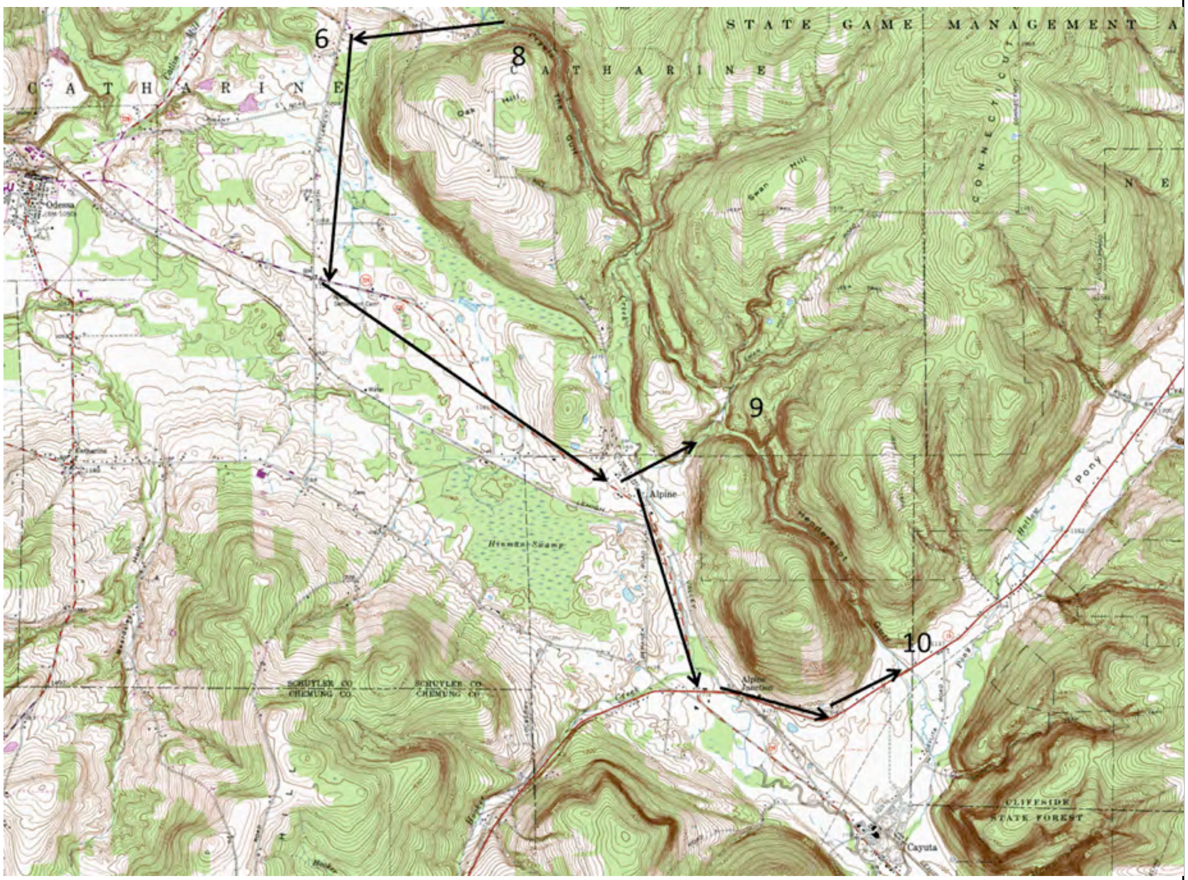

Figure 6. The drainage through gorges southeast of Cayuta Lake into which it drains. #8 is at the entrance of "The Gulf"; #9 is one of the two breaks in the gorges where drainage direction changes over time; and #10 is the end of the hanging gorge which today has very little outlet.

The elevation of the top of the dike and around the valley indicate that when lake was at the top of the dike, the whole valley was filled, and at considerable depth. Currently the lake is relatively shallow, 5-10m deep, with a few deeper holes.

The dike and current drainage into "The Gulf" of Cayuta Creek (#8) suggest that the gorge was blocked for a long time before drainage began, possibly by glacial ice due to its depth and narrow shape. Also the bedrock that it runs through has a divide perpendicular to the gulf in a couple of places (7), and eventually the main stream channel became part of a wider valley floor, and abandoned the very narrow Hendershot Gulf south of the lake (8).

In addition to its identification as a northern point between the ice lobes that formed the VHM, the Cayuta Lake Basin is unusual in a number of other ways. A sponge species has been found in the lake, and is closest to a species found only in Russia (citation?). The basin's locations at the headwaters of tributaries for both the Cayuga and Seneca Lakes suggest it acted as some kind of reservoir for one or the other, maybe both, during the retreat of the ice lobes. The differences in drainage were possibly affected by changes in the ice sheets, alluvial deposition, and isostatic movement.

Latitude	Longitude	Stop or View Description
42.31648	-76.71359	STOP 11 The Gap on Swan Hill Road
42.29484	-76.69481	STOP 12. Henderson Gulf Exit

REFERENCES CITED:

Griggs, CB, B Kromer. 2008. Wood macrofossils and dendrochronology of three mastodon sites in upstate New York. In: Allmon, W., Nester, P. (Eds.) Mastodon paleobiology, taphonomy, and paleoenvironment in the Late Pleistocene of New York State: Studies on the Hyde Park, Chemung, and Java Sites. *Palaeontographica Americana* 61: 49–61.

Muller, EH, PE Calkin. 1993. Timing of Pleistocene glacial events in New York State. Canadian Journal of Earth Sciences, 1993, 30:1829-1845, https://doi.org/10.1139

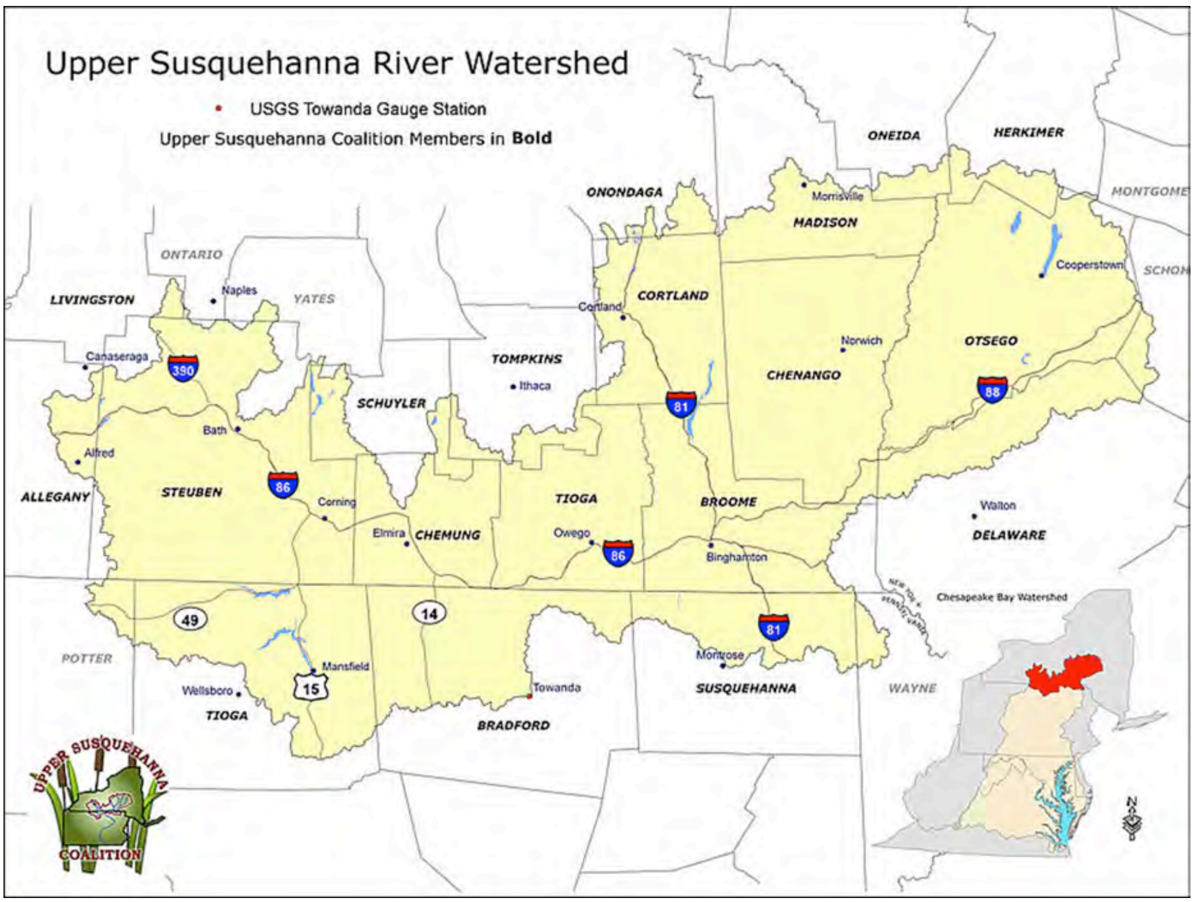

Addendum 1. The northern boundary of the Upper Susquhanna Watershed is very close to the location of the Valley Heads Moraine (e.g. Muller and Calkin 1993). Cayuta Lake is the small lake in the yellow background diagonal to the “R” in “SCHUYLER”. Map is available at http://www.chesapeakebay.net/

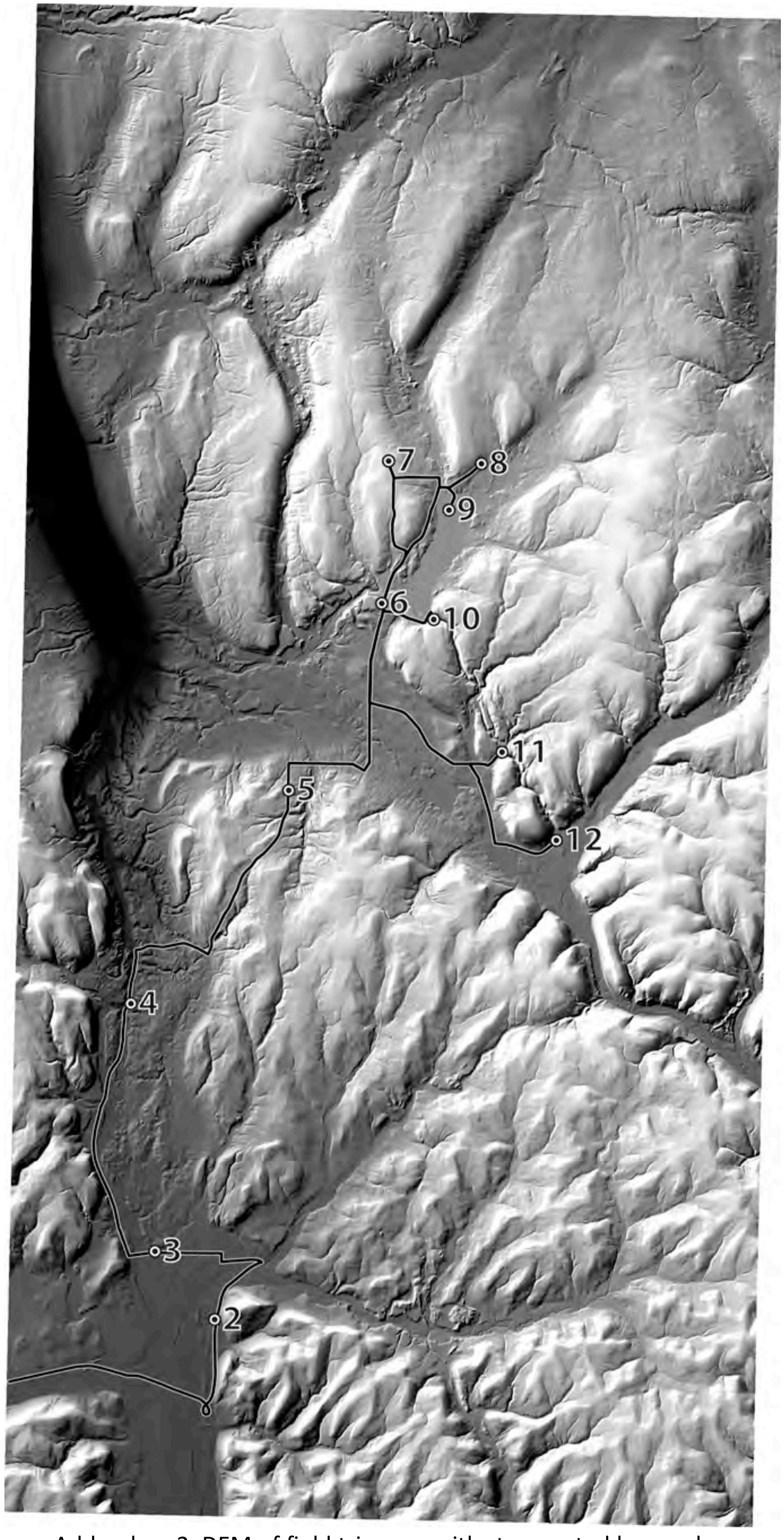

Addendum 2. DEM of field trip area with stops noted by number

W2: KEY TOOLS AND W2: STRATEGIES FOR MAKING AND USING VIRTUAL FIELDWORK EXPERIENCES

DON DUGGAN-HAAS AND ROBERT M. ROSS
Paleontological Research Institution | Museum of the Earth | Cayuga Nature Center
Ithaca, NY 14850

Fieldwork is a signature pedagogy (Shulman, 2005) for the geosciences, but it can be challenging to bring groups of students into the field. Likewise, it can be difficult to replace valuable aspects of fieldwork in settings like large college lecture halls or K-12 classrooms. Virtual Fieldwork Experiences (VFEs) are helpful in meeting these challenges. We do not suggest that VFEs replace actual fieldwork; rather, they can act as a dynamic bridge between field and classroom. In carrying out actual fieldwork and associated complementary VFEs, key questions to consider include:

- What are the most important features and results of fieldwork?
- What aspects can be replicated through the use of multimedia? To what extent?
- How can the creation of VFEs be used to catalyze, extend, document, and share what is learned from doing actual fieldwork?

Over a decade ago, we began developing curriculum materials and offering professional development programming in which VFEs are a key feature. Over the last ten years, both the technologies available and our pedagogical approaches have changed substantially. Technologically, things that used to take hours to create can now be done in minutes, and other things that were simply not practical have become simple for users to create.

The rate of change of pedagogy is slower. Our initial goal of creating VFEs that offer a true inquiry experience by themselves has been tempered over time. While VFEs can offer inquiry experiences for students, a shorter route to inquiry is through student-created VFEs that document fieldwork and learning done by students (Granshaw and Duggan-Haas, 2012).

One of the most important outcomes of our work is the development of a series of questions that can be productively asked and investigated for any site, all supporting the driving question of this work: *Why does this place look the way it does?* The set of questions is included in a virtual fieldwork template in a chapter on fieldwork in each regional volume of *The Teacher-Friendly Guide to the Earth Science of the U.S.* (available free at http://teacherfriendlyguide.org; see, e.g., Duggan-Haas and Kissel 2016).
The effective creation and use of VFEs is dependent upon Technological Pedagogical Content Knowledge (TPACK; see, e.g., Mishra and Koehler, 2006), the suite of understandings and skills that educators apply to teaching scientific content with technology. Educators working with VFEs often find themselves pushing their limits in one or more of the different realms of TPACK. Pushing limits is fundamental to professional growth.

Our work has led to three key ideas for VFE development and use.

- There are scientific and historical questions that can be productively asked and investigated about any site.
- Investigating a landscape is an exercise in Earth systems science – no landscape is the product of a single process.
- Virtual fieldwork is a student-friendly way of documenting, analyzing, and sharing lessons learned from studying a field site.
- And scruffy VFEs are okay. That is, VFEs are always works in progress and can be useful for teaching and learning from early stages of development and without professional-looking design and graphics.

This workshop will introduce a range of technological tools and teaching resources for the creation of VFEs (Duggan-Haas, 2015). Participants will have the opportunity to try out technologies on their own smartphones, tablets, or laptops, as well as explore VFEs we have created. We will explore options that are low-cost or free and that can be mastered by science educators who are not technology specialists. Categories of standard digital tools that together can be used to create a multimedia representation of a field site include the following:

- gigapixel-resolution panoramic images (e.g., Gigapan), made from numerous photos stitched together into one high resolution image, and lower resolution panoramic images (e.g., Google Street View);
- digital 3-D images at multiple spatial scales, including topography (e.g., TouchTerrain) and outcrops and specimens (e.g., Trnio), making them available online (e.g., via Sketchfab), and printing those shapes with 3-D printers;
- field video, time lapse animations, and simple GIF animations;
- digital maps of numerous kinds of spatial data that can be overlain upon each other (e.g., Google Earth, Google Maps, Esri products);
- platforms for sharing multimedia (e.g., Prezi, Esri Story Maps, Powerpoint/Keynote); and
- videoconferencing, e.g., from field to classroom and from classroom to classroom (e.g., Zoom).

Additional information about virtual fieldwork experiences can be found at PRI's website dedicated to the topic of VFEs, http://virtualfieldwork.org. At that site are examples of VFEs that have been created using a variety of media and for a variety of places and purposes.

REFERENCES

Duggan-Haas, D. 2015, About making Virtual Fieldwork Experiences: Resources from the ReaL Earth Inquiry project and the Critical Zone Observatory network, Prezi-style presentation for the Shale Hills RET/REU Program, Summer 2015, https://prezi.com/fvs9pabda-te/about-making-virtual-fieldwork-experiences-resources-from-the-real-earth-inquiry-project-the-critical-zone-observatory-network/?utm_campaign=share&utm_medium=copy&webgl=0

Duggan-Haas, D., and Kissel, R. A., 2016, Real and Virtual Fieldwork: "Why Does This Place Look the Way it Does?", In: Swaby, A. N., Lucas, M. D., and Ross, R. M. (Eds.). *The Teacher-Friendly Guide to the Earth Science of the Southwestern US*. Paleontological Research Institution (Special Publication 51), Ithaca, NY, pp. 373–395.

Granshaw, F. & Duggan-Haas, D., 2012, Virtual Fieldwork in geoscience teacher education: Issues, techniques, and models, In: Whitmeyer, S.J., Bailey, J. E., De Paor, D. G. , and Ornduff, T. (Eds.), *Google Earth and Virtual Visualization in Geoscience Education and Research*, Geological Society of America Penrose Special Paper 492, Boulder, CO, pp. 285-303.

Mishra, P., and Koehler, M., 2006, Technological Pedagogical Content Knowledge: A Framework for Teacher Knowledge, *The Teachers College Record,* v. 108, no. 6, pp. 1017–1054.

Shulman, L.S., 2005, Signature Pedagogies in the Professions, *Daedalus,* v. 134, no. 3, pp. 52–59.